ABSTRACT

Title of dissertation: DEBATING SPACE SECURITY: CAPABILITIES AND VULNERABILITIES

Jaganath Sankaran, Doctor of Philosophy, 2012

Dissertation directed by: Professor John D. Steinbruner
School of Public Policy

The U.S. position in the debate on space security has been that (1) space-based systems could be developed and used to obtain decisive warfighting superiority over an adversary, and (2) these space-based systems, because they might give such an inordinate advantage over any adversary, will be attacked. The Russians and Chinese, in contrast, claim to be threatened by U.S. aspirations in space but deny that they pose a serious threat to U.S. space-based systems. They view the development of advanced military space systems by the United States as evidence of a growing gap of military capabilities limited only by technological–not political–constraints. They argue that U.S. missile defense systems operating in coordination with advanced satellite sensors would weaken their nuclear retaliatory potential.

This dissertation argues that the positions held by both of these parties are more extreme than warranted. An analytical evaluation quickly narrows the touted capabilities and assumed vulnerabilities of space systems to a much smaller set of concerns that can be addressed by collaboration. Chapter 2: *Operationally Responsive Space (ORS): Is 24/7 Warfighter Support Feasible?* demonstrates the infea-

sibility of dramatically increasing U.S. warfighting superiority by using satellites. Chapter 3: *What Can be Achieved by Attacking Satellites?* makes the case that although U.S. armed forces rely extensively on its satellite infrastructure, that does not immediately make them desirable targets. The functions performed by military satellites are diffused among large constellations with redundancies. Also, some of the functions performed by these satellites can be substituted for by other terrestrial and aerial systems. Chapter 4: *The Limits of Chinese Anti-Satellite Missiles* demonstrates that anti-satellite (ASAT) intercepts are very complex under realistic conditions and that a potential adversary with space capabilities comparable to China's has very limited capability to use ASATs in a real-world battle scenario. Finally, in order to evaluate the chief concern raised by the Russians and Chinese, chapter 5: *Satellites, Missile Defense and Space Security* simulates a boost-phase missile defense system cued by the advanced Space Tracking and Surveillance (STSS) sensors. It demonstrates that even under best case assumptions, the STSS sensors are not good enough for the boost-phase missile defense system to successfully intercept and destroy an ICBM.

Together, these chapters aim to narrow the contentions in the debate on space security thereby fostering the international colloboration and data sharing needed to ensure safe operations in space.

DEBATING SPACE SECURITY: CAPABILITIES AND VULNERABILITIES

by

Jaganath Sankaran

Dissertation submitted to the Faculty of the Graduate School of the
University of Maryland, College Park in partial fulfillment
of the requirements for the degree of
Doctor of Philosophy
2012

Dissertation Advisory Committee:
John D. Steinbruner, Ph.D. (Chair)
William Dorland, Ph.D.
Nancy Gallagher, Ph.D.
Steve Fetter, Ph.D.
David Wright, Ph.D.

Acknowledgments

The ambitious dimensions of this thesis was feasible due to the large intellectual leeway I was permitted. I am very grateful to my thesis advisor, John Steinbruner for providing the freedom to explore the problem as I saw fit and in a number of occasions defending my right to do so.

Since I arrived at the Center for International and Security Studies at Maryland (CISSM), Dr. Nancy Gallagher has been my mentor and has constantly supported me with time and resources. She has backed my credentials and has striven to keep me funded at various instances in the last six years. Without her, I would not have done this. I am greatful to her for believing in me and supporting me.

All the other members of committee, Drs. Steve Fetter, William Dorland and David Wright have been very generous in sharing their time and thoughts with me. I am thankful to all of them for their involvement in this thesis.

I am grateful to my family for not trying too hard to understand what I was doing or why. My parents and brother have been patient with my pursuits and for that I am thankful. My lovely wife, *Magee Ammu* is a constant source of love and intimidation. Without her constant warnings asking me to finish my dissertation and to find a real job this thesis would have arrived late. She deserves a great deal of appreciation for untethering me many a time from my work and helping me live a more fulfilling life. Without her the process of producing this thesis would have been very painful. I proclaim both my love and thanks to her as ordered.

Table of Contents

List of Tables v

List of Figures vi

1 Debating Space Security: Capabilities and Vulnerabilities 1

2 Operationally Responsive Space (ORS): Is 24/7 Warfighter Support Feasible? 10
2.1 PnPSat: Assembly, Integration and Test (AIT) Constraints 14
2.2 Launch Site Constraints 22
2.3 Launch Cost Constraints 26
2.3.1 Falcon Launcher 26
2.3.2 Pegasus Launcher 29
2.3.3 Minotaur Launcher 29
2.3.4 Taurus Launcher 30
2.3.5 Falcon SLV Launcher 31
2.3.6 Eagle Launcher 32
2.4 Evaluating TacSats 33
2.4.1 TacSat Orbit Optimization 35
2.4.2 FOR Constraints on Optimized Orbits 44
2.4.3 Tactical Performance of Optimized Orbits 51
2.4.4 Constellation of TacSats 58
2.4.5 Elliptical Orbits for Communications 59
2.4.6 The Futility of TacSats 65
2.5 ORS missions vis-a-vis DOD space programs 67
2.6 Conclusions 73

3 What Can be Achieved by Attacking Satellites? 76
3.1 Is There a Benefit to Attacking GPS Satellites? 78
3.2 Is There a Benefit to Attacking Reconnaissance Satellites? 93
3.3 Is There a Benefit to Attacking Communication Satellites? 101
3.3.1 Operation Desert Storm: Theater Communications Infrastructure 102
3.3.2 Operation Desert Storm: Theater Voice and Data Network . . 108
3.4 Conclusions 114

4 The Limits of Chinese Anti-Satellite Missiles 117
4.1 Conceptualizing an ASAT Missile Attack 120
4.2 Case I: Cone of Vulnerability 122
4.2.1 Physics of Cone of Vulnerability Simulation 123
4.2.2 ASAT Missile Guidance System 126
4.2.3 The Extent of the "Cone of Vulnerability" for a Zero-Lag Flight Control System 130
4.2.4 3^{rd} Flight Control System 133

4.2.5 The Extent of the "Cone of Vulnerability" for a 3^{rd} Flight Control System . . . 135
4.3 Case II: Head-On Collision . . . 139
4.3.1 Satellite Orbit Simulation . . . 140
4.3.2 Limits on Achieving a "Head-On Collision" . . . 141
4.4 Conclusion: The Limits of Chinese Anti-Satellite Missiles . . . 142

5 Satellites, Missile Defense and Space Security 148
5.1 Outline of the Chapter . . . 151
5.2 Evolution of STSS: "Holy Grail" for Missile Defense . . . 154
5.3 Modeling the Target Ballistic Missile . . . 157
5.3.1 Simulating the North Korean ICBM . . . 159
5.4 Modeling the Interceptor Ballistic Missile . . . 162
5.4.1 Determination of Interceptor Location . . . 163
5.4.2 Simulating the Interceptor Missile . . . 167
5.4.3 Interceptor Guidance System . . . 170
5.4.4 Simulation Results With Zero-Lag Interceptor Guidance System 174
5.4.5 Third Order Flight Control System . . . 177
5.4.6 Simulation Results With 3^{rd} Order Interceptor Guidance System 180
5.5 Sensors: Radar . . . 182
5.5.1 Determination of Radar(s) Location . . . 186
5.5.2 Simulation of Target ICBM RCS as Seen by the Radars . . . 191
5.5.3 Operating Parameters of the Radar . . . 193
5.5.4 Simulation of Target Position Data as Determined by the Radars 195
5.6 Sensors: Space Tracking and Surveillance Systems (STSS) . . . 202
5.6.1 Target ICBM IR Spectroscopy . . . 206
5.6.2 Focal Plane Array (FPA) requirements . . . 210
5.6.3 SNR for a QWIP FPA . . . 212
5.6.4 Simulation of Target Position Data as Seen by STSS . . . 216
5.7 Sensors: Kill Vehicle (KV) Sensors . . . 221
5.8 Simulation Results: STSS vs. Ground-based radars . . . 222
5.9 Conclusion: Satellites, Missile Defense and Space Security . . . 225

A Failure Causes and Test Requirements for Spacecraft 227

B Defining Field of Regard (FOR), Field of View (FOV) and Resolution 232
B.1 FOR and FOV . . . 232
B.2 Resolution . . . 236

C Validation of Ergodic Theory 238

D Effect of FOR Constraints on Optimized Orbits: *Jakarta* and *St. Petersburg* 240
D.1 *Jakarta*: Communication Mission Constraints . . . 240
D.2 *Jakarta*: ISR Mission Constraints . . . 241
D.3 *St. Petersburg*: Communication Mission Constraints . . . 244

D.4 *St. Petersburg*: ISR Mission Constraints 246

E Effect of FOR constraints Across Latitudes 248
E.1 100 NM (185 km) Altitude 248
E.1.1 Effect of FOR Constraint on Equatorial and Polar Regions . . 248
E.1.2 Effect of FOR Constraint on Mid-Latitude Regions 249
E.2 500 km Altitude 253
E.2.1 Effect of FOR Constraint on Equatorial and Polar Regions . . 253
E.2.2 Effect of FOR Constraint on Mid-Latitude Regions 254

F Operationally Responsive Space (ORS) Definitions and Stakeholders 258

Bibliography 261

List of Tables

2.1 Costs of Selected National Security TacSat Like Demonstration Missions 73

3.1 Percentage of Precision Munitions Used in Battle Operations 93
3.2 Total Reconnaissance Sorties, 17 January - 28 February 1991 94
3.3 1991 Gulf War Communications Effort 102

4.1 Assumed Properties of Chinese DF-21 ASAT Missile 123
4.2 Maximum Radial Reach of SC-19 ASAT Missile at Given Altitude (Zero-Lag Flight Control System) 131
4.3 Maximum Radial Reach of SC-19 ASAT Missile at Given Altitude (3^{rd} Order Flight Control System) 135
4.4 Spherical Coordinates for Target Satellite at a Given Time 141

5.1 Target Missile Properties: Peacekeeper Missile 159
5.2 Target Missile Dimensions: Peacekeeper Missile 159
5.3 Interceptor Missile Properties 163
5.4 Interceptor (IM-1) Siting Parameters (for ICBM targeting San Francisco) 166
5.5 Interceptor (IM-2) Siting Parameters (for ICBM targeting Washington D.C.) 168
5.6 Gain and Antenna Diameter for a Given Half-Power Beamwidth . . . 194
5.7 Radar Parameters 195
5.8 STSS Parameters 217

A.1 Factors in Establishing Space Vehicle Test Requirements 227
A.2 Spacecraft Components and Subsystems Failure Causes 228
A.3 Spacecraft Components and Subsystems Failure Causes 229
A.4 Spacecraft Qualification Test 230
A.5 Spacecraft Acceptance Test 231

B.1 Off-Nadir Capabilities of Private for-profit Satellite Systems 234
B.2 Examples of Spatial Resolution 237

C.1 Total Access Duration for 24 Hours 239

F.1 ORS Definitions 258
F.2 ORS Stakeholders 259

List of Figures

2.1 Spacecraft Discrepancy Distribution Spectrum 19
2.2 Spacecraft Subsystem Discrepancy Distribution Spectrum 20
2.3 On-Orbit Spacecraft Failures 21
2.4 CONUS Satellite Launch Facilities 24
2.5 Maximum Average Satellite Coverage (at HORIZON FOR) Over *Jakarta* (minutes per day) 38
2.6 Maximum Average Satellite Coverage (at HORIZON FOR) Over *Baghdad* (minutes per day) 39
2.7 Maximum Average Satellite Coverage (at HORIZON FOR) Over *St. Petersburg* (minutes per day) 39
2.8 HORIZON FOR Maximum Average Satellite Coverage From 100 NM (185 km) (minutes per day) 43
2.9 HORIZON FOR Maximum Average Satellite Coverage From 500 km (minutes per day) 43
2.10 Maximum Average Satellite Coverage Over *Baghdad* with a 5 Degree Above the Horizon FOR (minutes per day) 45
2.11 Maximum Average Satellite Coverage Over *Baghdad* with a 10 Degree Above the Horizon FOR (minutes per day) 46
2.12 Maximum Average Satellite Coverage Over *Baghdad* with a 45 Degree Off-Nadir FOR (minutes per day) 48
2.13 Maximum Average Satellite Coverage Over *Baghdad* with a 30 Degree Off-Nadir FOR (minutes per day) 48
2.14 Field of Regard (FOR) from 500 km 50
2.15 Average Pass Durations Per Satellite Pass 52
2.16 Daily Satellite Coverage at 100 NM (185 km) altitude 54
2.17 Daily Satellite Coverage at 500 km altitude 54
2.18 Number of Passes, Average Gap Time, and Cost Per Hour of Visibility for a TacSat at 100 NM (185 km) 55
2.19 Number of Passes, Average Gap Time, and Cost Per Hour of Visibility for a TacSat at 500 km 57
2.20 Approximate number of satellites required for 24/7 persistence at 100 NM (185 km) 59
2.21 Approximate number of satellites required for 24/7 persistence at 500 km 60
2.22 Average Contact Time vs. Argument of Perigee for MAJIC Orbit . . 62
2.23 Apparent Motion and Range of a MAJIC Satellite Over *Jakarta* (24 hours; 10 minutes interval) 63
2.24 Apparent Motion and Range of a MAJIC Satellite Over *Baghdad* (24 hours; 10 minutes interval) 64
2.25 Apparent Motion and Range of a MAJIC Satellite Over *St. Petersburg* (24 hours; 10 minutes interval) 65

2.26 Comparison between Original Cost Estimates and Current Cost Estimates for Selected Major Space Acquisitions Program 68
2.27 Total Number of Estimated Months from Program Start to Initial Launch 70

3.1 AOR - 2D Image 82
3.2 AOR - 2D Image (close-up) 82
3.3 Figure with caption indented on both sides and single-spaced. 83
3.4 AOR GDOP Pre-Attack (11 Mar 2012 00:00:00.000 UTCG to 13 Mar 2012 00:00:00.000 UTCG) 83
3.5 Facilities GDOP Pre-Attack (11 Mar 2012 00:00:00.000 UTCG to 13 Mar 2012 00:00:00.000 UTCG) 84
3.6 GPS Satellite Distribution (11 Mar 2012 00:00:00.000 UTCG to 13 Mar 2012 00:00:00.000 UTCG) 85
3.7 AOR GDOP Post-Attack (11 Mar 2012 00:00:00.000 UTCG to 13 Mar 2012 00:00:00.000 UTCG) 86
3.8 Facility 1 GDOP Post-Attack (11 Mar 2012 00:00:00.000 UTCG to 13 Mar 2012 00:00:00.000 UTCG) 87
3.9 Facility 7 GDOP Post-Attack (11 Mar 2012 00:00:00.000 UTCG to 13 Mar 2012 00:00:00.000 UTCG) 88
3.10 Facility 13 GDOP Post-Attack (11 Mar 2012 00:00:00.000 UTCG to 13 Mar 2012 00:00:00.000 UTCG) 89
3.11 Facility 19 GDOP Post-Attack (11 Mar 2012 00:00:00.000 UTCG to 13 Mar 2012 00:00:00.000 UTCG) 90
3.12 Facility 25 GDOP Post-Attack (11 Mar 2012 00:00:00.000 UTCG to 13 Mar 2012 00:00:00.000 UTCG) 91
3.13 AOR GDOP Post-Attack (11 Mar 2012 00:00:00.000 UTCG to 20 Mar 2012 00:00:00.000 UTCG) 92
3.14 Operation Desert Storm JSTARS Coverage 97
3.15 Desert Storm JSTARS Image During Left Hook Maneuver 99
3.16 Desert Storm JSTARS Image During Left Hook Maneuver 100
3.17 Desert Storm: Satellite Communication Architecture 104
3.18 Microwave Communications Relay Sites Providing Communications Link Between XVIII Airborne Corps and Rear Area 106
3.19 Desert Storm: Terrestrial Communication Architecture 107
3.20 Desert Storm: Terrestrial Communication Architecture (Close-up View) 107
3.21 USCENTAF Voice Network 109
3.22 ARCENT Command and Control Information Systems 111
3.23 USCENTAF TADIL Network 113

4.1 ASAT Missile Proportional Navigation Guidance System Diagram . . 127
4.2 SC-19 ASAT Missile: Cone of Vulnerability (Top View) 131
4.3 SC-19 ASAT Missile: Cone of Vulnerability (Top View) 132
4.4 SC-19 ASAT Missile: Cone of Vulnerability (Side View) 132
4.5 SC-19 ASAT Missile: Cone of Vulnerability (Side View) 133

4.6 SC-19 ASAT Missile: Cone of Vulnerability (Top View) 136
4.7 SC-19 ASAT Missile: Cone of Vulnerability (Side View) 137
4.8 SC-19 ASAT Missile: Cone of Vulnerability (Side View) 137
4.9 Zero-Lag Flight Control System ASAT Missile: Lateral Acceleration and Divert 138
4.10 3^{rd} Order Flight Control System ASAT Missile: Lateral Acceleration and Divert 139
4.11 Head-on Collision (0 Minutes After 0 Mean Anomaly Passage) 144
4.12 Head-on Collision (5 Minutes After 0 Mean Anomaly Passage) 145
4.13 Head-on Collision (10 Minutes After 0 Mean Anomaly Passage) . . . 146
4.14 Head-on Collision (12 Minutes After 0 Mean Anomaly Passage) . . . 147

5.1 ICBM Trajectories Targeting San Francisco and Washington D.C. . . 161
5.2 ICBM Velocity Profile 162
5.3 ICBM Track Direction 164
5.4 ICBM Track Direction with Possible Interceptor Missile Locations . . 165
5.5 Interceptor Proportional Navigation Guidance System Diagram . . . 170
5.6 Interception Geometry (San Francisco on left; Washington D.C. on right) 175
5.7 Height vs. Distance for Target ICBM and Interceptor (San Francisco on left; Washington D.C. on right) 175
5.8 Velocity for Target ICBM and Interceptor (San Francisco on left; Washington D.C. on right) 176
5.9 Acceleration of Target ICBM as Seen by the Interceptor Missile (San Francisco on left; Washington D.C. on right) 177
5.10 Lateral Divert Demands on the Interceptor (San Francisco on left; Washington D.C. on right) 178
5.11 Acceleration Experienced by Interceptor Missile (San Francisco on left; Washington D.C. on right) 178
5.12 Lateral Divert demands on the Interceptor (San Francisco on left; Washington D.C. on right) 181
5.13 Acceleration Experienced by Interceptor Missile (San Francisco on left; Washington D.C. on right) 182
5.14 RCS Calculation of Target ICBM at Various Stages 185
5.15 Possible X-Band Radar Locations 186
5.16 Average RCS for Various Azimuth Angles and Distances - San Francisco Trajectory 187
5.17 Average RCS for Various Azimuth Angles and Distances - Washington D.C. Trajectory 188
5.18 RCS of the San Francisco Bound Target ICBM 191
5.19 RCS of the Washington D.C. Bound Target ICBM 192
5.20 SNR for San Francisco Trajectory 196
5.21 SNR for Washington D.C. Trajectory 197
5.22 Radar-1 Position Error for San Francisco Trajectory 199
5.23 Radar-2 Position Error for San Francisco Trajectory 199

5.24 Radar-1 Position Error for Washington D.C. Trajectory 200
5.25 Radar-2 Position Error for Washington D.C. Trajectory 200
5.26 Fused Radar Position Error for San Francisco Trajectory 201
5.27 Fused Radar Position Error for Washington D.C. Trajectory 202
5.28 LWIR Tracking of Delta-II Launch Vehicle 204
5.29 ICBM (Boost-Phase) Plume Radiant Exitance at 1400^{o}K 207
5.30 Radiant Exitance of Sun at 5500^{o}K 208
5.31 Radiant Exitance of Earth at 300^{o}K 209
5.32 Radiant Exitance of Post-Boost ICBM at 200^{o}K 210
5.33 QWIP FPA wafers 212
5.34 Geometry between STSS satellites and target ICBM 218
5.35 STSS Position Error for San Francisco Trajectory 220
5.36 STSS Position Error for Washington D.C. Trajectory 220
5.37 STSS vs. Ground-based Radar Performance (San Francisco Trajectory) 224
5.38 STSS vs. Ground-based Radar Performance (Washington D.C. Trajectory) 224

B.1 Field of Regard (FOR) from 100 NM (185 km) 235
B.2 Field of Regard (FOR) from 500 km 235

C.1 Size and Extent of Baghdad as Used in the Orbital Propagator (11 Apr 2012 12:00:00.000 UTCG to 12 Apr 2012 12:00:00.000 UTCG) . . 239

D.1 Maximum Average Satellite Coverage Over *Jakarta* with a 5 Degree Above the Horizon FOR (minutes per day) 241
D.2 Maximum Average Satellite Coverage Over *Jakarta* with a 10 Degree Above the Horizon FOR (minutes per day) 242
D.3 Maximum Average Satellite Coverage Over *Jakarta* with a 45 Degree Off-Nadir FOR (minutes per day) 243
D.4 Maximum Average Satellite Coverage Over *Jakarta* with a 30 Degree Off-Nadir FOR (minutes per day) 243
D.5 Maximum Average Satellite Coverage Over *St. Petersburg* with a 5 Degree Above the Horizon FOR (minutes per day) 245
D.6 Maximum Average Satellite Coverage Over *St. Petersburg* with a 10 Degree Above the Horizon FOR (minutes per day) 245
D.7 Maximum Average Satellite Coverage Over *St. Petersburg* with a 45 Degree Off-Nadir FOR (minutes per day) 247
D.8 Maximum Average Satellite Coverage Over *St. Petersburg* with a 30 Degree Off-Nadir FOR (minutes per day) 247

E.1 HORIZON FOR Maximum Average Satellite Coverage From 100 NM (185 km) (minutes per day) 250
E.2 5 Degree Above the HORIZON FOR Maximum Average Satellite Coverage From 100 NM (185 km) (minutes per day) 251
E.3 10 Degree Above the HORIZON FOR Maximum Average Satellite Coverage From 100 NM (185 km) (minutes per day) 251

E.4 45 Degree Off-Nadir FOR Maximum Average Satellite Coverage From 100 NM (185 km) (minutes per day) 252
E.5 30 Degree Off-Nadir FOR Maximum Average Satellite Coverage From 100 NM (185 km) (minutes per day) 252
E.6 HORIZON FOR Maximum Average Satellite Coverage From 500 km (minutes per day) 255
E.7 5 Degree Above the HORIZON FOR Maximum Average Satellite Coverage From 500 km (minutes per day) 255
E.8 10 Degree Above the HORIZON FOR Maximum Average Satellite Coverage From 500 km (minutes per day) 256
E.9 45 Degree Off-Nadir FOR Maximum Average Satellite Coverage From 500 km (minutes per day) 256
E.10 30 Degree Off-Nadir FOR Maximum Average Satellite Coverage From 500 km (minutes per day) 257

List of Abbreviations

AC2IS	ARCENT Command and Control Information System
AAA	Antiaircraft artillery
ABCCC	Airborne Battlefield Command and Control Center
ABM	Anti-Ballistic Missile
AEHF	Advanced Extremely High Frequency
AGM	Air-to-ground guided missile
AIT	Assembly, Integration, and Testing
AOR	Area of Responsibility
APAM	Anti-personnel, anti-material
APS	American Physical Society
ARCENT	U.S. Army Central Command
ASAT	Anti-Satellite
ASOC	Air Support Operations Center
ATACM	Army Tactical Missile System
ATO	Air Tasking Order
AUTODIN	Automatic Digital Network
AUTOVON	Automatic Voice Network
AWACS	Airborne Warning and Control System
BDA	Bomb-damage assessment
BFT	Blue Force Tracking
BLIP	Background Limited Infrared Photo detection
BLOS	Beyond Line-of-Sight
BMD	Ballistic Missile Defense
C^3	Command, Control, and Communications
CAFMS	Computer-aided Force Management System
CALCM	Conventional Air-Launched Cruise Missile
CBU	Cluster Bomb Unit
CCAFS	Cape Canaveral Air Force Station
CENTAF	CENTCOM's Air Force component
CENTCOM	U.S. Central Command
CINC	Commander-in-Chief
CONUS	Continental United States
DAGR	Defense Advanced GPS Receiver
DIA	Defense Intelligence Agency
DMA	Defense Mapping Agency

DOD	Department of Defense
DOP	Dilution of Precision
DOT	Department of Transportation
DSMAC	Digital Scene Mapping Area Correlator
DSN	Defense Switched Network
DSP	Defense Support Program
EFOG-M	Enhanced Fiber Optic Guided Missile
FAA	Federal Aviation Administration
FOR	Field of Regard
FOV	Field of View
FPA	Focal Plane Array
FLIR	Forward-looking infrared
GAM	Global Positioning System Aided Munition
GDOP	Geometric Dilution of Precision
GMF	Ground Mobile Force
GPS	Global Positioning System
GWAPS	Gulf War Air Power Survey
HARM	High-Speed Anti radiation Missile
HEO	Highly Elliptical Orbit
IADS	Integrated Air Defense System
ICBM	Inter-Continental Ballistic Missile
INS	Inertial navigation system
IIR	Imaging infrared
IR	Infrared
ISR	Intelligence, Surveillance, and Reconnaissance
JDAM	Joint Direct Attack Munition
JFC	Joint Force Commander
JSOW	Joint Standoff Weapon
JSTARS	Joint Surveillance Target Attack Radar System
KKMC	King Khalid Military City
KV	Kill Vehicle
LANTIRN	Low-Altitude Navigation and Targeting Infrared for Night System

LEO	Low Earth Orbit
LGB	Laser-Guided Bomb
LOROP	Long-Range Oblique Photograph
MAJIC	Microsatellte Area-Wide Joint Information Communication
MARCENT	CENTCOM's Marine component
MARS	Mid-Atlantic Regional Spaceport
MDA	Missile Defense Agency
MLRS	Multiple Launch Rocket System
MTI	Moving Target Indicator
MUOS	Mobile User Objective System
MWIR	Mid-Wave Infrared
NASA	National Aeronautics and Space Administration
NAVCENT	CENTCOM's Navy component
NOAA	National Oceanic and Atmospheric Administration
NPOESS	National Polar-Orbiting Operational Environmental Satellite System
ORS	Operationally Responsive Space
ORSO	Operationally Responsive Space Office
PDOP	Position Dilution of Precision
PGM	Precision-guided munition
PnP	Plug and Play
PnPSat	Plug and Play Satellite
PPS	Precise Positioning Service
PTSS	Precision Tracking and Surveillance System
QWIP	Quantum Well Infrared Photo detector
RCS	Radar cross section
SA	Situational Awareness
SADARM	Sense and Destroy Armor Munition
SAM	Surface-to-air missile
SAR	Synthetic Aperture Radar
SBIRS	Space Based Infrared System
SEAD	Suppression of Enemy Air Defenses
SFW	Sensor Fuzed Weapon
SHF	Super High Frequency

SIGINT	Signal Intelligence
SLAM	Standoff Land Attack Missile
SLAM-ER	SLAM-Expanded Response
SLAR	Side-Looking Aperture Radar
SNR	Signal-to-Noise Ratio
SpaceX	Space Exploration Technologies Corporation
SPS	Standard Positioning Service
STSS	Space Tracking and Surveillance System
SWIR	Short-Wave Infrared
TACC	Tactical Air Control Center
TACS	Tactical Air Control System
TACP	Tactical Air Control Party
TADIL	Tactical Data Links
TARPS	Tactical Air Reconnaissance Pod System
TASM	Tomahawk Anti-Ship Missile
TBIP	Tomahawk Baseline Improvement Program
TERCOM	Terrain Contour Mapping
TFR	Terrain-following radar
THAAD	Terminal High Altitude Area Defense
TLAM	Tomahawk Land Attack Missile
U.S.	United States of America
USAF	U.S. Air Force
USCENTAF	U.S. Central Command Air Force
UTCG	Universal Coordinated Time - Gregorian Format
VAFB	Vandenberg Air Force Base
WGS	Wideband Global SATCOM

Chapter 1

Debating Space Security: Capabilities and Vulnerabilities

The recent debate on space security was primarily sparked by two assertions that emanated from the U.S. policy apparatus: (1) satellites and other space-based systems could be developed and used to obtain decisive warfighting superiority over an adversary, and (2) these space-based systems, because they might give such an inordinate advantage over any adversary, will be attacked.

The *Joint Vision 2010* issued by the U.S. Joint Chiefs of Staff in 1996 was the first policy document to outline a number of ambitious mission areas[1] where space-based systems could be utilized to significantly alter the status quo and give the U.S. armed forces a decisive advantage over an adversary. In 2001, the Rumsfeld Commission[2] extended the debate by claiming that U.S. military satellites, because they might provide an array of capabilities, would be considered an attractive target by adversaries. The Rumsfeld Commission in its report stated, "*If the U.S. is to avoid a 'space Pearl Harbor' it needs to take seriously the possibility of an attack on U.S. space systems. The U.S. is more dependent on space than any other nation. Yet the threat to the U.S. and its allies in and from space does not command the*

1. These mission areas were reiterated by the *Joint Vision 2020* document issued by the Joint Chiefs of Staff in 2010. The ambitious mission areas identified by these documents include[39, 40]: (i) Long-Range Precision Strike; (ii) Dominant Battlespace Awareness; (iii) Information Superiority; (iv) Dominant Maneuver; and (v) Full Dimensional Protection.

2. Formally, it was called Commission to Assess United States National Security Space Management and Organization and was headed by Donald Rumsfeld.

attention it merits."

The other key players influencing the debate, Russia and China, argue otherwise. They claim to be threatened by U.S. aspirations in space and deny that they pose any threat to U.S. space-based systems. They view the development of advanced military space systems by the U.S as evidence of a growing gap of military capabilities. Many Russian experts believe that U.S. activities in the military use of space are currently limited only by technological—not political—constraints[3]. It is assumed that the number of U.S. military space-based systems will grow with improvements in their technical characteristics and with their increased ability to operate as part of an extensive and well coordinated network[229]. A capability of this kind would introduce new uses of military force, and it is not yet understood how these would affect Russia's reliance on the strategic nuclear force that exist today. The resulting uncertainty is one of the reasons the Russian military is wary of the continued militarization of space, as it is unclear if Russia would be able to deal with the new situation.

Russian military officials are worried that Washington could eventually obtain the capability to launch a surprise missile attack in which space-based systems

3. From their perspective, the U.S. decision to expand capabilities into outer space represents the collapse of the Cold War political bargains[146]. In the years of the Cold War, satellites were given protected status due to their role as "national technical means" to verify arms control treaties and as early-warning systems of nuclear strikes. The 1971 Strategic Arms Limitation Treaty and the 1972 Anti-Ballistic Missile Treaty represented the first of several agreements to designate satellites as "national technical means" for treaty verification. Other agreements including, the 1971 Agreement on Measures to Reduce the Risk of Outbreak of Nuclear War committed the superpowers to consult immediately in the event of interference with communications or early-warning satellites and the 1971 Hot Line Modernization Agreement which specified the use of Soviet Molniya and American Intelsat satellites for crisis communication and committed both sides to ensure their continuous and reliable operation[144].

would be used both for striking Russian targets and blinding its command, control, communications, and reconnaissance networks. It is assumed that missile defense systems would operate in coordination with advanced satellite sensors to further weaken Russia's retaliatory potential. Russians do not discount the possibility of a disarming "bolt-from-the-blue" U.S. strike from space as Washington seeks undisputed, unilateral military advantages[154].

The Chinese have similar concerns about U.S. missile defense and space plans. Though not a party to the Anti-Ballistic Missile (ABM) Treaty, China has viewed it as a cornerstone of strategic stability and an important legal instrument for preventing the deployment of weapons in space. Even a limited missile defense system using advanced satellite sensors could in principle neutralize China's limited number of single-warhead ICBMs capable of reaching the U.S. A space enabled boost-phase missile defense system would be particularly threatening. Many Chinese fear that whether or not U.S. missile defenses are as effective as planned, decision makers could become incautious in their actions, willing to risk a disarming first strike because they believe they have the capability to intercept any surviving Chinese missiles[154].

This thesis is an attempt to analytically evaluate these various claims of capabilities and vulnerabilities made by the U.S., Russia, and China. This thesis will demonstrate that most of these concerns are overblown. Chapter 2: *Operationally Responsive Space (ORS): Is 24/7 Warfighter Support Feasible?* posits that obtaining decisive warfighting superiority using space-based systems is so difficult and costly that they might not be feasible. Chapter 2 will show that many of the

developments needed to achieve such warfigthing superiority have not been accomplished. The chapter arrives at this conclusion by systematically examining the four areas of innovation[4] that supporters of ORS propose will provide 24/7 dominant battlespace awareness[5]. The chapter demonstrates the infeasibility of succeeding in the four areas of innovation.

Chapter 3: *What Can be Achieved by Attacking Satellites?* evaluates the military benefits that could accrue to an adversary by attacking U.S. military satellites. Three types of target satellites were considered: GPS satellites, reconnaissance satellites and U.S. military communication satellites. This chapter makes the case that although U.S. armed forces rely extensively on their satellite infrastructure that does not immediately make them desirable targets. The functions performed by satellites like navigation, reconnaissance, and communications are diffused among large constellations. These constellation of satellites possess design redundancies that enable them to serve the U.S. armed forces even after some of them are lost. The GPS constellation is used to demonstrate this particular point by a simulation exercise. Also, some of the functions performed by these satellites can be substituted for by other terrestrial and aerial systems as observed in the case of reconnaissance missions. Even though these other systems will not completely compensate for lost satellites,

4. The four areas of innovation are: (1) Developing Plug and Play Satellite (PnPSat) manufacturing architectures to accelerate satellite design, development and manufacturing; (2) Innovating launch site operations to be able to rapidly and continuously launch satellite to create satellite constellations; (3) Developing cheap and operationally responsive launch vehicles ; and (4) Designing innovative satellite orbits to produce tactically mission relevant information that will give the U.S. warfighter an asymmetric advantage against his adversary.

5. For this chapter, 24/7 dominant battlespace awareness includes beyond line of sight (BLOS) signal intelligence (SIGINT); intelligence, surveillance, and reconnaissance (ISR); blue force tracking and situational awareness (BFT/SA); and continuous uninterrupted communications missions.

there is no analytical evidence that suggests the U.S. would be completely disabled if some of its military satellites are lost. For example, the communication architecture created during Operation Desert Storm in 1991 illustrates that the capability was spread across various satellites, terrestrial systems and self-sufficient radio relays. Disrupting satellite communications might momentarily affect U.S. capabilities but would also provide it with the legitimacy to escalate the battle as it desires. These factors should dissuade an adversary from attacking U.S. military satellite systems. While the threat to space assets ranks high among the threats that concern U.S. strategists, it need not follow that enemies of the U.S. will do so, or will invest in the weapons required to do so. The U.S. armed forces possess many important vulnerabilities that adversaries have opted not to attack in past conflicts, typically due to resources limitations, a desire to avoid escalation, or fear of the reaction of third party audiences. Moreover, it is quite possible that if a potential enemy did want to develop the ability to disrupt U.S. space functions, it could choose to do so in ways that would not involve targeting satellites[115].

The analysis in chapter 3 was conducted under the assumption that a potential adversary like China possessed the capability to attack a number of U.S. satellites simultaneously. Chapter 4: *The Limits of Chinese Anti-Satellite Missiles* demonstrates that anti-satellite (ASAT) intercepts are very complex under realistic conditions and that even a potential adversary with space capabilities comparable to China's has very limited potential, if any, to use ASATs in a real-world battle scenario. This chapter arrives at this conclusion by analytically evaluating the technical capabilities required of a missile to perform a direct ascent hit-to-kill anti-satellite

intercept. The evidence presented in the chapter will show that even under the ideal conditions of a non-varying orbit satellite as a target, the reach of a Chinese SC-19 ASAT missile is very limited. In the case of an ASAT engaging a satellite target emerging over the horizon in a "head-on collision"–which is a more appropriate real-world scenario–the capabilities of the SC-19 are insufficient[6]. To maintain a manageable miss distance, an ASAT attack has to be launched simultaneously as the emerging target is being tracked. However, doing so requires a continuous thrusting capability that would enable the ASAT to fly out and intercept the target satellite. The ASAT missile can, however, generate thrust only during its boosting phase. This limitation makes any real-world operational ASAT mission infeasible.

Given the arguments made in chapter 3 and 4, a more logical reaction for China would be to create its own system of military satellites to offset the advantages U.S. armed forces obtain from space-based systems. That would narrow the capability gap without having to resort to the extremely difficult task of a synchronized multi-satellite ASAT attack. There are indications that this is happening. In the period 1992–2002, China deployed both LEO and GEO weather satellites (the Fengyun series) as well as improved GEO communications satellites (the Dongfanghong-3 series) and recoverable satellites with varying payloads (the Fanhui Shi Weixing-2 series). Chinese earth observation capabilities also improved during this period. In

6. A target satellite at 800 km is traveling at approximately 7.5 km/s. In the three minutes of boost available to the SC-19 missile the satellite travels a distance of 1350 km. In the same three minutes the ASAT missile will have to travel to the altitude of 800 km and at the same time compensate for the 1350 km the satellite traverses using its lateral acceleration forces. The ASAT mission must accomplish this while starting from 0 km/s velocity and flying at a average velocity of approximately 5.42 km/s during its 3 minutes of boosted flight.

cooperation with Brazil, China in 1999 deployed the China Brazil Earth Resource Satellite (CBERS), its first electro-optical imaging satellite capable of beaming pictures directly down to Earth. China has subsequently launched several similar satellites without Brazilian involvement; these are known as the Ziyuan series to distinguish them from the CBERS satellites. In 2000, China became only the third country to deploy a navigational satellite system, launching two Beidou regional navigation satellites into GEO. China has also deployed a variety of additional satellites, including new remote sensing satellites (the Yaogan series), microsatellites such as the Shijian series, and improved versions of the Fengyun and Ziyuan series[53].

Finally chapter 5: *Satellites, Missile Defense and Space Security* evaluates the improvements that a futuristic satellite sensor, the Space Tracking and Surveillance System (STSS), would provide to missile defense systems. By modeling and simulating a boost-phase missile defense system cued by the advanced STSS sensors, this chapter demonstrates that although the STSS sensors reduce the intercept miss distances substantially it is still not good enough to enable a successful intercept of a solid-propellant target ICBM. However, it is possible that against a slow burning liquid-propellant target ICBM, the STSS satellite sensors could produce more accurate information needed to enable a successful intercept. The estimation of that possibility is left to future iterations of this work.

Together, chapters 2 through 5 aim to narrow the points of contentions in the debate on space security thereby fostering the international collaboration and data sharing needed to ensure safe operations in space. There is already a growing interest in such measures. The U.S. is seeking a direct line with Beijing–similar to

one recently established with Moscow–to prevent collisions and potentially destabilizing events in space. Washington has proposed a bilateral space security dialogue with China patterned after a U.S.-Russian forum that kicked off in mid-2010 and expanded last summer into a direct hotline connecting U.S. Strategic Command's Joint Space Operations Center (JSpOC) in California with the Russian Space Surveillance and System Command Center in Moscow.

Arguing for similar collaboration with China, Frank Rose, U.S. Deputy Assistant Secretary of State of Space and Defense Policy said, "JSpOC in California has direct contact with space operations centers throughout the world, as well as with commercial operators...so that when there's a close approach, they call companies or countries directly. We'd very much like a number to call in China,"[25]. Absent a direct line with Chinese space authorities, notifications of impending debris threats will be passed from JSpOC to the State Department, then to the Chinese Foreign Ministry. Such a case occurred about 18 months ago, when JSpOC detected a piece of space debris from China's 2007 ASAT test that was heading close to a Chinese satellite, Rose said. "At first, my initial reaction was, 'Why do we want to notify them? But then I caught myself and realized that if a piece of debris hit their satellite, then we'd have more debris threatening our own satellites, and that would not be in anyone's interest." He added, "As China continues their economic expansion, they will become ever more dependent on space systems, and that's one of the reasons why we want to talk with them[7]. We believe it's in the interest of all

7. Gen. William Shelton, the Air Force Space Command chief made a similar point recently saying, "Trying to watch traffic in every search volume in the 73 million cubic miles of space be-

nations not to have collisions in space[25]."

Ultimately, this mutual interest and the reduction in the perceived difference of interests as argued above should impel the U.S., Russia, China and other space-faring nations to negotiate an agreement on space activities in the future in line with contemporary challenges. In the interim to that agreement, the pressure to ensure safe and reliable satellite operations will force the major space players to create measures of selective cooperation and data sharing similar to those as articulated above between the U.S. Russia and China.

---

tween Earth's surface and GEO altitude, it's nigh on impossible." "So tell me before you're going to maneuver, tell me before you're going to launch, tell me before you're going to create some debris[197, 192]."

Chapter 2

Operationally Responsive Space (ORS): Is 24/7 Warfighter Support Feasible?

Operational Responsive Space (ORS) is a recently proposed project[1] for providing warfighters with uninterrupted 24/7 access to satellite-enabled services. As U.S. warfighters' areas of operation become larger in modern conflicts, and distributed operations become more the norm, deficits in the tactical[2] warfighters' ability to conduct beyond-line-of-sight (BLOS) signal intelligence (SIGINT); intelligence, surveillance, and reconnaissance (ISR); blue force tracking and situational awareness (BFT/SA); and continuous uninterrupted communications missions could become detrimental and dangerous[14]. ORS proponents claim that their project aims to eliminate these deficits and provide the war fighter with 24/7 SIGINT, BFT/SA and communications capability through the extensive use of tactical satellites (TacSats).

According to ORS supporters, TacSats will be designed and launched with

1. The Operationally Responsive Space (ORS) Office was established in May of 2007 in response to section 913 of the FY07 National Defense Authorization Act[236].

2. Tactical is used in this chapter with the understanding and intent as defined here: Tactical in reference to units are those of the size to operate independently for a short period of time and/or toward limited mission goals, in our case, units at or below Army Brigades. Tactical in reference to missions are those executed in a period that the unit tasked can operate autonomously without continuous resupply or control from higher headquarters. At the tactical level, battles and engagements are planned and executed to accomplish military objectives. Activities at this level focus on the ordered management and maneuver of combat elements in relation to each other and to the enemy to achieve combat objectives[113, 135].

the explicit aim of serving the field commanders' tactical needs as opposed to usual strategic missions that satellites serve[91, 139]. In the future, should a commander spontaneously require a possible satellite capability over a region or should an adversary take away a space capability from a JFC, he will be able to turn to the ORS office, and request replacement of that capability, and see that capability returned through TacSats within days or weeks rather than years[3][95]. TacSats are envisioned to provide direct real-time support to the commanders in the field in a "hyper-tactical" mode i.e., they can task, process data on-board, and downlink a required product to users all in one overhead pass[169]. A rough outline of how ORS proponents envision their TacSat capabilities could be used is listed below.

> *Unit X in-theater is not receiving the ISR data they need in a timely manner.*
>
> *Their U-2's and Global Hawks do not have access to the airspace, but they need*

3. Apart from aiming to satisfy the JFCs immediate needs, ORS also aims to address other users' needs for improving the responsiveness of space capabilities to meet national security requirements[166]. These aims of the ORS are to be accomplished in three varied time scales ranging from days to a year at maximum referred to as Tier-1, Tier-2, and Tier-3 operations. *Tier-1* uses existing or on-orbit capabilities to provide highly responsive space effects through the employment/modification/revised application of existing, fielded space capabilities. The targeted time period for application of Tier-1 solutions is **immediate-to-days** from the time at which the need is established. *Tier-2* solutions would utilize field-ready capabilities or deploy new or additional capabilities that are field-ready. The targeted time frame for delivering usable Tier-2 solutions is **days-to-weeks** from the time at which the JFC need is established. The focus of activities in Tier-2 solutions is on achieving responsive exploitation, augmentation, or reconstitution of space force enhancement or space control capabilities through rapid assembly, integration, testing, and deployment of a small, low cost satellite. *Tier-3* involves development of capabilities. In some cases, an expressed need may not be addressable through existing capabilities (Tier-1) or through the rapid deployment of field-ready capabilities (Tier-2). In such cases, ORS efforts must focus on the rapid development and deployment of a new capability. The goal for execution of Tier-3 approaches is **months-to-one year** from established need to presentation of operational capability. Achieving such a time line will be very challenging, and cannot be accomplished unless the amount of new development involved is very limited. Consequently, much of the ORS work will be anticipatory in nature-identifying the most probable emergent space needs and preparing the elements required (via S&T and development/acquisition) to ensure highly responsive delivery of needed capabilities.

to know what is over the hill. The wait for up-to-date ISR products could be days long and they don't have that kind of time. Luckily, their Modular Interoperable Surface Terminal (MIST), used to communicate with the U-2 and Global Hawk is also configured for communications with a Tactical Satellite (TACSAT) Common Data Link (CDL) radio that will be overhead in a matter of minutes. With the flip of a switch, Unit X now has a satellite command and control station at their fingertips. As the satellite comes over the horizon, the MIST will lock on to the satellite and provide direct commanding access to the war fighter. Now he can task the satellite for ISR collection overhead but only has a few minutes to do it. But with an interface as easy to use as Orbitz.com, tasking the satellite can be done very quickly. Now that the satellite has been tasked, all he has to do is sit back and wait—but not for long! In a matter of minutes, a high speed downlink begins and the image can be displayed on the computer right in front of him[125].

The question immediately arises: can this be done? At what expense? The stated goals of a generalized TacSat program as proposed in various open source documents by their supporters is to:

1. quickly launch the energy equivalent of a 1000 lbs payload into a 100 NM (185 km) circular orbit (or a combination of payload weight and operational altitude that is within the same energy capability)

2. keep it there for between six months and a year[4] to provide real-time persis-

4. This time period is derived from the average duration of conflicts the U.S. has been involved in recently including Vietnam, Grenada, Panama, Iraq, Yugoslavia, and Afghanistan[139, 100].

tent battlefield coverage for SIGINT, ISR, BFT and communication missions during the entire course of a tactical engagement

3. for an acquisition cost of about USD 20 million per satellite and booster combined

ORS supporters intend to achieve their envisioned capabilities within the constraints of the goals outlined above by innovating in four focus areas:

- Developing methods to accelerate satellite design, development and manufacturing. ORS aims to reduce satellite production time lines from years to months and in some cases to weeks. The aim is to create Plug and Play satellites (PnPSats) manufacturing architectures. PnP architectures will produce satellites that have a "standard" satellite bus that can be used to quickly tailor satellite capabilities in response to immediate war fighting needs[170]. Section 2.1 of this chapter will discuss the infeasibility of creating such manufacturing architectures cost efficiently within the desired time.

- Innovating launch site operations to be able to rapidly and continuously launch satellites to create TacSat constellations. The aim is to be able to launch and populate a complete constellation in a matter of days. Section 2.2 will discuss the difficulty for such rapid continuous launches.

- Developing cheap and operationally responsive launch vehicles to reduce and bring the cost of TacSat to within the reach of a tactical commander. Open source documents show that ORS supporters claim to meet an acquisition cost

of about USD 20 million per satellite and launch vehicle combined[5]. Section 2.3 will evaluate the feasibility of attaining these cost goals. That section will show that there is very little reason to believe that such cheap launchers would be available for ORS payloads.

- Designing innovative satellite orbits that can employ TacSats (in constellations) within the above cost restriction to produce *tactically* mission relevant information that will give the U.S. war fighter an asymmetric advantage against his adversary. Section 2.4 will evaluate the operational feasibility and limitations of TacSats.

In order to achieve the goal of ORS, all the above focus areas need to be satisfied at minimum. This chapter will demonstrate that is not the case.

2.1 PnPSat: Assembly, Integration and Test (AIT) Constraints

This section will discuss one of the principal conceptual innovations needed to realize ORS missions: the ability to rapidly manufacture a satellite. The ORS Tier-2 solution, for example, focuses on using space-qualified field-ready components and subsystems to rapidly assemble and manufacture a satellite. The targeted time frame for delivering usable Tier-2 solutions is days to weeks from the time at which the need is established (in contrast to years for regular satellite manufacturing).

5. This comparative cost metric for TacSats is pegged to not exceed the the operational cost to field a UAV mission. Suggested TacSat operational goal is to meet the costs of a deployed Predator team, consisting of UAVs and a control van. This was found to be approximately USD 25 million[139, 100, 99].

ORS proponents envision achieving this time frame by using a rapid satellite manufacturing facility, currently referred to as "Chileworks," that will function more like an aircraft depot with quick turn-around sortie rates, than a one of a kind satellite AIT facility[124, 151, 200].

In this Chileworks concept of operations, all spacecraft components/subsystems will be preordered, pretested and sitting on shelf to avoid long wait times. These components/subsystems along with the main spacecraft bus on which the components are assembled must have passed all qualification tests to be accepted into the Chileworks inventory. From this stock of fully qualified components/subsystems a Tier-2 spacecraft will be assembled. This assembled spacecraft will be rapidly tested, qualified and launched.

The Chileworks spacecraft assembling process would use a Plug and Play (PnP) design architecture where they would be connected to a spacecraft bus using a standardized mechanical interface such as a grid pattern of screw holes. All components will also be connected electrically to the spacecraft using a standardized electrical interface[15]. It should be noted that proponents of the concept have neither provided any prior examples of such rapid satellite manufacturing processes nor have they conducted and published any detailed analysis that examines the economics and feasibility of such an innovation. Irrespective of that, discussion in the ORS community has extended so far as to predict a industrial-like capability for the Chileworks concept. These predictions project that by 2015, Chileworks should have both a steady-state and surge capability, that is throttleable depending on the assessed level of threat. In the steady-state mode, it would be constantly active with

system testing and exercises to build competence and confidence. As the assessed need for satellite augmentation or reconstitution arises, increasing amounts of component stock would be brought into the Chileworks to support a space capability augmentation or reconstitution response so rapid that the war fighter truly retains assured access to space. At any given time, the Chileworks satellite manufacturing facility will be able to respond to a single time-critical need at a rate of one per week for first spacecraft, promising a full constellation response within a month[15].

A prime goal of the ORS mission is, however, immediately violated by this "Chileworks" concept: cost. To operationalize the Chileworks concept, new organizations would have to be created to train, exercise, and eventually conduct operations at such accelerated pace. Creating, staffing and funding such organizations and facilities would place a significant cost burden on ORS missions. AIT and launch personnel in a stand-by mode are necessary to rapidly respond to a need to build and launch a Tier-2 satellite. It will also be highly cost-intensive to maintain on hold the inventory and the workforce needed to achieve such PnP satellite time lines. Storage facilities must be adequate to maintain the desired storage life of the components, as certain components may require environmentally controlled facilities (clean rooms etc.) and special storage facilities (e.g., for batteries or propellants)[63]. Inventory management requires periodic assessment and update of inventory content and level, such as checking and testing of components and re-stocking components as necessary.

None of these factors are well defined, which creates a large uncertainty about the cost-effectiveness of Chileworks manufacturing[236]. Frequency of launch, num-

ber of satellites to be launched, satellite testing standards and requirement, and the level of modularity of satellite components influence the required Chileworks depot capacity and use of the depot (i.e., how often is the depot producing and launching Tier-2 satellites). Cost escalation beyond stated ORS goals (of USD 20 million per satellite and launch vehicle combined) immediately arise from the uncertainty in these variables.

Also underappreciated is the issue of AIT constraints that are involved in this concept (see figure A.1 in Appendix A on page 227 for a list of factors influencing AIT process). The entire AIT phase for a unique spacecraft can last many years and includes extensive qualification and acceptance tests. AIT is a documented, formal, and sequential process[6] of integrating and testing components/subsystems and the satellite system to verify if specifications and requirements are met. The spacecraft integration and test plan[7] includes tests/activities to identify unanticipated interactions among the subsystems, failure modes and recovery procedures, faulty workmanship, and component/subsystem infant mortality or failure. A list of possible failures is shown in figures A.2 and A.3 on pages 228 and 229 respectively in Appendix A.

The tests are designed to replicate the actual operational environment and scenarios. Vibration and thermal vacuum tests are designed to replicate the launch

6. The primary military standards that define spacecraft AIT programs are: MIL-STD-1540D Product Verification Requirements for Launch, Upper Stage, and Space Vehicles; MIL-STD-340 Test Requirements for Launch, Upper Stage, and Space Vehicles; and DOD-HDBK-343 Design, Construction, and Testing Requirements for One of a Kind Space Equipment.

7. Typical test plans are shown in figures A.4 and A.5 on pages 230 and 231 respectively in Appendix A.

and on-orbit environments, respectively. Other tests, like payload functionality tests, electromagnetic compatibility tests, and attitude determination and control subsystems tests, duplicate operational scenarios. When deviations or anomalies occur, discrepancy reports are written to identify the problem and facilitate a solution. As mentioned previously, the entire AIT phase for a unique spacecraft can last many years and includes extensive qualification and acceptance tests. The importance of a comprehensive AIT process at all levels of spacecraft assembly and manufacturing is illustrated in figure 2.1[8].

Almost one-third of spacecraft discrepancies occur at the system level where Chileworks intends to accelerate. Even if components and subsystems are pretested and readily available, it is still necessary to test the assembled spacecraft rigorously, unless there is a tolerance for high risk margin or multiple redundancies are present in the satellite. A similar restriction on rapid satellite AIT emerges from figure 2.2. The non-flight ground support equipment cause one-third of the total spacecraft discrepancies. The final spacecraft assembly and launch process involves significant interaction with support equipment, thereby necessitating a careful and lengthy process in the end stages of satellite assembly and launch. The Chileworks concept is in opposition to both these observations and there is no explanation by the supporters of ORS on how they intend to address these concerns.

Tosney, Arnheim, and Clark collected data on 454 satellites encompassing all

8. Weigel[13] studied 23,000 spacecraft discrepancies (from 224 spacecraft representing 20 different programs) as part of a MIT Lean Aerospace Initiative to arrive at the data displayed in figure 2.1 and figure 2.2.

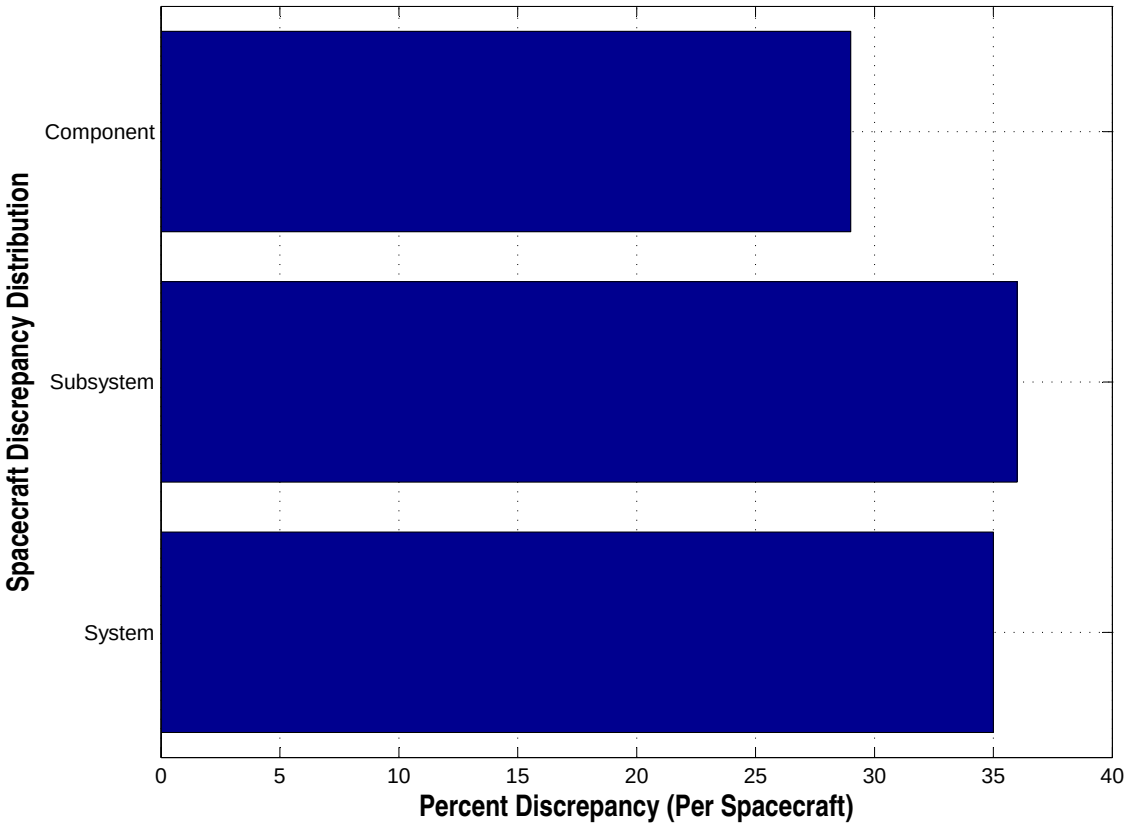

Figure 2.1: Spacecraft Discrepancy Distribution Spectrum[13]

U.S. manufactured satellites launched from 1980 to 1999 to correlate test thoroughness (ETTI[9]), design complexity, launch mass, and production sequence with on-orbit mission failures[209]. Strong correlation was found between on-orbit failures and ETTI (see figure 2.3): an exponential decrease in failures occurred as testing increased. This data again underscores the need for comprehensive testing. The data also suggests that as mass and complexity increased so does the number of

9. The Environmental Test Thoroughness Index is a qualitative technique to subjectively assign a measure of adequacy to spacecraft testing and qualification programs based on compliance with MIL-STD-1540.

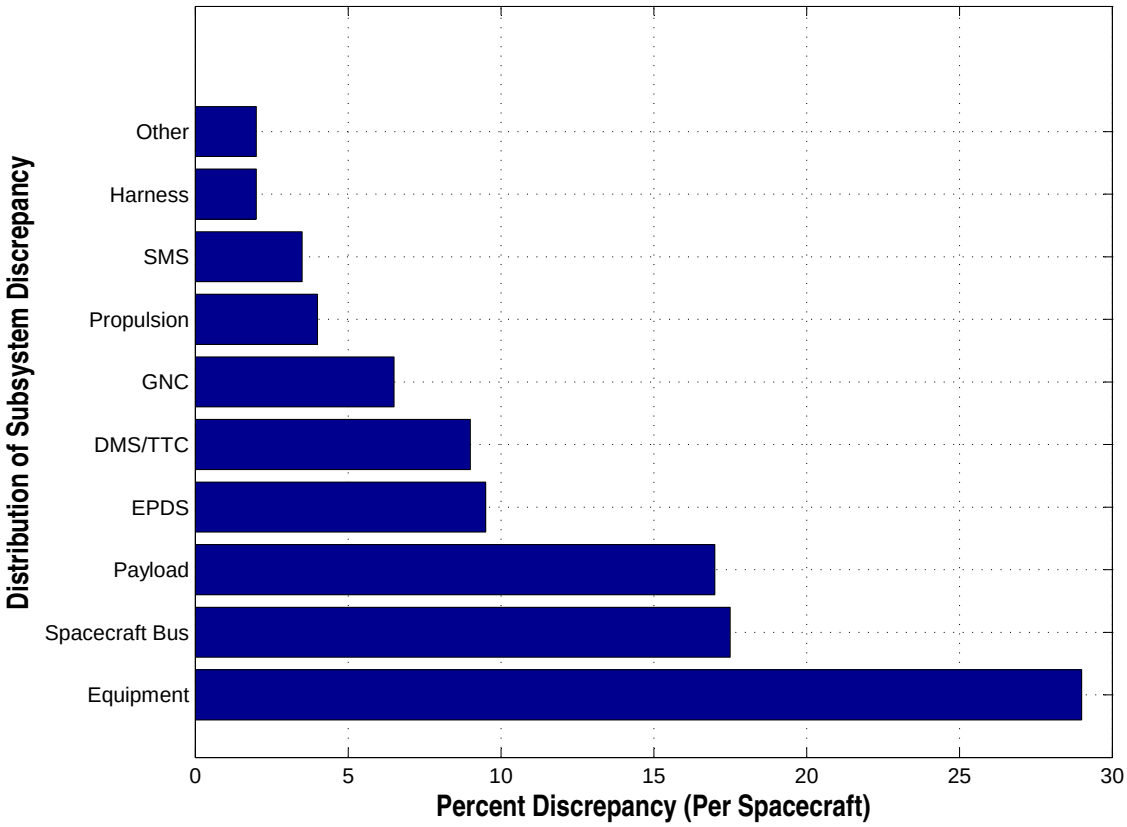

Figure 2.2: Spacecraft Subsystem Discrepancy Distribution Spectrum[13]

failures[10].

The Chileworks idea of accelerating spacecraft assembly, integration and testing by using pretested components/subsystems is poised against the standard industry practice. For a true Chileworks-like capability to materialize requires the satellite manufacturing industry to be on-board with the proposed standards and architectures. However, it is highly uncertain whether wide market acceptance of these standards and architectures could be achieved. There is initial industry reluctance

10. With the exception of lowest mass and complexity category; this outlying category is probably due to the experimental nature of most small satellites.

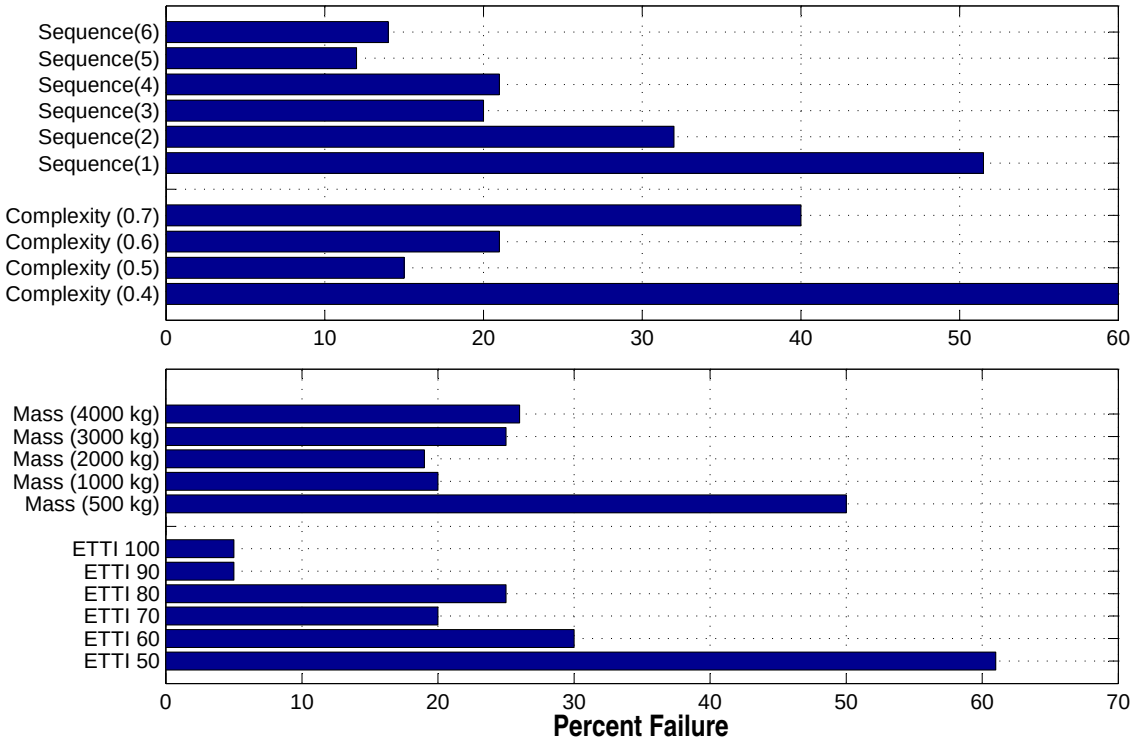

Figure 2.3: On-Orbit Spacecraft Failures[209]

because the business case is not clear. Adopting new standards and architectures requires industry (satellite manufacturers and suppliers) to make some initial capital investment, such as in new tooling and equipment, even though the return on the investment is unclear because of what still appears to be a low-volume satellite market.

Industry is concerned that the ORS market may never attain a sufficient volume to support standardization and PnP technology. Further satellite manufacturers are concerned about sustaining a competitive edge. They have their own

"standards" and other streamlining approaches that are often proprietary, which allows them to be competitive. Many bus standards and interface standards have been developed, but they have not achieved wide acceptance across the space industry.

In 2008 the Integrated Systems Engineering Team (ISET) completed development of bus standards that could be used to support a range of ORS missions. Industry members were key participants in the development. However, the progress in maturing these standards and gaining industry has been stagnant. The ISET business case team reported that a block buy would be necessary to realize any standardization and production benefits[236].

There has been only one attempt to achieve Chileworks-like spacecraft production timelines. The Air Force Institute of Technology conducted a trial of PnP satellite AIT in 2009 using the PnPSat-1[124]. Although the trial was able to attain AIT of the satellite within 24 hours, the process was undertaken in highly scripted and controlled conditions with a large proportion of standard tests eliminated. The PnPSat-1 was a smaller and less complex satellite than planned ORS Tier-2 satellites and most of its components were not flight qualified. Flight qualification would have been a hard requirement for any other spacecraft mission. There is no further evidence to suggest that the Chileworks concept can be attained.

2.2 Launch Site Constraints

Another hoped-for innovation of the Operationally Responsive Space (ORS) community is the ability to rapidly launch satellites in response to an immediate

tactical requirement. The aim is to launch satellites rapidly and continuously within a time line that must fit the joint force commander's mission requirements. Such rapid satellite launch operations have not been demonstrated to date. The launch facilities in the United States cannot readily accommodate quick-response vehicles. The Vandenberg Air Force base, one of the two major launch sites in the US, for example, has lengthy and detailed scheduling processes and strict safety measures for preparing and executing a launch, making it impossible to launch satellites within the tight time frames required for mounting constellation of satellites within weeks.

Processing at the launch site can alone take weeks to months depending on the size of the launch vehicle and spacecraft. Numerous stakeholders are involved in the entire process: the spacecraft manufacturer and customer, launch vehicle manufacturer, USAF, NASA, DOT (FAA), Coast Guard, and others. Extensive documentation, permits, launch clearances, frequency allocation, etc. are all required before a launch can occur. After a launch, maintenance and refurbishment of the launch pad is typically required and can take several days to weeks before another launch can occur[139]. Advocates of responsive launch capabilities do not address how these limitations will be overcome to attain the advertised timelines of ORS missions.

There are also constraints that emerge from the location and operational limitations of launch sites. Figure 2.4 shows the geographical location of various launch sites within CONUS; namely (1)Spaceport Florida at Cape Canaveral Air Force Station (CCAFS) (2)California Spaceport at Vandenberg Air Force Base (VAFB) (3)Mid-Atlantic Regional Spaceport (MARS) at Wallops Island, Virginia and (4)Ko-

diak Launch Complex on Kodiak Island, Alaska[74, 75, 163]. All of these launch sites have limitations of launch corridor to avoid direct overflight over populous regions. These limitation have a significant effect on ORS operations. For example, none of the eastern or western launch sites in CONUS have the capability to launch directly into a 63.4 degree inclination[11] that is a strict requirement for operating the elliptical MAJIC orbits that are proposed by TacSat supporters[12].

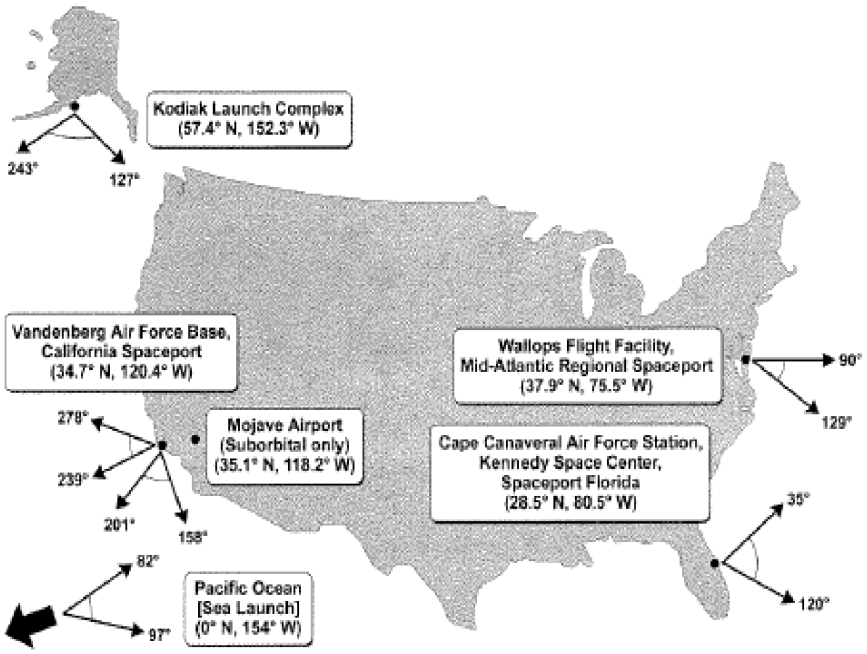

Figure 2.4: CONUS Satellite Launch Facilities

11. Doing so require the launch vehicle and boosters to make a low-altitude pass over populated land mass posing an unacceptable risk to these areas should the launch vehicle fail.

12. To achieve maximum coverage over a region of interest from a MAJIC orbit the angle of inclination needs to be fixed at 63.4 degrees to prevent the location of perigee/apogee from moving. The earth is not perfectly spherical. This imperfection causes several orbital perturbations including the rotation of the perigee and apogee of an orbit. By placing the MAJIC orbit at an inclination of 63.4 degrees this rotation is prevented.

Current launch infrastructure at the various spaceports around the country are often unique and designed around a given vehicle architecture. Facility and infrastructure accommodations for a new architecture tend to take considerable time, on the order of several years. ORS aims to use high-risk low-cost launch vehicles assembled, tested and launched at an accelerated pace. That idea goes against established paradigms and thereby precludes the sharing of existing facilities and infrastructure without significant ground infrastructure investment or costly insurance arrangements[33]. SpaceX Falcon launchers, a candidate low cost ORS launcher, have experienced such difficulties. SpaceX's launch of TacSat 1 at Vandenberg was put on hold when because of the potential risks it posed to a billion-dollar satellite that was waiting to be launched from a nearby pad. The Air Force had licensed the use of another nearby pad at Vandenberg to a contractor for large-scale launches. Given the proximity of launch pads, SpaceX's insurance premium increased ten-fold, from about USD50,000 to as much as USD500,000. Because of these issues, SpaceX decided to use the Reagan Test Site facility on Kwajalein Atoll, in the Pacific Ocean for its first launch[75]. The potential effect of such launch site constraints or the need to transport satellite to distant locations on ORS mission cost has not been documented and addressed by ORS supporters. It seems fair to conclude that these constraints would push ORS mission costs above the stated goals of USD 20 million per satellite and launch vehicle combined.

2.3 Launch Cost Constraints

In order to be cost competitive with UAVs for performing the same mission, ORS supporters want to to achieve an acquisition cost of about USD 20 million per satellite and launch vehicle combined[13]. However, all potential responsive launch vehicles alone currently cost close to or more than the USD 20 million for launches to LEO, essentially limiting all possible responsive spacelift systems to LEO. Satellites launches to higher orbits require larger, more complex and expensive boosters for launch. This section will discuss the status of various responsive launch vehicle candidates, their anticipated cost and their ORS mission feasibility.

2.3.1 Falcon Launcher

Name: Falcon[14] 1, 1e, 5, & 9.

Developer: Space Exploration Technologies Corporation (SpaceX)

Class: Partially Reusable

Description[179, 75, 72]: The partially reusable Falcon 1 is a two stage, liquid

13. The comparative cost metric for TacSats is to not exceed the the operational cost to field a UAV mission. Suggested TacSat goal is to meet the costs of a deployed Predator team, consisting of UAVs and a control van. This was found to be approximately USD 25 million[139, 100, 99].

14. At the end of 2002 DOD directed the Air Force and DARPA to combine their individual projects on hypersonic research into a common program. The resulting joint program was called Force Application and Launch from Continental US (FALCON), which consisted of two components: (1) Small Launch Vehicle (SLV): develop a low-cost, quick-response booster, which could launch small payloads into orbit, suborbit, or potentially launch hypersonic technology vehicles, and (2) Hypersonic Technology Vehicles (HTV): develop conceptual design, demonstrate technology, and flight test a low-risk first generation hypersonic technology vehicle. In 2004, the global strike or force application component of DARPA's FALCON project was canceled and "FALCON" was subsequently renamed "Falcon". Adding to the confusion, two of Project FALCON Phase IIa developers used the name "Falcon" for their launch vehicles: (1) SpaceX and its Falcon boosters (2) Lockheed Martin and its Falcon SLV hybrid rocket.

oxygen and rocket grade kerosene powered launch vehicle designed to place up to 670 kilograms (1,477 pounds) into LEO. The first stage of this vehicle is to be recovered from the ocean after a parachute landing, refurbished, and reused. The Falcon 1 achieved orbit on its fourth attempt, on 28 September 2008, with a mass simulator as a payload. On 14 July 2009, Falcon 1 successfully delivered the Malaysian RazakSAT satellite to orbit on SpaceX's first commercial launch (fifth launch overall). Following its fifth launch, the Falcon 1 was retired in favor of an enhanced variant, the Falcon 1e. The Falcon 1e consists of a new first stage, the same second stage used on the Falcon 1, and a new, larger payload fairing. Falcon 1e's payload capacity is 1,010 kilograms (2,200 pounds) into LEO.

Falcon 5 was based on much of the same technology developed for Falcon 1; the larger Falcon 5 was supposed to use five SpaceX-developed Merlin engines in the first stage with an engine-out capability to enhance reliability. Falcon 5 has been replaced by Falcon 9. Falcon 9 is a spaceflight launch system that uses rocket engines designed and manufactured by SpaceX. Both stages of the two-stage-to-orbit vehicles use liquid oxygen (LOX) and rocket-grade kerosene (RP-1) propellants. Multiple variants are planned with payloads of 10,450 to 26,610 kilograms (23,000 to 58,700 pounds) to LEO, and 4,450 to 15,010 kilograms (9,800 to 33,100 pounds) to geostationary transfer orbit, which will place the Falcon 9 design in the medium-lift to heavy-lift range of launch systems.

The first Falcon 9 flight was successfully launched from Cape Canaveral Air Force Station on June 4, 2010 with a successful orbital insertion, after several delays. The Falcon 9 is the launch vehicle for the SpaceX Dragon spacecraft. The Falcon 9

and Dragon combination won a Commercial Resupply Services (CRS) contract from NASA to resupply the International Space Station under the Commercial Orbital Transportation Services (COTS) program. The second Falcon 9 launch, and the first launch of the Dragon spacecraft, occurred at on December 8, 2010 from Cape Canaveral. The launch was successful, with the Dragon spacecraft completing two orbits before splashing down in the Pacific Ocean.

Recently, on May 22, 2012 Falcon 9 successfully flew the Dragon spacecraft for its first ISS resupply mission. SpaceX has a launch manifest of over 40 launches, including the space station resupply and the Iridium constellation. At the end of this launch volume there should be sufficient data to establish the reliability and price of SpaceX launch vehicles. However, all of these launches are for the heavy-lift Falcon 9 launcher. From the perspective of TacSat missions this is of little direct consequence, since for the TacSat missions Falcon 1e is the appropriate launcher. It is, however, possible that SpaceX might be able to subsidize some of the costs of its Falcon 1e launcher from the profits of its Falcon 9 launcher and Dragon spacecraft missions.

Assessment: Viable. Falcon 1e has a quoted cost of USD 10.9 million for a payload of 1010 kg and Falcon 9 has a quoted cost of USD 54 million to USD 59.5 million. The company owner, Elon Musk, is investing his own money into building a technically viable launch family. He plans to sell these vehicles for a price far below his competition. There is still queries among the aerospace community whether the advertised launch prices will last.

2.3.2 Pegasus Launcher

Name: Pegasus XL

Developer: Orbital Sciences Corporation

Class: Expendable

Description: Pegasus was specifically developed to orbit small satellites weighing up to 1,000 pounds into low-Earth orbit. It is a winged, 3 stage expendable booster. The launch vehicle is carried aloft by an L-1011 carrier aircraft to approximately 40,000 feet over open ocean, where it is released and then free-falls in a horizontal position for five seconds before igniting its first stage rocket motor.

Assessment: Viable. Pegasus is expensive (USD 20 to 24M) but is the launcher of choice for small payloads. Unless SpaceX can deliver a cheap small launcher, Pegasus will continue to be the primary U.S. small launcher[179, 75].

2.3.3 Minotaur Launcher

Name: Minotaur[173]

Developer: Orbital Sciences Corporation

Class: Expendable

Description: Minotaur was developed for the USAF Orbital/Suborbital Program as a low-cost, four-stage vehicle using a combination of government-supplied surplus Minuteman II intercontinental ballistic missile motors and existing technologies. Proposed growth versions would use surplus Peacekeeper rocket stages. Minuteman

motors serve as the first and second stages while the third and fourth stages, structures, and payload fairing are from Orbitals Pegasus XL rocket[179, 75]. Several derivatives of Minotaur were developed or proposed:

- Minotaur I can deliver a payload of 580 kg to a 185 km, 28.5 degree orbit from Cape Canaveral; or 310 kg to a 740 km sun-synchronous orbit from Vandenberg.
- Minotaur IV can deliver a payload of 1720 kg to a 185 km, 28.5 degree orbit from Cape Canaveral; or 1000 kg to a 740 km sun-synchronous orbit from Vandenberg.
- Minotaur V can put small spacecraft on high-energy trajectories, such as GTO, HEO, and lunar with a Star 48V fourth stage and Orion 38 fifth stage. For example, it can place 560 kg to a geosynchronous transfer orbit (GTO).

Assessment: Viable. Minotaur has been successful, but is limited to Government payloads. The Minotaur is not very cheap, costing between USD 15-20 million.

2.3.4 Taurus Launcher

Name: Taurus

Developer: Orbital Sciences Corporation

Class: Expendable

Description: The Taurus was developed under DARPA sponsorship for easy transportability and rapid set-up and launch. Since 1994, it has conducted six of seven

successful missions launching 12 satellites for commercial, civil, military, and international customers. The vehicle is a ground-based variant of the Pegasus rocket. The four-stage, all solid propellant vehicle can deploy 1,350 kg (3,000 lbs) to LEO. Two fairing sizes offer the option of single or multiple payloads[179, 75]. Taurus uses horizontal integration of the upper stages and offline encapsulation of the payload within the fairing to expedite integration.

Assessment: Viable. Taurus is successful, but is not cheap, costing between USD 25 and USD 30 million a launch.

2.3.5 Falcon SLV Launcher

Name: Falcon SLV

Developer: Lockheed Martin

Class: Expendable

Description: One of the four DARPA Force Application and Launch from CONUS (FALCON) Phase 2a contracts to develop concepts for a low-cost (USD 5M) small launch vehicle. Falcon SLV approach uses an all-hybrid propulsion approach and a mobile launch system. Lockheed was not selected to continue in the Phase 2b of the FALCON project[179, 75].

Assessment: Not likely to be viable. Lockheed conducted several test firing of its new hybrid rocket. Hybrid rocket technology is estimated to be more expensive than conventionally fueled rockets. Lockheed was not selected to continue in Phase

2b of the FLACON project. While a competitor in FLACON 2a, Lockheed test fired its engine several times but never developed integrated rocket plans. A hybrid rocket has issues with environmental impact and does not have the performance of cryogen propellants.

2.3.6 Eagle Launcher

Name: Eagle SLV (Scorpius)

Developer: Microcosm, Inc.

Class: Expendable

Description: Part of the Scorpius family of expendable launch vehicles, marketed for suborbital and orbital missions. Microcosm, Inc. the developer plans to eventually market up to eight Scorpius variants: two suborbital vehicles, the SR-S and SR-M launchers; three light-lift orbital vehicles, the Sprite Mini-Lift, the Eagle SLV, and the Liberty Light-Lift launchers; one intermediate-lift orbital vehicle, the Antares Intermediate-Lift launcher; one medium-lift vehicle, the Exodus Medium-Lift launcher; and one heavy lift vehicle, the Space Freighter. Each Scorpius variant is based on a scalable modular design featuring simple liquid oxygen, kerosene pressure-fed motors without turbo pumps and with low-cost avionics equipped with Global Positioning System internal navigation. Microcosm was one of the FALCON Phase 2a contractors but was not selected for further work[179, 75].

Assessment: This system is not currently viable. Microcosm is a small company

surviving largely on small business study contracts. They launched two suborbital rockets in the past (SR-S and SR-XM-1). However, the Scorpius family is designed around an inappropriate technology: pressure-fed liquid propulsion. The structure mass has to be strengthened to accommodate high pressure. Because the performance is so poor, there are not any currently operational launch vehicles that use this technology for their main stage. The vehicles cannot compete in the marketplace.

All of the potential responsive launch vehicles discussed above are beyond the cost margin of ORS with the possible exception of Falcon 1e. However, even that launch vehicle costs approximately 50 percent of the cost budget of one ORS TacSat raising questions on its utility for ORS missions. Given the current launcher market, it would be extremely difficult to execute ORS missions without exceeding the cost constraints significantly. Proponents assert that launch costs would come down once the demand for launch services had increased substantially, but this claim has been made for decades and is yet to be demonstrated in practice.

2.4 Evaluating TacSats

This section will evaluate TacSats, their orbits, and their utility to the tactical war fighter. The evaluation will test if suggested SIGINT, ISR, BFT and communication missions can be achieved by designing innovative satellite orbits that can employ TacSats (in constellations) within the above cost restriction to produce *tactically* mission relevant information that will give the U.S. war fighter an asymmetric

advantage against his adversary.

Subsection 2.4.1 below will begin the evaluation by outlining the analytical method used to optimize a TacSat for coverage over a particular region of interest. This optimization is initially performed for the ideal case of a satellite with no sensor constraints. The next subsection 2.4.2 on page 44 will then impose the real-world sensor constraints like minimum elevation angle or maximum off-nadir imaging angle to the analysis. This process will normalize the optimized TacSat orbits to realistic conditions. The maximum average daily coverage over the region of interest will be numerically determined using the analytical method in this subsection. Then in subsection 2.4.3 on page 51 more mission relevant parameters like satellite pass duration, gap time between passes, etc., will be estimated for the optimized orbits.

Subsection 2.4.4 on page 58 will progress from the previous subsection and estimate the number of satellite needed to obtain 24/7 coverage over the region of interest for the various missions. It will shown that an unrealistically large number of satellites will be needed to obtain 24/7 communication or ISR coverage over a region of interest when employing TacSats. Finally, subsection 2.4.5 on page 59 will evaluate TacSats operating in Highly Elliptical Orbits (HEO) called MAJIC (Microsatellite Area-Wide Joint Information Communication Orbit), which are the suggested orbits to accomplish communication and BFT missions for the tactical war fighter using fewer satellites[170, 63, 97, 30]. This subsection will discuss the difficulties of realizing the MAJIC orbits.

All the subsections outlined above will in sequence demonstrate that even if the cost and timeline requirements of the TacSat concept are met, there are oper-

ational limitations emerging from orbital mechanics that make the idea of TacSats unrealistic. A combination of *physical constraints* placed on satellites by orbital mechanics and *operational requirements* placed on their payloads by the mission that can be performed from space prevent all but the most rudimentary missions from being attainable.

2.4.1 TacSat Orbit Optimization

TacSats by their definition require optimizing for a specific location, perhaps a city or a small region of a country, but most definitely not for continental or global coverage. Therefore, the first step in evaluating TacSats is to determine how to optimize a TacSat's orbit for maximum coverage over the region of interest. This subsection will outline that process of optimizing a single satellite[15] for tactical operations i.e., maximize the contact time over a specific city/region at a particular latitude. The optimization is initially performed assuming a TacSat sensor with a horizon Field of Regard (FOR)[16] with no constraints. The next subsection will impose satellite sensor FOR constraints[17].

TacSat orbit optimization is done by numerically estimating the average long-

15. Satellite constellations will be examined later.

16. The Field of Regard (FOR) of a satellite is the total extent of *"the area of Earth that can be covered by its sensor by altering the satellite orientation (in space)."* Satellites are never able to operate in their entire FOR. Satellites operate in a much narrower Field of View (FOV) which is *"the area of Earth that a sensor has coverage over at any moment without moving its sensor."* More explanation on FOR and the distinction between FOR and FOV is detailed in Appendix B.

17. The missions of a satellite dictates the FOR constraints that is imposed on it. For example, in order to operate without interference communication satellites have a 5/10 degree above-the-horizon FOR requirement. Similarly, ISR satellites have a 45/30 degree off-nadir FOR constraint in order to capture images with sufficient resolution.

term contact time over the latitude of interest[18] and then interpolating for the averaged maximum per-day satellite coverage over the target location in that latitude. The optimization is accomplished by applying the concept of ergodic theory[19] to satellite orbit coverage analysis [137, 138]. Using ergodic theory, a definite integral is obtained that gives the average view period of a ground location from a spacecraft in orbit. This method avoids the propagation of the orbit, which requires a lot of time and computation resources, and simplifies the computation of satellite coverage[20]. Lo[138] applying ergodic theory defines the long-term coverage ρ as

$$\rho = \lim_{T \to \infty} \frac{P(T)}{T} = \int_{\phi_1}^{\phi_2} g(\phi) h(\phi) d\phi \tag{2.1}$$

where

$$g(\phi) = 2\,(acos[(\cos\beta_0 - \sin\phi \sin\phi_0)/\cos\phi_0 \cos\phi])$$

$$h(\phi) = \cos\phi/(2\pi^1\sqrt{\sin^2 i - \sin^1\phi})$$

18. For a generalized optimization study, we are not interested in the exact day-to-day times that a particular satellite will be overhead. Instead, our true interest lies in the long-term average contact time of the satellite with the target location latitude. As TacSat proponents intend the satellites to have a life of six months to a year, this study will perform satellite optimization for a period of one year. The Long term average calculations mean that we really only need to specify the latitude of the target; all longitudes crossing the specified latitude will have the same long term average contact times due to the symmetry of the Earth. Symmetry also implies that northern and southern latitudes will have the same long-term average contact times.

19. Ergodic theory studies the statistical behavior of the solutions of differential equations.

20. Ergodic theory optimizes the coverage over a single point on the ground at a latitude of interest. This raises the question of accuracy. In reality, operations are conducted over a finite area of the size of a city. How does this affect the results of this paper? Not much in reality. Appendix C will show that the difference in coverage durations obtained from simulating a orbit coverage over the city of Baghdad and obtained from applying ergodic theory are trivial and does not affect the validity of the results as applied in this chapter.

$$\phi_0 = station latitude\ latitude$$

$$\beta_0 = station\ mask\ angular\ radius$$

$$i = satellite\ inclination$$

P(T) in equation 2.1 is the total time the satellite has coverage over the target latitude from time 0 to time T. Implying, ρ is the fraction of time the satellite has coverage over target latitude.

Of the four variable parameters in equation 2.1 (orbital altitude, orbital inclination, satellite FOR, and target location) for TacSat orbit optimization, there is real flexibility in only two. The analysis in this subsection is done assuming the TacSat is able to perform its mission from a horizon FOR. Once the satellite FOR and target location (i.e., latitude) are chosen, only the satellite's inclination and altitude can be varied to determine the maximum coverage. Figures 2.5, 2.6 and 2.7 below plot the maximum average daily contact time a single TacSat with a horizon FOR would have over three cities at different latitudes:

1. *Jakarta*, Indonesia (6 deg south latitude)

2. *Baghdad*, Iraq (33 deg north latitude)

3. *St. Petersburg*, Russia (60 deg north latitude)

These cities were chosen to give representative samples across southern and northern hemisphere and between low, mid, and high latitudes. Altitudes are varied between 150 km to 600 km; the lower limit is where the atmosphere becomes thick enough to bring a satellite down in a matter of several days and the upper limit is somewhat

around the published value for the funded TacSat programs. Inclinations are varied between zero degrees (equatorial orbits) and 105 degrees (sun synchronous orbits).

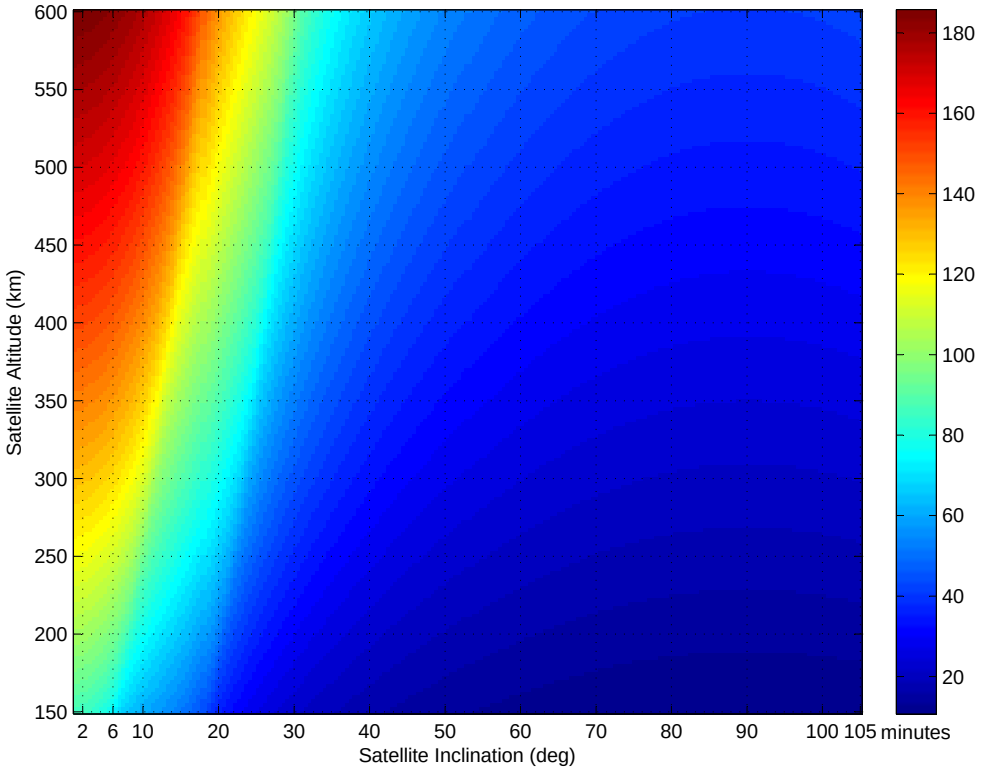

Figure 2.5: Maximum Average Satellite Coverage (at HORIZON FOR) Over *Jakarta* (minutes per day). The sidebar graph key denotes the maximum minutes of coverage per day over Jakarta for a given satellite inclination (x-axis of the graph) and satellite altitude (y-axis of the graph).

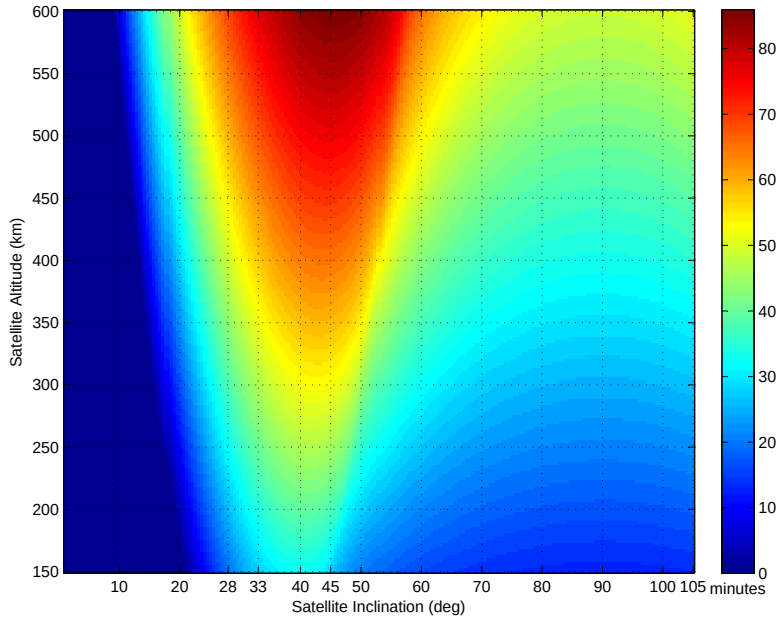

Figure 2.6: Maximum Average Satellite Coverage (at HORIZON FOR) Over *Baghdad* (minutes per day)

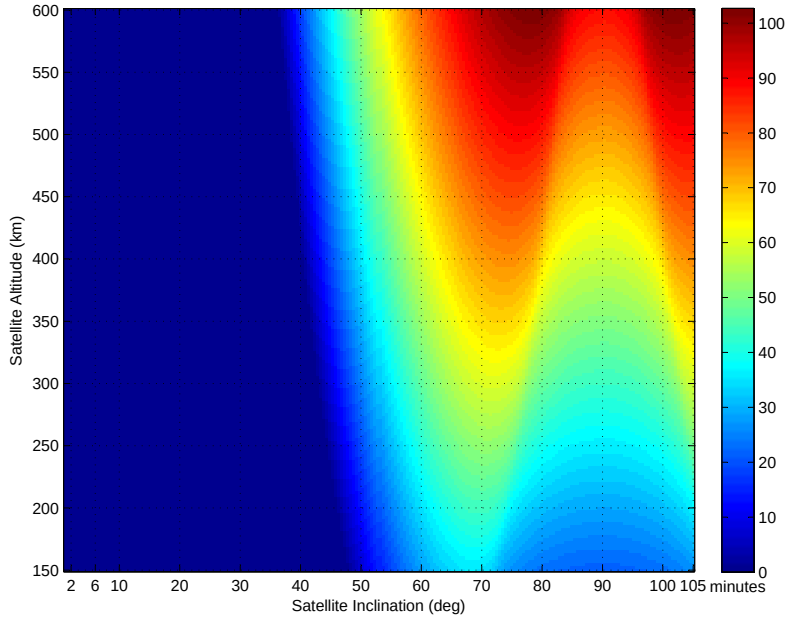

Figure 2.7: Maximum Average Satellite Coverage (at HORIZON FOR) Over *St. Petersburg* (minutes per day)

From the plots above the following inferences can be made:

Inference 2.1 *There is a certain orbital inclination that, for any given altitude, maximizes average daily contact time*[21]*. In most cases, this optimal orbital inclination will be slightly larger than the target's latitude* [22]*. For example, on examining figure 2.6 on page 39 it becomes clear that for a given satellite altitude as the satellite inclination increases from 0 to around 33 degrees (the target latitude of Baghdad) the coverage goes from 0 minutes to a value close to the maximum; it reaches maximum at a slightly larger inclination than 33 degrees*[23]*. Furthermore, as the satellite inclination continues to increase the coverage duration starts to taper off. The same phenomenon can be observed in the case of Jakarta and St. Petersburg.*

Inference 2.2 *As a direct consequence of the first inference it becomes apparent that to optimize contact time, the inclination of the TacSat orbit should be higher than the latitude of the target. As a corollary, no satellite can be optimized for more than one target latitude. For example, observe that in figure 2.6 at the given satellite*

---

21. It should be noted that there might be a single day where the coverage exceeds this value; however, on average this is the maximum daily coverage that can be obtained from the satellite for the given altitude and inclination. This coverage is not obtained in a single orbital pass but is the averaged value of the cumulative coverage from multiple passes over the target latitude over a period of one year. It will be shown later that the duration of each pass and time gap between each pass is different.

22. The only case for which it is exactly equal to the target's latitude is for the theoretical case of a zero altitude orbit. As the satellite altitude increases above zero, the optimal inclination moves further away from the target's latitude, the magnitude of the shift being directly related to the size of the FOR. The reason the optimum inclination is generally larger than the target latitude is that the actual path the target location appears to trace through the FOR is not a straight line but instead a curve concave toward the equator. Also, there are more opportunities for access when inclination is greater than target latitude due to curvature of the Earth and longitude compression [180].

23. In fact there is analytical evidence that for mid-latitude regions, the optimal inclination is approximately equal to the target latitude plus 2 degrees for each 100 km increase in the altitude of the satellite[23].

inclination of 33 degrees the coverage drastically drops off for all latitudes not close to 33 degrees. It is, of course, true that all targets/locations at this latitude of 33 degrees would receive the maximum daily average contact time[24]*. It should also be noted that the corresponding latitude in the opposite hemisphere would receive exactly the same coverage, so technically there are two latitudes that are optimized for each orbit.*

Inference 2.3 *Increasing the orbital altitude increases contact time. Re-examining figure 2.6 it can seen that at a latitude of 33 degrees as the satellite altitude increases from 150 km to 500 km, the coverage duration increases approximately from 35 minutes to 75 minutes. This result is due to two causes. Further distance can be seen when altitude increases since increasing the altitude also physically increases the size of the FOR, which in turn increases the contact time. Additionally, moving to a higher orbit slows the satellite down a bit, more closely matching its speed with that of earth's angular velocity. The FOR thus moves more slowly across a target tending to increase the contact time. While boosting the satellite altitude to a more realistic 500 km does increase contact time, it simultaneously degrades image resolution by a factor of almost three and signal strength for all missions (communication, BFT, and SIGINT) by a factor of over seven. Overcoming these mission degradations involves adding large sensors and associated equipment, increasing weight and making it that much more difficult and expensive to get the payload to the higher orbit.*

---

24. It would be a rare event to have two battle engagement at two different regions of the world with the same latitude within the short lifetime (6 months/1 year) of a tactical satellite. Hence, tactical satellites are mostly useful only for a single battle situation.

Inference 2.4 *Targets near the equator and the poles receive better optimized coverage than mid-latitude targets. Notice from the plots above that the maximum average daily coverage time that Baghdad receives (approximately 85 minutes) is less than the maximum average daily coverage time that Jakarta and St. Petersburg receive (approximately 180 and 100 minutes, respectively). The layout of the plots (figures 2.5, 2.6, 2.7) above have to be changed to better demonstrate this inference. Instead of plotting the satellite altitude versus the inclination, the plots below in figure 2.8 and figure E.6 on page 43 vary satellite inclination against the target latitude (at two different altitudes). It is immediately apparent on examining the y-axis that maximum coverage is attained at the equator and at the poles. This is because it is possible to put a satellite in orbit directly over the equator, since the plane of the equator contains the center of the earth. If the target is on or close to the equator (like Jakarta), the satellite will pass over it every single time it goes around the earth. Similarly, if the target is at or close to one of the poles (like St. Petersburg), placing the satellite into a polar orbit with an inclination of 90 degrees makes the satellite pass over the target every time*[25]*. However, if the target is located at the mid-latitudes (like Baghdad), even an optimized orbit will not necessarily pass over it every single orbit; depending upon the match between the satellite's and the earth's rotational speeds, sometimes the satellite will reach its maximum inclination over the target and at other times it will reach its maximum inclination some distance away from the target.*

25. No matter what longitude along which the satellite makes it approach, it will pass directly over the pole on each orbit.

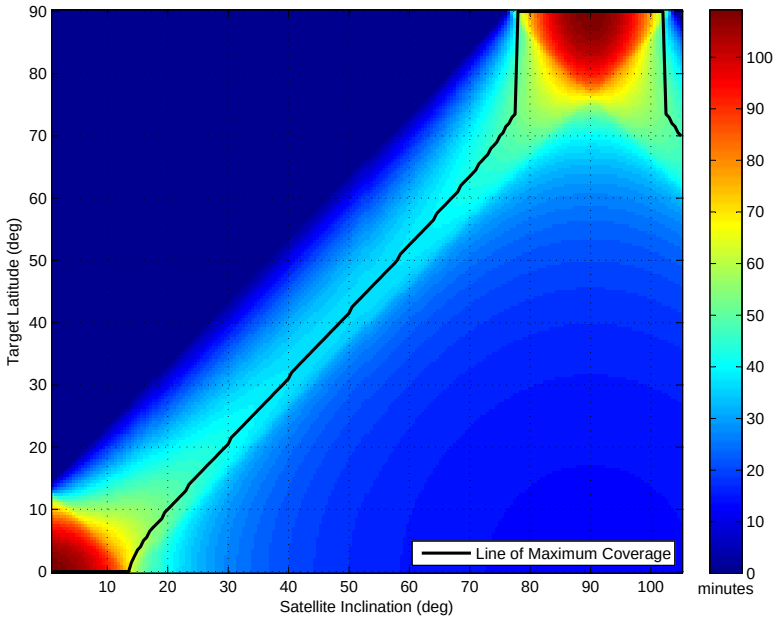

Figure 2.8: HORIZON FOR Maximum Average Satellite Coverage From 100 NM (185 km) (minutes per day)

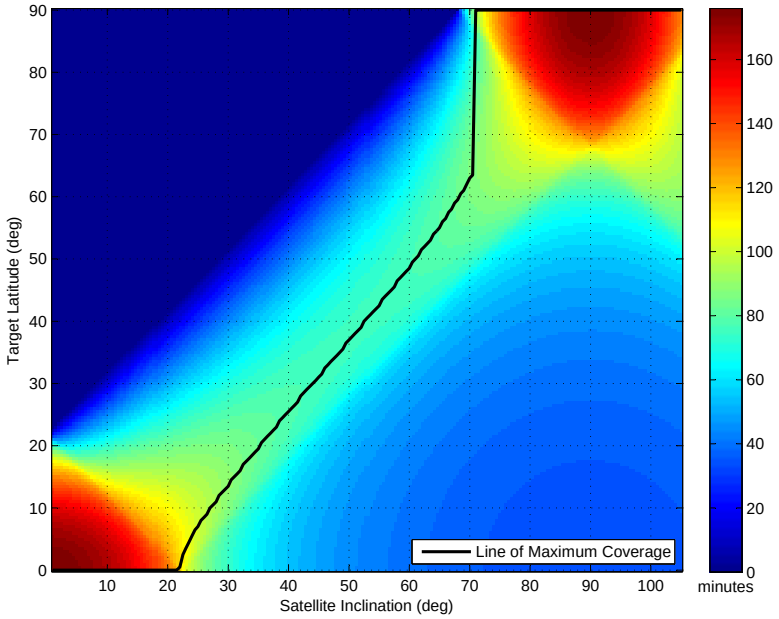

Figure 2.9: HORIZON FOR Maximum Average Satellite Coverage From 500 km (minutes per day)

Inference 2.5 *Hence, to optimize a TacSat (i.e., to obtain maximum average daily contact time over a specified target): place the satellite in a orbit as high as possible and match its inclination to (slightly higher than) the desired target's latitude.*

2.4.2 FOR Constraints on Optimized Orbits

In subsection 2.4.1 no real-world operational constraints were placed on the satellite sensors. The figures displayed in the previous subsection and the corresponding inferences drawn represent the best-case average contact times that can be obtained, limited only by orbital constraints on a satellite. Unconstrained and unobstructed FORs were assumed for the satellite.

However, actual tactical satellite missions will have limited FORs. Tactical satellites engaged in SIGINT mission are the only ones that can operate effectively at a horizon FOR. Since they are detecting radio transmissions, SIGINT TacSats only need to have line of sight to the emitter they are trying to detect, hence its FOR extends to the horizon as seen from the satellite[26]. For communication and BFT missions, the ground-based node of a ground-to-space communication/BFT link generally requires the satellite to be a specified angle above the horizon, usually five to ten degrees, to ensure connectivity. The FOR for such a mission would be the area on the ground from where the satellite is at least 5-10 degrees above the horizon.

---

26. This does not imply that SIGINT missions lend themselves well to TacSats. Military signals of interest span a range of frequencies, and this would obviously need to be taken into account in the design of any satellite collector, probably requiring a number of different antennas to be accommodated on the satellite. TacSats are not conceptualized to host multiple antennae. Also, typically SIGINT satellite collection concepts utilize three or perhaps four satellite working together in close formation in order to provide appropriate baselines between the satellites for "time difference of arrival" calculations[195].

Given a constraint of 5 or 10 degrees above the horizon FOR, the daily maximum coverage of a particular target latitude decreases significantly from a horizon FOR case. This is illustrated in figures 2.10 and 2.11 on pages 45 and 46 respectively.

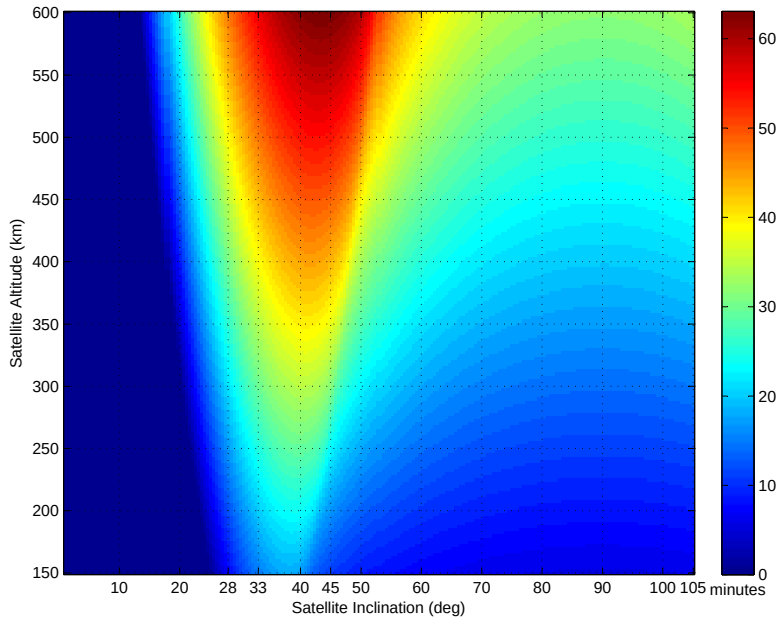

Figure 2.10: Maximum Average Satellite Coverage Over *Baghdad* with a 5 Degree Above the Horizon FOR (minutes per day)

Inference 2.6 *At a given satellite altitude and inclination, as the FOR becomes more constrained for operational reasons, the maximum average daily coverage over the target latitude decreases. For example, it can be seen in figure 2.6 on page 39 that at an altitude of 500 km and an inclination of 33 degrees (Baghdad being the target location at that particular latitude) the maximum daily coverage is approximately 70 minutes for a horizon FOR. In comparison, it is seen in figure 2.10 above that at the same altitude of 500 km and 33 degrees inclination for a 5 degree above the*

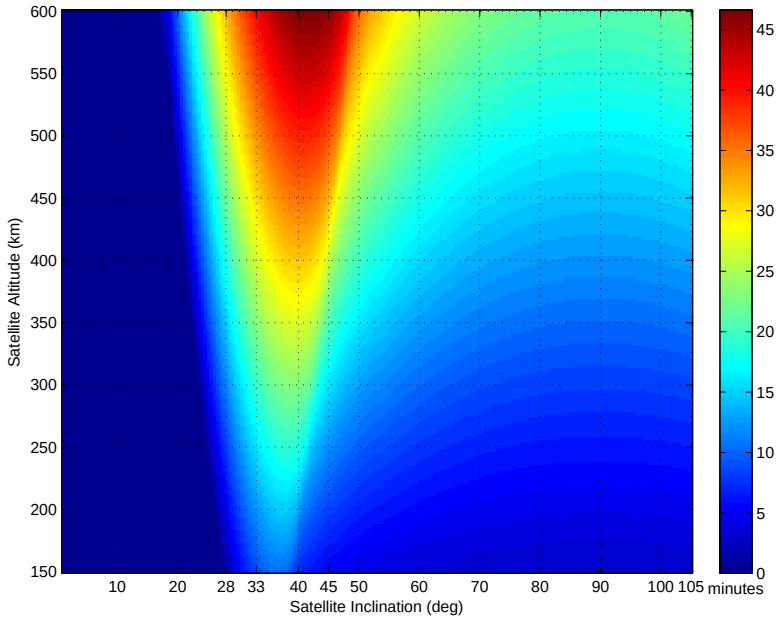

Figure 2.11: Maximum Average Satellite Coverage Over *Baghdad* with a 10 Degree Above the Horizon FOR (minutes per day)

horizon FOR constraint the maximum average daily coverage is approximately 50 minutes: a 29 percent decrease in coverage. Similarly, it is seen in figure 2.11 above that at the same altitude of 500 km and 33 degrees inclination for a 10 degree above the horizon FOR constraint the maximum average daily coverage is approximately 35 minutes: a 50 percent decrease in coverage (in comparison to the horizon FOR case). Similar trends in the decrease of coverage are seen in the cases of Jakarta and St. Petersburg. The graphs illustrating the reduction in coverage for Jakarta and St. Petersburg can be found in Appendix D on page 240.

ISR satellites have even more restrictive FORs. Not only must they have LOS like the other missions, but they cannot look too far away from the nadir[27] without

27. Nadir is the direction of an imaginary line extending from the satellite straight down toward the center of the Earth.

introducing a host of problems. In order to properly analyze overhead images, the images cannot be taken from too shallow an angle. Atmospheric effects are much more pronounced when the image is taken at a shallow angle due to the much greater distance through the atmosphere the light has to travel from the object. At shallower than certain angles, the images become useless as the information desired (discriminating between tank and truck, for example) can no longer be discerned[28].

The resolution of an image i.e.,, the ability to distinguish small, closely-spaced objects from each other, is directly related to how far away the object is. The smallest feature x that can be resolved by a circular aperture of diameter D at a range R from the target using an electromagnetic wavelength λ is approximately given by the formula $x = \frac{1.22R\lambda}{D}$, showing that the resolution power is linearly related to range[29]. Therefore, imagery satellites seldom look more than about 30 degrees off-nadir. A quick survey of currently operational private for-profit satellite systems proves this (see table B.1 on page 234 of Appendix B).

The figures 2.12 and 2.13 below illustrate the effects of 45 degree[30] and 30 degree off-nadir satellite sensor FOR constraint on coverage durations.

Inference 2.7 *Similar to the previous inference, when the FOR is constrained by*

---

28. For discrimination resolution requirements for various military targets see table B.2 on page 237 of Appendix B.

29. For example, as shown in table B.2 on page 237 to detect a radar from a satellite a 3 meter resolution is required. Operating in visible band at a wavelength λ of 20 nm with a 20 cm diameter aperture, the maximum distance (that can tolerated without loss of detection) between the satellite and radar location can be 984 km. If the satellite is operating at 500 km altitude, this distance translates into a maximum off-nadir angle of 30 degrees at a slant range of 984 km.

30. The 45 degree off-nadir imaging scenario is given to illustrate the drastic loss in coverage even at a highly biased value in favor of TacSats.

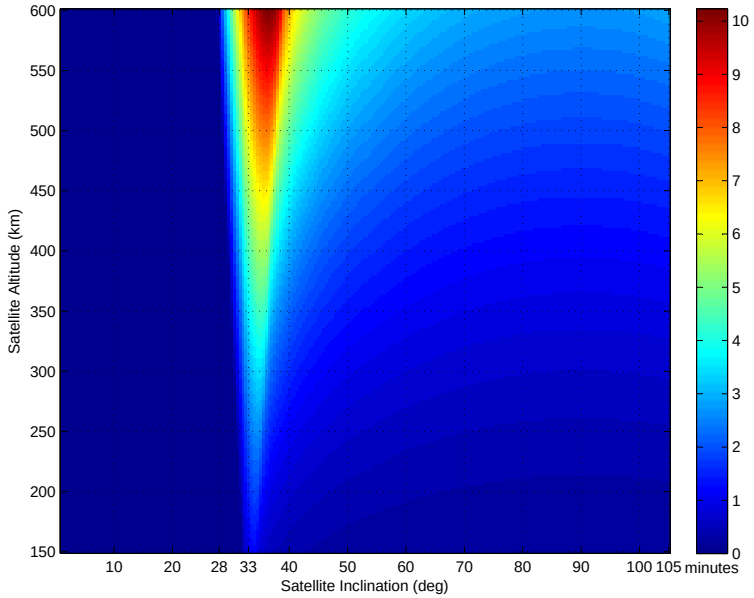

Figure 2.12: Maximum Average Satellite Coverage Over *Baghdad* with a 45 Degree Off-Nadir FOR (minutes per day)

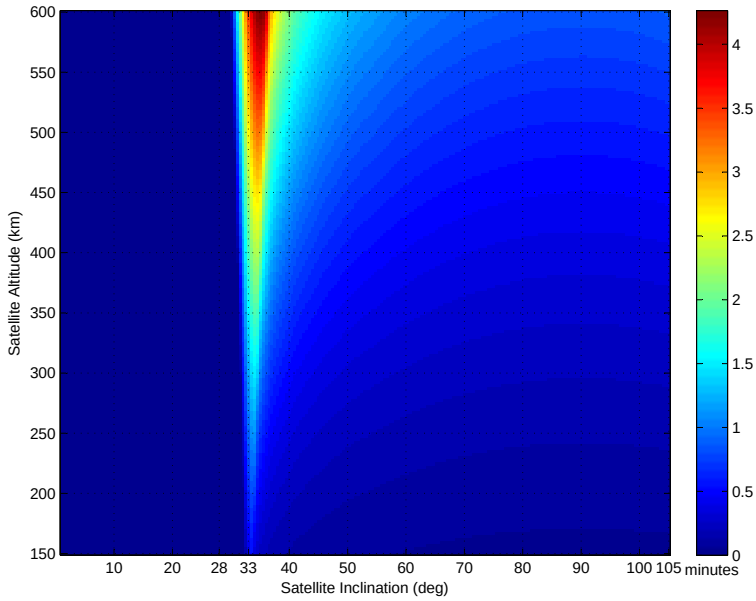

Figure 2.13: Maximum Average Satellite Coverage Over *Baghdad* with a 30 Degree Off-Nadir FOR (minutes per day)

ISR requirements there are drastic losses in coverage time. For example, it can be seen in figure 2.12 that at an altitude of 500 km and an inclination of 33 degrees with a 45 degree off-nadir FOR constraint the maximum daily coverage is approximately 8 minutes: a 90 percent decrease in coverage from the horizon FOR case. Similarly, it is seen in figure 2.13 that at the same altitude of 500 km and 33 degrees inclination with a 30 degree off-nadir FOR constraint the maximum average daily coverage is approximately 3 minutes: a 95 percent decrease in coverage (in comparison to the horizon FOR case).

The dramatic fall in coverage between the ideal case of horizon FOR and the 5/10 degree above the horizon FOR requirement for communication satellites or the 30/45 degree off-nadir FOR for ISR satellites can be comprehended by examining figure 2.14[31] below. It is immediately clear that as FOR becomes more constrained, the area on the ground accessible for the particular mission gets smaller hence leading to reduced mission coverages[32].

Inference 2.8 *Once a tactical satellite is optimized for a particular target location, the operational mission constraints on the satellite's sensors drastically limit the maximum daily average coverage possible. This is true across all latitudes (see Appendix E on page 248 for evidence). However, the decrease in coverage is more drastic at mid-latitude regions in comparison to equatorial and polar regions*[33].

31. This figure has been copied from [67]. An articulate and detailed review of the discussion above can also be found here.

32. More details are in Appendix B on page 232.

33. See inference E.1 in Appendix E on page 248 for illustration and proof.

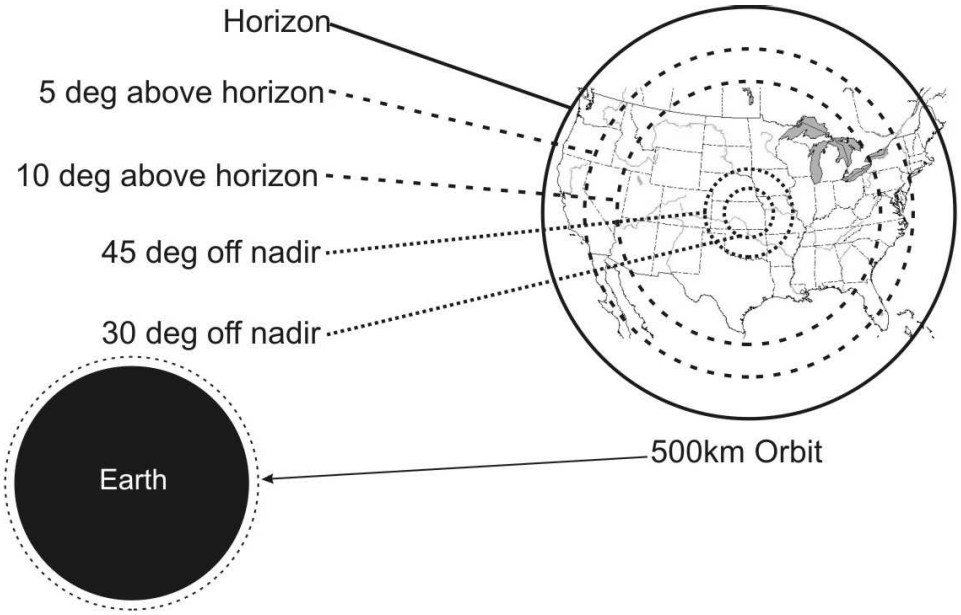

Figure 2.14: Field of Regard (FOR) from 500 km. The solid line (Horizon) represent the SIGINT FOR, the dashed lines (5/10 degree above horizon) represent communication/BFT FOR and the dotted lines (45/30 degree off-nadir) represent ISR related FOR[67].

Up to this point, it has been assumed that there is only FOR constraints and no FOV constraints. It is important to realize that just because a target is in the FOR of the satellite, it is not necessarily being imaged by the payload. Satellites typically do not image their entire FOR during a single pass. Especially for the high resolution imagery necessary for the tactical war fighter, only a tiny fraction of the whole FOR can be seen by the camera's FOV at any instant[34]. Similarly, the

34. For example, the FOR for earthbound photographers with a camera would be everything they can possibly see from their location through their camera (i.e.,, zero to 360 degrees in azimuth and zero to 90 degrees in elevation); their FOV, on the other hand, would be the substantially reduced portion of the world that can be seen through their camera at any instant[67].

power from the main lobe of a communication satellite would be concentrated in a smaller region of its FOR. These FOV constraints will further diminish the average daily coverage durations. Also, this analysis has ignored the non-trivial limitations of weather and darkness and assumed an ability for imagery sensors to operate at full capacity 24/7.

2.4.3 Tactical Performance of Optimized Orbits

In the previous two subsections, the maximum average coverage over a latitude of interest for a optimized satellite was estimated under various FOR constraints. To more fully appreciate the limitations of these estimations, this subsection will discuss other tactically relevant parameters like satellite pass duration, number of passes per day, average coverage gaps between passes and cost per-hour of satellite coverage.

To calculate the pass duration, a generalized average metric is used again. A pass occurs when the FOR of the satellite passes over the target. However, as the FORs on the earth's surface are circles centered on the subsatellite point, different contacts have different pass durations. Their duration depends on the distance of the subsatellite point to the target location[67]. Assuming the FOR passes over the target in a straight line, the minimum pass duration would be an almost instantaneous flicker should the target location pass at the very edge of the FOR circle; on the other hand, if the satellite passes directly over the target location dragging the entire diameter of the FOR circle across it, the pass duration would

be maximum.

For the calculations in this subsection, the average pass duration is related to the average chord length of a circle equal to the FOR diameter. The maximum chord length is the FOR diameter and is dependent on the orbital altitude. Applying the relationship that distance traversed is equal to the product of the velocity and time, the average pass durations can be found by dividing the chord lengths by the ground speed of the FOR which is again altitude dependent. Figure 2.15 below shows the results of applying this discussion.

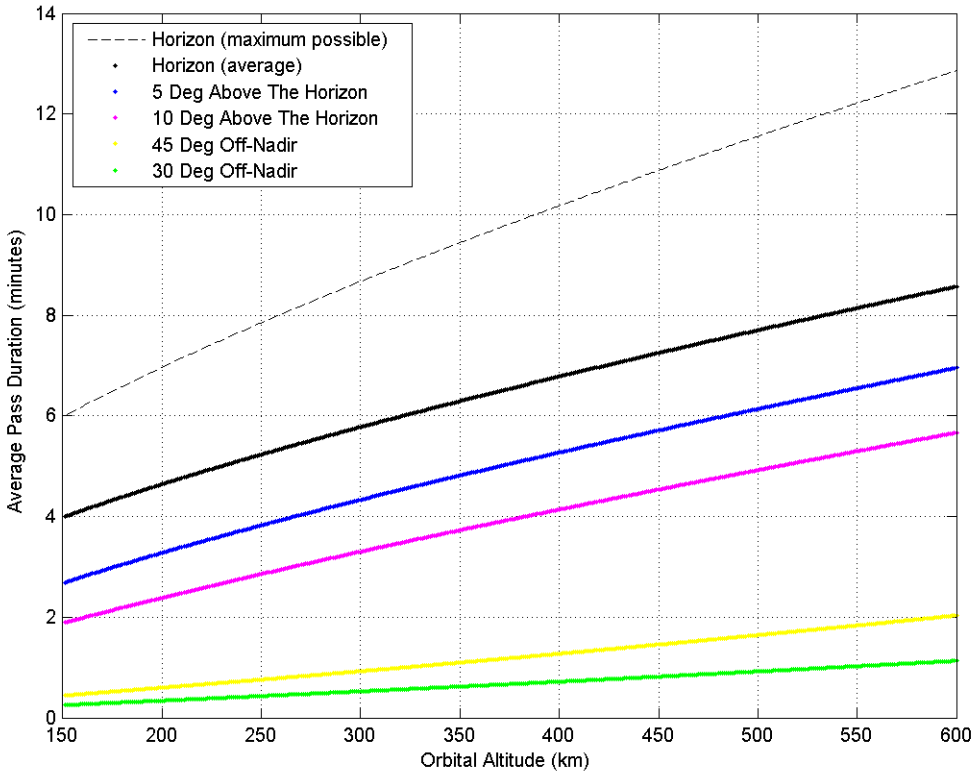

Figure 2.15: Average Pass Durations Per Satellite Pass

Figure 2.15 illustrates the average pass durations (y-axis) against a range of satellite altitudes (x-axis) accounting for the various FOR constraints. For example, at an altitude of 500 km, a satellite with horizon FOR would have an average pass duration of approximately 8 minutes whereas a satellite with 10 degree above the horizon FOR constraint would have an average pass duration of 5 minutes. The maximum pass duration (i.e., when the FOR diameter passes directly over the target latitude) is shown for illustrative purposes. It would almost never be attained. Along with the *individual* pass durations shown in Figure 2.15 above, the optimized coverage *per day* at various latitudes that was calculated in subsections 2.4.1 and 2.4.2 is reproduced below in figures 2.16 and 2.17. Using the information embedded in figures 2.15, 2.16 and 2.17 on can calculate the other parameters of interest like average number of passes per day, average gap time between passes, and cost per-hour overhead for a TacSat.

By dividing the optimized average daily contact time by the average pass durations, the average number of passes per day can be determined. By inverting the number of passes per day, the average revisit time between passes is determined. The average gap time is the difference between the revisit time and pass duration. The cost per hour overhead can be calculated by dividing the aspirational TacSat cost of USD 20 million by the total of number of hours the satellite would be overhead during its life time (one year for the purpose of calculations). Evaluating these metrics shows the insufficiency and inefficiency of TacSats in performing their missions. On examining figure 2.18 below, for the case where the TacSat is orbiting at an altitude of 100 NM (185 km) with a horizon FOR, a single satellite will have

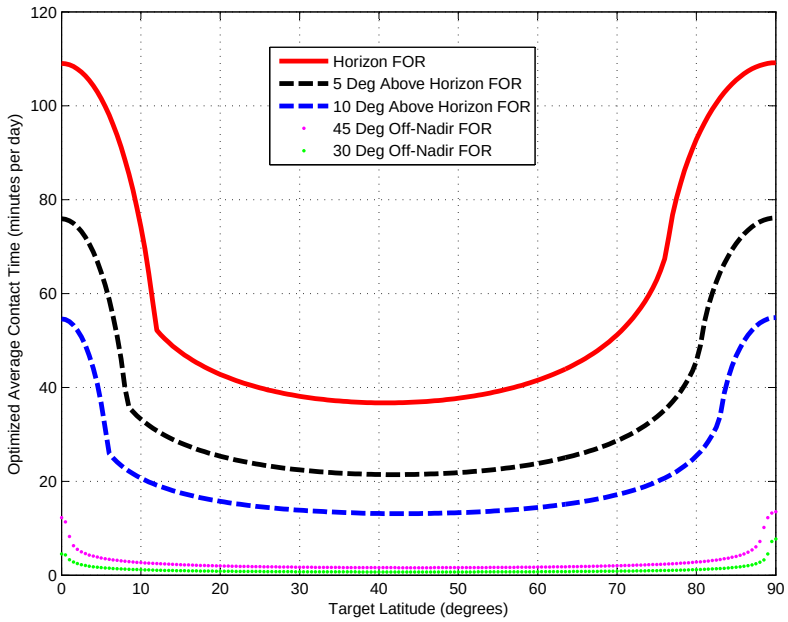

Figure 2.16: Daily Satellite Coverage at 100 NM (185 km) altitude

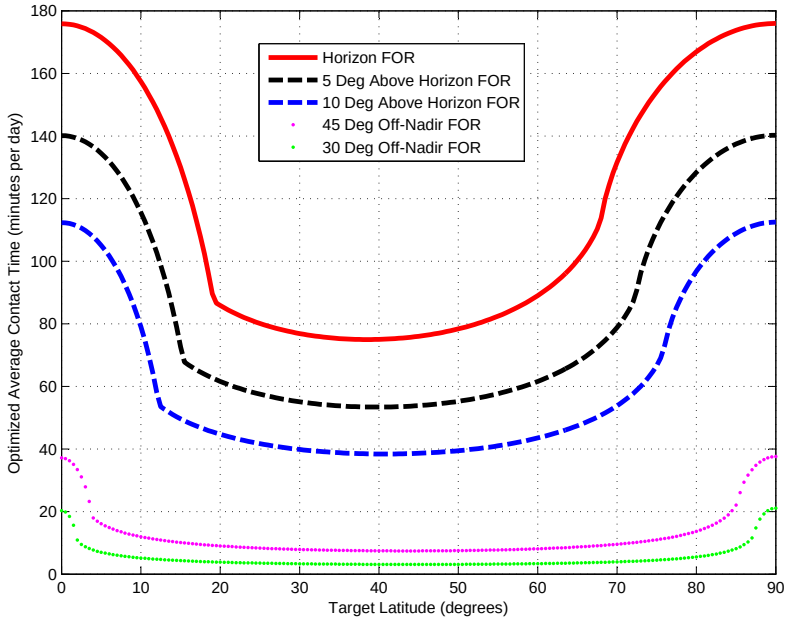

Figure 2.17: Daily Satellite Coverage at 500 km altitude

approximately 8 passes over Baghdad (33 degrees latitude) per day with an average pass duration of 4.5 minutes (from figure 2.15) per pass. The gap time between each successive passes on average would be approximately 3 hours.

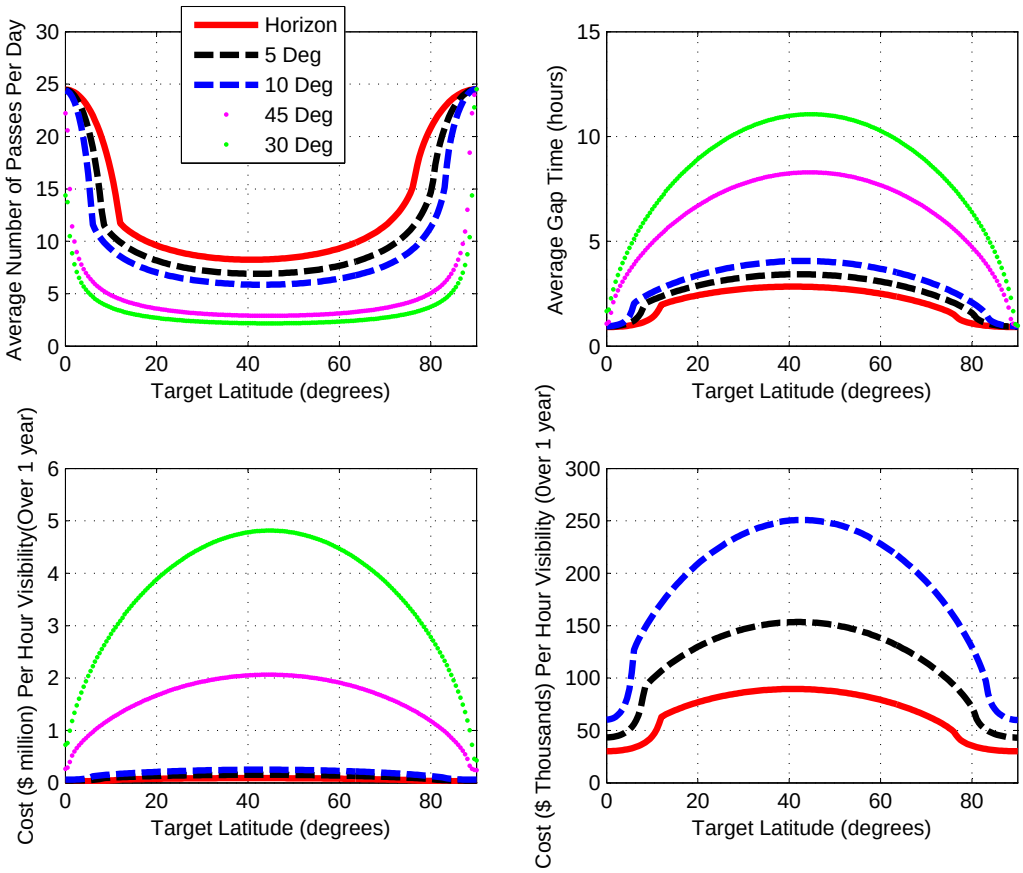

Figure 2.18: Number of Passes, Average Gap Time, and Cost Per Hour of Visibility for a TacSat at 100 NM (185 km)

Similarly, on examining figure 2.19 on page 57 for the case where the TacSat is orbiting at an altitude of 500 km with a horizon FOR, a single satellite will have approximately 10 passes over Baghdad (33 degrees latitude) per day with an average

pass duration of 8 minutes (from figure 2.15) per pass. The gap time between each successive passes on average would be approximately 2 hours. Finally, the cost per hour of overhead visibility (over Baghdad) is approximately USD 40,000 per hour. Placing the satellite at a higher altitude does give some improved performance. There is a limit, however, on the achievable altitude since the TacSats intend to use COTS technology that limit the operational altitude of ISR sensors[35]. Any attempt to use state-of-the-art sensors that can provide high resolution at greater orbital altitudes will place the cost of the TacSat in the range of strategic satellites.

Even at a higher operational altitude of 500 km, the performance obtained from a optimized TacSat is completely unsuitable for tactical operations. It would be impossible to undertake a tactical mission that lasts for a duration of 8 minutes with an average gap of 2 hours between each pass. The emphasis on average in the previous sentence is to illustrate another important limitation that all TacSats suffer from: pseudorandom distribution of passes. Pseudorandom passes implies that although the time of each satellite pass can be calculated, there will be no apparent regular schedule between passes with some occurring quite close together in time, while at other times there will be substantial gaps. The tactical war fighter will have no control over exactly when a satellite will pass over the location of interest. This will be detrimental to mission accomplishment as regular, predictable information is needed by tactical commanders. On the other hand, a fairly sophisticated adversary would be able to predict the passes and employ counter strategies to defeat the

35. The effect of the Van Allen belt radiation on TacSats can be severe as they are designed using cheaper COTS electronics that might not be manufactured to withstand these radiations.

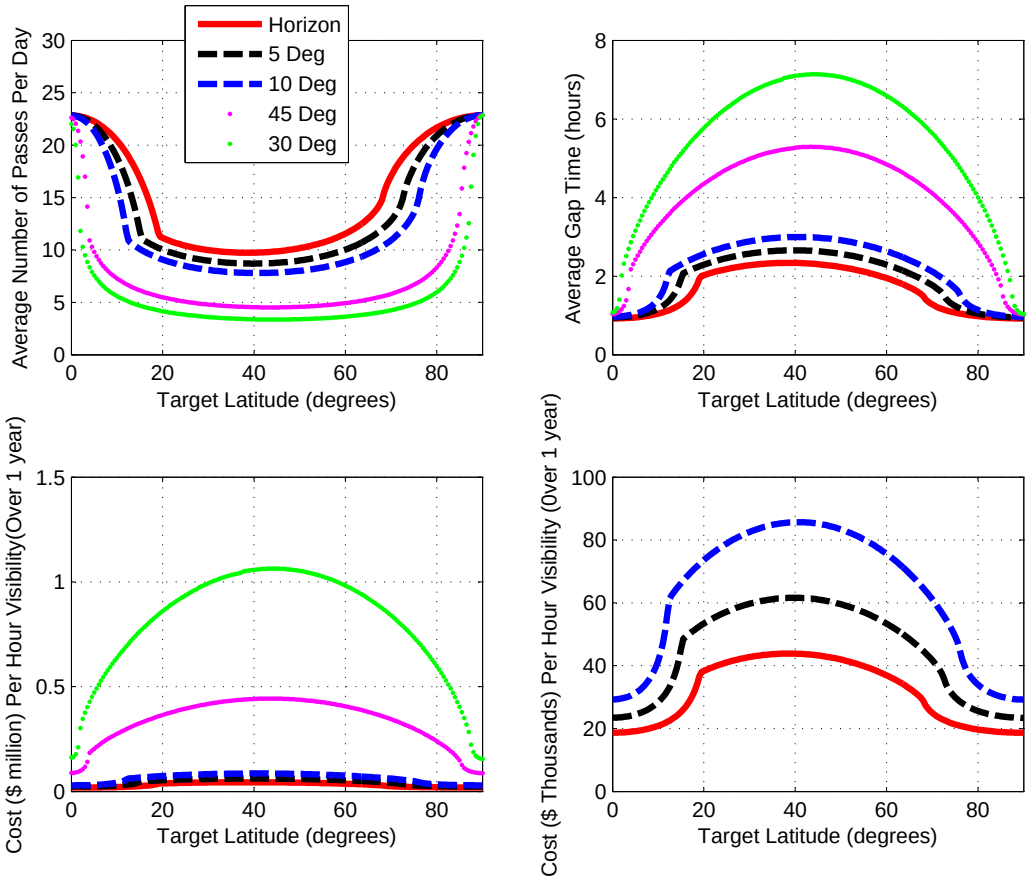

Figure 2.19: Number of Passes, Average Gap Time, and Cost Per Hour of Visibility for a TacSat at 500 km

purpose of the tactical satellite[67].

Inference 2.9 *To operationalize a tactical engagement under a best-case scenario using a single optimized LEO satellite, its mission would be have to be defined as: "Mission lasting for an average of 8 minutes with repeat engagement possibly 2 hours (more or less)". It would be inept for a commander to use such a vague time line for engaging in a military mission. A tactical war fighter needs persistent imagery and*

constant communication. Getting a snapshot or minutes of communications every two hours or so is not very useful at the tactical level, where the time scale of the action is measured in minutes or seconds[67].

2.4.4 Constellation of TacSats

One of the mechanisms advocated by the ORS community to eliminate the limitations of a single optimized TacSat and to obtain 24/7 persistence is to use a constellation of these satellites. This subsection will evaluate the improvement in performances obtained by employing such TacSat constellations.

A simple approach to approximate the number of satellites required to gain 24/7 persistence of the target location is to divide the minutes in a day by the average number of minutes per day spent overhead by a single satellite. This number of satellites would be the chain of satellites required to pass sequentially over the target to provide 24/7 persistence. For example, as shown in figure 2.20 below the minimum number of satellites required on average to ensure persistent 24/7 coverage over Baghdad from an orbital altitude of 100 NM (185 km) with a best case scenario horizon FOR is 40 satellites. At an aspirational cost of USD 20 million per satellite this would be a total of USD 800 million for one tactical mission over one city. The number of satellite required and the total cost goes up rapidly as the FOR becomes more constrained. If the orbital altitude of is increased to 500 km, for the same best case scenario horizon FOR the total number of satellite required to create 24/7 persistence over Baghdad is approximately 20 satellites (see figure 2.21

below). At a cost of USD 20 million per satellite this would be a total of USD 400 million for one tactical mission over one region. This still is much higher than the possibly obtainable funding for any one tactical mission's communication or ISR requirements.

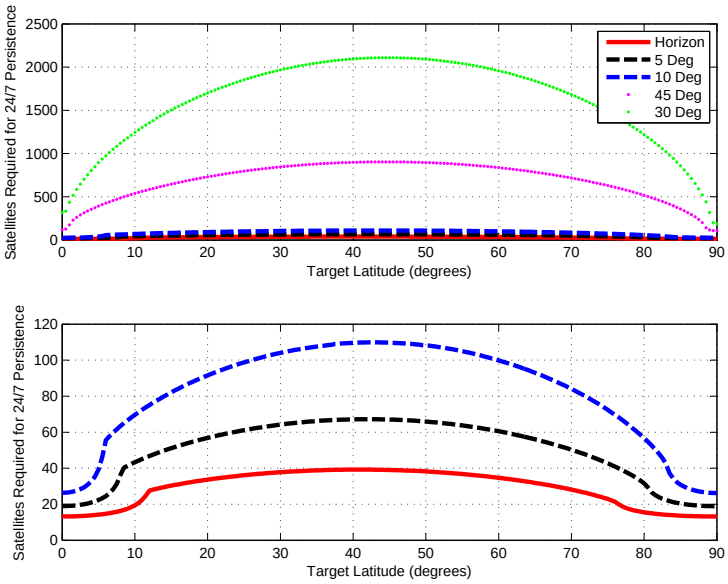

Figure 2.20: Approximate number of satellites required for 24/7 persistence at 100 NM (185 km)

2.4.5 Elliptical Orbits for Communications

In an attempt to prevent the large costs involved with optimized LEO orbits (as demonstrated in the previous subsections), ORS proponents have proposed a Highly Elliptical Orbit (HEO) for TacSat communications missions called MAJIC (Microsatellite Area-Wide Joint Information Communication) Orbit (500 x 8000 km, 63.4 degrees inclination)[170, 63, 97, 30]. The advantage of a MAJIC orbit is

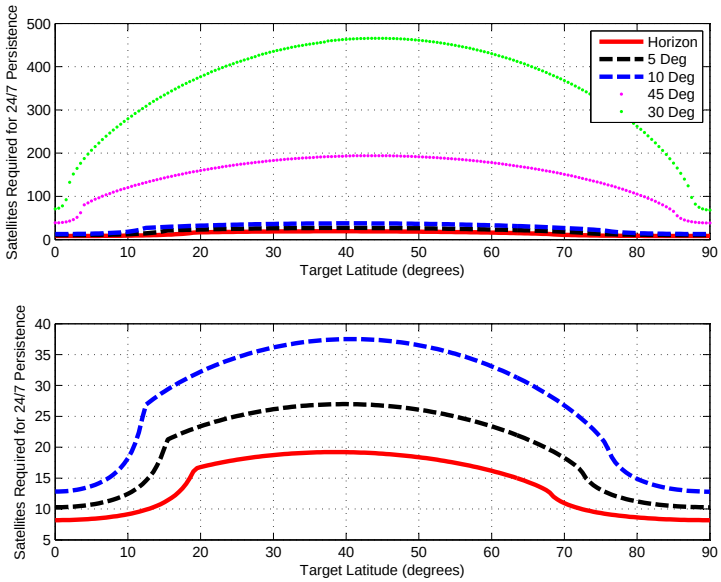

Figure 2.21: Approximate number of satellites required for 24/7 persistence at 500 km

that it greatly reduces the number of satellite required for 24/7 persistence of a tactical area and can be reached within the launch budget constraints of a TacSat. However, when at the useful part of its orbit, a satellite in a MAJIC orbit is about 8000 km above the earth, over 16 times further than a likely 500 km circular tactical satellite orbit. At this distance, conventional imagery missions are ineffective due to resolution limitations. Therefore MAJIC orbit TacSats could only be used for communication missions.

Studying figure 2.22 below on page 62 it can be seen that at an optimized argument of perigee[36] of 270 degrees, a single satellite in MAJIC orbit will provide

36. Argument of perigee is the angular distance between the point where the satellite crosses the equatorial plane in a northerly direction and the point of closest approach to the earth.

close to 8 hours of coverage at horizon FOR[37], implying that 24/7 persistence can be obtained by employing just three satellites. The reason for this highly improved coverage is because the orbital period of the MAJIC orbit is 1/8th of a day and therefore TacSats at the MAJIC orbit move slower with respect to earth. The satellite and its FOR move very slowly at apogee when the satellite is above the location of interest spending the major portion of its orbit there. As the satellite accelerates back towards perigee, it zips past the target providing very little coverage then.

TacSats employing the MAJIC orbit and orbiting at an optimized argument of perigee do provide significantly improved coverage per satellite, removing the need for large number of satellites to provide 24/7 persistence. On the other hand, employing MAJIC orbits introduces other problems that negate their utility as tactical assets. Satellites in MAJIC orbit are on average 17 times further from a location in comparison to a 500 km orbit. At this range, signal strength can be very problematic. Using the simple $1/r^2$ metric for signal strength attenuation, it becomes obvious that at MAJIC orbit altitudes the satellite antennae and signal power density have to be substantially higher than LEO requirements. To illustrate, for a communications antenna in a MAJIC orbit satellite to be as sensitive to signals as

37. For highly elliptical orbits, to maximize contact time over regions in the northern hemisphere like *Baghdad* and *St. Petersburg* the argument of perigee needs to be close to 270 degrees. Similarly, for regions in the southern hemisphere like *Jakarta* the argument of perigee that maximizes contact is 90 degrees. Additionally, HEO orbit missions require the angle of inclination of the orbit needs to be fixed at 63.4 degrees to prevent the location of the perigee/apogee from moving, The earth is not perfectly spherical. This imperfection causes several orbital perturbations including the rotation of the perigee and apogee point of an orbit. By placing the MAJIC orbit at an inclination of 63.4 degrees this rotation is prevented.

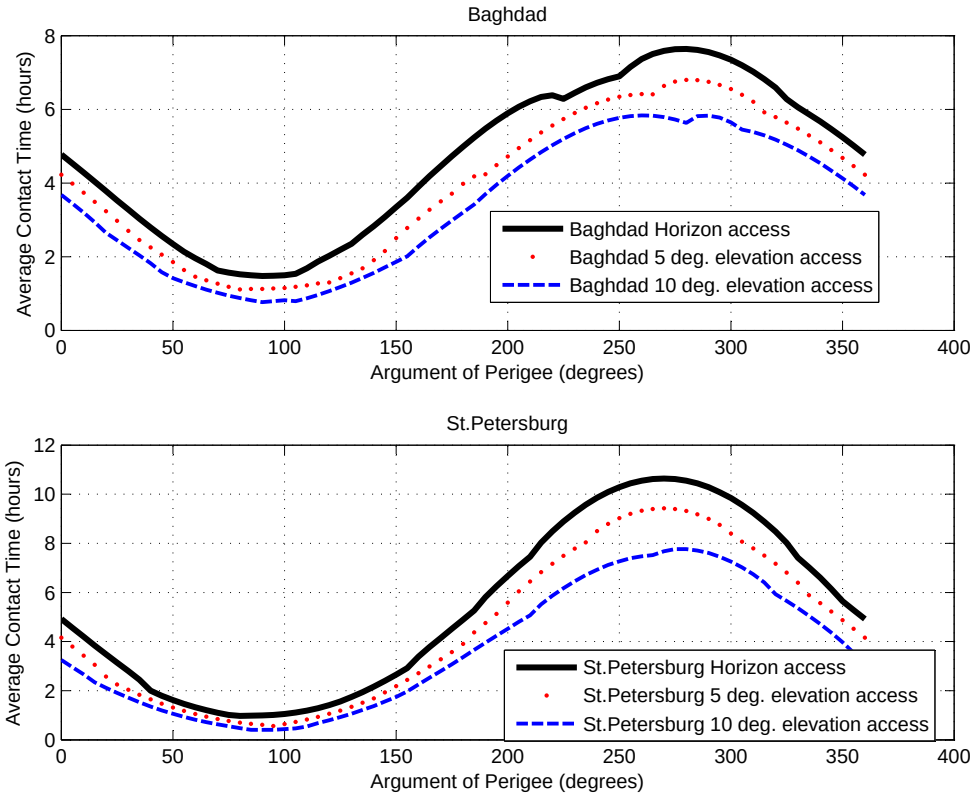

Figure 2.22: Average Contact Time vs. Argument of Perigee for MAJIC Orbit

the Iridium SATCOM system (which has a set of three 1.6 square-meter antennae for reception) its antennae should be about 200 square-meter. The weight and energy requirements for such a large antennae are outside the design and cost margins of a tactical satellite[67, 125]. Additionally, unlike traditional GEO communication satellites which have a fixed position in the sky in reference to the tactical user, MAJIC orbit TacSats will be operating in such a manner that the satellite will have complex and unpredictable apparent motion and range to the tactical user (see figure 2.23 below). This is a more involved form of pseudorandom motion.

For the case of MAJIC orbit satellite passage over Jakarta, as illustrated in left panel of figure 2.23 below, the direction of apparent motion and time gap between each satellite pass is highly variable, exhibiting the characteristics of a pseudorandom motion. Similarly, it can be inferred from studying the right panel of figure 2.23 that the range between the satellite and the target location and the apparent velocity of the satellite with respect to the location is varying randomly. A similar pattern of behavior is observed for MAJIC orbit TacSats over *Baghdad* and *St. Petersburg* as shown below in figures 2.24 and 2.25 respectively.

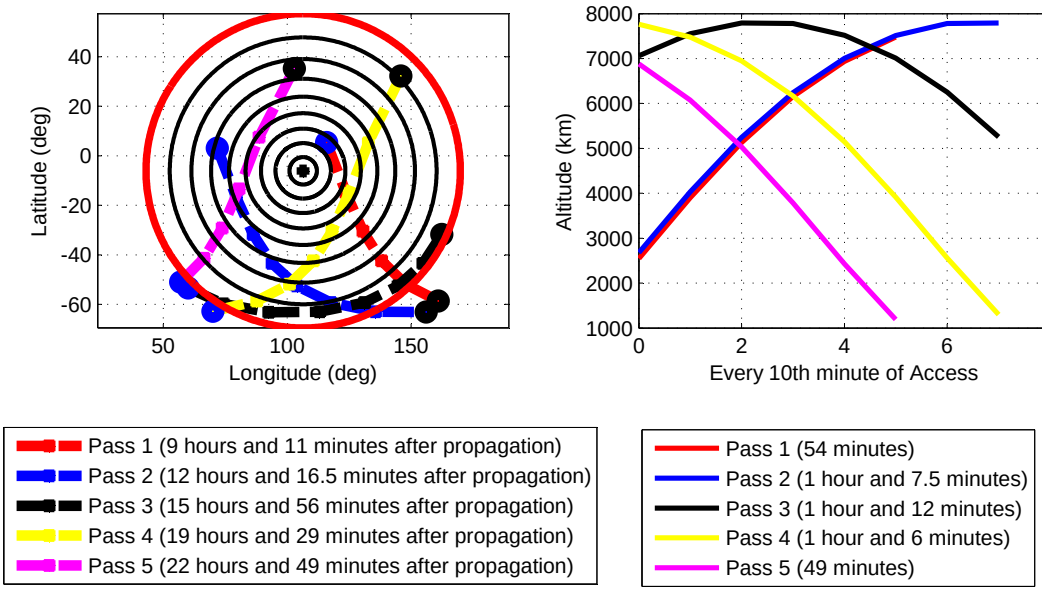

Figure 2.23: Apparent Motion and Range of a MAJIC Satellite Over *Jakarta* (24 hours; 10 minutes interval)

Inference 2.10 *In operational terms, the pseudorandom motion of a satellite in MAJIC orbit would require the tactical unit employing a MAJIC orbit-based satellite for communication to stop, set up a dish antenna, and point it toward the tactical*

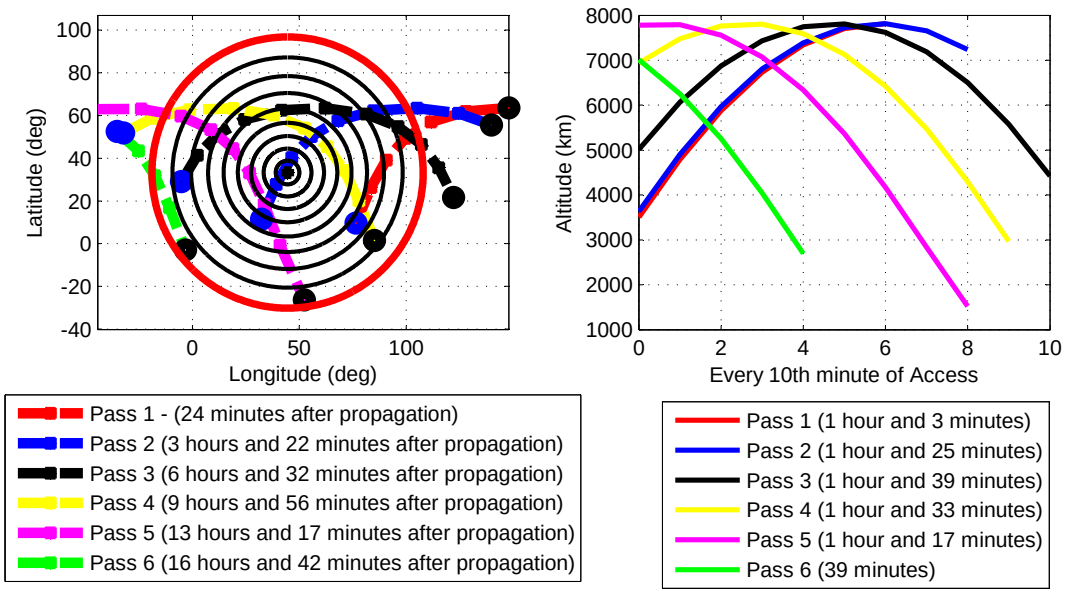

Figure 2.24: Apparent Motion and Range of a MAJIC Satellite Over *Baghdad* (24 hours; 10 minutes interval)

satellite and then continuously estimate its position and track it. At the current time, one of the biggest limitations on tactical use of satellite for communications is that the tactical squad unit must stop its vehicle and point a high gain antenna towards the stationary satellite GEO to get reception. The reason for this limitation is that communication satellites are very far away and the signals they emit are relatively weak. The signal from a satellite in a MAJIC orbit would be about 20 times stronger, but instead of coming from a stationary communications satellite it would come from a moving one. The soldier's problem is now compounded; he has to stop and acquire a satellite that is constantly changing location[67]. Doing so in the middle of a tactical engagement is prohibitive.

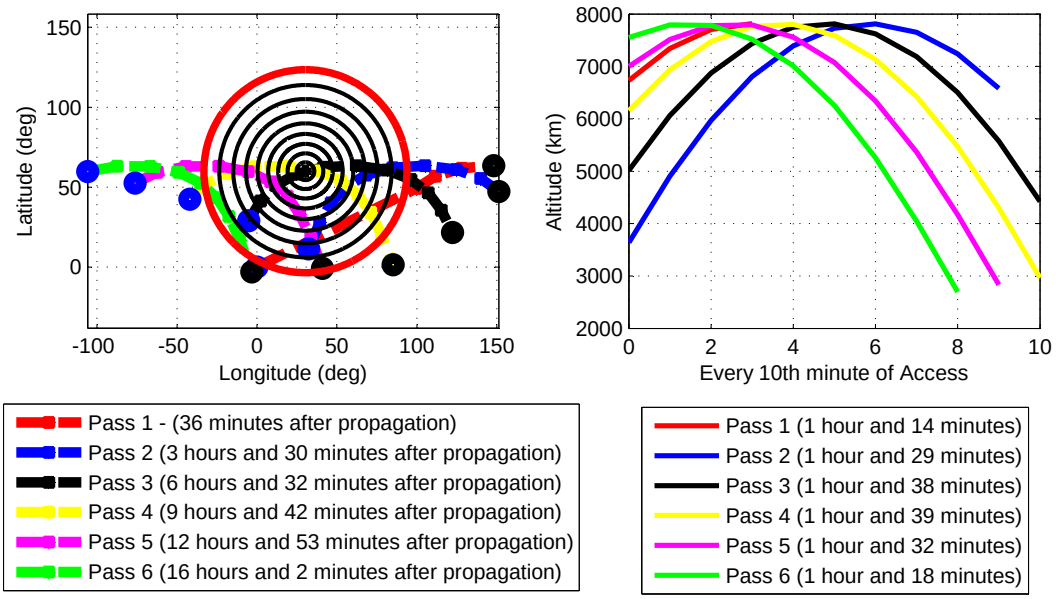

Figure 2.25: Apparent Motion and Range of a MAJIC Satellite Over *St. Petersburg* (24 hours; 10 minutes interval)

2.4.6 The Futility of TacSats

The fundamental laws of orbital mechanics work against the idea of TacSats. A combination of *physical constraints* placed on satellites by orbital mechanics and *operational requirements* placed on their payloads by the mission that can be performed from space prevent all but the most rudimentary missions from being attainable cost-efficiently. Choosing an orbit that slows down the satellite pass to improve persistence ends up requiring huge increase in payload size in order to maintain the standard of performance. Neither the operational constraints from orbital mechanics and FOR/FOVs nor the cost constraints involved in mounting and populating a TacSat constellation have been resolved by TacSat advocates.

Unless there is a significantly new paradigm of satellite development or there is

a technological revolution in space launch, there is very little chance of satellites being used a tactical battle asset. Furthermore, the effect of orbiting tens to hundreds of satellites on the space control network has not been studied and might well turn out to be a significant deciding factor. TacSat supporters have also not adequately addressed the issue of data management and the training required for tactical U.S. war fighters to operate a possible TacSat network.

This entire chapter on evaluating TacSats has demonstrated that the use of high-risk low-cost quick-response satellites for tactical battle missions is questionable. It is conceivable that cheaper small satellites (in the weight range of 100-150 kg) that cost less than USD 20 million might have some battle management applications. These satellites may have possible augmentation missions of DSP, DMSP, and GPS satellites. However, they might not be ideal candidates for the purposes of tactical missions as outlined by TacSats proponents. These cheaper small satellites have limited on-board processing capability which might inhibit rapid image processing in order to provide real-time intelligence to the warfighter. Also, most of these satellites are launched as piggyback payloads. Such a launch schedule does not suit TacSat missions. Finally, for TacSat missions supporting warfighters a certain level of reliability is needed. It is not clear if these cheap smaller satellites possess that level of reliability. The TacSat community is yet to have to demonstrate both the physical viability and the economic feasibility of using these cheaper small satellites for TacSat missions.

2.5 ORS missions vis-a-vis DOD space programs

The previous sections of this chapter demonstrated the infeasibility of attaining the goals outlined by proponents of ORS mission in each of the four areas of innovation. Those arguments should convince an impartial evaluator about the futility of spending scarce resources on ORS missions. Indeed, the White House's fiscal year 2013 budget has called for terminating the Operationally Responsive Space office[191]. Testifying before the House Armed Services strategic forces subcommittee, Air Force Gen. William Sheldon, commander of Air Force Space Command, said the move was necessary as part of the Air Force contribution to the USD 487 billion in planned reduction in defense spending over the next decade mandated by the Budget Control Act of 2011[204].

There is, however, resistance against the move. For example, Rep. Martin Heinrich (D-N.M.) in whose state the ORS is headquartered at the Kirkland Air Force Base characterized the cancellation as "penny-wise and pound-foolish" given the minimal investment involved[204]. However, when the goals and achievements of the ORS mission are investigated in reference to the current situation in DOD's space acquisition activities they come out to be futile and very inefficient.

Despite a growing investment in space, the majority of large-scale acquisition programs in the Department of Defense's (DOD) space portfolio have experienced problems during the past two decades that have driven up cost and schedules and increased technical risks. The reasons cited for these cost escalations and schedule delays are also present in ORS-TacSat missions as discussed below. Figure 2.26

below illustrates that the yearly combined cost[38] of various space programs have been steadily climbing[39]. The combined estimated costs for the major space acquisitions programs have increased by about USD 11.6 billion–321 percent–from initial estimates for fiscal year 2011 though 2016.

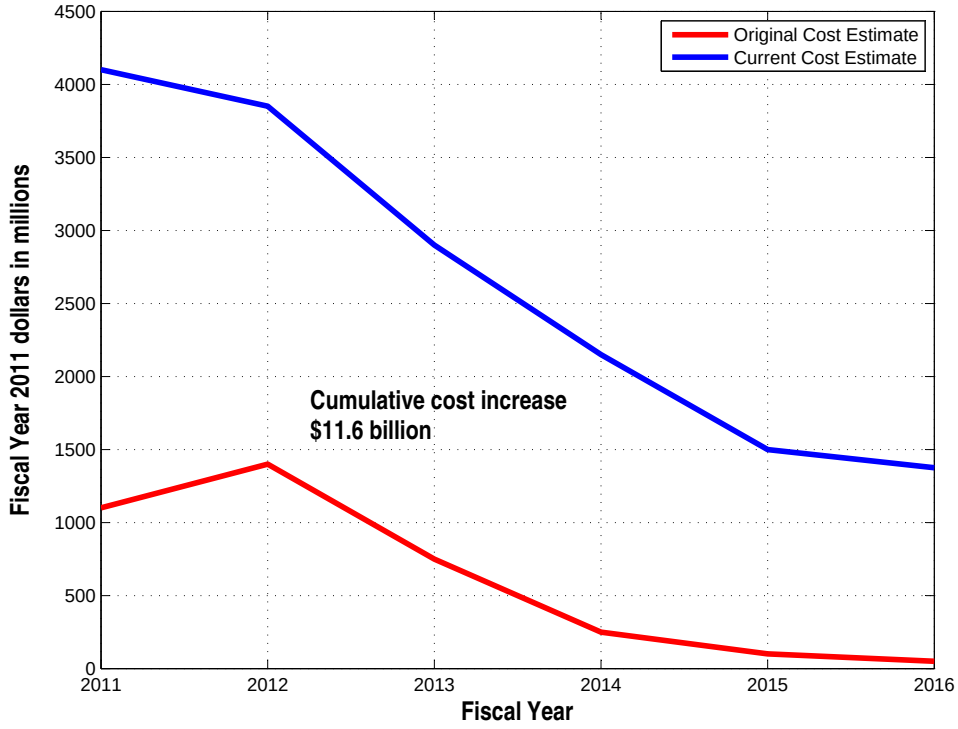

Figure 2.26: Comparison between Original Cost Estimates and Current Cost Estimates for Selected Major Space Acquisitions Program[226]

38. Programs included in the combined cost estimate are the Advanced Extremely High Frequency (AEHF), Global Broadcast System, Global Positioning System II and III, Mobile User Objective System (MUOS), Space Based Infrared System (SBIR), and Wideband Global SATCOM (WGS).

39. It's worth noting that the declining investment in later years is the result of mature programs that have planned lower out-year funding, cancellation of a major space acquisition program and several development efforts, and the exclusion of several major space acquisition efforts like the Space Fence, Space Based Space Surveillance, and the Defense Weather Satellite effort for which the total cost data were unavailable[226].

Figure 2.27 illustrates the additional months of delay not anticipated at the programs' start dates. These delays in space acquisitions are leading to potential gaps in the delivery of critical capabilities. For example, DOD faces a potential gap in protected military communications caused by delays in the AEHF program and the proposed cancellation of the TSAT program. DOD also faces a potential gap in ultra high frequency (UHF) communications capability caused by the unexpected failure of two satellite already in orbit and the delays resulting from the MUOS program. Similarly DOD faces potential gaps or decrease in positioning, navigation and timing (PNT) capabilities because of late delivery of GPS IIF satellites and the late start of the GPS IIIA program. There are also concerns about potential gaps in missile warning and weather monitoring capabilities because of delays in SBIRS and NPOESS[223, 225, 226].

GAO has cited a number of reasons for the cost growth and time delays in DOD's space acquisitions[225, 223]:

- DOD has tended to start more weapons programs that it can afford, creating a competition for funding that encourages low cost estimating, optimistic scheduling, overpromising, suppressing bad news, and for space programs, forsaking the opportunity to identify and assess potentially more executable alternatives. Programs focus on advocacy at the expense of realism and sound management. Invariably, with too many programs in its portfolio, DOD is forced to continually shift funds to and from programs–particularly as programs experience problems that require additional time and money to address.

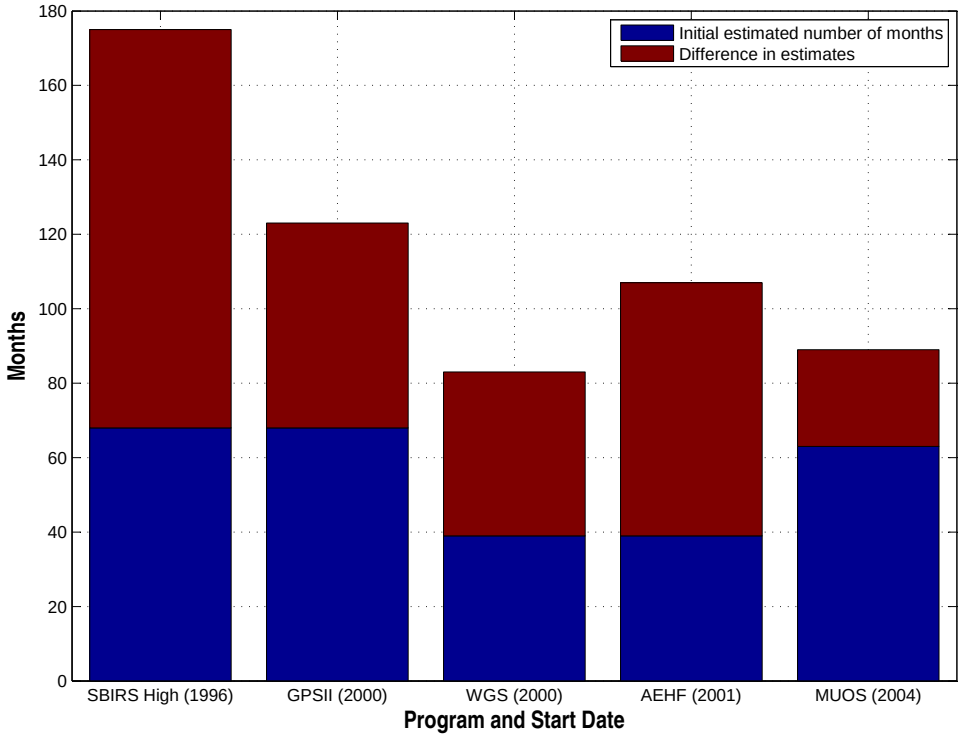

Figure 2.27: Total Number of Estimated Months from Program Start to Initial Launch[225, 224]

Such shifts, in turn, have had costly, reverberating effects.

- DOD has tended to start its space programs too early, that is, before it has the assurance that the capabilities it is pursuing can be achieved within available resources and time constraints. This tendency is caused largely by the funding process, since acquisition programs attract more dollars than efforts concentrating solely on proving technologies. Nevertheless, when DOD chooses to extend technology invention into acquisition, programs experience technical problems that require large investments of time and money to fix. Moreover, when this approach is followed, cost estimators are not well positioned to de-

velop accurate cost estimates because there are too many unknowns. Put more simply, there is no way to accurately estimate how long it would take to design, develop, and build a satellite system when critical technologies planned for that system are still in relatively early stages of discovery and invention.

- Programs have historically attempted to satisfy all requirements in a single step, regardless of the design challenges or the maturity of the technologies necessary to achieve the full capability. DOD has preferred to make fewer but heavier, larger, and more complex satellites[40] that perform a multitude of missions rather than larger constellations of smaller, less complex satellites that gradually increase in sophistication. This has stretched technology challenges beyond current capabilities in some cases and vastly increased the complexities related to software.

- Many of the cost and schedule problems identified were tied in part to diffuse leadership and organizational stovepipes throughout DOD, particularly with respect to DOD's ability to coordinate delivery of space, ground, and user assets. Additionally DOD faces a situation where satellites with advances in capability will be residing for years in space without users being able to take full advantage of them because investments and planning for ground, user, and space components were not well coordinated.

---

40. This preference stems from the satellite "real estate" constraint. With space launch prices ranging from around USD 100 million to well over USD 200 million, space programs often seek to maximize the "real estate" on board a satellite by including more capabilities that can sometimes be handled by a single program or within the time period desired for the program.

All of these criticisms of DOD's legacy space acquisitions projects will also apply to the missions of ORS. A variety of offices undertake ORS-related operations and a number of important personnel have provided their own version of what ORS is meant to accomplish (see Appendix F). The ORS concept is not commonly understood by all members of the war fighter and national security space communities. Key stakeholders do not share a common understanding of the ORS concept for two primary reasons-the ORS concept is not clearly defined in its initial guidance documents and DOD has not adequately communicated the concept to key stakeholders[41]. Also, there has been very little scrutiny of the technical feasibility of TacSats before project commitments were extended. Proponents have claimed that TacSats would quickly and cheaply provide 24/7 capabilities to warfighters across a number of mission areas and the DOD seems to have accepted that premise with very little proof. However, all recent ventures to orbit tactical satellites have surpassed estimates of cost and time (see Table 2.1 below for cost estimates).

Almost of all the experimental TacSat missions have crossed the target price of USD 20 million. Even though these TacSats have much simpler and less complex mission objectives than the strategic space systems discussed above they have suf-

41. The first extensive outreach to the combatant commands by the ORS Office was in preparation of the the November 2007 ORS senior War fighters Forum, which took place 6 months after the standup of the Joint ORS office. As stated in a recent GAO report a senior space planner, who is the lead for ORS for one combatant command, has mentioned that during preparatory briefings for the ORS Senior War fighters Forum, participants were told that the purpose of the forum would be to learn what space capabilities the various combatant commands needed that ORS might be able to address. However, after a couple of briefings, the purpose of the ORS Senior War fighters Forum had shifted to that of educating the combatant commands on the ORS process. The senior space planner explained that rather than asking the war fighter what they need, the focus was now on placing their needs into a process that had already developed. This would derail the technology from having user buy-in[222].

fered from cost escalation and schedule delays. It is then valid to conclude that if these satellites are used as visualized by ORS proponents they will end up costing much more. Given this it is very unrealistic to expect the DOD to support TacSats when there is a real and immediate need for resources in the strategic legacy space systems.

Table 2.1: Costs of Selected National Security TacSat Like Demonstration Missions[179, 188]

Satellite	**Organization**	**Cost (Millions) in 2006 USD)**	**Year Launched**
Mightysat I	AFRL/Phillips Lab	7.4	1998
Space Technology Experiment (STEX)	NRO	88.0	1998
Mightysat II	AFRL	42.6	2000
XSS-10	AFRL	43.6	2003
XSS-11	AFRL	67.1	2005
TacSat 2	AFRL	39	2006
TacSat 3	AFRL	40	2009
TacSat 4	NRL	41	2011 Scheduled
TacSat 1	NRL	9.3	Mission canceled

2.6 Conclusions

This chapter has systematically demonstrated the difficulty in achieving success in each of the four focus areas that supporters of ORS hope to innovate in. Section 2.1 of this chapter outlined the difficulties in achieving the "Chileworks"

like rapid satellite manufacturing model. To operationalize the Chileworks concept, new organizations would have to be created to train, exercise, and eventually conduct operations at a accelerated pace. It will also be highly cost-intensive to maintain on hold the inventory and the workforce needed to achieve such rapid time lines. None of these factors are well defined and accounted for, which creates a large uncertainty about the cost-effectiveness of Chileworks manufacturing concept. Also, the ORS community has not addressed how the Assembly, Integration and Testing (AIT) requirements that underlie current satellite manufacturing operations would affect the Chileworks concept.

Section 2.2 of this chapter examines the ability to rapidly launch satellites within days to weeks in response to an immediate tactical requirement. The aim of ORS proponents is to launch satellites rapidly and continuously within a time line that must fit the joint force commander's unfolding mission requirements. Such rapid satellite launch operations have not been demonstrated to date. The ORS community has not identified any mechanism to compress the current satellite launch times. Section 2.3 evaluates the cost of launchers and its effect on ORS missions. In order to be cost competitive, ORS supporters want to to achieve an acquisition cost of about USD 20 million per satellite and launch vehicle combined. However, all potential responsive launch vehicles alone currently cost close to or more than the USD 20 million for launches to LEO. This raises doubts on the viability of accomplishing ORS missions within the stated cost.

Section 2.4 demonstrates the operational limitations emerging from orbital mechanics that make the idea of TacSats unrealistic. A combination of physical

constraints placed on satellites by orbital mechanics and operational requirements placed on their payloads by the mission that can be performed from space prevent all but the most rudimentary missions from being attainable within the cost goals and launch time constraints. Finally, section 2.5 concludes this chapter by making the case that scarce DOD resources would be more usefully spent in addressing the immediate requirements in legacy space systems rather than diverting it to ORS missions whose purpose and viability rest on weak foundations.

Chapter 3

What Can be Achieved by Attacking Satellites?

A pivotal question in the debate on space security is: what could be achieved by attacking satellites? A significant portion of that debate in the U.S. proceeds under the assumption that there are substantial benefits for an adversary in attacking U.S. satellites. A sampling of this notion is given below.

- America's reliance on space is so extensive that a widespread loss of space capabilities would prove disastrous for both its military security and its civilian welfare. The Armed Forces would be obliged to hunker down in a defensive crouch awaiting withdrawal from dozens of no-longer-tenable foreign deployments[73].

- The sudden major loss of satellite function would quickly throw U.S. military capabilities back twenty years or more and substantially damage U.S. and world economies. While backup systems could partially compensate for this loss, U.S. military forces would be significantly weakened[32].

- The U.S. now, more than at any point in its history, depends on space systems for its national security-and much more so than any other country. This combined, with the fact that those systems are becoming vulnerable to a growing number of potential adversaries, suggests that first-strike stability in space is eroding. If locked in a confrontation with the U.S., were the aggressor to con-

clude that war was inevitable, it would also realize that it would eventually have to pay a higher price if it did not attack U.S. space systems[80].

This chapter will make the case that these concerns are exaggerated. Although U.S. armed forces rely extensively on its satellite infrastructure, that does not immediately make them desirable targets. The functions performed by satellites like navigation, reconnaissance, and communications are diffused among large constellations. These constellations of satellites possess redundancies that enable them to serve the U.S. armed forces even after some of them are lost. Also, some of the functions performed by these satellites can be substituted for by other terrestrial and aerial systems. Even though these other systems will not completely compensate for lost satellites, there is no analytical evidence that suggests the U.S. would be completely disabled if some of its military satellites are lost.

Section 3.1 below will examine the benefits of attacking the GPS satellite system. Section 3.2 will then examine the benefits of attacking U.S. satellite reconnaissance platforms. Finally, section 3.3 will examine the benefits of attacking U.S. communication satellites. These sections of this chapter will demonstrate in detail why feasible attacks on US satellite systems cannot be expected to confer decisive advantage in a military engagement.

It is possible, however, to conceive of more limited motivations for an adversary to attack U.S. satellites. An adversary could arguably attack U.S. satellites as a warning of further escalation in response to a certain U.S. military action, based on the assumption that attacking U.S. satellite assets would be less severe than

attacking U.S. battle ships or U.S. ground troops. This chapter does not study the logic behind such an action by an adversary nor does it try to formulate political arrangements that would prevent that event. Those questions are left to future developments of this chapter. This chapter only attempts to evaluate the military advantages that might induce an adversary to attack U.S. satellites.

3.1 Is There a Benefit to Attacking GPS Satellites?

In order to evaluate the effort required and benefits accrued from attacking GPS satellites, a simulation is performed in this section. The various steps of the simulation and the conclusions drawn from the simulation are outlined below:

- An Area of Responsibility (AOR) encompassing Taiwan and the part of East China Sea between China[1] and Taiwan was modeled in STK[2]. The modeled region is shown in figures 3.1 and in 3.2 on page 82. A 3D illustration of the model is shown in figure 3.3 on page 83.

- Once the AOR has been defined, it is granulated into finer points along every latitude and longitude direction. This is done to determine the cumulative GPS Geometric Dilution of Precision[3] (GDOP) in the entire AOR. Figure 3.4

1. For the purposes of illustration only, China is chosen as the candidate nation that is attempting to attack GPS satellites. This dissertation does not attribute such an intention to China.
2. STK or Satellite Tool Kit is a commercial software for orbital analysis. An evaluation copy of the software was used to undertake the analysis in this chapter.
3. Geometric Dilution of Precision (GDOP) is a common measure of GPS 3D positioning error. Generally, if the GDOP rises above six, the satellite geometry is not very good and there will increased positioning error. The operational GPS constellation is designed to provide a world-wide GDOP of less than six, assuming at least four satellite are visible[141].

on page 83 shows the cumulative GDOP over the entire AOR. Also, 25 facilities are defined in the AOR as shown in figure 3.2 on page 82. This is done to determine the individual GPS GDOP values at specific locations in the AOR. Figure 3.5 on page 84 shows the GDOP at the individual facilities distributed along the diagonal of the AOR. It can be seen that the GDOP is below 3 over the entire AOR and at each of the individual facilities. An adversary like China would prefer to degrade this value to above 6.

- The simulation is performed over a period of 48 hours starting from 00:00:00.000 UTCG on 11 March, 2012 to 00:00:00.000 UTCG 13 March, 2012.

- Now, in the simulation it is assumed that China intends to attack GPS satellites in the AOR at 00:00:00.000 UTCG on 12 March, 2012. In order to determine which satellites China should attack to obtain the best possible advantage over U.S., the 5 satellites contributing the most to the GDOP values at the instant of attack are chosen. Figure 3.6 on page 85 shows the 5 satellites that could be attacked. To model the attack scenario, these satellites are removed one after the other from the simulation in order to evaluate the effect of on an attack on GPS satellites.

- Figure 3.7 on page 86 shows the effect of removing the 5 selected satellites one-by-one on the defined AOR. It is observed that removing up to 3 satellites does not significantly degrade the GDOP. When 4 or 5 satellites are removed (i.e., attacked) the GDOP values are degraded above 6. The GDOP degrades around the time chosen for the attack. However, the degradation lasts only

for approximately 2 hours. After that the redundancy of the GPS satellite constellation makes up for the degradation that occurred due to the attack on the GPS satellites.

- The same phenomenon is also observed in the case of the individual facilities distributed diagonally across the AOR. For example, figure 3.8 on page 87 shows that removing up to 3 satellites does not affect the GDOP value over facility 1. Removing 4 or 5 satellites, degrades the GDOP over facility 1 for a period of 42 minutes. After that the redundancy of the GPS satellite constellation makes up for the effects of the attack on GPS satellites.

- Figure 3.9 on page 88 shows that the effect of removing 4 or 5 GPS satellites degrades the GDOP over facility 7 for a period of 48 minutes. Figure 3.10 on page 89 shows that the effect of removing 4 or 5 GPS satellites degrades the GCOP over facility 13 for a period of approximately 2 hours. Figure 3.11 on page 90 shows that the effect of removing 4 or 5 GPS satellites degrades the DCOP over facility 19 for a period of approximately 2 hours. Finally, Figure 3.12 on page 91 shows that the effect of removing 4 or 5 GPS satellites degrades the GDOP over facility 25 for a period of approximately 2 hours.

- In sum, to affect the GDOP over the AOR, the Chinese would have to simultaneously attack at least 4 GPS satellites. The next chapter on ASATs will demonstrate that China does not possess such a capability.

- Even if it did possess such a capability, there does not seem to be any abiding

tactical logic in attacking GPS satellites. As previously argued, any benefits of the attack last only for a period of 2 hours at most. After that, the redundancy of the GPS satellite constellation makes up for the effects of the attack on GPS satellites.

- Also, the degradation of the GDOP values shows a periodic pattern after the modeled attack. Figure 3.13 on page 92 shows that the degradation of GDOP occurs at the same time everyday. This makes it easier for the U.S. to respond and adapt its strategy after the attack. The U.S. would still be able to navigate on land or sea without GPS, albeit with lesser accuracy for that period. As for its ability to use precision munitions, table 3.1 below on page 93 shows that the percentage of GPS-based Joint Direct Attack Munitions (JDAMs) usage has been around 25% in recent U.S. operations. The U.S. could easily shift to its other precision-guided munitions or non-precision munitions[4] during the 2 hour time period when GPS is not available at the required accuracy.

- All that China would obtain from executing the attacks on the GPS satellites is a two hour window. That outcome does not seem to be worth the retribution the action would entail.

---

4. Uncertainty as to what is being targeted and where weapons will fall can have a significant psychological effect on an enemy. Interviews of captured Iraqi soldiers during the Gulf War revealed that their greatest fear was being attacked by B-52s, each dropping 38,250 pounds of conventional, non-precision ordinance. It is especially true for troop formations, but reasonably, applicable at all echelons, that the shock, noise, and disruption of an air attack can have a paralyzing and demoralizing effect out of all proportion to the amount of physical destruction achieved[109]. By attacking GPS satellites China might bring out an undesirable situation of this sort.

Figure 3.1: AOR - 2D Image

Figure 3.2: AOR - 2D Image (close-up)

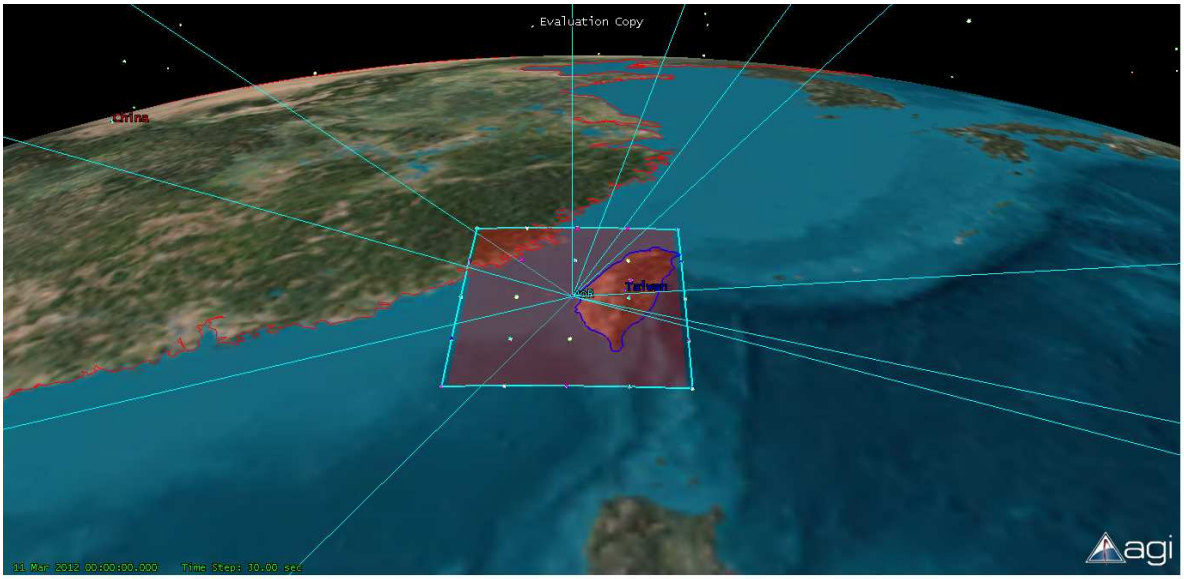

Figure 3.3: AOR - 3D Image

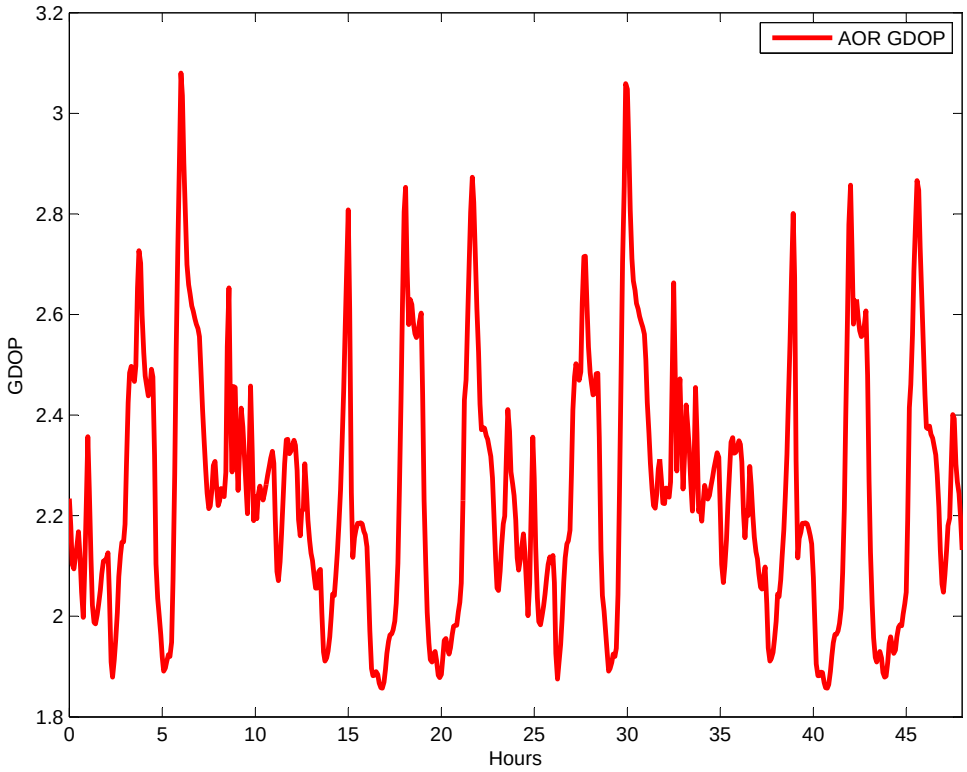

Figure 3.4: AOR GDOP Pre-Attack (11 Mar 2012 00:00:00.000 UTCG to 13 Mar 2012 00:00:00.000 UTCG)

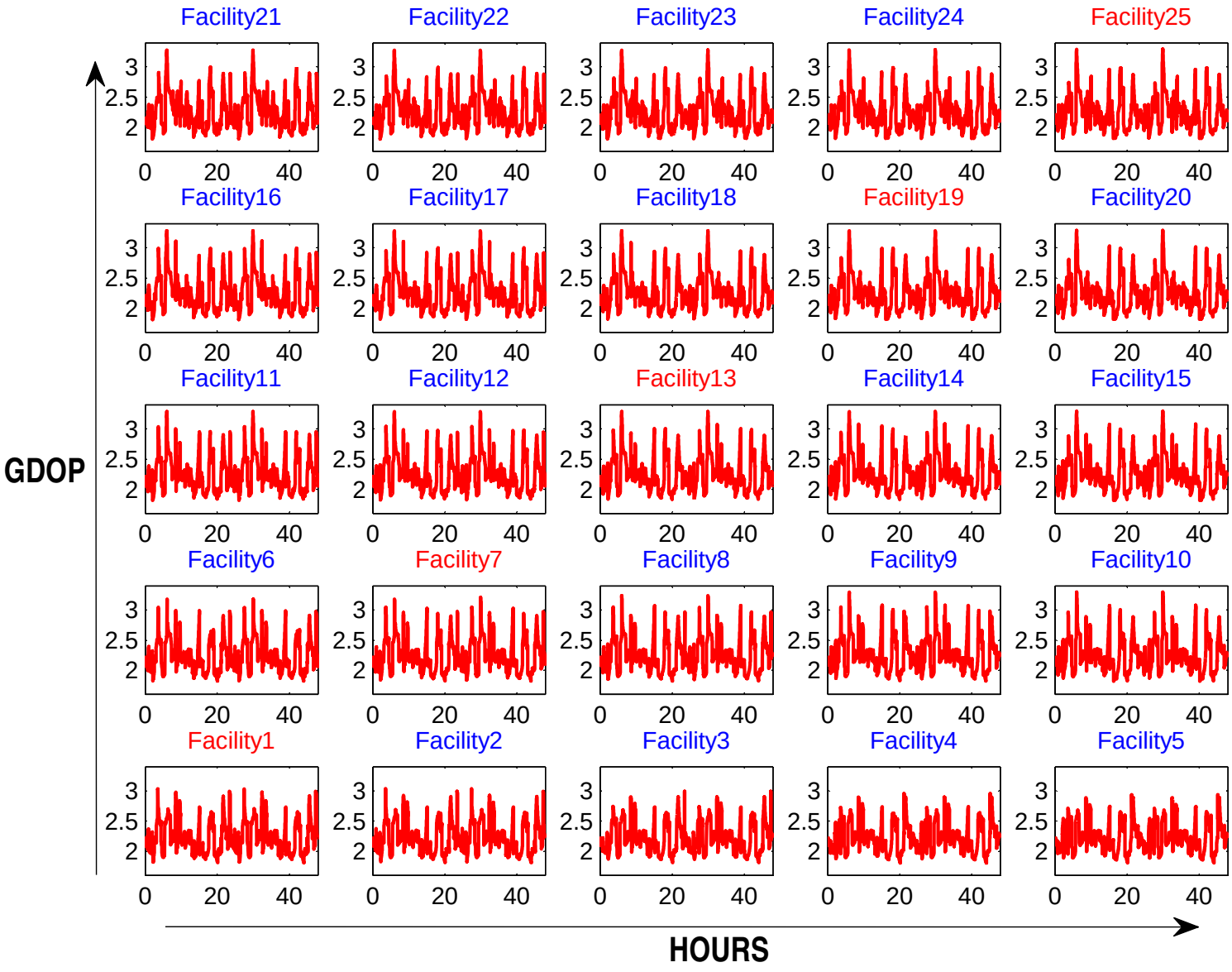

Figure 3.5: Facilities GDOP Pre-Attack (11 Mar 2012 00:00:00.000 UTCG to 13 Mar 2012 00:00:00.000 UTCG)

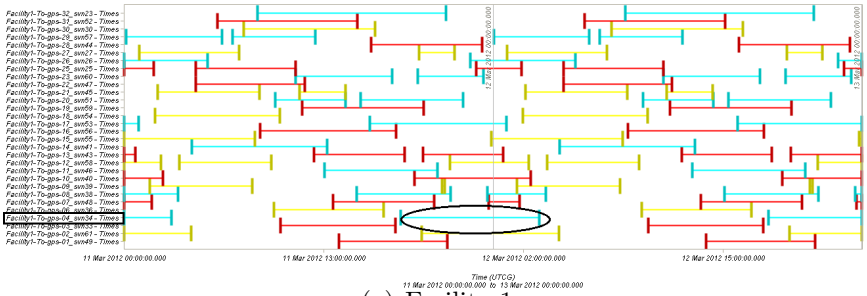

(a) Facility 1

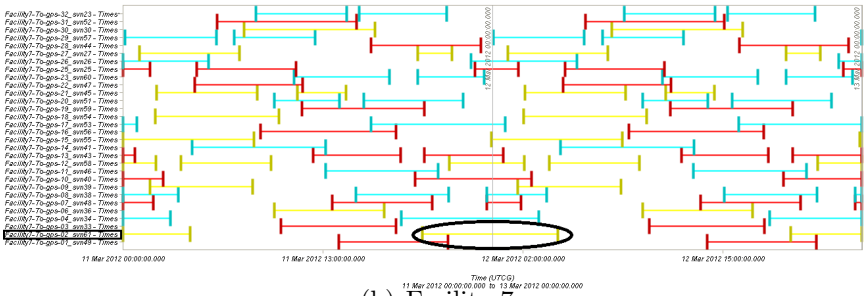

(b) Facility 7

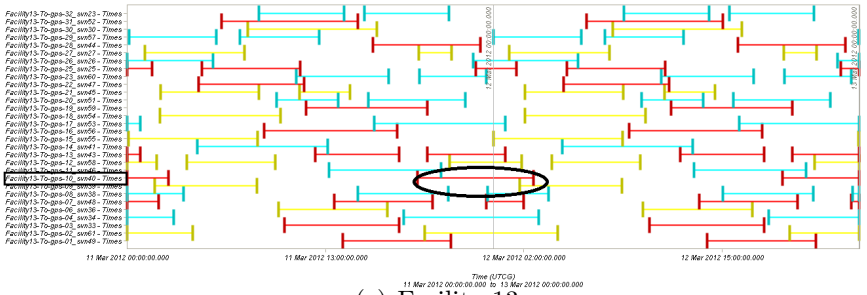

(c) Facility 13

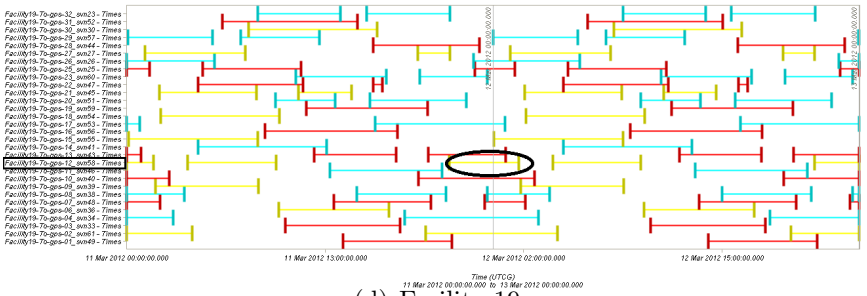

(d) Facility 19

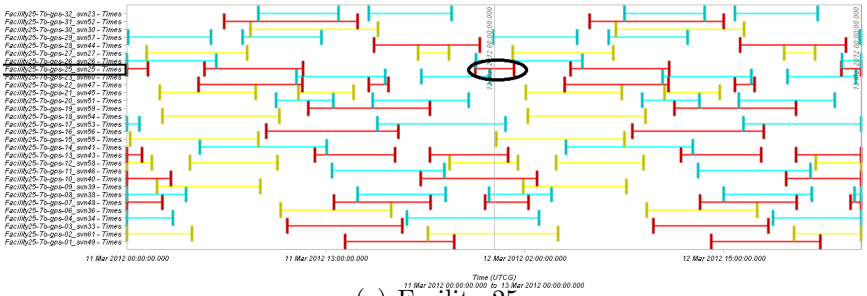

(e) Facility 25

Figure 3.6: GPS Satellite Distribution (11 Mar 2012 00:00:00.000 UTCG to 13 Mar 2012 00:00:00.000 UTCG)

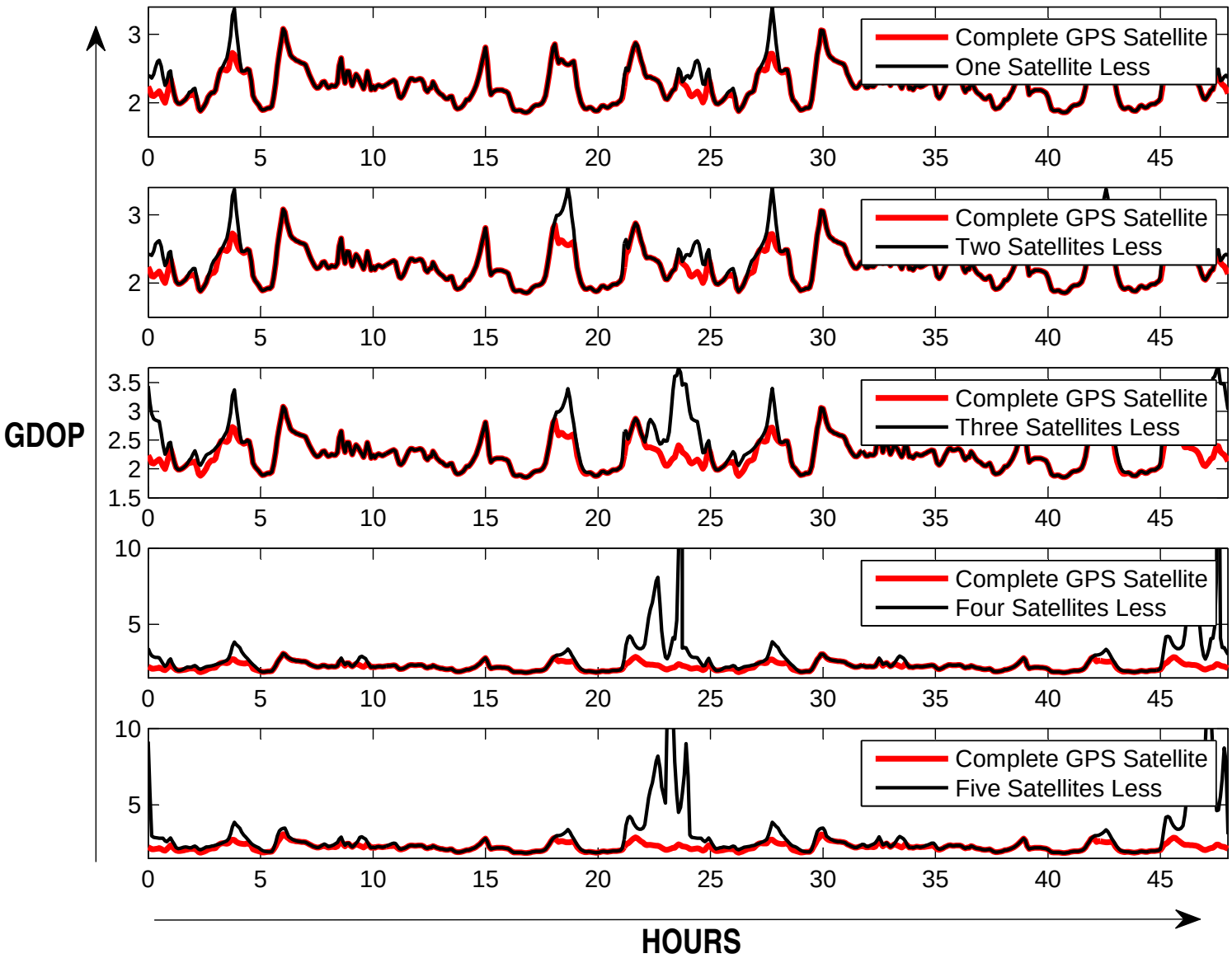

Figure 3.7: AOR GDOP Post-Attack (11 Mar 2012 00:00:00.000 UTCG to 13 Mar 2012 00:00:00.000 UTCG)

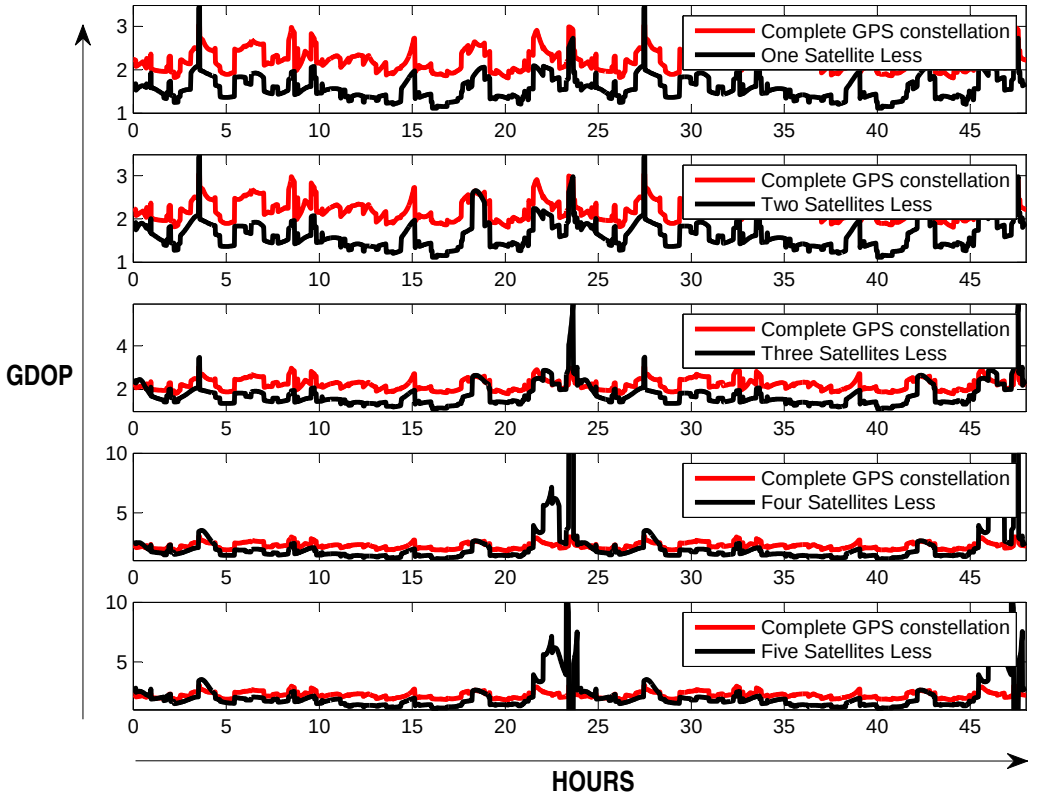

(a) Facility 1 GDOP Post-Attack

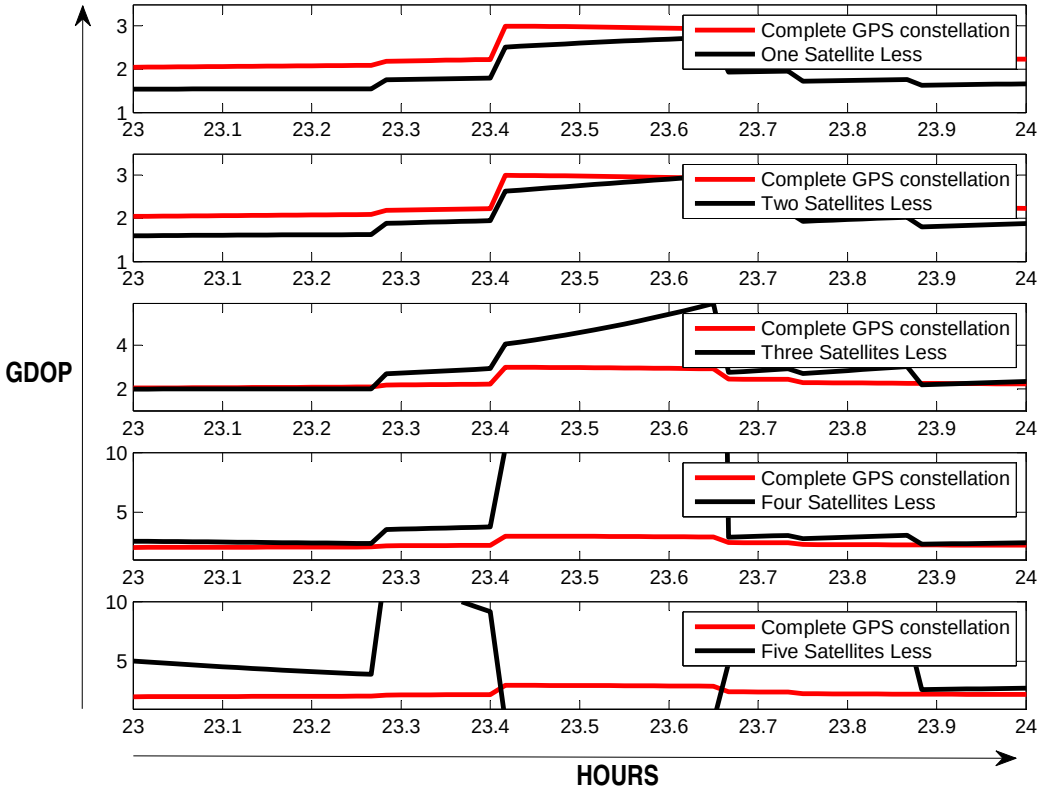

(b) Facility 1 GDOP Post-Attack (close-up)

Figure 3.8: Facility 1 GDOP Post-Attack (11 Mar 2012 00:00:00.000 UTCG to 13 Mar 2012 00:00:00.000 UTCG)

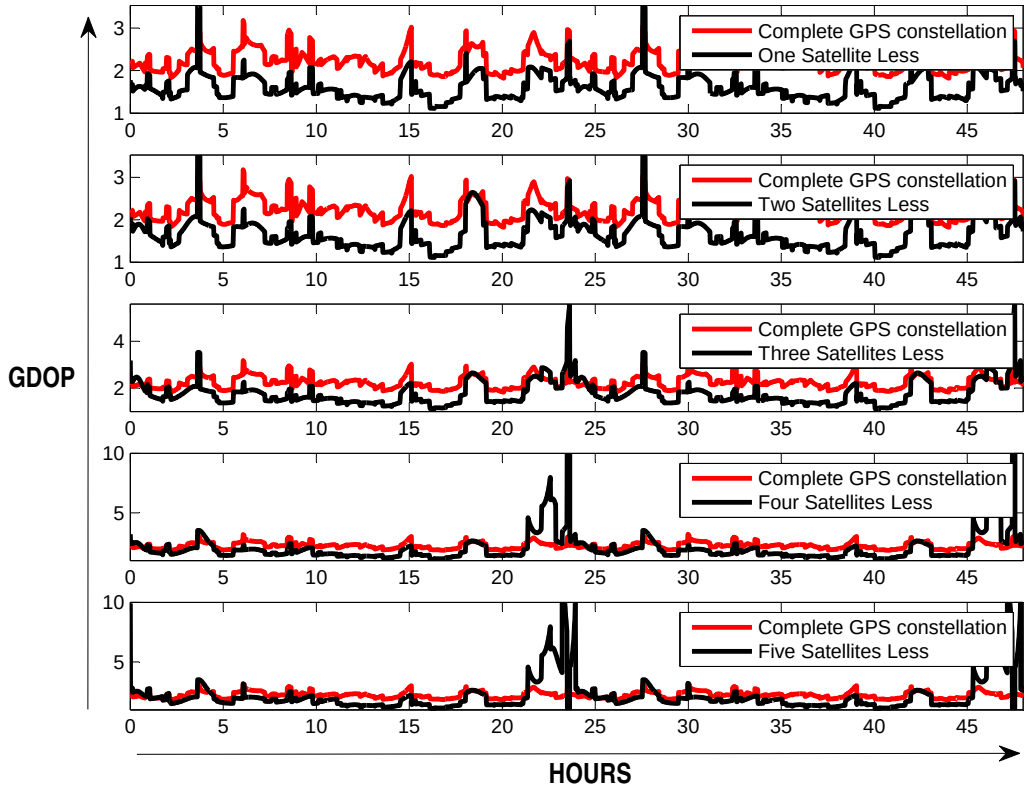

(a) Facility 7 GDOP Post-Attack

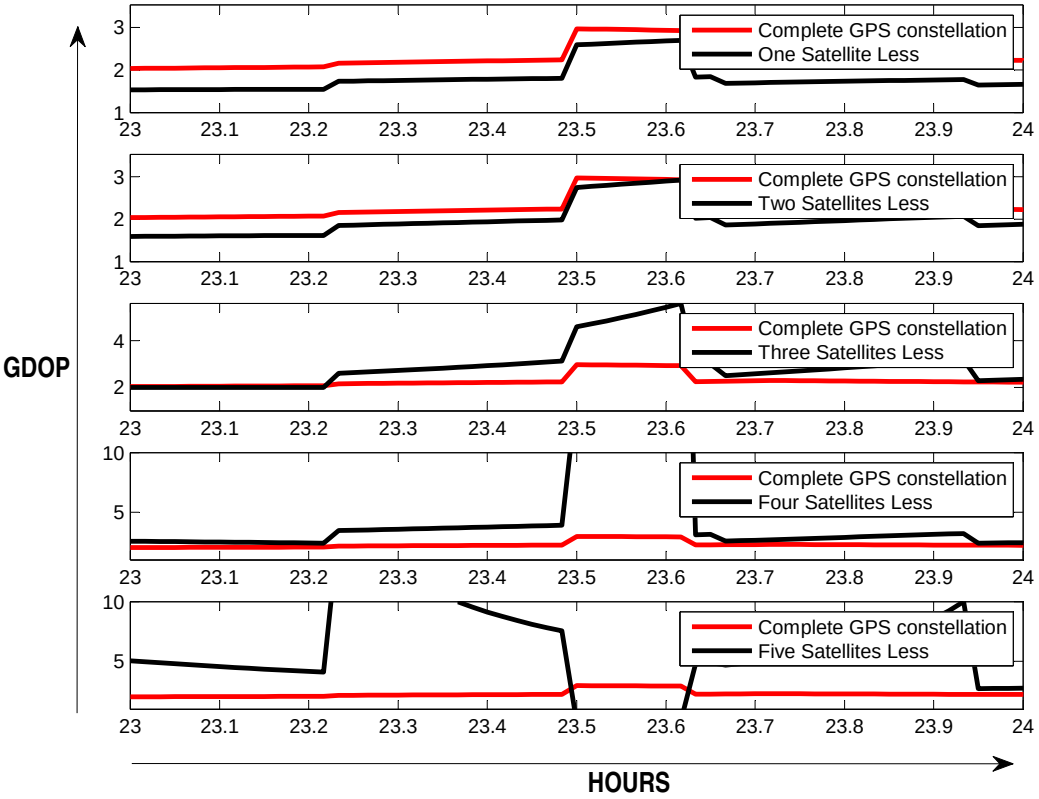

(b) Facility 7 GDOP Post-Attack (close-up)

Figure 3.9: Facility 7 GDOP Post-Attack (11 Mar 2012 00:00:00.000 UTCG to 13 Mar 2012 00:00:00.000 UTCG)

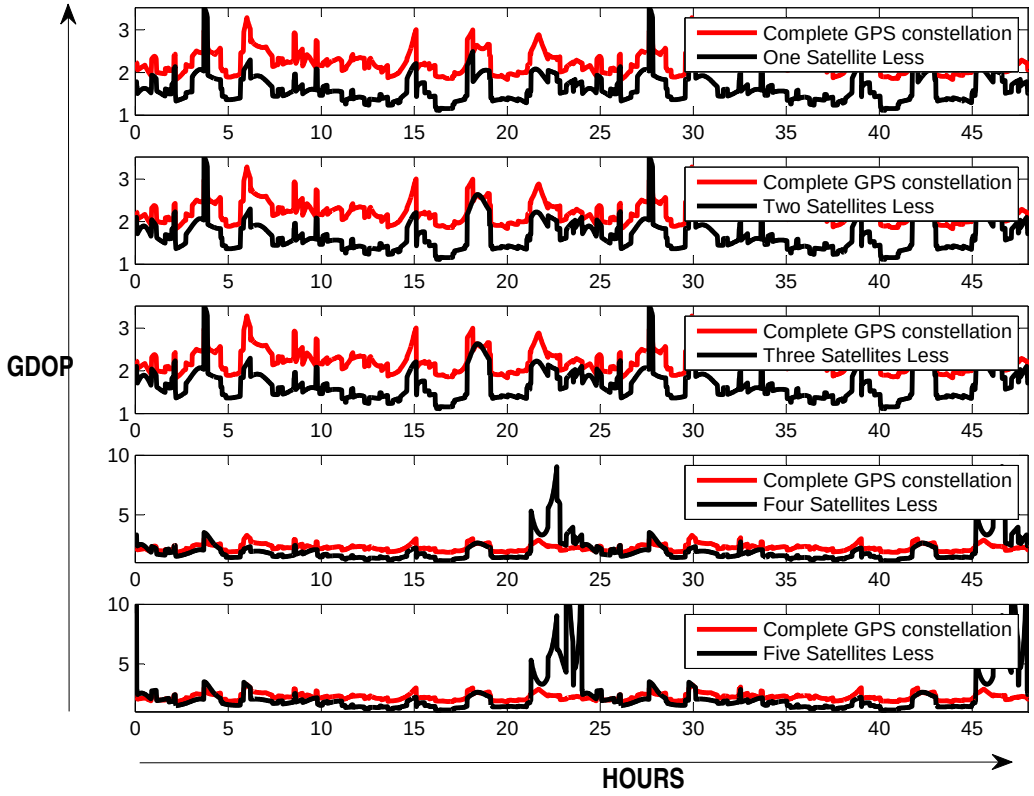

(a) Facility 13 GDOP Post-Attack

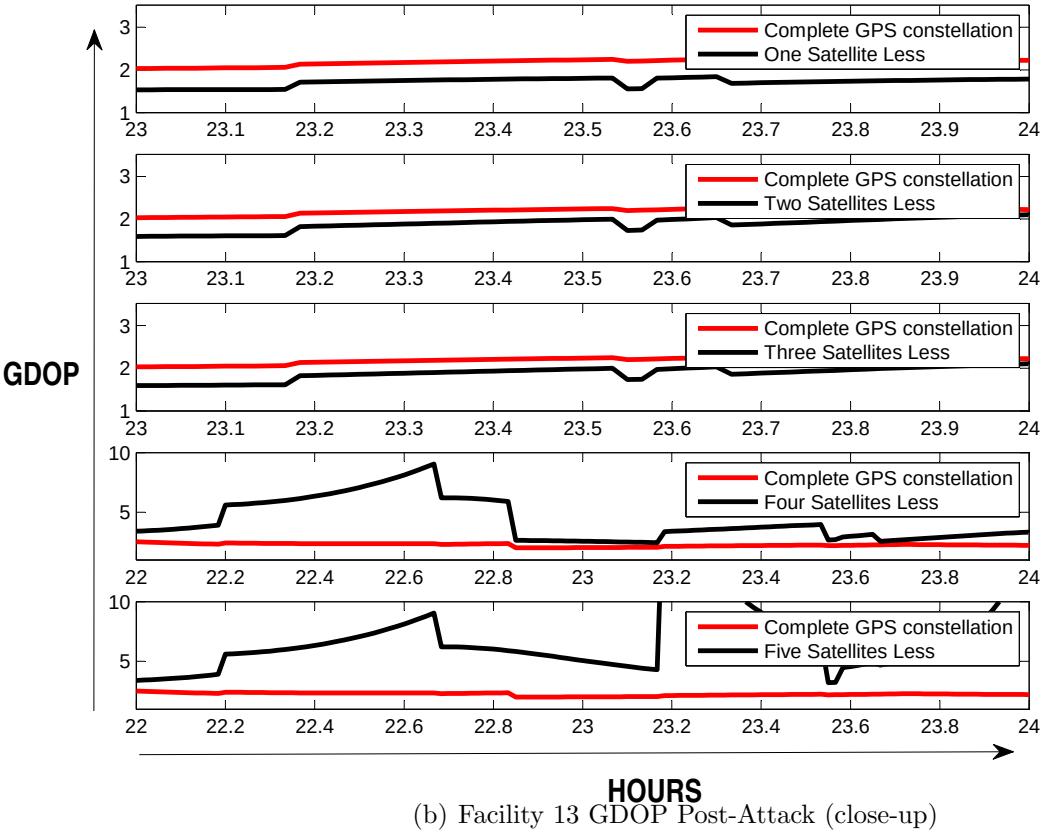

(b) Facility 13 GDOP Post-Attack (close-up)

Figure 3.10: Facility 13 GDOP Post-Attack (11 Mar 2012 00:00:00.000 UTCG to 13 Mar 2012 00:00:00.000 UTCG)

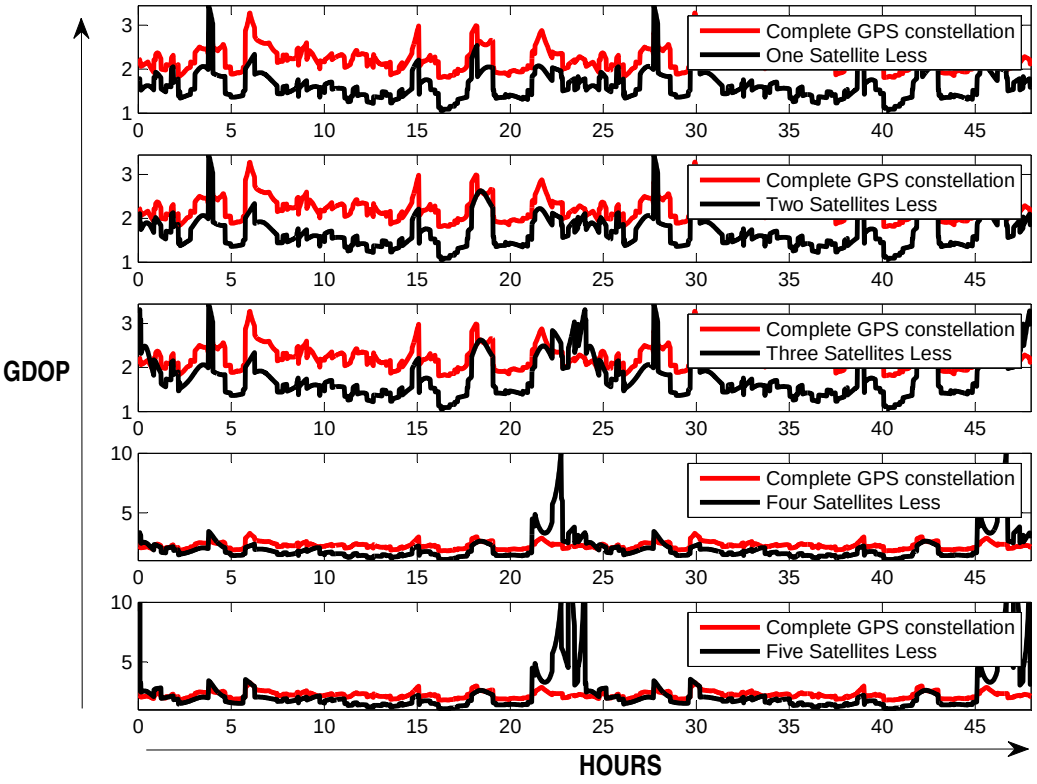

(a) Facility 19 GDOP Post-Attack

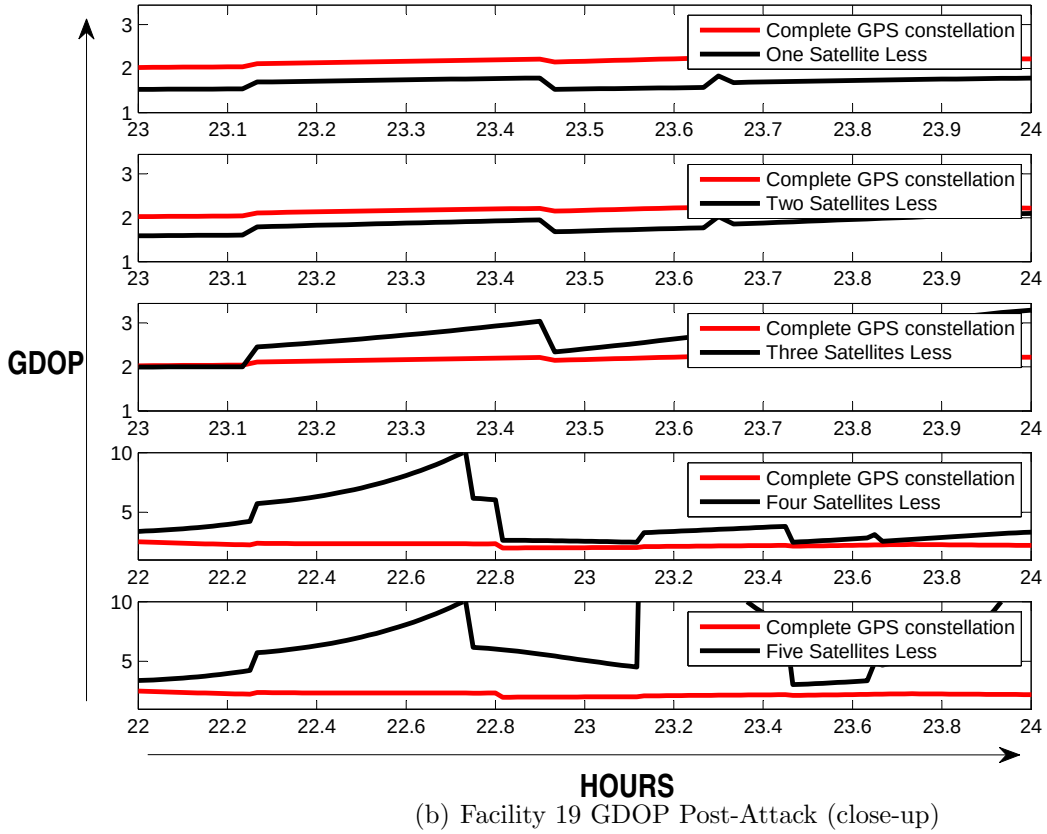

(b) Facility 19 GDOP Post-Attack (close-up)

Figure 3.11: Facility 19 GDOP Post-Attack (11 Mar 2012 00:00:00.000 UTCG to 13 Mar 2012 00:00:00.000 UTCG)

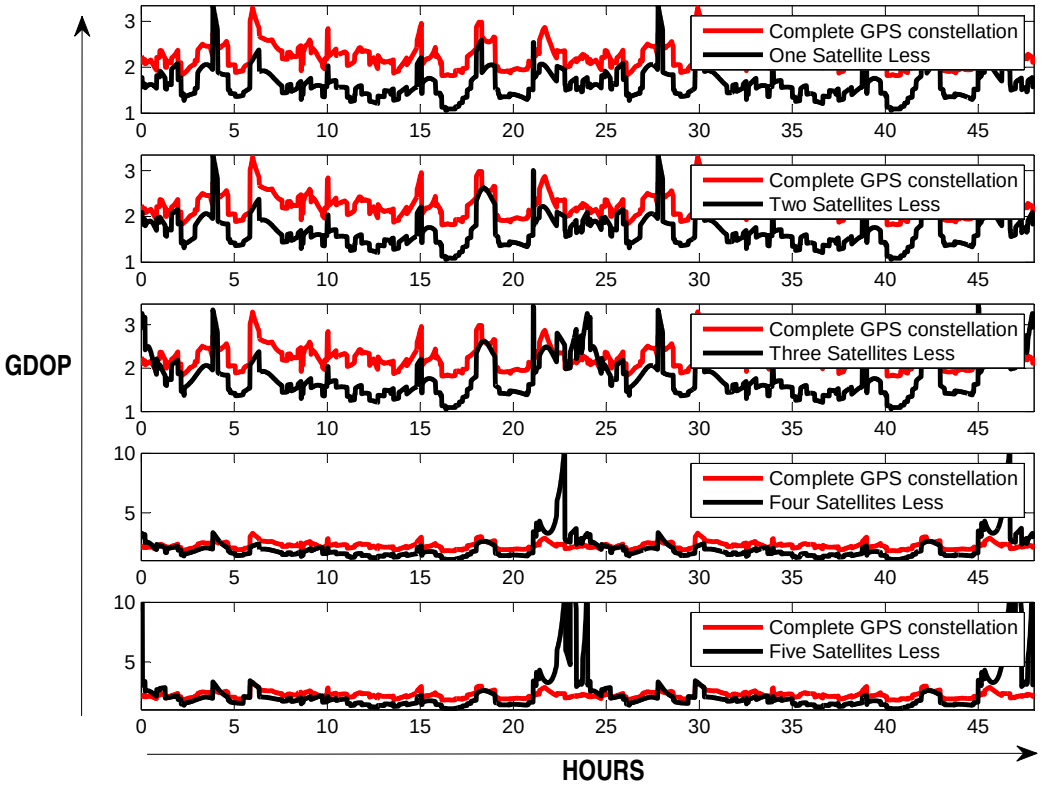

(a) Facility 25 GDOP Post-Attack

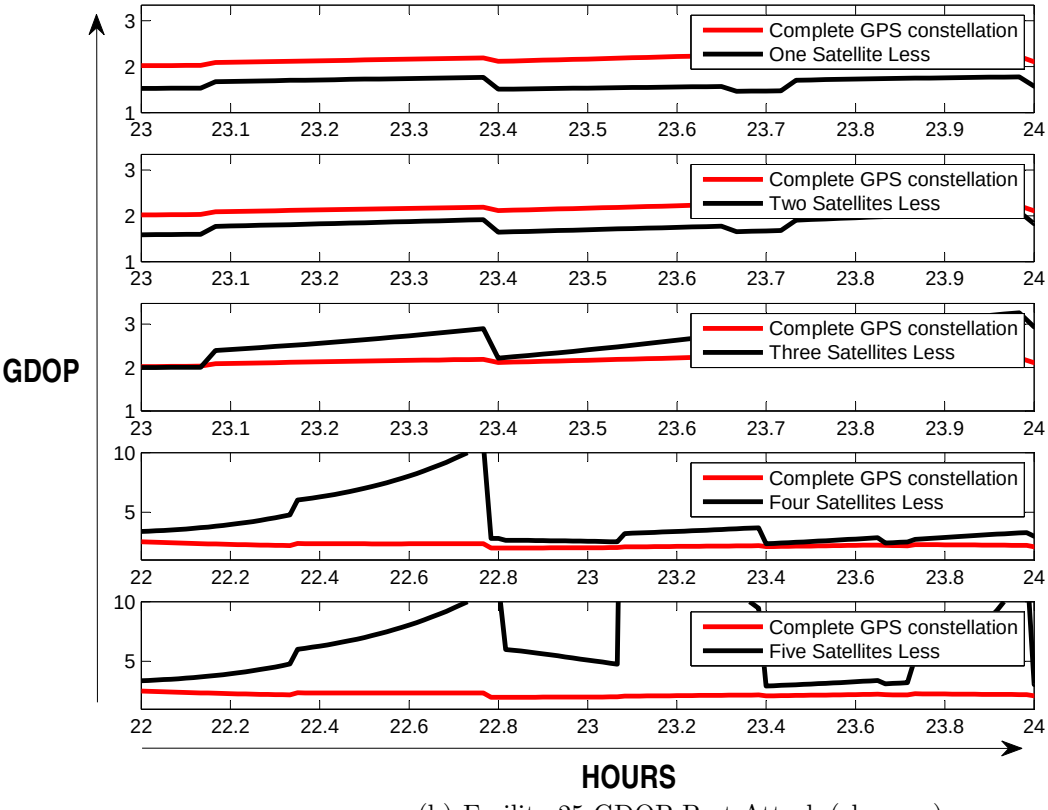

(b) Facility 25 GDOP Post-Attack (close-up)

Figure 3.12: Facility 25 GDOP Post-Attack (11 Mar 2012 00:00:00.000 UTCG to 13 Mar 2012 00:00:00.000 UTCG)

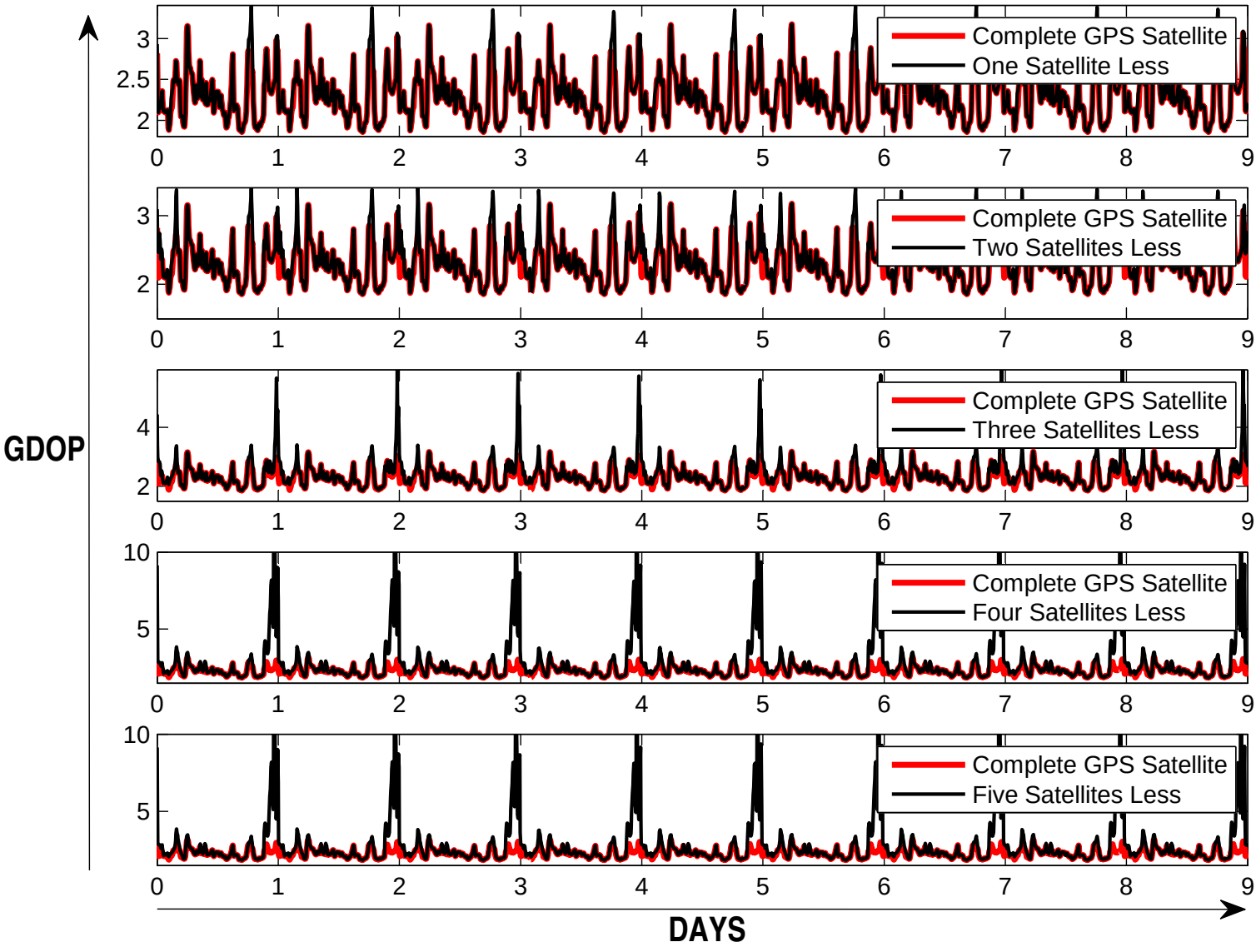

Figure 3.13: AOR GDOP Post-Attack (11 Mar 2012 00:00:00.000 UTCG to 20 Mar 2012 00:00:00.000 UTCG)

Table 3.1: Percentage of Precision Munitions Used in Battle Operations[37, 230, 88, 111, 194]

	Operation			
	Desert Storm (1991)	**Allied Force (1999)**	**Enduring Freedom (Oct. 2001-Feb. 2002)**	**Iraqi Freedom (2003)**
Total Air Delivered Weapons	227,648	23,644	17,459	29,199
Total PGMs delivered	17,644	7,057	10,548	19,948
% of PGMs Employed	7.70%	29.80%	60.40%	68.32%
Total JDAMs Used	0	652	5000	6,542
% of JDAMs Used	0	0.30	28.64	22.40

3.2 Is There a Benefit to Attacking Reconnaissance Satellites?

This section of the chapter will argue that although U.S. reconnaissance satellites have important applications in a battle, it does not immediately render them as uniquely desirable targets. The satellite reconnaissance capability is spread across many satellites. Attacking all of them might be impossible for an adversary like China. Also, for most tactical battlefield reconnaissance needs, aerial platforms are more appropriate. The publicly available data on Operation Desert Storm reveals that battlefield intelligence was often obtained from aerial platforms (see table 3.2 below).

General Horner, Commander of coalition Air Forces' during Operation Desert Storm pulled in every reconnaissance platform the coalition possessed. That included the high-flying TR-1/U-2R aircraft, the RF-4C for tactical information, the

Table 3.2: Total Reconnaissance Sorties, 17 January - 28 February 1991[70]

Reconnaissance	**Side-Looking Aperture Radar (SLAR)**	**Observation Flight**
2,406	147	683
Reconnaissance missions flown by U.S. A-6, A-7, EA-6B, F-14, F/A-18, P-3, RC-135, RF-4C, S-3, MH-60, and coalition RF-5, Tornado GR-1, Jaguar, Mirage F1-CR and Mirage 2000 aircraft. SLAR missions flown by U.S. OV-1D and RC-12 aircraft. Observation flight missions flown by U.S. A-6, F-16, F/A-18, and S-3B aircraft.		

RC-135 Rivet Joint to monitor electronic emissions, the Boeing E-3B/C Airborne Warning and Control System (AWCACS) and the EC-130E Airborne Battlefield Command and Control Center (ABCCC) for combat management, the E-8A Joint Surveillance Target Attack Radar System (JSTARS) to find ground targets, the Navy F-14s equipped with TARPS (Tactical Air Reconnaissance Pod System) and remotely-piloted vehicles. Details on the role played by each of these platforms are discussed below. Importantly, all of these platforms (some in more advanced versions) are still in service with the U.S. forces, raising questions on the value of attacking U.S. reconnaissance satellites. Its seems that these aerial platforms would be more attractive targets tactically and would have the additional advantage of not escalating the conflict.

- The TR-1A and U-2R carried a multitude of sensors, including infrared, radar, and long-range optical systems for all-weather capability, day or night. The aircraft can be tailored for specific intelligence missions by changing the sensors in the wing pods. Other SAR-equipped aircraft also played a vital part in the

Gulf War. When the TR-1As could not take off due to excessive winds, Army SAR-equipped OV-1Ds were called in to fill in some of the intelligence gaps[92].

- The 117th deployed to Saudi Arabia during Desert Storm was provided with six RF-4Cs equipped with the long-range oblique photograph (LOROP) camera. The RF-4C squadron provided photographs of key targets while staying outside of enemy defenses[92].

- During Desert Shield, General Horner repeatedly sent F-15s, Tornados, and F/A-18s racing toward the Iraqi border to locate Iraqi air defenses and discern operating frequencies and types of communications. They would turn around before reaching the border but not before triggering an Iraqi response. Big RC-135 Rivet Joint electronic reconnaissance aircraft monitored the Iraqi radar and communications response, gradually building a comprehensive knowledge of Iraqi defensive systems and capabilities.

- TARPS transforms the F-14 into a reconnaissance platform. The pod contains three sensors and ancillary control components. The sensors include two high resolution cameras–one for forward oblique and vertical photography and the other for panaromic views–and a sophisticated infrared sensing system. Although conceived as a low-to-medium altitude strike planning and battle damage assessment system, TARPS was employed at high altitude during Desert Storm because of the heavy air defense batteries[92].

- During Operation Desert Storm, the E-3B/C AWACS controlled the air-to-

air war and EC-130E ABCCC controlled the air-to-ground war. The flexible, mobile, jam resistant E-3B/C Sentry was a highly modified Boeing 707 transport. The large aircraft carried an extensive complement of mission avionics, including a computer, radar, IFF, communications, display, and navigation systems. The AWACS radar provided a look-down capability and could acquire and track multiple targets. The ABCCC is a C-130 specially modified to carry a high-tech command, control, and communications module in the cargo compartment. It was used to coordinate the aerial operations.

- The JSTARS was an extremely useful reconnaissance platform that provided very high resolution imagery of ground troops during Operation Desert Storm. The JSTARS was a modified Boeing 707-300 equipped with a Norden AN/APY-3 phased array (electronically steered) multimode and a side-looking airborne radar (SLAR) antenna. The radar was capable of searching out targets over a 77,000-sq-km area with a line of sight range in excess of 250 km (see figure 3.14 below for an indication of the coverage into Kuwait and Iraq that JSTARS had during the 1991 Operation Desert Storm). It operated in two modes: Doppler (for slow-moving objects) and synthetic aperture (for stationary objects). In the former mode a moving target indicator (MTI) is used for wide-area airborne battlefield surveillance, while in the latter mode the synthetic aperture radar (SAR) is employed for fixed-target imagery[141, 92].

- The utility of JSTARS was starkly observed in three different events during Operation Desert Storm. On January 29 (4 weeks before the main coalition

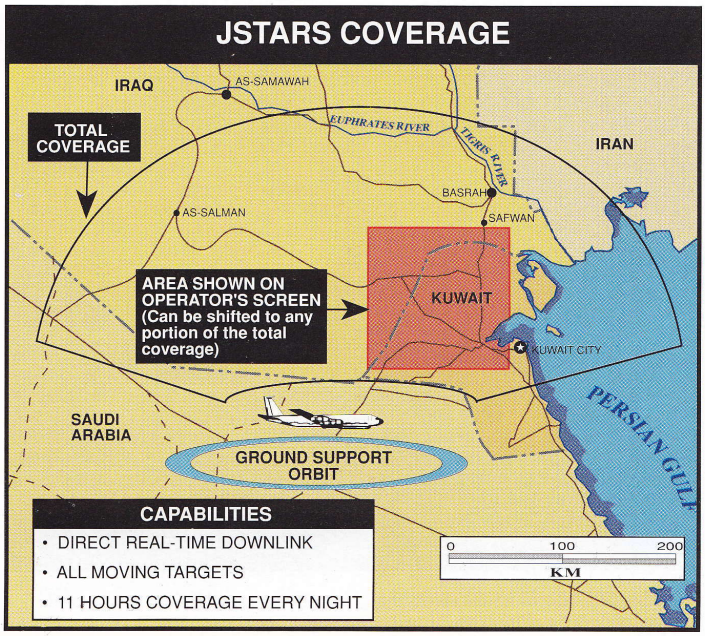

Figure 3.14: Operation Desert Storm JSTARS Coverage[164]

ground offensive), Saddam Hussein ordered an attack on Khajfi, just inside Saudi Arabia. Unfortunately for him, an E-8A Joint STARS aircraft was on the job, using its moving target indicator and side-looking radar to look deep inside the battle area. Joint STARS operators detected an armored division assembly area and a convoy of more than sixty vehicles moving through the night into Saudi Arabia. They called in two A-10s and an AC-130 gunship and vectored them onto the convoy and the staging area with the result that seventy-one vehicles were destroyed. Saddam therefore started his attack on Khafji short-handed. U.S. officials claim that, during the battle for the Saudi border town of Khafji early in the war, Joint STARS crew members informed allied forces that no Iraqi units were coming to support their comrades who had

entered the town. Armed with this information, allied commanders launched an immediate and highly effective counterattack. Coalition air forces attacked the Iraqis in and around Khafji. After two days of fighting, most of Saddam's remaining forces withdrew and the rest surrendered[92].

- JSTARS aircraft was also used to watch Iraqi ground reaction when coalition troops moved into position for the "Left Hook" flanking movement. During the coalition ground offensive, JSTARS aircraft provided highly detailed images on Iraqi troop movements (see figures 3.15 and 3.16 below) using which the coalition forces were able modify their attack posture. Finally, on February 29 the JSTARS was able to capture the retreat in its radars. Using these images the retreating was targeted and stopped very effectively. This event was given the moniker, "the highway of death" because of the devastating effect it had on the Iraqis. Aerial platforms like JSTARS would have a much higher target value than reconnaissance satellites.

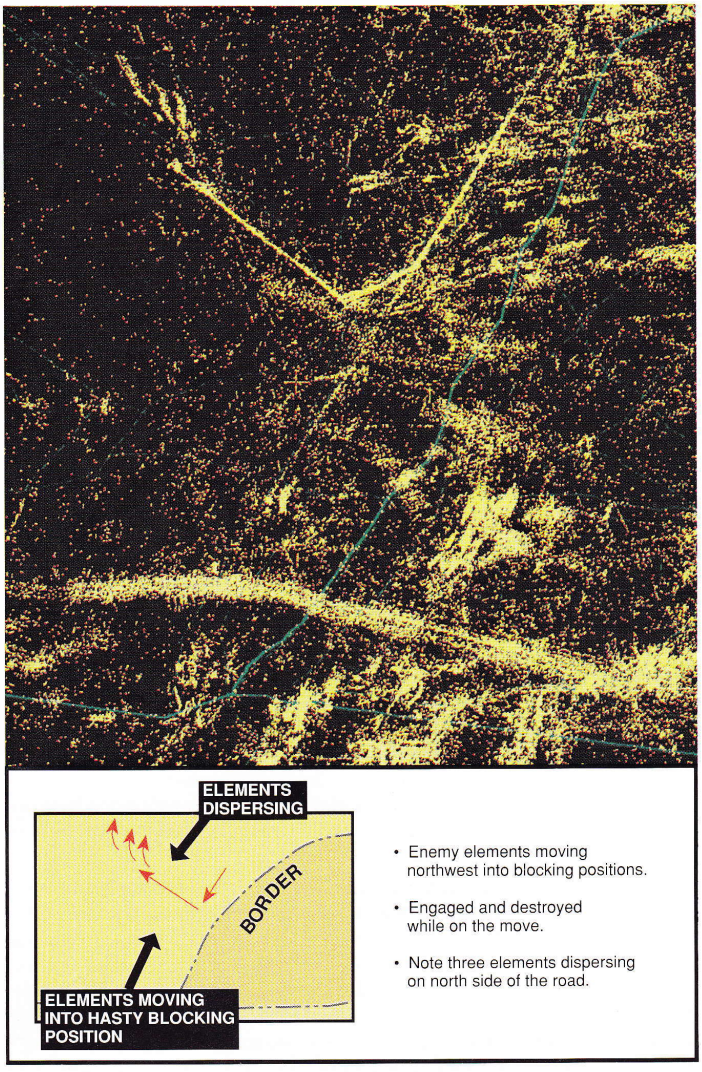

JSTARS readout, G plus 1, depicted 12th Armored Division and Republican Guard elements moving into blocking positions. This picture allowed General Stewart to track the Iraqi GHQ battle plan as it developed on the ground.

Figure 3.15: Desert Storm JSTARS Image During Left Hook Maneuver[164]

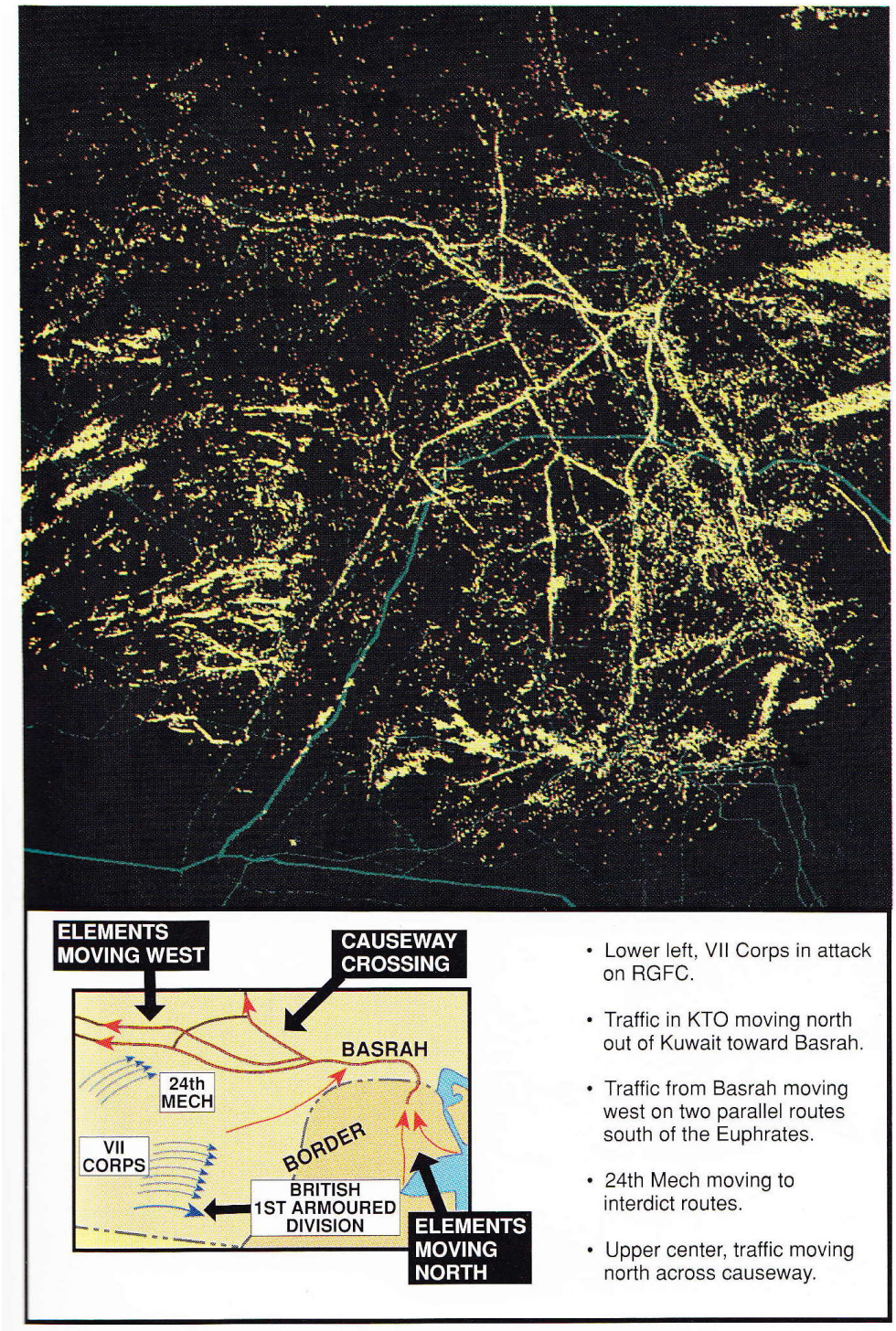

JSTARS readout, G plus 2, depicted VII Corps and 24th Infantry Division elements closing on the Republican Guard. Note that the Iraqis continued to move toward Basrah and to use the causeway over the Euphrates River.

Figure 3.16: Desert Storm JSTARS Image During Left Hook Maneuver[164]

3.3 Is There a Benefit to Attacking Communication Satellites?

This section of the chapter will make an argument similar to the one made above about reconnaissance satellites. Although U.S. communication satellites are a chief component in the U.S. battlefield communication architecture, there are also other terrestrial components, like tropospheric scatter (tropo) and microwave systems, that play an equally important role. U.S. battlefield voice and data networks are spread across satellite, terrestrial and other radio relay components as shown in this section. For an adversary attempting to degrade U.S. performance in battle, it is not apparent that attacking U.S. communication satellites could directly translate into a particularly predictable advantage. Although an attack on communication satellites might slow down U.S. actions, it would also provide the U.S. with the legitimacy to escalate the battle as it desires. That might not be a positive outcome for the adversary.

In order to understand the communication network employed in warfare, the 1991 Operation Desert Storm communications' architecture will be examined in this section. What evolved during the 1991 Gulf War was the largest single communications mobilization in military history (see Table 3.3 below). It was a network of multiple systems that was stretched and stressed to provide the connectivity for a theater-wide communications system. Subsection 3.3.1 below will describe the development of the Operation Desert Storm theater communication infrastructure and subsection 3.3.2 will describe how a combined satellite and terrestrial theater communication infrastructure was used to establish a battlefield voice and data

network.

Table 3.3: 1991 Gulf War Communications Effort[5]

SINGLE LARGEST COMMUNICATIONS MOBILIZATION IN HISTORY
110 SHF earth terminals 3 commercial T-1 satellite terminals 1050 USAF circuits 1000 miles of terrestrial systems: 29 tropo (AN/TRC-170) and microwave links 6 DCS entry points 19 automatic telephone switches (72 AUTOVON trunks) 17 manual switches 3 message switches: 132,012 message transmitted; 1,293,775 message received 59 communication centers 29,542,121 calls 7000+ radio frequencies
AIR TRAFFIC
350,000 operations for Desert Shield 225,000 operations for Desert Storm Air Tasking Order often exceeded 950 pages 12 Combat Communications Squadron

3.3.1 Operation Desert Storm: Theater Communications Infrastructure

When on August 2, 1990, Saddam Hussein announced the invasion of Kuwait to a shocked world, the United States had a single administrative unit in Bahrain and two training mission in Saudi Arabia, served by satellite communications. U.S. Army and Air Force communicators were hard pressed to provide means for adequate connectivity among the rapidly growing number of bases and to the nodes in the

United States that provided those units with logistic and intelligence. Connections had to be quickly made if the planned initial air campaign could hope to blunt the expected Iraqi attacks into Saudi Arabia.

The only immediate solution to the theater connectivity problem was in use of Ground Mobile Force (GMF) Super-High Frequency (SHF) tactical satellite communications[5]. The ground network of GMF SHF tactical satellite infrastructure was created from scratch during the buildup to Operation Desert Storm. Thumrait, Oman was selected for the initial hub location because it was believed to be outside the range of Scud or air attack. Soon the buildup of air power required a second hub at Riyadh and then a third at Al Dhafra, UAE. This latter hub providing inter-theater trunking to Europe via a UK Syknet satellite and the Indian Ocean DSCS satellite. Figure 3.17 on page 104 shows the network for the USCENTAF as it

5. During the 1991 Gulf War, the flexibility of space communications was demonstrated by U.S. authorities by reconfiguring their space segment to match traffic demands. Prior to hostilities, the U.S. space communications workhorse, the SHF Defense Satellite Communications System (DSCS) provided the telecommunications coverage of the area through its Eastern Atlantic (EA) and Indian Ocean (IO) satellites. The total DOD traffic throughput over these two satellites was about 4.5 Mb/s–equivalent to around 70 commercial voice circuits. A little more than 1 month later, with the first U.S. forces in theater, 48 tactical terminals had been deployed; the traffic throughput had risen to 38 Mb/s (600 voice channels); and DSCS IO was saturated. Traffic demands were still building. By mid-September, DSCS 9E was reconfigured (in a novel realignment of its high gain and multibeam antennas) to increase its Gulf traffic capability. At the same time, under longstanding agreements, the United Kingdom provided U.S. forces with capacity on its Skynet 4B satellite positioned at 53^oE. In the meantime, the U.S. tactical terminal population had risen to 53. It was at this time that President George Bush announced the deployment of 200,000 more U.S. troops to the Gulf. The decision was then made to boost Gulf traffic capability by relocating the DSCS reserve West Pacific (WP) satellite from its 180^o geostationary parking slot to 65^oE. Shortly after DSCS WP began operation, traffic had risen to 44 Mb/s (710 voice circuits), 60 U.S. earth stations were operating in theater and the United Kingdom's Skynet 4A at 30^oE was providing additional reserve capability. By the time traffic to U.S. forces in the Gulf had peaked, yet another SHF satellite, DSCS Indian Ocean Reserve, was available, the throughput had risen to 68 Mb/s (1,100 voice circuits) and the earth station population was 110. In addition to DSCS SHF services, U.S. forces in the Gulf were also served by UHF geostationary satellites, the Fltsatcom/AFsatcom and Leasat/Syncom families[185].

ultimately evolved. Commercial satellite communications eventually supplemented each of USCENTAF's satellite hubs, becoming the primary means of extending DSN, AUTODIN, weather and several other services from CONUS to theater[5, 64].

However, the interim theater network provided by the Ground Mobile Force (GMF) satellite terminals provided an initial, if precarious capability. Communications were almost totally dependent upon the theater satellite hubs and would remained so until airlift could be obtained for the AN/TSC-170 tropospheric scatter and microwave terminals. By mid-August, engineers from the 5th Combat Communications Group had completed initial studies[6] and concluded that it was feasible to construct what would become the "longest tactical, digital, terrestrial transmission system ever assembled." The first increment of the tropo network would connect the communications hubs at Riyadh with Al Dhafra, through the tactical air bases on the eastern side of the Saudi Arabian peninsula. Later it would extend north through King Khalid Military City (KKMC) to Rahfa on the border with Iraq. This northward extension provided circuitry from the Tactical Air Control Center (TACC) in Riyadh to the radar control and reporting center at KKMC and to three air support operations centers co-located with the XVIIIth Airborne Corps, the VII Corps and other coalition ground forces (Figure 3.18 on page 106 shows microwave sites connecting the XVIIIth Airborne Corps). Figures 3.19 and 3.20 below show the final configuration of the terrestrial transmission system, consisting of 29 links of tropospheric and microwave, covering over 1,000 miles.

6. Design parameters called for a transmission rate of 2,304 kbps with a link availability of .90 and a bit error rate of not more than 1 x 10^{-5}.

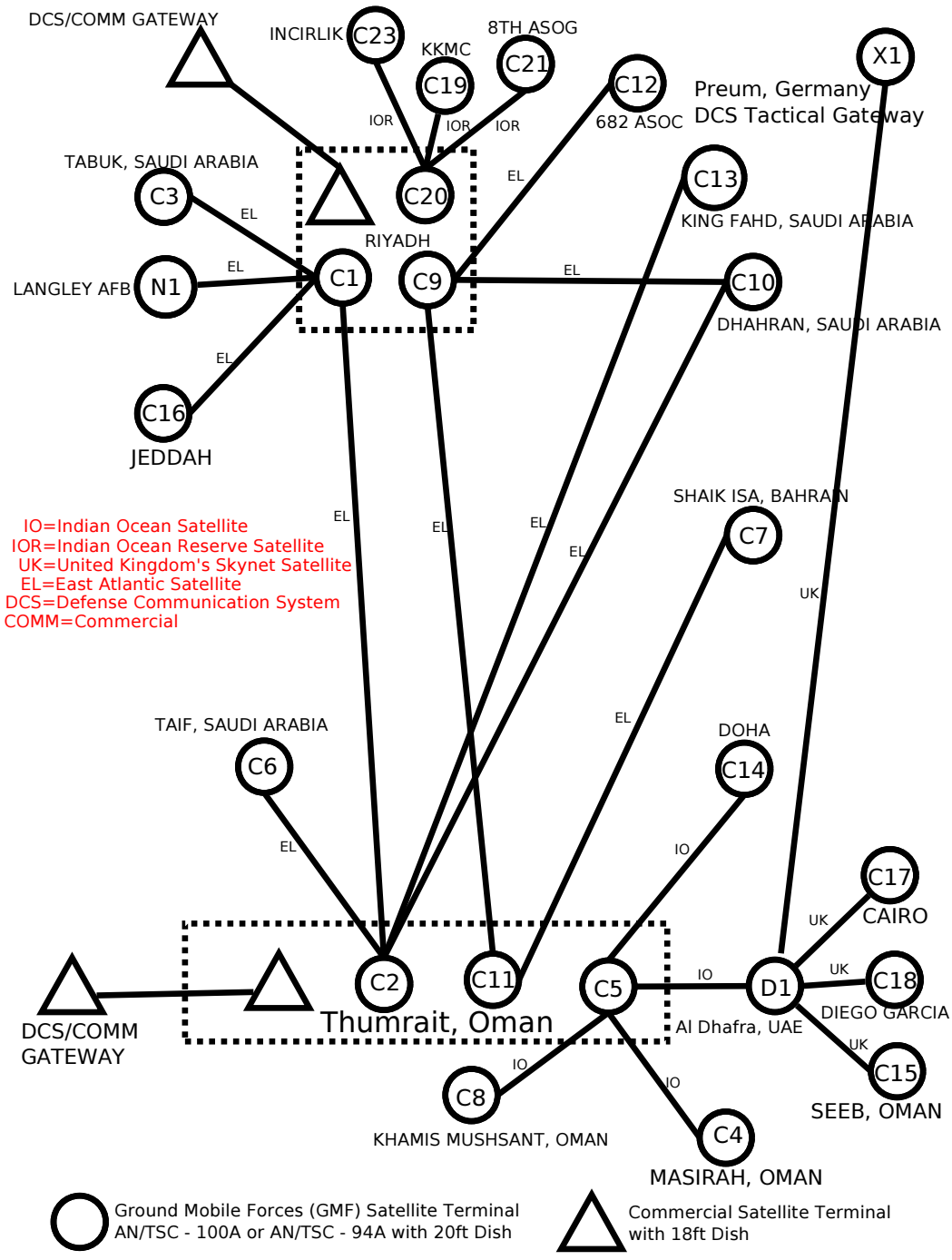

Figure 3.17: Desert Storm: Satellite Communication Architecture[64]

Figure 3.18: Microwave Communications Relay Sites Providing Communications Link Between XVIII Airborne Corps and Rear Area[214]

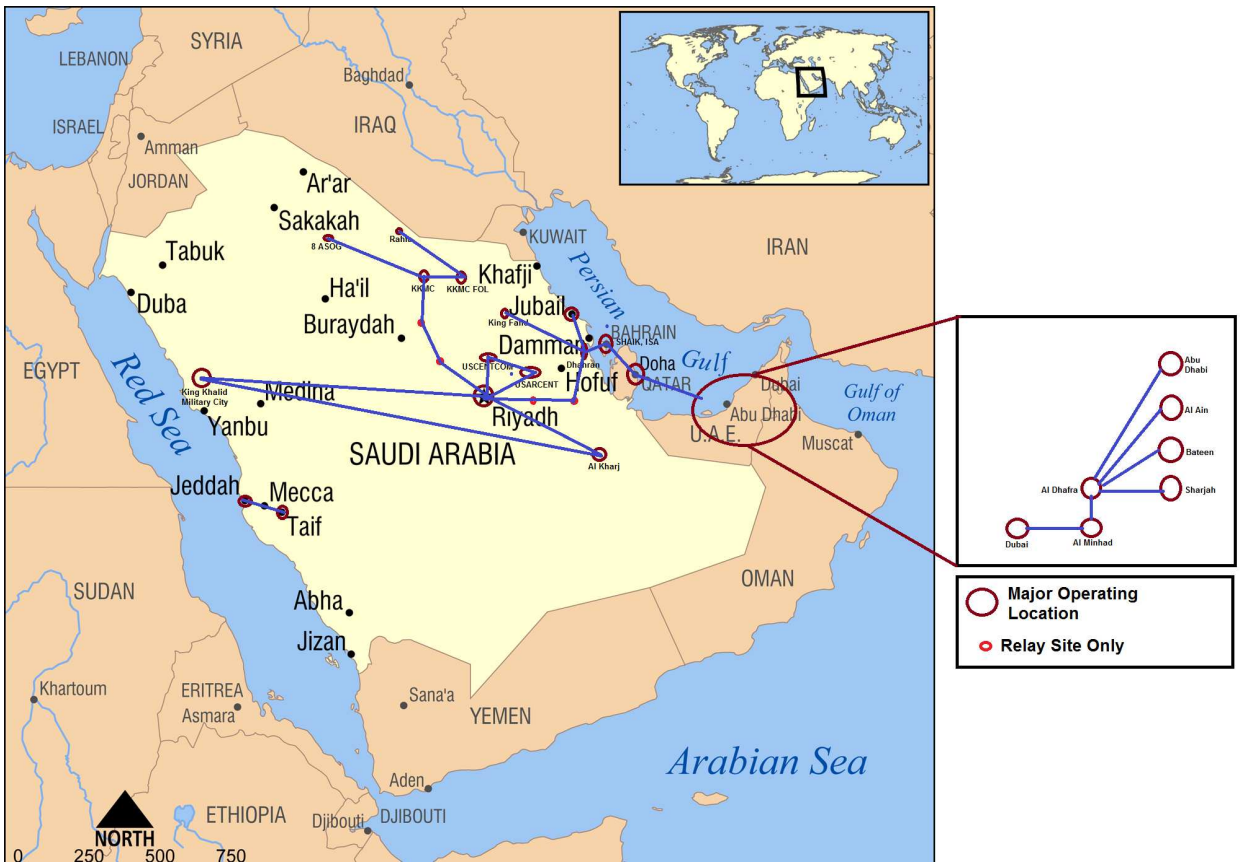

Figure 3.19: Desert Storm: Terrestrial Communication Architecture[64]

Figure 3.20: Desert Storm: Terrestrial Communication Architecture (Close-up View)[64]

This subsection demonstrates that both satellite and terrestrial communication architectures were created during Operation Desert Storm. Though, it should be acknowledged that satellite-based communications systems came into operation much earlier due to the easy availability of GMF terminals during the operations. The next subsection will discuss how the satellite and terrestrial communication architectures were used to establish a theater voice and data network.

3.3.2 Operation Desert Storm: Theater Voice and Data Network

Figure 3.21 below shows the U.S. voice network that drew its trunking from both the satellite and terrestrial systems described above. It contained 19 automatic and 17 manual switchboards and processed just under 30 million calls through 70 AUTOVON trunks. By January 1991 there would be an additional 169 telephone switches brought into the theater by the other military services.

This networks eventually evolved to satisfy customer needs for both voice and message traffic, but had little capability to handle large volumes of bit-oriented data traffic. Planners had greatly underestimated the volume and the variety of data transmission that would be required by automated combat support systems. A significant proportion of warfare was automated during Operation Desert Storm requiring the ability to transmit large volumes of data.

At the higher levels of command, enemy formations and strengths are tracked and analyzed with computers, courses of action were war-gamed with computer programs and logistical and personnel information was compiled and tracked on

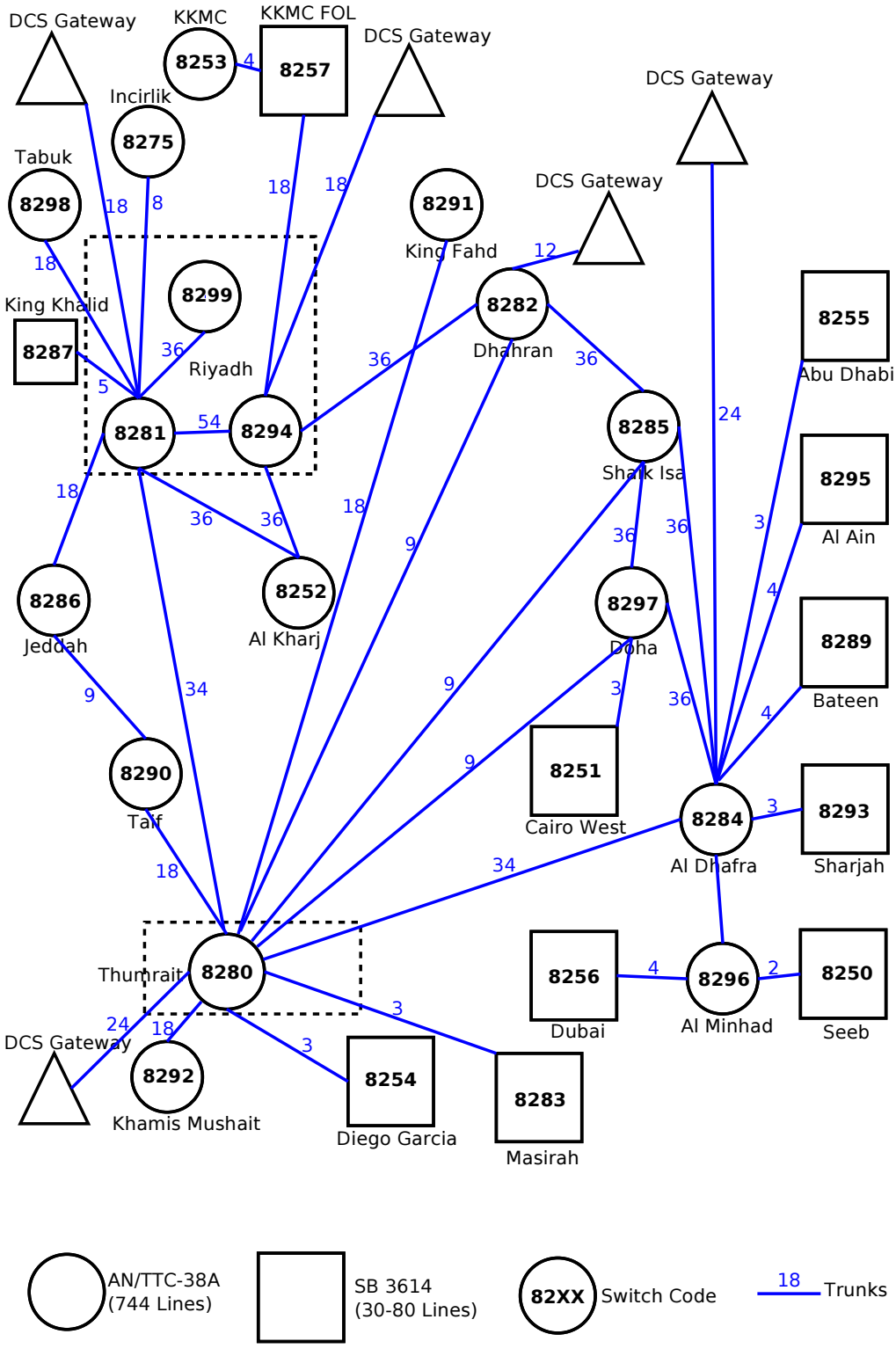

Figure 3.21: USCENTAF Voice Network[64]

computer spreadsheets. Once this information was analyzed and compiled by computers, the same machines were used to pass the information between commanders and staff organizers. During Desert Storm, staff officers regularly used spreadsheets and databases to track the arrival and location of units and supplies. Briefing charts, with operational information for senior commanders, were changed and distributed daily to other headquarters through computer systems. There was a need to send large amounts of information securely over long distances. For example, the daily theater logistic report was prepared at the 22nd Support Command Headquarters in Dhahran in eastern Saudi Arabia. This report was medium sized (approximately fifty kilobytes) Lotus 1-2-3 spreadsheet that was compiled with data from both the Dhahran area and from King Khalid Military City (KKMC) which is 380 miles north-west of Dhahran. Once officers at the 22nd Support Command Headquarters compiled and briefed the report to their commander, they sent the report to the Army Headquarters in Riyadh, 350 miles to the southwest. The Army headquarters staff made any changes necessary for their purposes, presented it to their commander, and then forwarded it 8000 miles to the rear Army headquarters in the United States.

All the data requirements for computer-based planning discussed above was met by the Army Central Forces (ARCENT) Command and Control Information System (AC2IS). AC2IS provided Army level staff officers with a secure means to quickly pass electronic messages and transfer data files long distances[203]. AC2IS was designed to use the existing theater communications architecture. The transmission medium ran the gamut from short line-of-sight microwave and tropospheric-

scatter systems to communications satellites as shown in figure 3.22. AC2IS was accurate and could transfer the file to any other station on the network, including stations in the United States or Germany, in less time than it took to make a connection on a secure FAX machine. A dedicated data system like AC2IS also reduced the load on the tactical switching system.

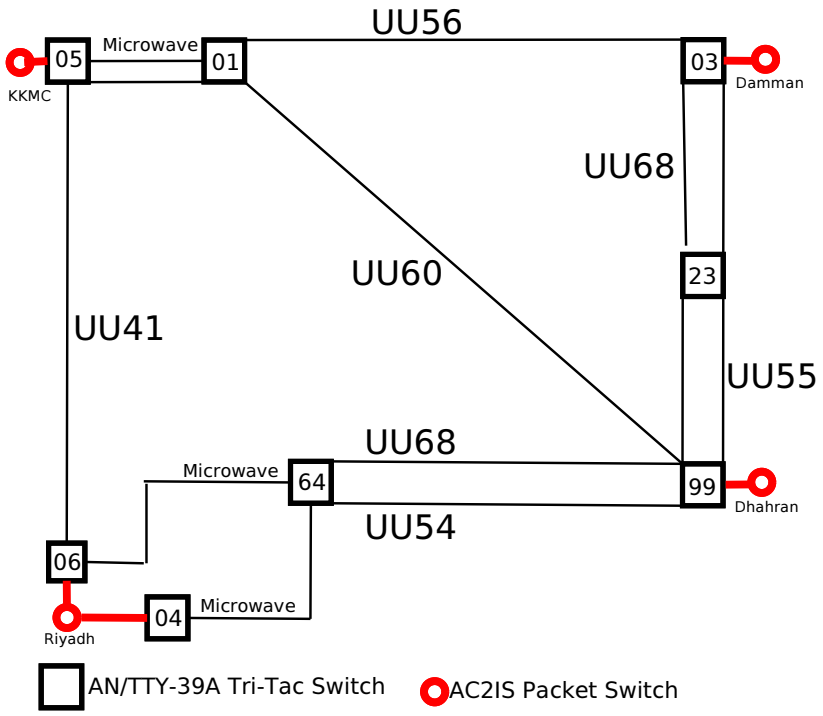

Circuit	From	To	Type
UU60	Dhahran	KKMC	Satellite
UU54	Riyadh	Dhahran	Tropo & Microwave
UU55	Dhahran	Damman	Microwave
UU41	Riyadh	KKMC	Tropo
UU56	Damman	KKMC	Satellite
UU68	Riyadh	Damman	Tropo & Microwave

Figure 3.22: ARCENT Command and Control Information Systems[7]

Another system that was used to handle the large volumes of bit-oriented data traffic among the elements of the U.S. Air Force was the Tactical Data Links[7] (TADIL) (see figure 3.23 below). A key component of the successful Desert Storm air campaign, TADIL enabled real time exchange of voice and radar displays. This network had to be improvised during the operation. The challenge to USCENTAF communicators was to provide communications connectivity between the Tactical Air Control Center (TACC) in Riyadh and its eyes and ears now embarked on a growing family of aircraft, some of which were orbiting at greater distances from Riyadh[8] than could be reliably supported through conventional ground-air-ground communications nets. Also, these nets were not suitable for transferring data in near real-time. TADIL served that purpose by connecting the various components of the TACC. TADIL used satellite, terrestrial and other self-sufficient radio relays

---

7. Tactical Data Links or TADIL consists of: TADIL-A (also known as Link-11A) employs netted communication techniques using standard message formats. TADIL-A radios can operate in the HF band, giving a range of up to 300 nautical miles(nm), or the UHF band, giving a range of approximately 25 nm surface-to-surface or up to 150 nm surface-to-air. TADIL-A data links operate at rates of 1,364 bps (HF/UHF) or 2,250 bps (UHF). TADIL-A is used commonly in the sea environment for the exchange of air, surface, and subsurface tracks, EW data, and limited command data among connected terminals. TADIL-B (also known as Link-11B) provides a secure, full-duplex, point-to-point digital data link utilizing serial transmission frame characteristics and standard message formats at 2,400, 1,200, or 600 bps. It interconnects tactical air defense and air control units. Tactical Data Link (TADIL-J) is a secure, high capacity, jam-resistant, nodeless data link which uses the JTIDS (Joint Tactical Information Distribution System) transmission characteristics and protocols, conventions, and fixed-length messages formats. TADIL-J operates in the UHF band in the frequency range of 960 to 1,215 MHz, and therefore provides LOS operation. TADIL-J is an all-informed nets. In the U.S. Army, TADIL-J terminals is now planned to be assigned to division, corps, and *echelon above corps* (EAC). These terminals will support engagement operations, command and control, surveillance, weapon status and coordination, *precise participant location and identification* (PPLI), and battlefield situation awareness (air and ground).

8. The airborne warning and control system (E3 AWACS), the airborne command and control center (ABCCC), the intelligence gathering RC-135 Rivet Joint and eventually the airborne radar Joint Stars (JSTARS) aircraft, were often ranging or orbiting well beyond limits of UHF radio range from the TACC in Riyadh.

to form its network.

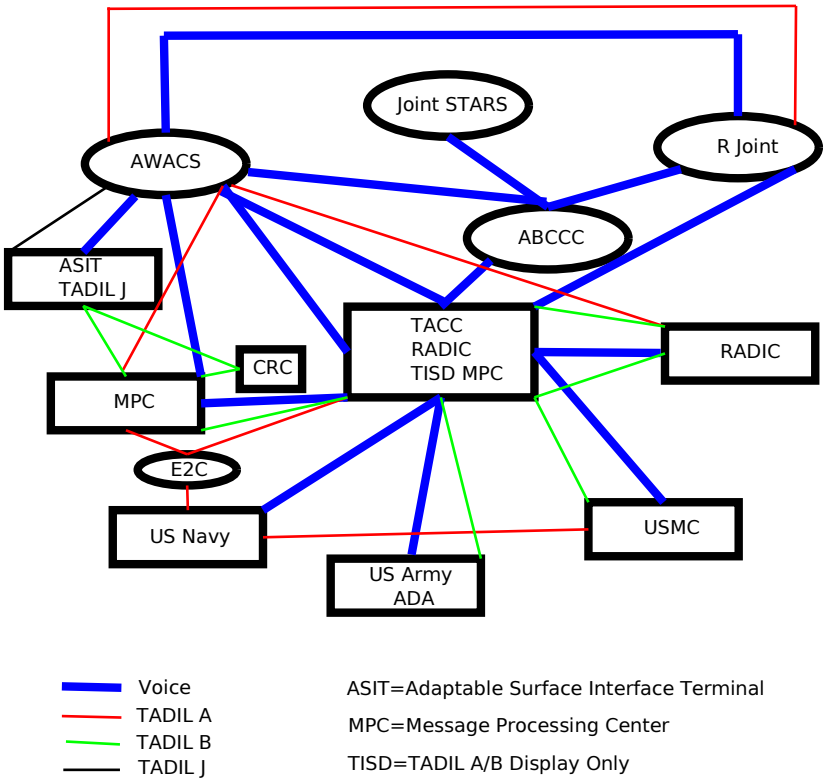

Figure 3.23: USCENTAF TADIL Network[64]

These operational descriptions of the voice and data networks used during Operation Desert Storm again reinforces the point that communication capabilities are spread across satellite, terrestrial and other radio relay components[9]. For an adversary attempting to degrade U.S. performance in battle it is not apparent that attacking U.S. communication satellites could directly translate into a particularly predictable advantage.

9. This multiple platform communication architecture will persist. Two of the DSCS satellites have failed. The replacement to the DSCS satellite, the Mobile User Objective System (MUOS) communications satellites has experienced both program delays and cost increases. The first Mobile User Objective System (MUOS) communications satellite was launched on February 24, 2012: a 26-month delay–from March 2010 to May 2012–in the delivery of on-orbit capability from the first satellite[226].

3.4 Conclusions

This chapter was intended to test the validity of the argument that there are substantial military motivations that might induce an adversary of the U.S. in attacking its satellite assets. In order test that argument, three classes satellite systems were examined in this chapter. Section 3.1 examined the benefits to an adversary from attacking the GPS satellite system. In that section, the GPS system was modeled and its performance was simulated under conditions of attack. The simulation revealed that that an adversary like China or one with capability similar to China, would have to simultaneously attack at least 4 GPS satellites to produce a militarily relevant benefit[10]. Any benefit, however, dissipates quickly within 2 hours. After that, the redundancy of the GPS satellite constellation makes up for the effects of the attack on the GPS satellite system. Also, the degradation of the GPS accuracy shows a daily periodic pattern after the attack. This would make it possible for the U.S. to respond and adapt its strategy after the attack. Given this, this section concludes that there does not seem to be any abiding tactical military logic in attacking GPS satellites.

Section 3.2 examined the benefits of attacking U.S. satellite reconnaissance platforms. Using the data from the 1991 Operation Desert Storm, the case is made that U.S. battle reconnaissance capabilities are spread across multiple platforms

10. The simulation discussed above was done assuming that the adversary would possess the capability to attack and disable 4 or more satellites simultaneously. The next chapter on anti-satellite (ASAT) missiles will argue that neither does China possess the satellite tracking infrastructure nor is there evidence it is developing the operational missile batteries needed to execute such an attack with a high probability of success.

including air-borne vehicles. These aerial reconnaissance platforms can perform as good as satellites and in some cases better. Also, the satellite reconnaissance infrastructure is composed of many satellites providing redundancies against attacks. In order to disrupt that infrastructure a number of those satellites will need to be attacked. Section 3.2 argues that although U.S. reconnaissance satellites do have important applications in a battle, that fact alone does not mean that they would be considered as desirable targets. For an adversary trying to obtain a military advantage, there seems to be little value in attacking reconnaissance satellites due to the presence of multiple systems capable of performing reconnaissance missions.

Finally, section 3.3 examined the benefits to an adversary from attacking U.S. communication satellites. Similar to the argument made in the section on reconnaissance satellites, even though U.S. communication satellites are a chief component in the U.S. battlefield communication architecture, there are other terrestrial components, like tropospheric scatter (tropo) and microwave systems, that play an equally important role. U.S. battlefield voice and data networks are usually spread across satellite, terrestrial and other radio relay components. For an adversary attempting to degrade U.S. performance in battle, it is not apparent that attacking U.S. communication satellites could directly translate into a particularly predictable battle advantage.

In sum, the various sections of this chapter make the case there are no obviously evident benefits for an adversary in attacking U.S. satellite systems for purely military advantage. Those arguing otherwise would need to provide evidence to the contrary.

Chapter 4

The Limits of Chinese Anti-Satellite Missiles

A recurrent refrain in the debate on space security has been about the threat to U.S. military space assets. The most dramatic characterization of this refrain is the "space Pearl Harbor" analogy used by the 2001 Rumsfeld Commission[1] report. The Rumsfeld Commission in its report stated, "*If the U.S. is to avoid "a space Pearl Harbor" it needs to take seriously the possibility of an attack on U.S. space systems. The U.S. is more dependent on space than any other nation. Yet the threat to the U.S. and its allies in and from space does not command the attention it merits.*

Other participants in the debate on space security have also expressed similar concerns on the safety of U.S. military space assets in various forms:

- Among many complex and diverse lessons, Chinese analyses of U.S. military operations in the Persian Gulf wars, Kosovo and Afghanistan have yielded one critical insight: the U.S. is inordinately dependent on its complex but exposed network of sophisticated command, control, communications and computer-based intelligence, surveillance, and reconnaissance systems operating synergistically in and through space. In other words, while American military power derives its disproportionate efficacy from its ability to leverage critical space

1. Formally, it was called Commission to Assess United States National Security Space Management and Organization. It was headed by Donald Rumsfeld.

assets, these very resources are simultaneously a font of deep and abiding vulnerability. Chinese strategists concluded, that any effort to defeat the U.S. would require a riposte against its Achilles heel: its space-based capabilities and their organic ground installations[21].

- The Chinese consider American intelligence, surveillance, and reconnaissance satellites, and even meteorological satellites, to be "space weapons" and therefore legitimate targets. According to Kevin Pollpeter, China Project Manager of the Center for Intelligence Research and Analysis of Defense Group Inc., a common theme in practically every Chinese book and magazine article about space is that "whoever controls space controls the Earth." Its almost obligatory to put this in a book or article[65].

- The fragility of space systems, and the very limited number of spares, means that the functions these systems provide can be quickly and in some cases easily cut off[49].

- This (U.S.) dependence on space will offer opportunities for low-cost, "asymmetric" strategies for inflicting significant damage to the U.S. without having to confront the full brunt of U.S. military forces[82].

- Due to the dramatic war fighting advantage that space support provides to U.S. forces, security analysts are nearly unanimous in their judgment that future enemies will likely attempt to "level the playing field" by attacking U.S. space systems in efforts to degrade or eliminate that support[80].

This chapter challenges the validity of the concern raised above about the feasibility of an attack on U.S. space systems[2]. It does so by systematically evaluating the question: How vulnerable are satellites to a targeted attack? More specifically, can nominated adversaries like China be able to destroy with high probability specific U.S. military satellites employing a direct-ascent hit-to-kill anti-satellite (ASAT) missile? Direct-ascent hit-to-kill ASAT missiles are required to ensure a high probability success in attacking and destroying satellites. An operational direct-ascent hit-to-kill ASAT missile capability is, therefore, a clear indication of a nation's intent to attack satellites.

In the discussions within the community that subscribes to the idea of an imminent threat to U.S. military space systems, China is invariably considered as the most likely potential adversary. For example, the Defense Intelligence Agency (DIA) director, Army Lt. Gen. Ronald Burgess, recently told a Senate committee while presenting the DIA's 2012 worldwide threats report that the agency believes China is developing a space weapon program that can be used against satellites worldwide[116]. He argued that it would take "*only*" (emphasis added) about two dozen ASAT missile attacks from China to cause serious damage to U.S. military operations.

The evidence usually provided to make the case for China's ability to successfully execute such comprehensive ASAT missions is the 2007 Chinese ASAT test[3].

---

2. The question on the utility of attacking U.S. military satellites was addressed in the previous chapter.

3. The 2010 Chinese missile defense test is also used by some as a potential demonstration of China's ASAT capabilities. On 11 January 2010, China launched an SC-19 missile from the Korla Missile

In 2007, China used a modified version of its DF-21 (NATO CSS-5) missile called the SC-19 ASAT missile to intercept and destroy one of its non-functional weather satellite (the FY-1C of Fengyun series) at an altitude of roughly 865 kilometers.

Those making the case for Chinese ASAT capabilities argue that this test was a clear indication of the capability to engage in an advanced ASAT mission. The analytical evidence presented in this paper, however, argues against that idea. The results demonstrate that ASAT intercepts are very complex under realistic conditions and that China's has very limited to potential, if any, to use direct ascent hit-to-kill ASATs in a real-world battle scenario.

4.1 Conceptualizing an ASAT Missile Attack

This chapter will examine the two different ways to understand a direct ascent hit-to-kill anti-satellite (ASAT) mission profile.

- The first one is the simpler case of a target satellite on a non-varying[4] orbit for the duration of the ASAT attack mission. In this scenario, the satellite being targeted has been tracked and its orbit mapped for a substantial period of time. This means that the nation engaging in the ASAT attack can predict with high accuracy the position of the satellite at each instant of time. The mission then reduces to flying out the intercepting ASAT missile to a pre-determined location on the path of the satellite at the right time. Put simply,

---

Test Complex and supposedly successfully intercepted a near-simultaneously launched CSS-X-11 medium-range ballistic missile launched from the Shuangchengzi Space and Missile Center[27].

4. The satellite is on a predicted orbit and will not undergo any maneuvers.

the target here reduces to a fixed point in space. The Chinese ASAT test is an example of this kind of intercept. The region of outer space in which the ASAT missile can successfully intercept a non-varying orbit satellite is referred to as the "cone of vulnerability" in this chapter. The extent of the cone of vulnerability is a function of the ASAT missile boost-phase flight velocity profile. Section 4.2 of this chapter will discuss in detail the simulation and estimation of the "cone of vulnerability."

- The second type of ASAT mission profile is more complex and realistic. In this scenario the targeted satellite has performed a maneuver or there is no prior information available on its orbit. Either way, the satellite has be tracked as it flies towards the territory of the nation (or its allies) engaging in the ASAT attack while the ASAT missile is in flight towards a "head-on collision" with the satellite. This is a more realistic representation of how an ASAT attack will unfold. Section 4.3 will discuss in detail the simulation of a "head-on collision" scenario.

The evidence presented in the chapter will show that even under the ideal conditions[5] of a non-varying orbit satellite as target the reach of Chinese SC-19 ASAT missile is very limited. In the case of an ASAT engaging an emerging satellite target in a "head-on collision" the capabilities of the modeled SC-19 are insufficient. To maintain a manageable miss distance, an ASAT attack has to be launched simul-

5. Ideal conditions refer to perfect targeting information of the target satellite. This enables the ASAT to aim at a fixed point in space to achieve intercept collision at the same time the satellite traverses it.

taneously as the emerging target is being tracked. Doing so requires a continuous thrusting capability that would enable the ASAT to fly out and intercept the target satellite. The ASAT missile can, however, generate thrust only during its boosting phase.

4.2 Case I: Cone of Vulnerability

The "cone of vulnerability" is broadly defined as the region in space in which a satellite with a non-varying orbit is vulnerable to attack from a particular ASAT missile. Any satellite passing through the cone can be destroyed by the ASAT with a high probability of success. The cone of vulnerability is centered at the launch location of the ASAT missile and its maximum radial and altitude range depends on the boost-phase velocity profile and dynamics of the ASAT missile.

In the first part of this section, the cone of vulnerability will be determined for a ASAT missile with a zero-lag guidance system i.e., the ASAT missile is able to spontaneously satisfy all its lateral divert requirements (subject to 10 g limit on lateral acceleration at any instant). In the second part of this section, the the zero-lag guidance system will be replaced by a more realistic 3^{rd} order flight control system (subject to 10 g limit on lateral acceleration at any instant). A third-order flight control system creates a time lag between commanded and achieved lateral divert of the ASAT missile and it is not able to spontaneously satisfy all of its lateral divert requirements.

The "cone of vulnerability" for both of these analyses is generated using an

SC-19 Chinese ASAT missile (the parameters of the missile are shown Table 4.1 below) launched from the Xichang Satellite Launch Center ($28^o12'00''N$ latitude and $102^o02'00''E$ longitude). These parameters were chosen to mimic the 2007 Chinese ASAT test.

Table 4.1: Assumed Properties of Chinese DF-21 ASAT Missile

	Total Mass(lb)	**Propellant Mass(lb)**	**Isp(s)**	**Burn Time(s)**
Stage-1	20,800	19,136	300	60
Stage-2	11,200	10,304	300	60
KV Stage	1,325	1,200	300	60
KV Payload	125	0	0	0

As previously stated, the "cone of vulnerability" analyses discussed in this section are done by assuming that the target satellite will arrive at a particular point in space inside the vulnerability cone at the same time the ASAT missile reaches that point in space. Subsection 4.2.1 and subsection 4.2.2 below will outline the equations used to model the flight dynamics and guidance laws of the ASAT missile used in a "cone of vulnerability" intercept scenario.

4.2.1 Physics of Cone of Vulnerability Simulation

There are two parts to simulating the dynamics of the ASAT intercept used to produce the data for generating the "cone of vulnerability." The first part involves modeling and simulating the parameters of the target satellite. For determining

the "cone of vulnerability," the satellite's flight path is not simulated. Instead the satellite is positioned at various points in space. The altitude of the satellite is varied from 300 km to 850 km, the inclination is varied from 0 degrees to 360 degrees, and the values of mean anomaly[6] are accounted for by placing the satellite at various radial distance from the launch location at the given altitude and inclination.

The second part involves modeling and simulating the ASAT missile which is described below. The simulation of the ASAT missile is accomplished by forcing the ASAT model to obey Newton's Second Law at each time step[235]. The ASAT missile also has a built-in guidance system designed to reduce the distance between itself and the target satellite in order to achieve collision. The guidance system generates a thrust component perpendicular to the velocity vector that forces the ASAT missile to move in a direction that achieves collision.

In vector form Newton's law is written as

$$\vec{F} = m\vec{a} \tag{4.1}$$

where $\vec{F}$ is the force vector (in Newtons) acting on the center of gravity of the ASAT missile, m is the total mass (in kg), and $\vec{a}$ is the net acceleration (in m/s^2). There are three major forces acting on the missile:

$$\vec{F} = \vec{T} + \vec{W} + \vec{D} \tag{4.2}$$

6. The mean anomaly of a satellite tells where the satellite is located in its orbital path

Thrust ($\vec{T}$) acting in the direction of the ASAT missile velocity vector, Weight ($\vec{W}$) acting in the direction of the center of the Earth, and Drag ($\vec{D}$) acting in the direction opposite to the ASAT missile velocity vector. Thrust ($\vec{T}$) is calculated as as

$$T = -I_{sp}\dot{W} = -I_{sp}\frac{dm}{dt}g \tag{4.3}$$

However, the Thrust ($\vec{T}$) is composed of $\vec{T_v}$ and $\vec{T_p}$ as shown in equation 4.4 below.

$$\vec{F} = \vec{T_v} + \vec{T_p} + \vec{W} + \vec{D} \tag{4.4}$$

$\vec{T_v}$ is the thrust component along the direction of the velocity vector (in m/s) and $\vec{T_p}$ is the thrust component perpendicular to the velocity vector (i.e. the lateral divert). The mechanism to calculate $\vec{T_v}$ and $\vec{T_v}$ is shown in subsection 4.2.2 below. The total magnitude of the two thrust components parallel and perpendicular to the velocity vector is always equal to the total thrust $\vec{T}$ provided by the rocket engine.

The magnitude of the other two forces are calculated as

$$W = mg \tag{4.5}$$

$$D = 0.5\rho V^2 C_d A_{projected} \tag{4.6}$$

where I_{sp} is the stage specific impulse (in s), $\dot{W}$ is the change in stage weight over

time, ρ is the atmospheric density at the current position of the ASAT missile, V is the velocity magnitude of the ASAT missile, C_d is the co-efficient of drag, and $A_{projected}$ is the projected area of the ASAT. $\dot{W}$ is the product of in-stage fuel consumption $\frac{dm}{dt}$ (in kg/s) and gravitational acceleration at the current distance from the center of the Earth g in (m/s^2).

4.2.2 ASAT Missile Guidance System

Proportional navigation guidance law is used for estimating $\vec{T_p}$, the guiding force used in driving the ASAT missile towards the target satellite[7]. Figure 4.1 on page 127 depicts the operational logic of the Proportional Navigation guidance system.

The first step in the guidance law is for the ASAT missile to measure/read the position vector of the target satellite $\vec{r_t}$ and compute the line of sight (LOS) vector $\vec{\lambda}$ by subtracting its own position vector $\vec{r_m}$ as shown in equation 4.7 below

$$\vec{\lambda} = \vec{r_t} - \vec{r_m} \tag{4.7}$$

This LOS vector $\vec{\lambda}$ is then differentiated to calculate the LOS rate vector $\dot{\vec{\lambda}}$

7. The proportional navigation guidance law is optimal for constant velocity targets. This condition is not satisfied for satellite targets. However, the aim in this simulation is not to design a guidance law for ASAT intercepts. The aim is to understand ASAT intercept physics in generic terms. Hence the simplified proportional navigation guidance law is used. More detailed studies for designing a tuned guidance system for an accelerating target can be found in the APS study on boost-phase intercept[16].

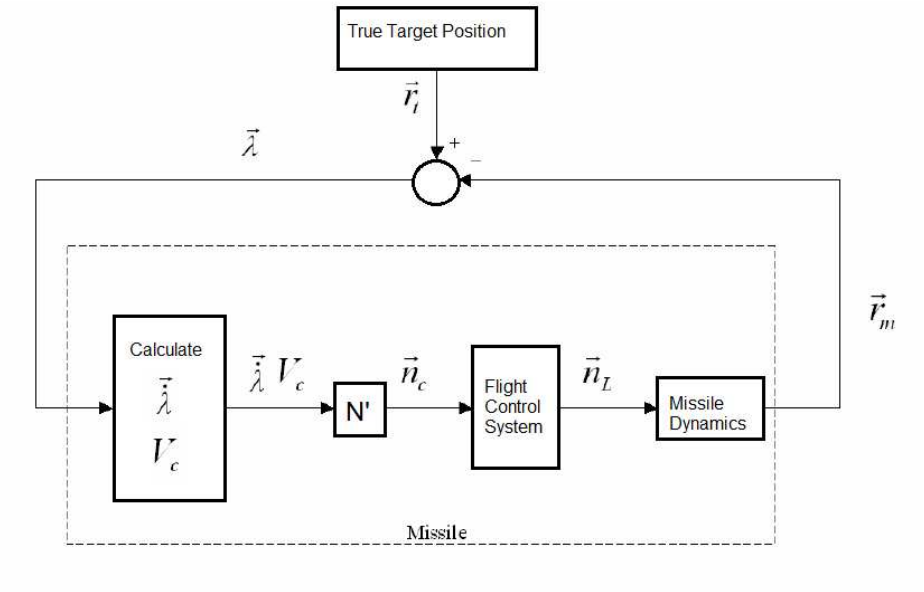

Figure 4.1: ASAT Missile Proportional Navigation Guidance System Diagram

and closing velocity V_c. The magnitude of the LOS rate is obtained by

$$|\dot{\lambda}| = \frac{|\Delta\hat{\lambda}|}{\Delta t} \tag{4.8}$$

where Δt is the simulation step time.

The closing velocity V_c is computed as the range rate. The range between the target satellite and the ASAT missile is the magnitude of the LOS vector $|\vec{\lambda}|$. This magnitude is calculated for each time step of the simulation and differentiated. Dividing the difference in the range by the simulation step time yields the closing

velocity as

$$V_c = \frac{|\Delta\vec{\lambda}|}{\Delta t} \tag{4.9}$$

The calculated parameters $\dot{\vec{\lambda}}$ and V_c are multiplied by the navigation coefficient N' to calculate the commanded lateral acceleration vector $\vec{n_c}$ as shown in equation below.

$$n_c = N' V_c \dot{\lambda} \tag{4.10}$$

The commanded acceleration is always applied perpendicular to the LOS. The flight control system uses the commanded lateral acceleration to change the attitude of the missile resulting in the achieved lateral acceleration vector $\vec{n_L}$. The achieved lateral acceleration vector $\vec{n_L}$ is integrated along with other accelerations acting on the system resulting in a new missile position $\vec{r_m}$.

The instantaneous LOS vector is normalized to obtain the LOS unit vector $\hat{\lambda}$. In the next time step, the new LOS is computed using equation 4.7 and converted to the unit vector. Vector subtraction of these two unit vectors is the direction in which the acceleration command is applied and is always perpendicular to the instantaneous LOS. After normalizing the acceleration command, the unit vector is

$$\hat{n_c} = \frac{\hat{\lambda} - \hat{\lambda}_{previous}}{|\hat{\lambda} - \hat{\lambda}_{previous}|} = \frac{\Delta\hat{\lambda}}{|\Delta\hat{\lambda}|} \tag{4.11}$$

where $\hat{n}_c$ is the unit acceleration command vector perpendicular to the LOS, $\hat{\lambda}$ is

instantaneous unit LOS vector, and $\hat{\lambda}_{previous}$ is the previous unit LOS vector.

Finally, the commanded acceleration vector is calculated. The magnitude of the commanded acceleration is computed by multiplying the navigation ratio, the closing velocity, and the magnitude of the LOS rate. Multiplying the magnitude of the acceleration command with the acceleration command unit vector yields the commanded acceleration command vector. This is expressed as

$$\vec{n}_c = \hat{n}_c N' V_c |\dot{\lambda}| \tag{4.12}$$

For a zero lag system, the achieved acceleration n_L is always equal to the commanded acceleration n_c and, for the moment it is assumed that the ASAT missile dynamics are free of lags.

The computed acceleration command is perpendicular to the LOS; however, missile acceleration commands ($\vec{T_p}$) can only be applied perpendicular to the velocity vector. Thus, only the commanded acceleration component perpendicular to the velocity vector contributes to the missile guidance. The thrust component perpendicular to the velocity vector, $\vec{T_p}$, is then given as

$$\vec{T_p} = \vec{n}_{c\perp} m_m \tag{4.13}$$

where m_m is the ASAT missile mass at the current time.

Using equation 4.4, the magnitude of the thrust component parallel to the

velocity vector is

$$\vec{T}_v = \sqrt{|\vec{T}|^2 - |\vec{T}_p|^2} \tag{4.14}$$

4.2.3 The Extent of the "Cone of Vulnerability" for a Zero-Lag Flight Control System

This section will show the results of applying the equations outlined above in subsection 4.2.1 and subsection 4.2.2 for a zero-lag flight control system. The dimensions of the "cone of vulnerability" i.e., the maximum radial distance at a given altitude of the target satellite up to which a successful interception can be accomplished are illustrated in figure 4.2 on page 131, figure 4.3 on page 132, figure 4.4 on page 132 and figure 4.5 on page 133 below. The dimensions of the "cone of vulnerability" are also listed in table 4.2 on page 131 along with other variables of the simulation. For example, at a target satellite altitude of 500 km, the maximum radial distance at which the SC-19 can successfully intercept and destroy the satellite is 360 km[8]. This maximum radial distance changes from altitude to altitude. The simulation also shows that the SC-19 has a very low radial outreach of 1 km at an altitude of 850 km.

8. The criteria for successful intercept is a miss distance of 5 m or less. In real-world operations a miss distance of 1 m or less is required. However, in a computer simulation 5 m is accepted due to the effects of the time resolution on the intercept.

Table 4.2: Maximum Radial Reach of SC-19 ASAT Missile at Given Altitude (Zero-Lag Flight Control System)

Altitude of Intercept (km)	**Max. Radial Distance at Altitude (km)**	**Miss Distance (m)**	**Lateral Divert (m/s)**	**Time to Interception (min)**
300	390	4.79	7629.47	3.00
400	410	3.77	4951.67	3.01
500	360	4.36	3236.05	2.99
600	280	2.54	2071.68	2.99
700	70	3.20	443.28	3.00
800	2	3.58	56.72	3.17
850	1	3.82	48.41	3.25

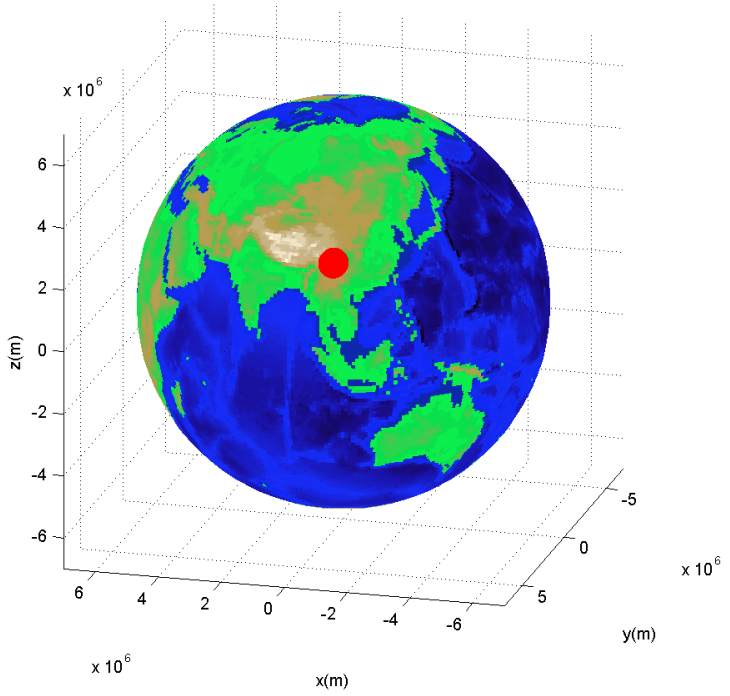

Figure 4.2: SC-19 ASAT Missile: Cone of Vulnerability (Top View)

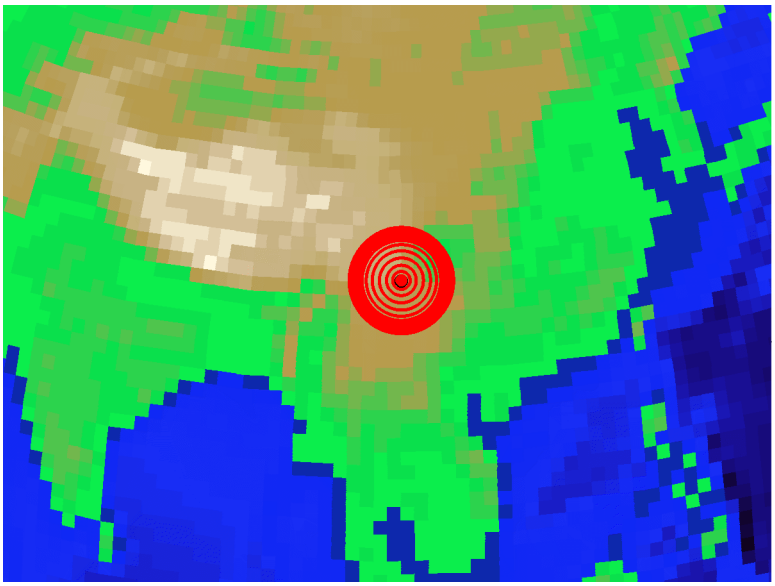

Figure 4.3: SC-19 ASAT Missile: Cone of Vulnerability (Top View)

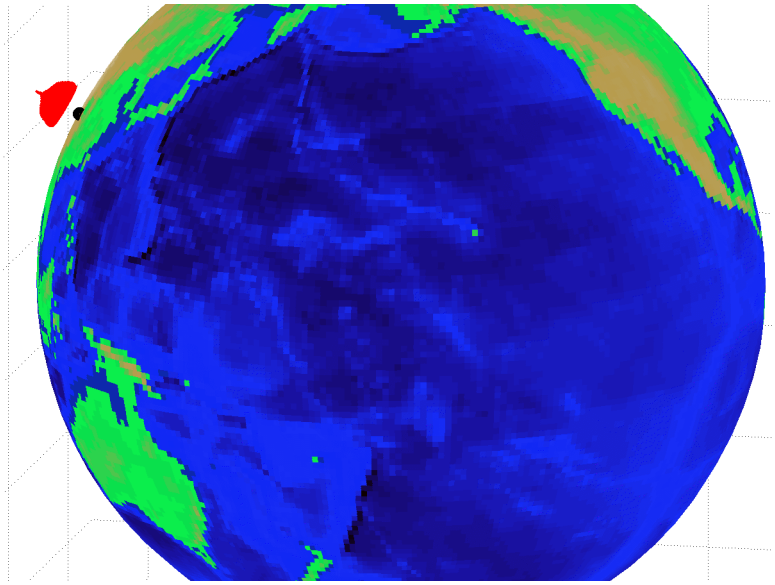

Figure 4.4: SC-19 ASAT Missile: Cone of Vulnerability (Side View)

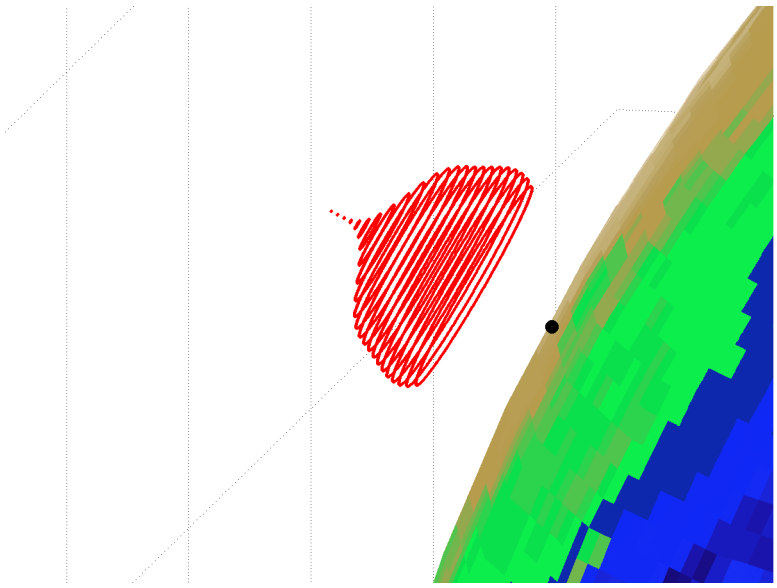

Figure 4.5: SC-19 ASAT Missile: Cone of Vulnerability (Side View)

4.2.4 3^{rd} Flight Control System

So far the ASAT missile guidance is assumed to be perfect. In other words, the achieved acceleration n_L is always equal to the commanded acceleration n_c. This type of model is known as a zero-lag guidance system, where the ASAT missile flight control system can respond to acceleration commands immediately and with 100 percent efficiency. In reality, guidance systems have lags (or delays) in their response. In this subsection, the simulation model is expanded to include a real-world flight control system.

If the flight control system lag is modeled as a 1^{st} order transfer function, the

relation between commanded and achieved acceleration can be given as

$$\frac{n_L}{n_c} = \frac{1}{1+sT} \tag{4.15}$$

where n_L is the achieved lateral acceleration that is integrated to obtained the ASAT missile lateral divert ($\vec{T_p}$), n_c is the commanded lateral acceleration, s is the complex frequency, and T is the system time constant[9].

The general form of an n^{th} order all-pole transfer function is written as

$$\frac{n_L}{n_c} = \frac{a}{bs^n + cs^{n-1} + \cdots + ds^2 + es + f} \tag{4.16}$$

where $a, b, c, \cdots, f$ are constants characterizing the system poles.

For the simulation executed in this chapter the ASAT missiles' flight control systems are modeled as a 3^{rd} order single time constant flight control system with the transfer function

$$\frac{n_L}{n_c} = \frac{1}{\frac{T^3}{27}s^3 + \frac{T^2}{3}s^2 + Ts + 1} \tag{4.17}$$

In the next subsection the simulation results obtained using this 3^{rd} order ASAT guidance system are shown.

9. The determination of optimal system time constant is study in itself. This was done in the background of the simulation in this chapter. It is however not detailed here. More information on designing a transfer function can be seen in Zarchan[152, 153].

4.2.5 The Extent of the "Cone of Vulnerability" for a 3^{rd} Flight Control System

This section will show the results of applying the third-order flight control equations to the ASAT missile. The dimensions of the "cone of vulnerability" under this condition are illustrated in figure 4.6 on page 136, figure 4.7 on page 137 and figure 4.8 on page 137 below. The dimensions of the "cone of vulnerability" are also listed in table 4.3 on page 135 along with other variables of the simulation.

Table 4.3: Maximum Radial Reach of SC-19 ASAT Missile at Given Altitude (3^{rd} Order Flight Control System)

Altitude of Intercept (km)	**Max. Radial Distance at Altitude (km)**	**Miss Distance (m)**	**Lateral Divert (m/s)**	**Time to Interception (min)**
300	5	4.70	57.00	2.14
400	4.8	4.72	47.83	2.39
500	4.4	4.89	41.71	2.62
600	5.1	4.48	44.88	2.82
700	5.1	4.28	42.00	3.00
800	0.8	4.89	7.16	3.17
850	0.8	4.61	8.45	3.25

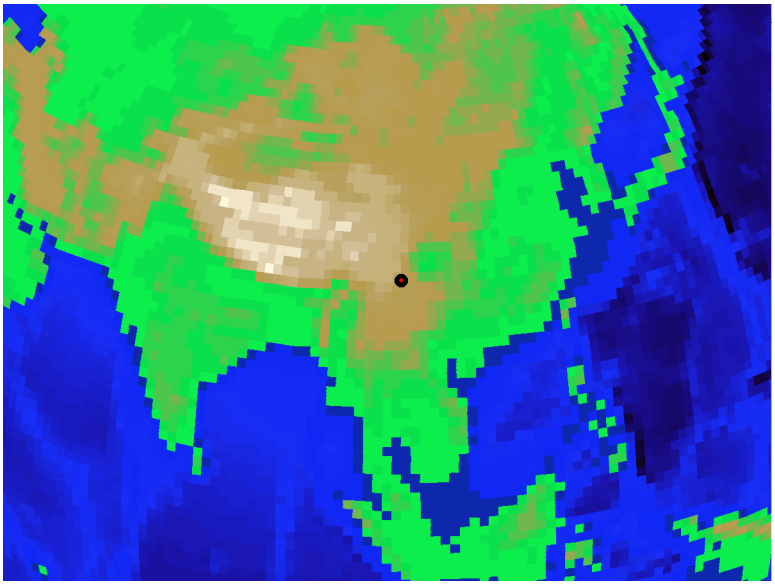

Figure 4.6: SC-19 ASAT Missile: Cone of Vulnerability (Top View)

It is immediately clear from observing figures 4.6, 4.8 and 4.7 generated for an ASAT missile with a 3^{rd} order flight control system that the region of space contained in the "cone of vulnerability" has dramatically reduced. The lags introduced into the ASAT missile by the third-order flight control system increases the miss distances above the tolerable limit of 5 m in almost every point in space.

To understand why that is happening, a comparison of the lateral acceleration and divert is made below between a ASAT missile with a zero-lag and a 3^{rd} order flight control system. For both cases, the ASAT is attempting to intercept a satellite that would pass through the point in space that is at an altitude of 500 km and radial distance of 360 km from the ASAT launch site (Xichang Satellite Launch Center). Figure 4.9 below shows the lateral acceleration and divert for a zero-lag

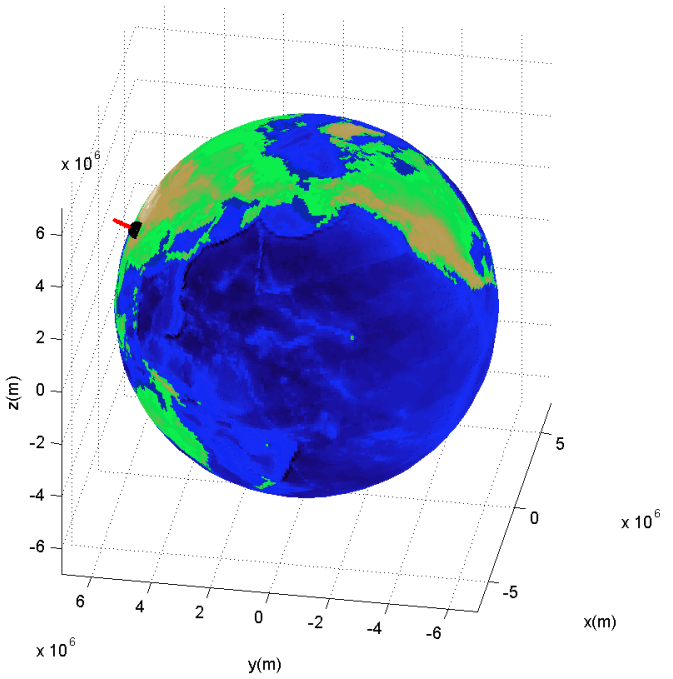

Figure 4.7: SC-19 ASAT Missile: Cone of Vulnerability (Side View)

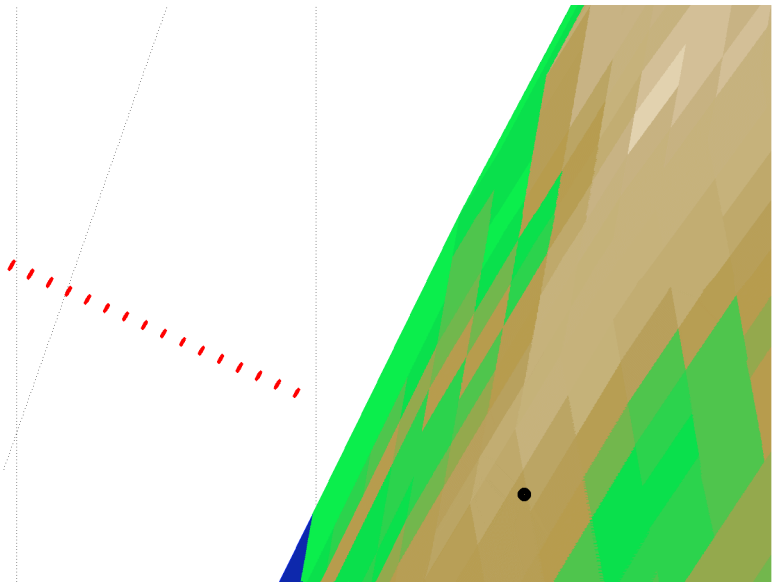

Figure 4.8: SC-19 ASAT Missile: Cone of Vulnerability (Side View)

flight control system ASAT whose intercept miss distance is 5.36 m. Figure 4.10 below shows the lateral acceleration and divert for a 3^{rd} order flight control system ASAT whose intercept miss distance is 110.73 m.

The increased miss distance for a 3^{rd} order flight control system ASAT can be explained by the constant lag between achieved and commanded lateral acceleration. The left panel of figure 4.10 shows that the achieved lateral acceleration lags behind the commanded lateral acceleration at every time instant for a 3^{rd} order flight control system. This lag causes the required lateral acceleration and divert for an intercept to rise in comparison to the zero-lag system. Although the increased lateral acceleration compensates for some of the effects of the constant lag, it is still insufficient to reduce the miss distance to manageable levels.

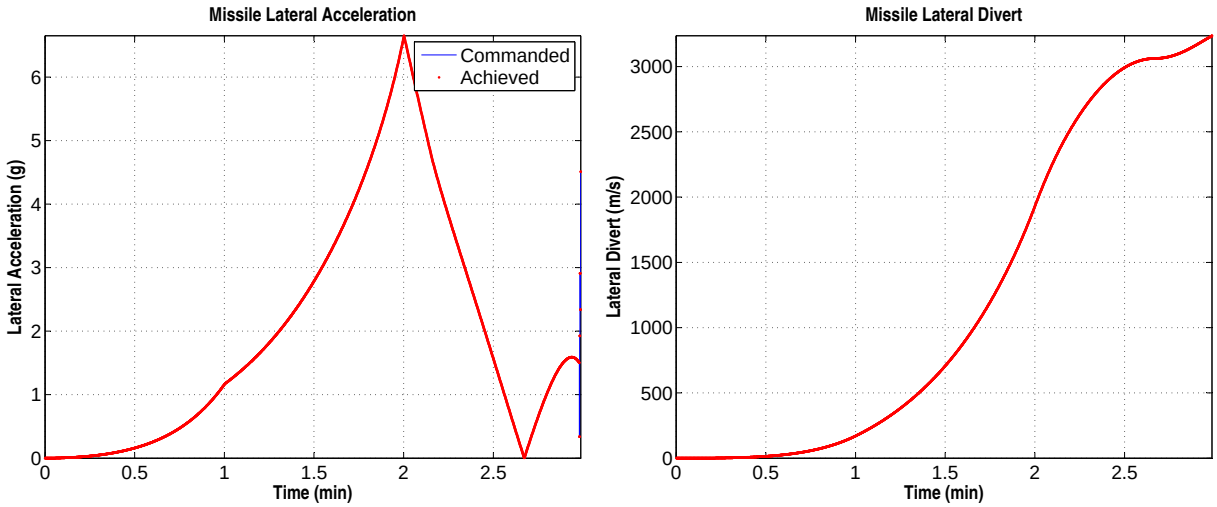

Figure 4.9: Zero-Lag Flight Control System ASAT Missile: Lateral Acceleration and Divert

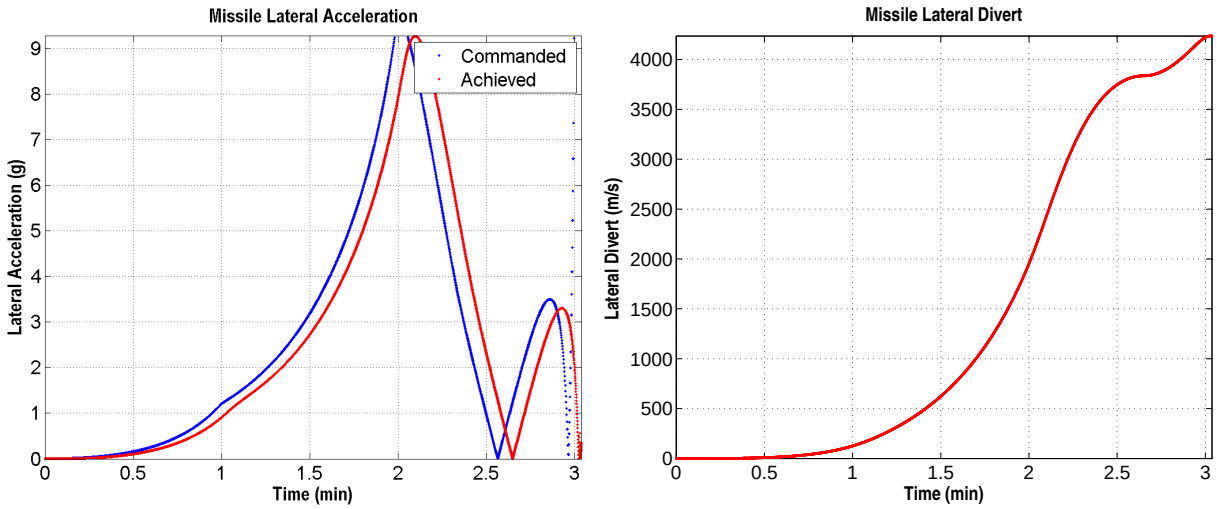

Figure 4.10: 3^{rd} Order Flight Control System ASAT Missile: Lateral Acceleration and Divert

4.3 Case II: Head-On Collision

The "head-on collision" type of ASAT mission profile is more realistic. An ASAT mission during wartime is much more likely to resemble the "head-on collision" intercept scenario described below. In this scenario, the targeted satellite has either performed a maneuver or there is no prior information available on its orbit. Either way, the satellite has to be tracked as it flies over the territory of the attacking nation (or its allies) while the ASAT missile is in flight towards a "head-on collision" with the satellite. This scenario is similar to a ballistic missile defense intercept.

There are two parts to simulating the dynamics of the ASAT-satellite "head-on collision" scenario. The first part involves modeling and simulating the parameters of the target satellite. This part is described in subsection 4.3.1 below. The second part involves the modeling of the dynamics, guidance law, and flight control system of the

ASAT missile, which was described in subsection 4.2.1 on page 123, subsection 4.2.2 on page 126 and subsection 4.2.4 on page 133 above.

4.3.1 Satellite Orbit Simulation

For the "head-on collision" simulation, the target satellite orbit is propagated in time. The altitude of the target satellite is 800 km. The inclination is set equal to the latitude of Xichang satellite launch center and the right ascension of ascending node (RAAN) is chosen to mimic an ideal situation where the satellite exactly passes the launch site. The mean anomaly at the beginning of the target satellite orbit propagation is, however, varied as a function of time ranging from 0 to 12 minutes after zero mean anomaly passage. The mean anomaly at various instants is given by

$$w = nt \tag{4.18}$$

Given the inclination, RAAN, and mean anomaly, the position of the target satellite during simulation is determined in spherical angles using the formulas given in table 4.4 below.

After calculating the spherical coordinates, the target satellite position vector at each time can be determined in an Earth-Centered Earth-Fixed (ECEF) coordi-

Table 4.4: Spherical Coordinates for Target Satellite at a Given Time [22]

	θ **(radians)**	ϕ **(radians)**
$0 < w \leq \frac{\pi}{2}$	$\frac{\pi}{2}$ - $\cos^{-1}(\sqrt{(}cos^2 w + sin^2 w.cos^2 i))$	$\omega + \tan^{-1}(\tan\ w.\cos\ i)$
$\frac{\pi}{2} < w \leq \pi$	$\frac{\pi}{2}$ - $\cos^{-1}(\sqrt{(}cos^2 w + sin^2 w.cos^2 i))$	$\omega + \pi$ - $\tan^{-1}$(-tan w.cos i)
$\pi < w \leq \frac{3\pi}{2}$	$\frac{\pi}{2}$ + $\cos^{-1}(\sqrt{(}cos^2 w + sin^2 w.cos^2 i))$	$\omega + \pi + \tan^{-1}(\tan\ w.\cos\ i)$
$\frac{3\pi}{2} < w \leq 2\pi$	$\frac{\pi}{2}$ + $\cos^{-1}(\sqrt{(}cos^2 w + sin^2 w.cos^2 i))$	$\omega + 2\pi + \tan^{-1}$(-tan w.cos i)

nate system by

$$X_{satellite} = \begin{bmatrix} rsin\theta cos\phi \\ rsin\theta sin\phi \\ rcos\theta \end{bmatrix}_{ECEF}$$

4.3.2 Limits on Achieving a "Head-On Collision"

Assuming that China is able to continuously track a satellite, this subsection will show that it is still not possible for China to engage an emerging satellite in a "head-on collision" using its SC-19 ASAT missile.

Figures 4.11, 4.12, 4.13 and 4.14 below illustrate the result of a "head-on collision" between the modeled SC-19 ASAT missile and a satellite at 800 km altitude. The left panel of each of these figures show an ideal scenario where the ASAT missile has a zero-lag flight control system with unlimited thrust. The right panel shows an operational real-world SC-19 missile with a 3^{rd} order flight control system that

has thrusting capability only when its rocket motors are ignited.

It can be seen from the right panel that for a real-world, operationally limited ASAT missile, the lateral acceleration starts to rise after the boost-period of the missile. However, the ASAT is not able to provide the required lateral acceleration. This leads to continuously rising lateral divert and growing target satellite maneuver as seen from the perspective of the ASAT missile. These effects lead to an inability of the SC-19 ASAT missile to engage the satellite in a "head-on collision". The same effect is observed for the various cases of 0, 5, 10 and 12 minutes after 0 mean anomaly passage shown below.

This difficulty in engaging a satellite in a "head-on collision" scenario can be understood as a result of the difference between the velocity of the target satellite and the ASAT missile. The satellite is traveling at approximately 7.5 km/s. In the three minutes of boost available to the modeled SC-19 missile the satellite travels a distance of 1350 km. In the same three minutes the ASAT missile will have to travel to the altitude of 800 km and, at the same time, compensate for the 1350 km the satellite traverses using its lateral acceleration forces. The ASAT mission must accomplish this while starting from 0 km/s velocity and flying at a average velocity of approximately 5.42 km/s during its 3 minutes of boosted flight.

4.4 Conclusion: The Limits of Chinese Anti-Satellite Missiles

This chapter has made the case even under ideal conditions, the reach of the Chinese SC-19 direct-ascent hit-to-kill ASAT missile is very limited. There seems

to be a thin region in space where a direct-ascent hit-to-kill ASAT mission might be feasible under the conditions of perfect satellite tracking. Given that, in order to have a high probability of success, an adversary like China would have to invest significantly in both satellite tracking infrastructure and ASAT missile batteries that would engage in salvo fire against target satellites.

There does not seem to be any sign that the Chinese are creating such an infrastructure. Those arguing otherwise would need to provide evidence proving the presence of such infrastructures or will have to demonstrate how the Chinese or an adversary with similar capability can execute a targeted ASAT attack against an U.S. satellite with a high probability of success.

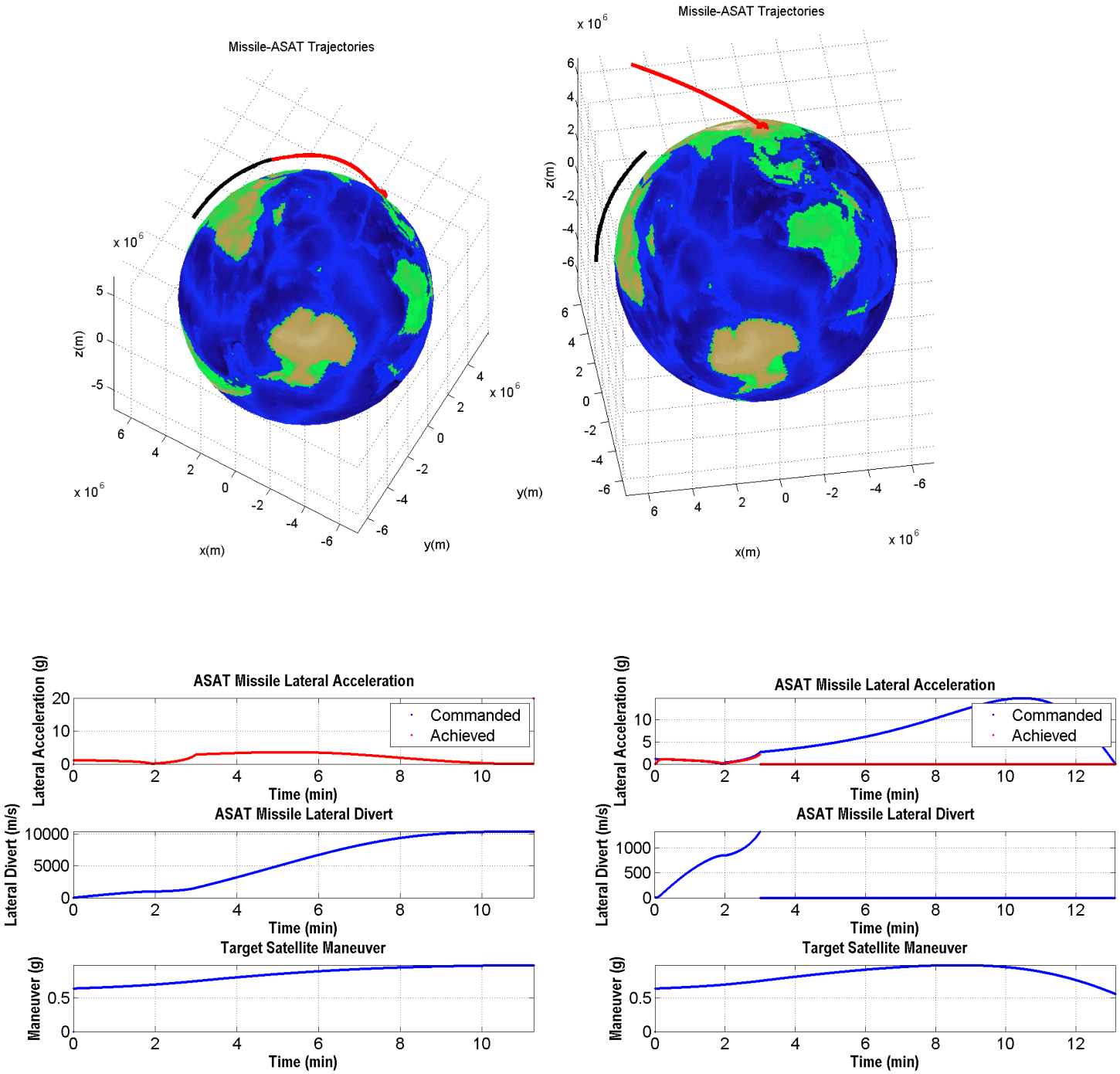

(c) **Ideal Case**: Zero-Lag flight Control System With Unlimited Thrust

(d) **Real-World Case**: 3^{rd} Order flight Control System With 3 Minutes of Thrust

Figure 4.11: Head-on Collision (0 Minutes After 0 Mean Anomaly Passage)

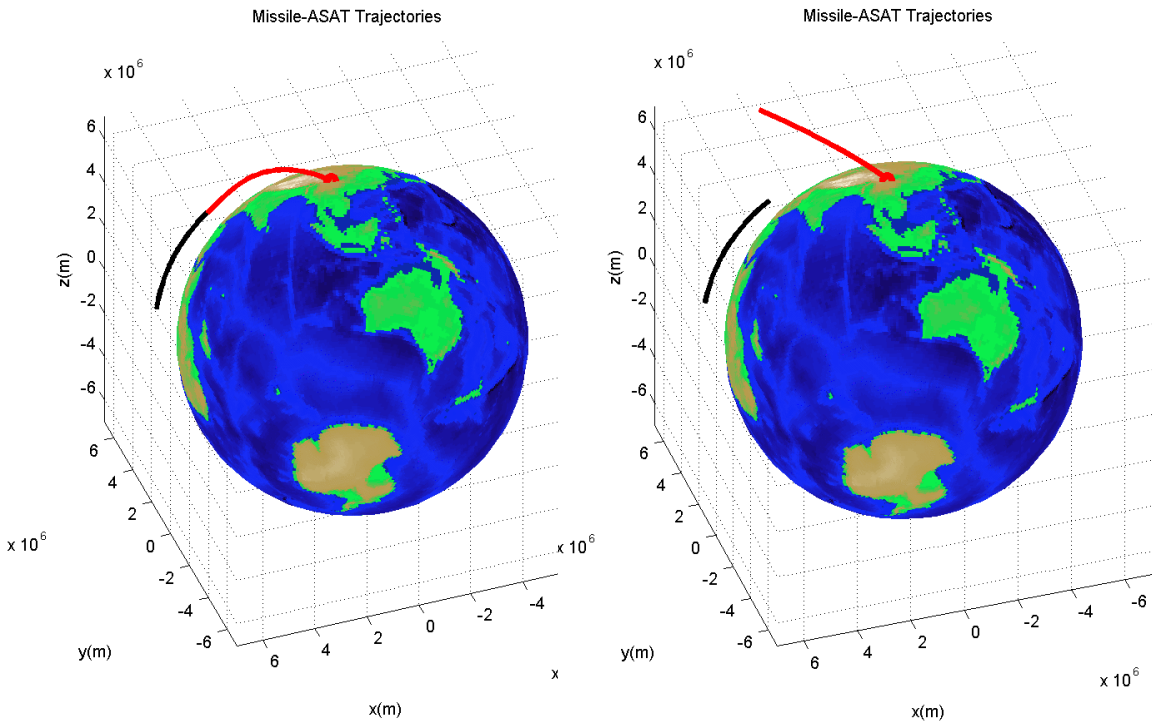

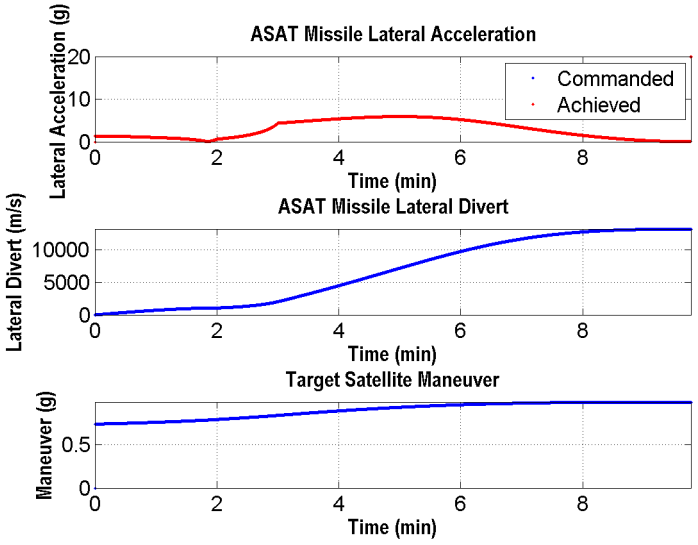

(c) **Ideal Case**: Zero-Lag flight Control System With Unlimited Thrust

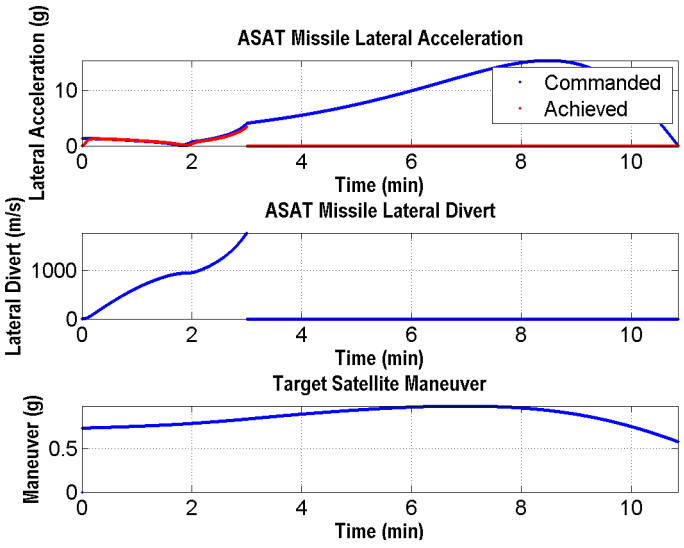

(d) **Real-World Case**: 3^{rd} Order flight Control System With 3 Minutes of Thrust

Figure 4.12: Head-on Collision (5 Minutes After 0 Mean Anomaly Passage)

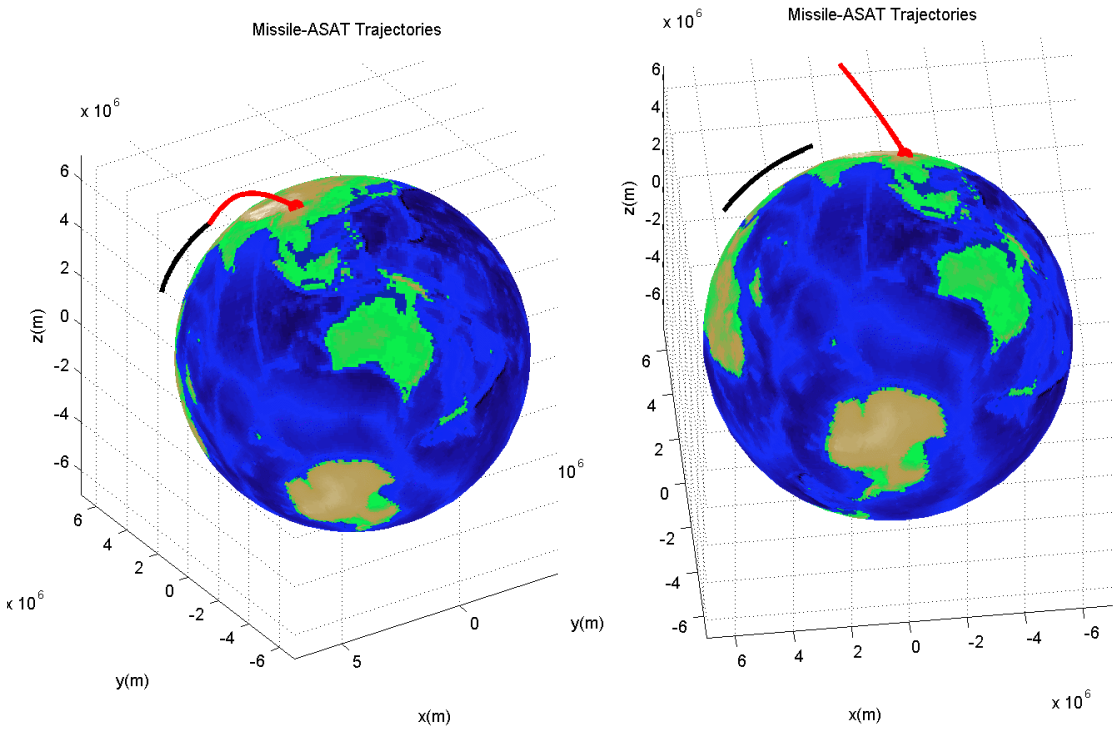

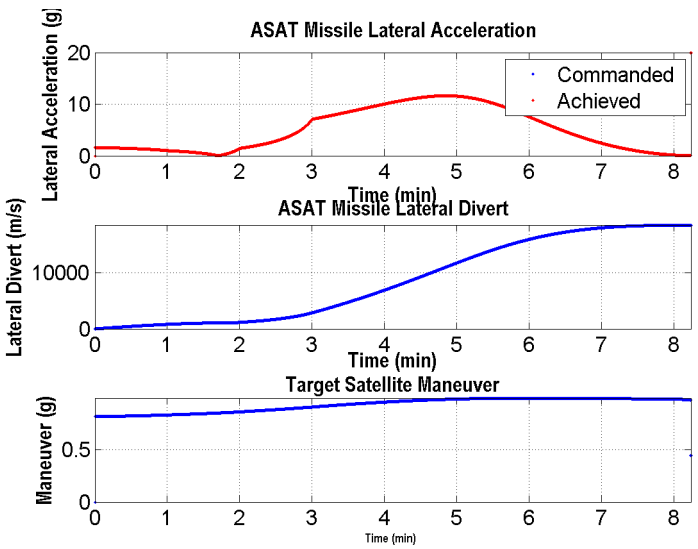

(c) **Ideal Case**: Zero-Lag flight Control System With Unlimited Thrust

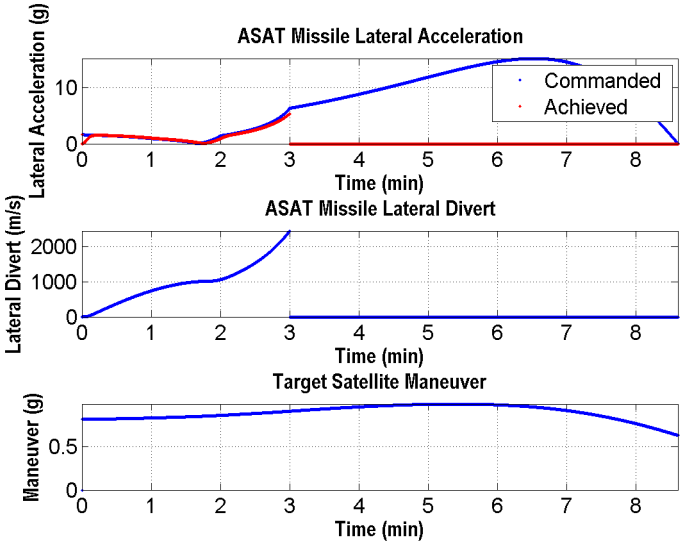

(d) **Real-World Case**: 3^{rd} Order flight Control System With 3 Minutes of Thrust

Figure 4.13: Head-on Collision (10 Minutes After 0 Mean Anomaly Passage)

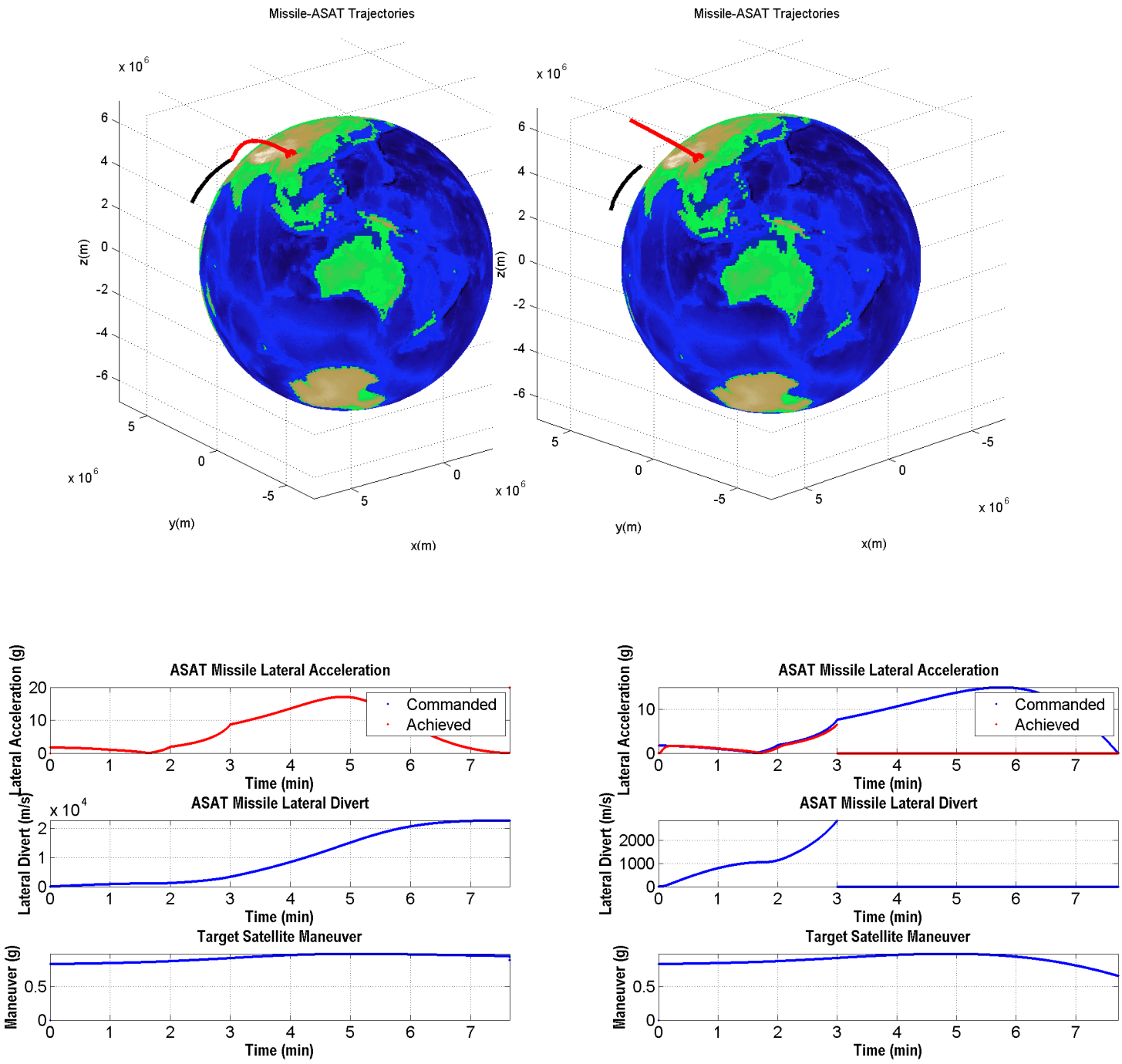

(c) **Ideal Case**: Zero-Lag flight Control System With Unlimited Thrust

(d) **Real-World Case**: 3^{rd} Order flight Control System With 3 Minutes of Thrust

Figure 4.14: Head-on Collision (12 Minutes After 0 Mean Anomaly Passage)

Chapter 5

Satellites, Missile Defense and Space Security

This chapter will investigate the role of modern satellite systems in U.S. missile defense operations and the effect of that linkage on space security. The Russians and Chinese contend that such a functional dyad, if and when operational and synchronized, could provide the U.S. with a false confidence in its ability to engage in a coordinated nuclear strike against them. This, they argue, upends the balance of strategic restraint between the U.S. and them. The Russians and Chinese frame the debate on space weaponization and arms control to include missile defense. The U.S. has argued that missile defense is a legitimate right that it preserves to protect itself. It is between these contrasting views that any agreement on space security will have to emerge.

U.S. missile defense systems have for a long time had a weak functional link to satellites. In the face of repeated claims and attempts to use satellites to significantly improve the efficiency of missile defense systems little was accomplished. The only implemented satellite system for missile defense purposes is the Defense Support Program (DSP)[1]. However, the utility of the DSP satellites for missile de-

1. DSP is the first operational constellation of satellites being used since 1970s for missile defense applications. Since then, DOD has attempted to replace DSP with the Advanced Warning System in the early 1980s; the Follow-on Early Warning System in the early 1990s; and the Alert, Locate, and Report Missiles system in mid-1990s. These attempts failed due to immature technology, high cost, and affordability issues[218]. Then in 1996, the Space-Based Infrared System (SBIRS) was initiated. However, negative trends in cost, schedule and performance estimates for the SBIRS-low

fense has been mostly trivial in comparison with the role played by other sensors. DSP satellites are capable of providing the position of missiles in flight to within a 1 km pixel once every 10 seconds in the early stages of flight[16]. This sampling rate is too low to enable independent guidance of the missile defense system interceptors. Therefore, the DSP satellites can only be used to construct a trajectory profile of the target ICBM missiles in the early stages of boost-phase flight. Once the target missile appears above the radar horizon all tracking and acquisition are accomplished by using ground-based radars.

This weak functional relationship between satellites and missile defense systems could however change substantially because of the advanced capabilities of the recently launched Space Tracking and Surveillance System (STSS) satellites. The two experimental LEO STSS satellites have dramatically more advanced capabilities than the DSP systems. They operate in stereo mode providing 3D positioning data on target ICBMs to within a 50 m pixel. The STSS satellites are based on a step-stare focal plane array (FPA) design than enables continuous tracking of target missiles in all phases of flight.

This chapter will study the improvements in intercept miss distances obtained by using STSS satellites for boost-phase missile defense. Boost-phase missile defense was chosen due to availability of detailed open-source information on the various processes involved in it. The "Report of the American Physical Society Study Group on Boost-Phase Intercept Systems for National Missile Defense: Scientific

---

program resulted in DOD taking it off an acquisition track, and converted it to a sustained and deliberate experimental technology development program called STSS in 2002[219].

and Technical Issues" published in October 2004[16] evaluated each of the processes involved in boost-phase missile defense in extensive detail. This report was used to benchmark and validate each of the steps undertaken in this chapter. This chapter is an initial attempt at studying the role of modern advanced satellite systems in missile defense. Future work of this chapter will extend the study to evaluate the effect of these advanced satellite systems on the mid-course phase of missile defense systems[2].

This chapter will demonstrate that the capability of STSS satellites when studied via computer simulations indicates that they reduce the attained miss distances in a boost-phase missile defense interception from the thousands of meters to less two hundred meters. These drastic reductions in intercept miss distances obtained with STSS is still insufficient to successfully execute a hit-to-kill boost-phase missile defense[3]. However, the improvements obtained with STSS are significant. Miss distances of less than two hundred meters shown in this chapter were obtained by modeling the parameters of the experimental STSS. It is conceivable that a technologically mature constellation could make STSS a credible mechanism for missile defense.

---

2. Tests are now being planned for the STSS satellites to see if the tracking data is good enough to cue the launch of ship-based interceptor missiles used in mid-course missile defense. As it stands now, the U.S. Navy Aegis ships can only launch interceptors if the ship's own radar is locked onto the missile. If it turns out that the satellite data is good enough to target missiles independently, it would drastically increase the effective range of each ship[41]. This would certainly threaten Russian and Chinese capabilities. The addition of a modern space-based missile detection network, which STSS is designed to demonstrate, could also give strategic, regional and theater defense systems more accurate warning of an enemy missile and permit the launch of interceptors against the threat earlier than ever before[190]. This again would be a matter of significant concern to China and Russia.

3. A successful hit to kill boost-phase intercept requires a miss distance of less than 1 m.

The potential capabilities of STSS adds a new and unique dimension to space security. To have a chance at successfully intercepting a rogue North Korean missile the STSS satellites have to be protected against any form of disruption. However, if the STSS based missile defense system is not operationally limited to rogue threats other nations including China and Russia perceiving themselves as potential targets will challenge its legitimacy and disrupt these satellites if needed. This scenario will evolve in some form in the future when the potential of STSS becomes more clear. Effective missile defense against rogue threats will require the U.S. to self-impose limitations on its space-based missile defense applications in order to obtain operational sanctuary for its satellites against disruption.

5.1 Outline of the Chapter

In order to investigate the role of the Space Tracking and Surveillance System (STSS) in missile defense operations, a simulation of a boost-phase ballistic missile defense (BMD) system utilizing STSS was undertaken in this chapter. There are multiple technical questions involved in estimating the utility of STSS to boost-phase missile defense. This section of the chapter will outline the various important sections and subsections that provide answers to those questions.

- Section 5.2 on page 154 will briefly describe the history behind the STSS satellites, their expected capabilities, their performance to date and future configurations.

- Section 5.3 on page 157 models and simulates the target ICBM threat that a

rogue state like North Korea could mount. The Peacekeeper missile is used as the baseline to model the threat ICBM missile.

- Section 5.4 on page 162 describes in detail the modeling and simulation of the boost-phase missile defense interceptors. Within Section 5.4, Subsection 5.4.1 on page 163 details the analysis done to decide the optimum interceptor basing location for given North Korean target ICBM parameters and other geopolitical considerations. Next, subsection 5.4.2 on page 167 details the equations governing the flight simulation, i.e., the dynamics of the interceptor. Subsection 5.4.3 on page 170 explains the Proportional Navigation guidance laws that direct the interceptor towards the target ICBM. Following subsection 5.4.3, subsection 5.4.5 on page 177 describes the flight control system of the interceptor.Finally, subsection 5.4.6 on page 180 shows the performance results of the modeled interceptor missile against the target North Korean ICBM.

- Section 5.5 on page 182 models and simulates a X-Band radar that could be used for boost-phase missile defense. Within section 5.5, subsection 5.5.1 on page 186 details the analysis done to decide the optimum radar basing distance and bearing for a given target ICBM launch location. Subsection 5.5.2 on page 191 details the method used to calculate the Radar Cross Section (RCS) of the target ICBM for a particular geometry between the radar and the interceptor. Finally, subsection 5.5.4 on page 195 shows the results of the modeled X-Band radar when it is tracking the target North Korean ICBM as

it flies to its intended target location. Also shown are the fused position error magnitudes for the two X-Band radars.

- Section 5.6 on page 202 explains the various new technologies like step-stare Focal Plane Arrays (FPA) and Quantum Well Infrared Photodetectors (QWIP) that are behind the performance of STSS. First, subsection 5.6.1 on page 206 configures the Infrared (IR) characteristics of the target ICBM during its flight in boost-phase and post-boost[4] for both day-time and night-time operations. Then subsections 5.6.2 and 5.6.3 on pages 210 and 212 respectively use the estimated IR characteristics of the target ICBM to determine the field of view, lens diameter, aperture area and signal-to-noise ratio (SNR) of the QWIP FPA of STSS. Finally, subsection 5.6.4 on page 216 explains the methodology used to estimate target ICBM position through stereoscopic satellite measurements. Also shown are the position error magnitudes obtained by STSS.

- Section 5.7 on page 221 describes the endgame simulation and the sensors used on the Kill Vehicle (KV) of the interceptor missile. The KV sensor parameters are taken from the American Physical Society (APS) report on boost-phase missile defense[16].

- Section 5.8 on page 222 shows the results of the complete simulation. Graphs in this section show the improvement in boost-phase missile defense miss distance on using STSS as compared to ground-based radars.

4. Post-boost phase is included since STSS is claimed to have multiband discrimination capability enabling seamless tracking from boost-phase to mid-course phase.

- Finally, section 5.9 on page 225 concludes by reiterating the linkage between missile defense and space security and the emerging need for U.S. acceptance of limits on its military space applications.

5.2 Evolution of STSS: "Holy Grail" for Missile Defense

The Space Tracking and Surveillance System (STSS) is the latest iteration of many space-based satellite IR systems intended to aid missile defense. STSS is the LEO component of a scaled down version of the Space Based Infrared System (SBIRS). Initially, SBIRS was designed to have two components: SBIRS-GEO and SBIRS-Low. There were to be 4 SBIRS GEO and 24 SBIRS-Low. However, escalating cost and schedule slips[5] lead to a reduced system of four GEO satellites and two experimental STSS payloads riding on classified host satellites in HEO[147].

---

5. Despite years of significant investment, most of the DOD large space acquisition programs have collectively experienced billions of dollars in cost increases, stretched schedules, and increased technical risk. Unit costs for the Space Based Infrared System (SBIRS), for instance, has climbed about 231 percent to over USD 3 billion per satellite. Moreover, the first satellite, GEO-1 was launched into geostationary orbit on May 2011, about 9 years later than predicted[226]. Total cost for the SBIRS High program is currently estimated at over USD 18 billion for six GEO satellites, representing a program unit cost of over USD 3 billion, about 233 percent more than the original unit cost estimate[225].Also, program officials are predicting a 1–year delay on production of the 3rd and 4th GEO satellites due in part to technical challenges, parts obsolescence and test failures. Along with the production delay, program officials are predicting a USD 438 million cost overrun for the 3rd and 4th GEO satellites. There were three identified primary reasons for the SBIRS program cost increases/schedule delays/technical problems: (1) latent defects, resulting from insufficient product assurance activity in earlier design and production activities; (2) insufficient schedule and budget to ensure robust GEO first article integration/test; and (3) process escapes due to human error/insufficient training/fragile processes. In mid-2006, Gary Payton, then the chief of Air Force space acquisition, trying to explain the delays in SBIRS, told *Aerospace America*: "In the beginning of the SBIRS High program, everybody said 'we're going to take a grand and glorious big leap forward to replace the old DSP missile warning satellites that are old and are not good enough any more.' The problem was that we didn't have the technology that would be needed....but we went ahead anyway." The Air Force and its SBIRS High contractors "began doing the research work without having the technology in hand for the sensor that was supposed to go on the spacecraft," he explained[90].

The two experimental STSS satellites were launched on the 25th of September 2009 on a single United Launch Alliance Delta 2 rocket[187]. They now fly in tandem in HEO at about 1350 km above the Earth and a couple of thousand kilometers apart. In that configuration, they provide a stereo view of the missile and warheads they track[233]. Each satellite has two sensors. During operation, first an acquisition sensor detects the short-wave infrared (SWIR) signature produced by the hot exhaust of a missile launch. As the missile passes through the boost-phase, the second sensor takes over, using mid-wave infrared (MWIR) to track upper stages of rockets and the small engines of post-boost vehicles[233, 211]. During an extended on-orbit check-out and calibration phase, the satellites tracked multiple missile launches in the early boost and post-boost phase and demonstrated the ability to relay data from one satellite to another.

On 6 June 2010, the twin STSS satellites observed the debut of the MDA's two-stage interceptor for the Ground-based Midcourse Defense System as it lifted off from Vandenberg Air Force Base, California, and flew over the Pacific Ocean. Ten days later, STSS observed an ICBM test launch from the same location. On 28 June 2010, the satellites observed a target missile that was launched from a mobile platform in the Pacific Ocean as part of a test of the Terminal High Altitude Area Defense System[212]. All this was done by only the acquisition sensor tracking in the boost-phase.

For the first time on the 16th of March 2011, STSS detected and tracked a ballistic missile launch through all phases of flight. The so-called "*birth-to-death*" tracking of a ballistic missile had never been done before from space and is the most

significant achievement to date for the STSS spacecraft. As Doug Young, Northrop Grumman's vice president of missile defense and warning programs said, "It's the Holy Grail for missile defense[210]." During the test, an ARAV-B short-range target missile was launched from the Pacific Missile Range Facility at Kauai, Hawaii. A STSS satellite detected the heat signature of the launch with its acquisition sensor, and then its tracking sensor locked on to the boosting missile[6]. It then passed the tracking data off to the second satellite, which followed the missile through space, re-entry and splashdown[210]. This is very significant as it demonstrated the ability to pass tracking data along from one spacecraft to another[41]. STSS sensor calibration was also done while tracking missile surrogate targets like ground-based Starfire laser and a NOAA weather satellite[190].

On October 5, 2011 the STSS demonstration satellites tracked two different missile targets and delivered data in real-time to support a successful flight test of the Terminal High Altitude Area Defense (THAAD), according to Northrop Grumman. During the live-intercept of both targets, the STSS demonstrators transmitted data in real-time to the U.S. MDA's Command, Control, Battle Management and

6. There have been significant problems in implementing the same sensor-to-sensor missile track transfer capability in the SBIRS GEO satellite. SBIRS GEO, similar to STSS, has two infrared sensors: a scanning sensor that sweeps over large swaths of territory watching for missile launches, and a staring sensor that can be trained constantly on a smaller area of interest to provide immediate notification of launches. Gen. William Shelton, head of Air Force Space Command, said the service will not be able to fully exploit data from the staring sensors on-board the SBIRS GEO satellites until 2016 or 2017. Shelton said the Air Force ran into "money issues" on the SBIRS program that led it to focus on getting the first satellite into orbit while deferring work on the ground segment. Moreover, he said, some of the ground software for the SBIRS satellite has proved more complex than anticipated[205]. Until the new software is ready, Shelton said, the Air Force will not be able to exploit the staring sensor data in real time[205]. Given this information, it seems rather questionable that STSS would have demonstrated the mentioned track transfer. All the information on STSS to date has been released by its contractor,Northrop Grumman, and its quite possible that the capabilities are being overstated.

Communications System. Known as FTT-12, the THAAD flight test took place at the Pacific Missile Range Facility at Kauai, Hawaii. FTT-12 is the second THAAD flight test that included STSS, with far more extensive participation by the demonstration satellites compared with the previous test on June 28, 2010 (FTT-14).

After the STSS demonstration mission is finished, the Missile Defense Agency (MDA) is planning to populate an operational constellation of missile tracking satellites based on STSS dubbed the Precision Tracking Space System (PTSS) scheduled to begin launch operations in 2018[210]. MDA hopes that the STSS program will set the stage for PTSS, a network of 9 and 12 satellites to join MDA operational assets in real-world defense efforts. The PTSS satellite fleet would be used by sea- and U.S.-based interceptors and future missile defense deployments in Europe[190].

5.3 Modeling the Target Ballistic Missile

This section of the chapter will detail the modeling and simulation of the target ICBM. It is the first step in determining the role of STSS in a boost-phase missile defense system.

In choosing a target ballistic missile, North Korea's space launcher/missile capabilities were used as a benchmark. The latest North Korean launchers Unha-2/3 are considered to represent a significance advance in capabilities. Unha-2 was estimated to have the potential to reach continental United States with a payload of 1 ton or more if North Korea modified it[52]. David Wright and Ted Postol[52] have

explained the possible capabilities of the Unha-2 and estimated its dimensions[7]. Although significant details on the Unha-2 were approximated by Wright and Postol, in order to simulate the physics of a ballistic missile intercept more detailed information like the magnetic permeability and electrical conductivity of the missile structure is required. Hence for the purposes of modeling it is assumed that a future North Korean ICBM would parallel the capabilities and designs of the early U.S. ICBM–Peacekeeper.

Peacekeeper is chosen as the model for simulation due to the extensive amount of information available on its design, capabilities, and structure. The detailed capabilities and dimensions of each stage of the Peacekeeper ICBM is shown below in table 5.1 and table 5.2. Choosing a solid-propellant target ICBM missile like Peacekeeper for analysis enforced a demanding requirement on the STSS satellite system being evaluated. A solid-propellant missile burns much faster than one built on liquid propellant. This implies that is there is less time for the STSS satellite system to form a trajectory track of the target ICBM missile. A missile tracking satellite system that works against a solid-propellant missile should also be able to work against a liquid-propellant missile as demonstrated in the APS report on missile defense[16]. Two models of the Peacekeeper (one targeting San Francisco and the other targeting Washington D.C.) were used in the simulation discussed in this chapter. This was done to model and simulate a boost-phase missile defense system

7. In their article, David Wright and Ted Postol argued that although this launcher could be modified to create a ballistic missile with capability to reach continental United States that any such missile would be significantly dependent on foreign components and technical expertise.

that should be able to operate against ICBMs attacking the entire the latitude and longitude range of the continental United States.

Table 5.1: Target Missile Properties: Peacekeeper Missile[78]

	Total Mass(lb)	**Propellant Mass(lb)** San Francisco Mass Fraction=0.85	**Propellant Mass(lb)** Washington D.C. Mass Fraction=0.90	**Isp(s)**	**Burn Time(s)**
Stage-1	108,000	91,800	97,200	300	60
Stage-2	61,000	51,850	54,900	300	60
Stage-3	17,000	14,450	15,300	300	60
Stage-4	5,000	0	0	0	0

Table 5.2: Target Missile Dimensions: Peacekeeper Missile[78]

Peacekeeper Missile Radar Cross Section (RCS) Model
Stage-1 Length=8.175 m Stage-2 Length=5.86 m Stage-3 Length=2.315 m Stage-4/Payload Length=5.45 m Diameter of the missile=2.3 m

5.3.1 Simulating the North Korean ICBM

The two models of the peacekeeper ICBM discussed above are simulated using slightly varying parameters. The first is modeled to be launched from Kilju-kun missile base in North Korea towards San Francisco. The second is modeled to be launched from Kilju-kun missile base in North Korea towards Washington D.C. The

launch towards Washington D.C. requires a more capable ICBM and is modeled to have a mass fraction of ninety percent, whereas the ICBM targeting San Francisco is modeled to have a mass fraction of eighty-five percent. The simulated trajectory and velocity profile of both the ICBM models are shown in figures 5.1 and 5.2 on page 161. The simulation of the ICBMs are accomplished by forcing the ICBM model to obey Newton's Second Law at each time step. In vector form Newton's law is written as

$$\vec{F} = m\vec{a} \tag{5.1}$$

where $\vec{F}$ is the force vector (in Newtons) acting on the center of gravity of the ICBM, m is the total mass (in kg), and $\vec{a}$ is the net acceleration (in m/s^2). There are three major forces acting on the missile: Thrust ($\vec{T}$) acting in the direction of the ICBM velocity vector, Weight ($\vec{W}$) acting in the direction of the center of the Earth, and Drag ($\vec{D}$) acting in the direction opposite to the ICBM velocity vector. The magnitude of the three forces are calculated as

$$T = -I_{sp}\dot{W} = -I_{sp}\frac{dm}{dt}g \tag{5.2}$$

$$W = mg \tag{5.3}$$

$$D = 0.5\rho V^2 C_d A_{projected} \tag{5.4}$$

where I_{sp} is the stage specific impulse (in s), $\dot{W}$ is the change in stage weight over time, ρ is the atmospheric density at the current position of the ICBM, V is the velocity magnitude of the ICBM, C_d is the co-efficient of drag, and $A_{projected}$ is the projected area of the ICBM. $\dot{W}$ is the product of in-stage fuel consumption $\frac{dm}{dt}$ (in kg/s) and gravitational acceleration at the current distance from the center of the Earth g in (m/s^2).

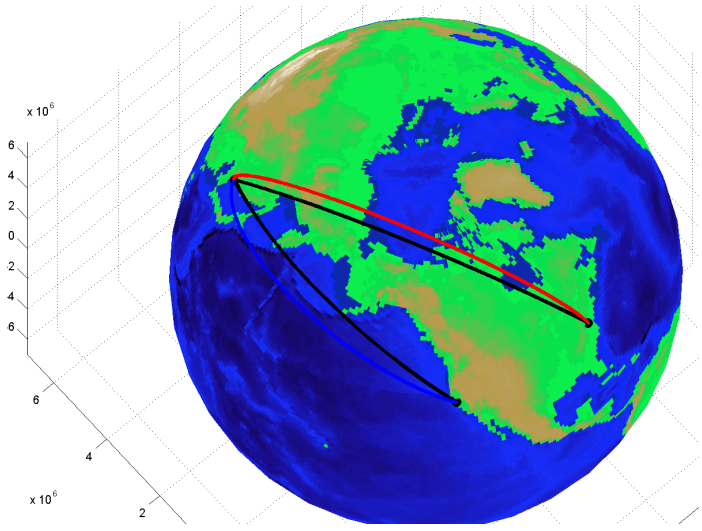

Figure 5.1: ICBM Trajectories Targeting San Francisco and Washington D.C.

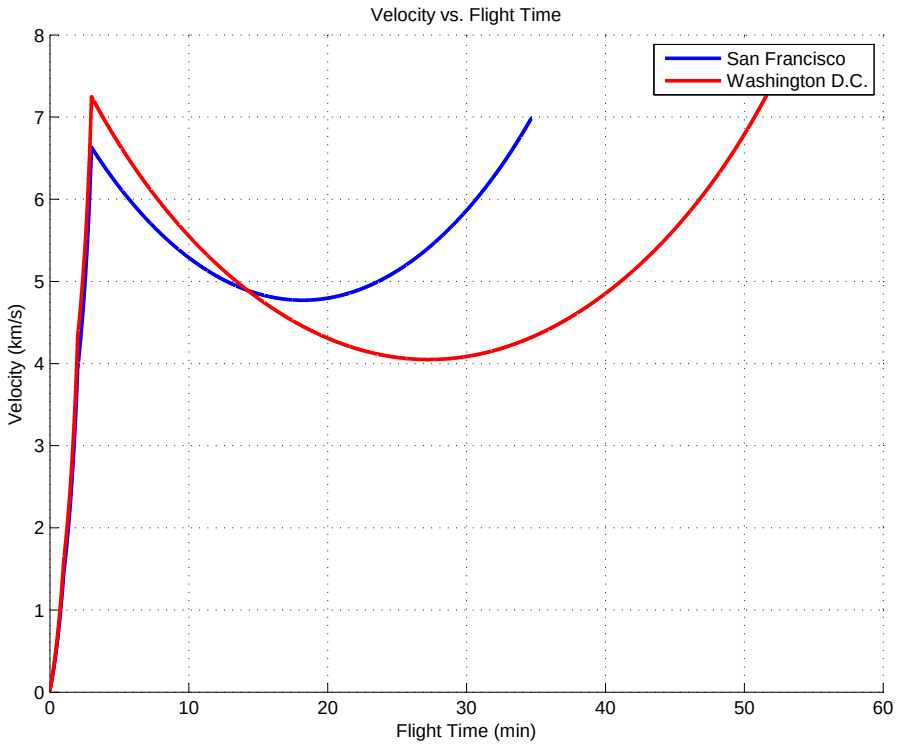

Figure 5.2: ICBM Velocity Profile

5.4 Modeling the Interceptor Ballistic Missile

Two types of missile defense interceptors are modeled and simulated (refer to table 5.3 below). The first interceptor IM-1 is meant to intercept and destroy the North Korean ICBM targeting San Francisco. The second interceptor IM-2 is meant to intercept and destroy the North Korean ICBM targeting Washington D.C.

As a mission requirement, both the interceptors should be more capable than the ICBMs. This is because usually there is a significant time delay between the ICBM and interceptor launch and the interceptor missile should be able to make up for this lost time. Therefore, both interceptors IM-1 and IM-2 are modeled to have ninety-five percent mass fraction. IM-2 is modeled with a specific impulse of 350

Table 5.3: Interceptor Missile Properties

	Total Mass(lb)	**Propellant Mass(lb)** Mass Fraction=0.95	**Isp(s)** IM-1	**Isp(s)** IM-2	**Burn Time(s)**
Stage-1	108,000	102,600	300	350	60
Stage-2	61,000	57,950	300	350	60
Stage-3	17,000	16,150	300	350	60
Stage-4	1,500/1,500	0	0	0	0

seconds whereas IM-1 is modeled with a specific impulse of 300 seconds. These mass fraction and specific impulse values were chosen to meet the minimum requirements for a successful boost-phase interception[8].

5.4.1 Determination of Interceptor Location

The first decision to be made concerning the architecture of a boost-phase BMD system is the location of the interceptors. This section will discuss the process involved in making that decision. Ideally, the interceptors should be located and launched in a direction opposite to the flight direction of the attacking missile i.e. a head-on collision geometry. However, that is not currently possible for the case of a North Korean ICBM targeting either San Francisco or Washington D.C. since the

8. These values are very high and is extremely difficult to achieve, if at all possible. However, as the APS report on boost-missile defense stated, "Boost Phase defense of the entire United States against solid-propellant ICBMs, which have shorter burn times than liquid-propellant ICBMs, is unlikely to be practical when all factors are considered, no matter where or how the interceptors are based. Even with optimistic assumptions, a terrestrial-based system would require very large interceptors with extremely high speeds and accelerations to defeat a solid-propellant ICBM launched from even a small country like North Korea." In order to evaluate the effect of STSS satellite systems it was assumed these values of the interceptor missiles are achievable.

direction of the ICBM flight requires basing the interceptors within Russia or its territorial waters to gain a head-on collision geometry. This difficulty is illustrated in figure 5.3 below.

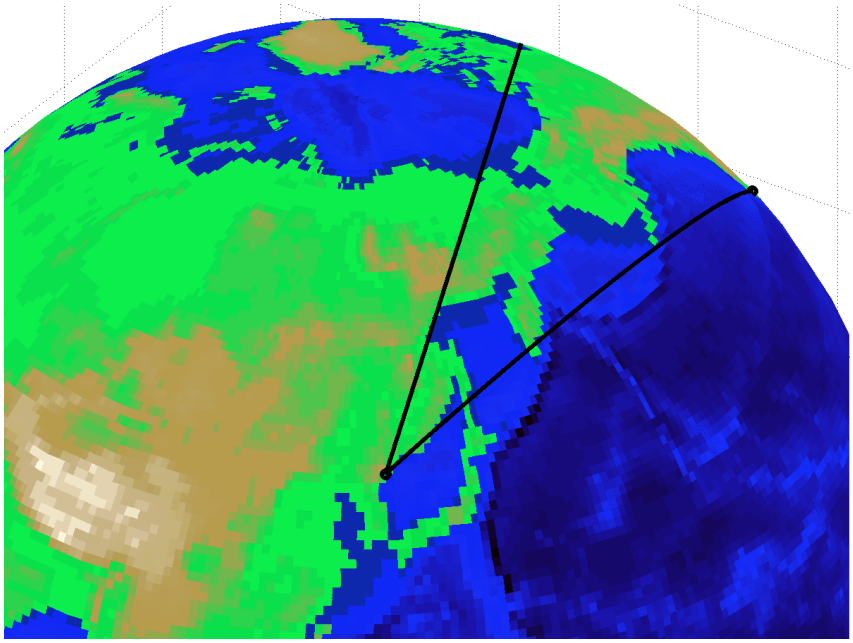

Figure 5.3: ICBM Track Direction

The next best feasible location for the interceptors is to the east of the ICBM launch location in the Sea of Japan or in Japan as shown in figure 5.4 below.

To determine the optimal interceptor launch site distance to the east of the IBCM launch site, a preliminary simulation was run with the assumption that an interceptor (IM-1) with perfect dynamics[9] was pursuing an San Francisco-bound

9. Meaning the interceptor possess no system lags is able to execute all guidance commands immediately and completely.

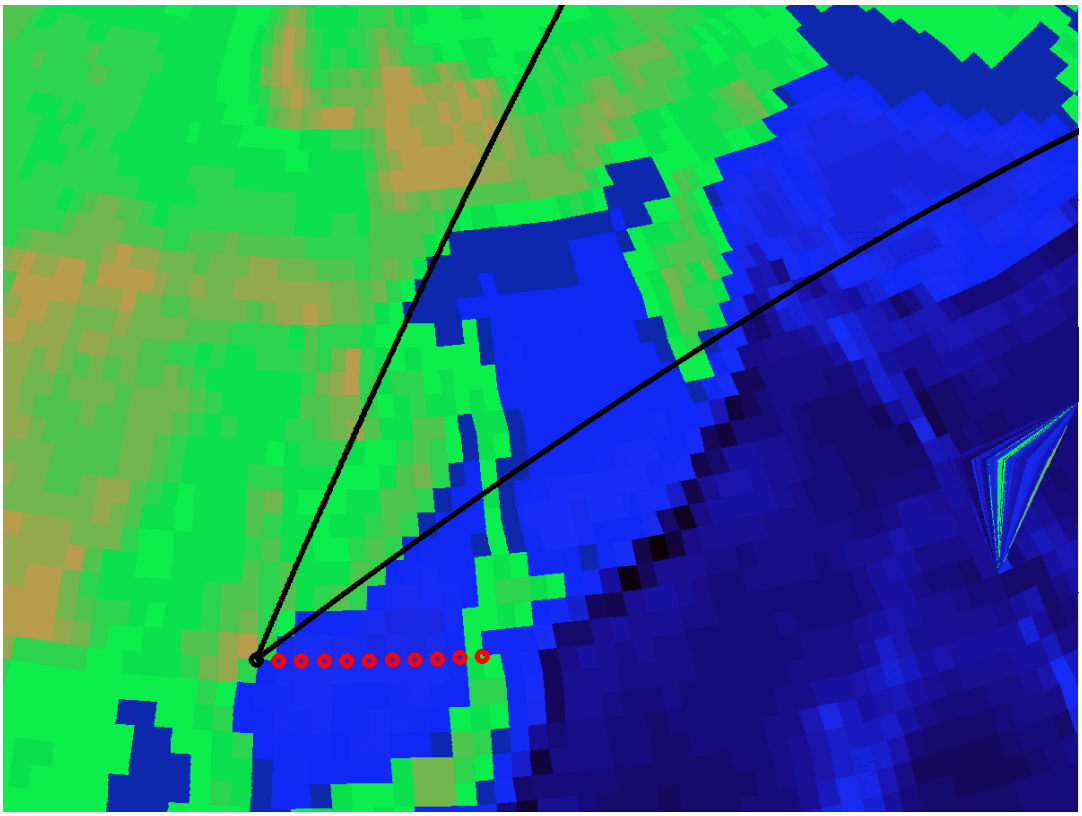

Figure 5.4: ICBM Track Direction with Possible Interceptor Missile Locations

North Korean ICBM with perfect targeting information[10]. The simulation was run multiple times with the interceptor located at distances ranging from 100 km to 1000 km to determine the optimal distance. For the case of an ICBM launched from North Korea targeting San Francisco, the results of the simulation are tabulated in table 5.4 below.

A distance of 900 km or more is rejected since the intercept takes more than

10. Meaning the interceptor possess perfect and immediate knowledge about the location and acceleration of the ICBM at every instant.

Table 5.4: Interceptor (IM-1) Siting Parameters (for ICBM targeting San Francisco)

Distance from ICBM launch site (km)	**Time (min)**	**Miss Distance (m)**	**Lateral Divert (m/s)**	**Max. Commanded Acceleration (G)**
100	1.50	1.95	1085.22	86.60
200	1.70	2.36	937.45	2.90
300	1.98	2.30	975.67	5.30
400	2.20	4.64	896.96	1.93
500	2.40	2.61	985.62	24.75
600	2.58	4.34	1081.05	11.56
700	2.74	3.55	1231.35	9.11
800	2.88	7.88	1508.25	19.05
900	3.00	6.74	2097.55	86.16
1000	3.11	7.98	2076.84	14.61

the 3 minutes of boost-phase. Interceptor location siting distances of 100 km, 500 km, 800 km, 900 km and 1000 km are rejected since interception from these distances results in excessive acceleration demands on the interceptor missile that are physically infeasible[11] (10 G is considered the limit). The lowest miss distance within acceptable values of interceptor acceleration demands is 2.30 m obtained at 300 km distance. This is a tolerable miss distance for a numerically approximated computer simulation. In a real-world case, a miss distance of less than 1 m is required to have a high probability of single-shot hit-to-kill intercept. At 300 km, the effort required

11. The high values of acceleration (i.e., any value above 10 G) show in table 5.4 would be physically impossible to realize due to structural limitations of the interceptor missile. It was possible only because the conputer programs used in these calculations did not enforce a maximum limit on the acceleration at this stage. Such limits will be enforced from the next step of the simulation algorithm.

to achieve a miss distance of 2.30 m is reasonable at 975.67 m/s of lateral divert. Therefore, the optimum interceptor location for the ICBM targeting San Francisco is taken to be at a distance of 300 km.

For the case of an ICBM launched from North Korea targeting Washington D.C. the results of the simulation are tabulated in table 5.5 on page 168. Any distance greater than 700 km is rejected since the intercepts takes more than the 3 minutes of boost-phase. Similarly, 100 km and distances greater than 500 km are rejected due to excessive acceleration demands on the interceptor missile. The lowest miss distance within acceptable values of interceptor acceleration demands is 2.74 m obtained at 200 km distance.

To mimic real-world conditions the interceptor should be located at a distance where it should at least be able to intercept and destroy ICBMs having the latitude and longitude spread of the San Francisco and Washington D.C. trajectories. This means a distance of 200 km is not acceptable since for the San Francisco-bound ICBM, a distance of 300 km is required. Therefore, all further calculation in this simulation is performed by modeling the interceptors as being located at distance of 300 km east from the ICBM launch location (Kilju-kin in North Korea).

5.4.2 Simulating the Interceptor Missile

The simulation of the interceptor (similar to the ICBM simulation) is accomplished by forcing the modeled interceptor to obey Newton's Second Law at each

Table 5.5: Interceptor (IM-2) Siting Parameters (for ICBM targeting Washington D.C.)

Distance from ICBM launch site (km)	**Time (min)**	**Miss Distance (m)**	**Lateral Divert (m/s)**	**Max. Commanded Acceleration (G)**
100	1.50	1.70	702.30	85.58
200	1.80	2.74	768.75	6.57
300	2.11	2.87	670.16	1.48
400	2.36	1.87	752.44	2.42
500	2.58	3.25	943.08	10.07
600	2.77	6.38	1335.29	15.66
700	2.93	5.75	2106.96	41.71
800	3.07	7.64	2916.93	27.27
900	3.20	7.55	3132.73	18.40
1000	3.34	5.86	3236.28	13.56

time step. In vector form, Newton's law is written as

$$\vec{F} = m\vec{a} \tag{5.5}$$

where $\vec{F}$ is the force vector (in Newtons) acting on the center of gravity of the ICBM, m is the total mass (in kg), and $\vec{a}$ is the net acceleration (in m/s^2). Similar to the ICBM modeling, there are three major forces acting on the missile as shown in equation 5.6.

$$\vec{F} = \vec{T} + \vec{W} + \vec{D} \tag{5.6}$$

However, the Thrust ($\vec{T}$) in the case of the interceptor missile is composed of $\vec{T_v}$ and $\vec{T_p}$ as shown in equation 5.7. The Weight ($\vec{W}$) is acting in the direction of the center of the Earth and Drag ($\vec{D}$) is acting in the direction opposite to the ICBM velocity vector.

$$\vec{F} = \vec{T_v} + \vec{T_p} + \vec{W} + \vec{D} \tag{5.7}$$

$\vec{T_v}$ is the thrust component along the direction of the velocity vector (in m/s) and $\vec{T_p}$ is the thrust component perpendicular to the velocity vector (i.e. the lateral divert). The mechanism to calculate $\vec{T_v}$ and $\vec{T_v}$ is shown in subsection 5.4.3 below. The total magnitude of the two thrust components parallel and perpendicular to the velocity vector is always equal to the total thrust $\vec{T}$ provided by the rocket engine.

The other two components of the force vector are estimated similar to the method used in the ICBM modeling. The magnitude of weight vector is given as

$$W = mg \tag{5.8}$$

and the magnitude of the drag vector is calculated as

$$D = 0.5\rho V^2 C_d A_{projected} \tag{5.9}$$

where ρ is the atmospheric density at the current position of the ICBM, V is the velocity magnitude of the ICBM, C_d is the co-efficient of drag, and $A_{projected}$ is

the projected area of the ICBM.

5.4.3 Interceptor Guidance System

The Interceptor Guidance System uses Proportional Navigation guidance law for estimating $\vec{T}_p$, the guiding force used in driving the interceptor missile towards the ICBM target[12]. Figure 5.5 on page 170 depicts the operational logic of the proportional navigation based guidance system.

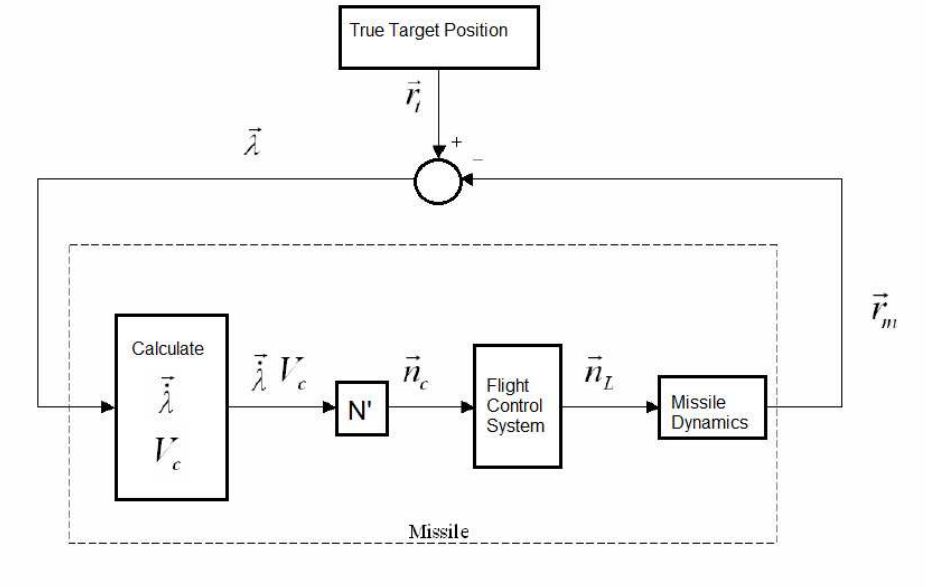

Figure 5.5: Interceptor Proportional Navigation Guidance System Diagram

12. The proportional navigation guidance law is optimal for constant velocity targets. This condition is not satisfied for acceleration ICBMs which are the targets in boost-phase BMD intercepts. However, the aim in this simulation is not to design a guidance law for boost-phase intercepts. The aim is to study the effect of STSS sensors. Hence the simplified proportional navigation guidance law is used. More detailed studies for designing a tuned guidance system for an accelerating target can be found in the APS study on boost-phase intercept[16].

The first step in the guidance law is for the interceptor missile to measure/read the position vector of the target $\vec{r_t}$ and computes the line of sight (LOS) vector $\vec{\lambda}$ by subtracting its own position vector $\vec{r_m}$ as shown in equation 5.10 below

$$\vec{\lambda} = \vec{r_t} - \vec{r_m} \tag{5.10}$$

This LOS vector $\vec{\lambda}$ is then differentiated to calculate the LOS rate vector $\dot{\vec{\lambda}}$ and closing velocity V_c. The magnitude of the LOS rate is obtained by

$$|\dot{\lambda}| = \frac{|\Delta\hat{\lambda}|}{\Delta t} \tag{5.11}$$

where Δt is the simulation step time.

The closing velocity V_c is computed as the range rate. The range between the ICBM and the interceptor is the magnitude of the LOS vector $|\vec{\lambda}|$. This magnitude is calculated for each time step of the simulation and differentiated. Dividing the difference in the range by the simulation step time yields the closing velocity as

$$V_c = \frac{|\Delta\vec{\lambda}|}{\Delta t} \tag{5.12}$$

The calculated parameters $\dot{\vec{\lambda}}$ and V_c are multiplied by the navigation coefficient N' to calculate the commanded lateral acceleration vector $\vec{n_c}$ as shown in equation

below.

$$n_c = N' V_c \dot{\lambda} \tag{5.13}$$

The commanded acceleration is always applied perpendicular to the LOS. The flight control system uses the commanded lateral acceleration to change the altitude of the missile resulting in the achieved lateral acceleration vector $\vec{n_L}$. The achieved lateral acceleration vector $\vec{n_L}$ is integrated along with other accelerations acting on the system resulting in a new missile position $\vec{r_m}$.

The instantaneous LOS vector is normalized to obtain the LOS unit vector $\hat{\lambda}$. In the next time step, the new LOS is computed using equation 5.10 and converted to the unit vector. Vector subtraction of these two unit vectors is the direction in which the acceleration command is applied and is always perpendicular to the instantaneous LOS. After normalizing the acceleration command, the unit vector is

$$\hat{n_c} = \frac{\hat{\lambda} - \hat{\lambda}_{previous}}{|\hat{\lambda} - \hat{\lambda}_{previous}|} = \frac{\Delta\hat{\lambda}}{|\Delta\hat{\lambda}|} \tag{5.14}$$

where $\hat{n}_c$ is the unit acceleration command vector perpendicular to the LOS, $\hat{\lambda}$ is instantaneous unit LOS vector, and $\hat{\lambda}_{previous}$ is the previous unit LOS vector.

Finally, the commanded acceleration vector is calculated. The magnitude of the commanded acceleration is computed by multiplying the navigation ratio, the closing velocity, and the magnitude of the LOS rate. Multiplying the magnitude of the acceleration command with the acceleration command unit vector yields the

commanded acceleration command vector. This is expressed as

$$\vec{n}_c = \hat{n}_c N' V_c |\dot{\lambda}| \tag{5.15}$$

For a zero lag system, the achieved acceleration n_L is always equal to the commanded acceleration n_c. For the moment, it is assumed that the interceptor dynamics are free of lags.

The computed acceleration command is perpendicular to the LOS; however, missile acceleration commands ($\vec{T_p}$) can only be applied perpendicular to the velocity vector. Thus, only the commanded acceleration component perpendicular to the velocity vector contributes to the missile guidance. The thrust component perpendicular to the velocity vector, $\vec{T_p}$, is then given as

$$\vec{T_p} = \vec{n}_{c\perp} m_m \tag{5.16}$$

where m_m is the interceptor missile mass at the current time.

Using equation 5.7, the magnitude of the thrust component parallel to the velocity vector is

$$\vec{T_v} = \sqrt{|\vec{T}|^2 - |\vec{T_p}|^2} \tag{5.17}$$

5.4.4 Simulation Results With Zero-Lag Interceptor Guidance System

Applying the equations derived earlier, simulations of the intercept were performed. The interception between IM-1 and the San Francisco-bound target ICBM produces very different flight profiles and demands as compared to the interception between IM-2 and the Washington D.C.-bound target ICBM as discussed below.

Interception Geometry

The intercept geometry of the two intercept is shown in figure 5.6 on page 175. There are some significant differences between the two. The intercept between IM-2 and Washington D.C.-bound target ICBM takes place at an altitude 40 km higher than the intercept of IM-1 and San Francisco bound-target ICBM as shown in figure 5.7. This would mean that the IM-2 intercept would have more and quicker exposure to space-based satellite Infrared (IR) sensors. The higher velocity of intercept in the case of the Washington D.C.-bound target ICBM as shown in figure 5.8 on page 176 is due to the relative superior capabilities of that ICBM and the IM-2 interceptor.

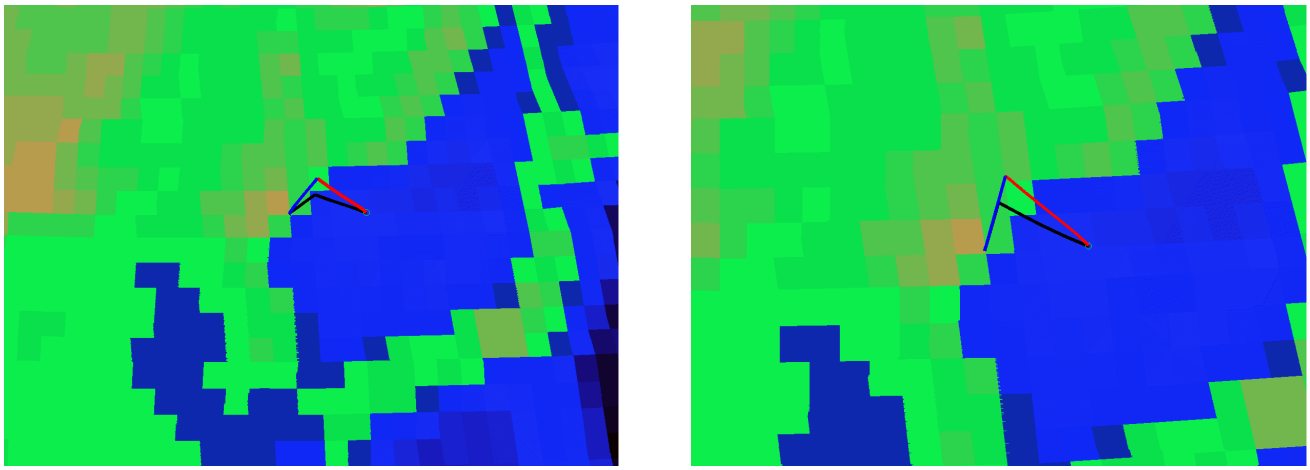

Figure 5.6: Interception Geometry (San Francisco on left; Washington D.C. on right)

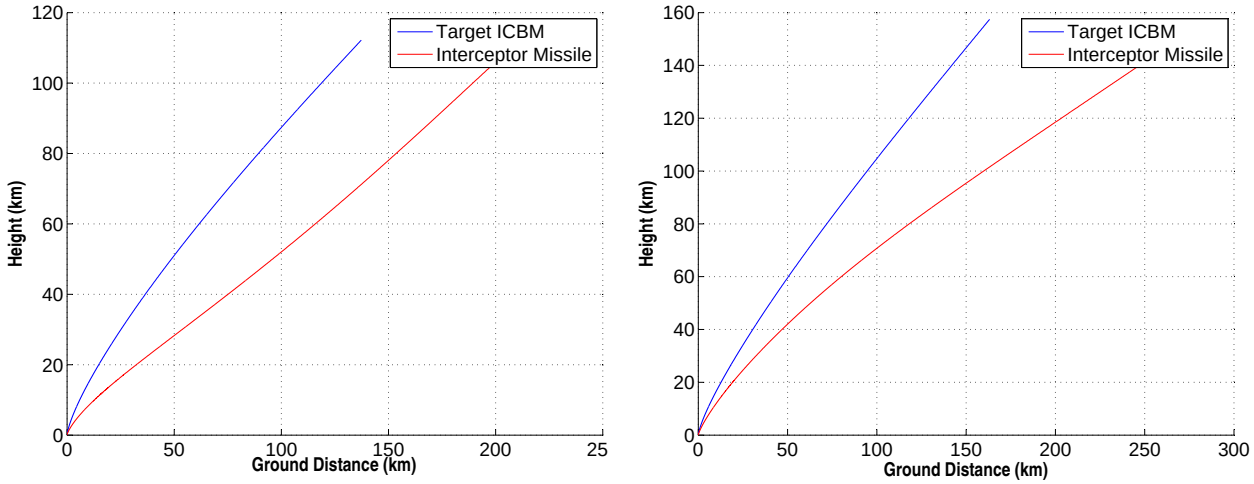

Figure 5.7: Height vs. Distance for Target ICBM and Interceptor (San Francisco on left; Washington D.C. on right)

Target Maneuver

Shown below in figure 5.9 on page 177 is the acceleration of the target ICBM for both intercept scenarios as seen by the respective interceptor, i.e., the observed

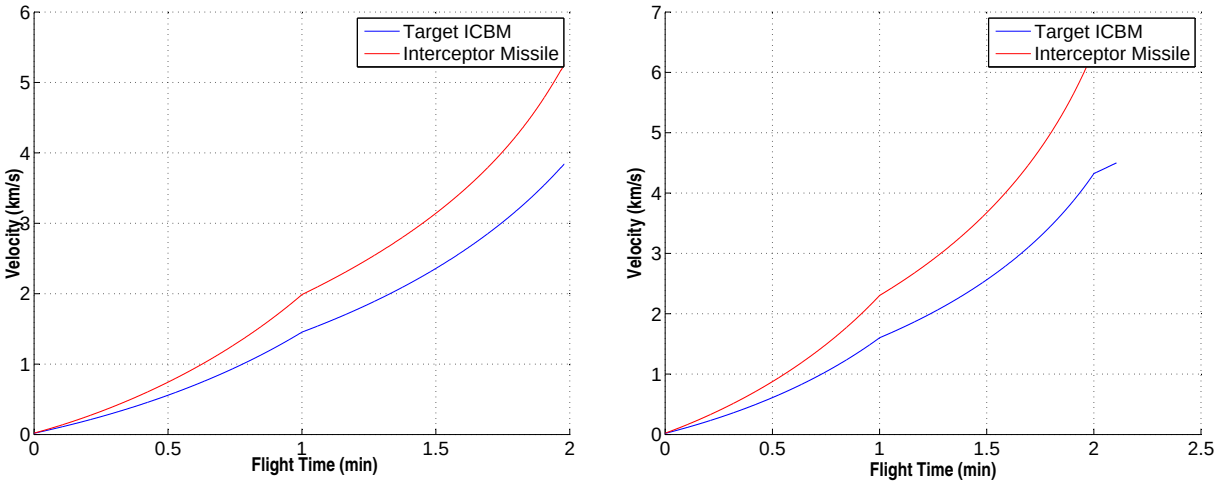

Figure 5.8: Velocity for Target ICBM and Interceptor (San Francisco on left; Washington D.C. on right)

target maneuvers. It is this acceleration viewed by the interceptor as a function of the interception geometry between itself and the target ICBM that influences the effort required and the miss distance produced. Constant target acceleration is ideal to achieve zero miss distances. Apparently, the interception between IM-2 and Washington D.C.-bound target ICBM produces appreciably more target maneuver than the other scenario.

Interceptor Effort

Two variables measure the effort made by the interceptor during the course of its mission. The lateral divert measures the change in velocity that is experienced by the missile due to the guidance force thrust perpendicular to the velocity vector, $\vec{T}_p$. The lateral divert values are shown below in the figure 5.10 on page 178 for both the interceptions. The second variable of interest is the acceleration experienced by

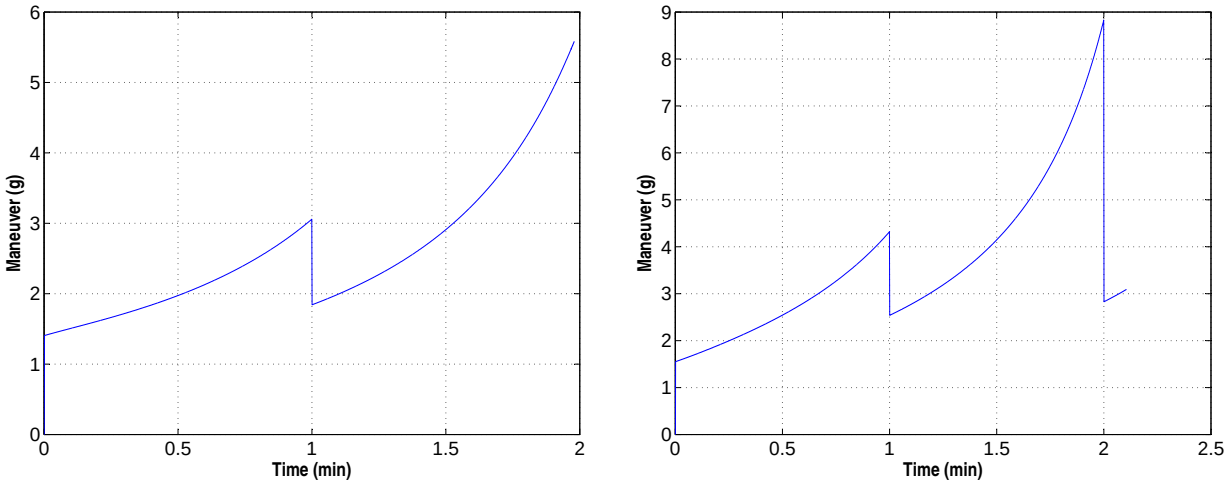

Figure 5.9: Acceleration of Target ICBM as Seen by the Interceptor Missile (San Francisco on left; Washington D.C. on right)

the interceptors (shown in figure 5.11 on page 178) during the course of its mission. Higher values of acceleration cause more stress on the interceptor's structure. The intercept between IM-1 and the San Francisco-bound ICBM seems to generate greater lateral divert and acceleration demands.

5.4.5 Third Order Flight Control System

So far, the missile guidance has been assumed to be perfect. In other words, the achieved acceleration n_L is always equal to the commanded acceleration n_c. This type of model is known as a zero-lag guidance system where the interceptor missile flight control system can respond to acceleration commands immediately and with 100 percent efficiency. In reality, guidance systems have lags (or delays) in their response. In this subsection the simulation model is expanded to include a

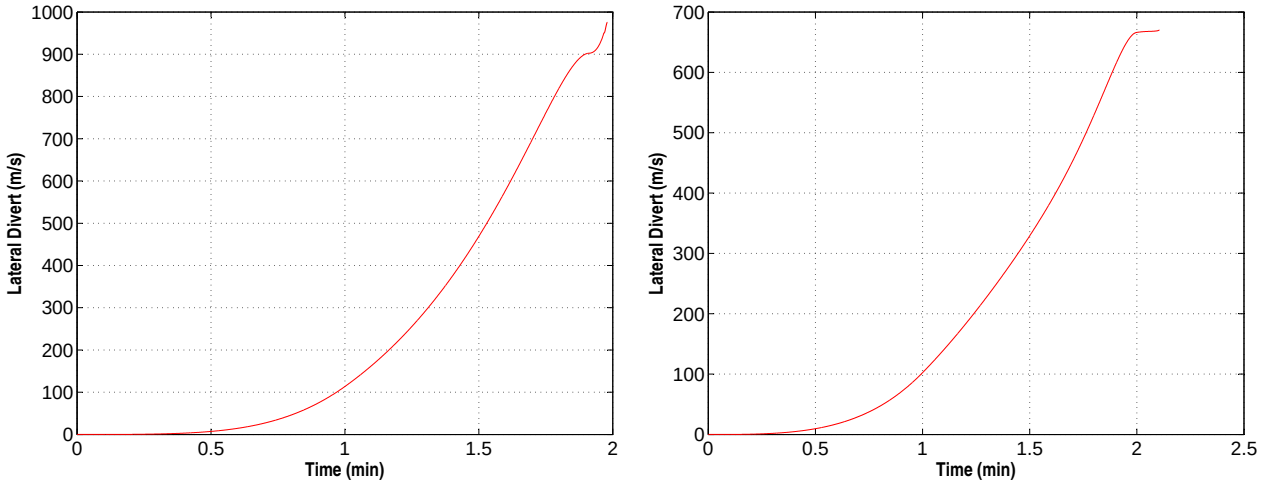

Figure 5.10: Lateral Divert Demands on the Interceptor (San Francisco on left; Washington D.C. on right)

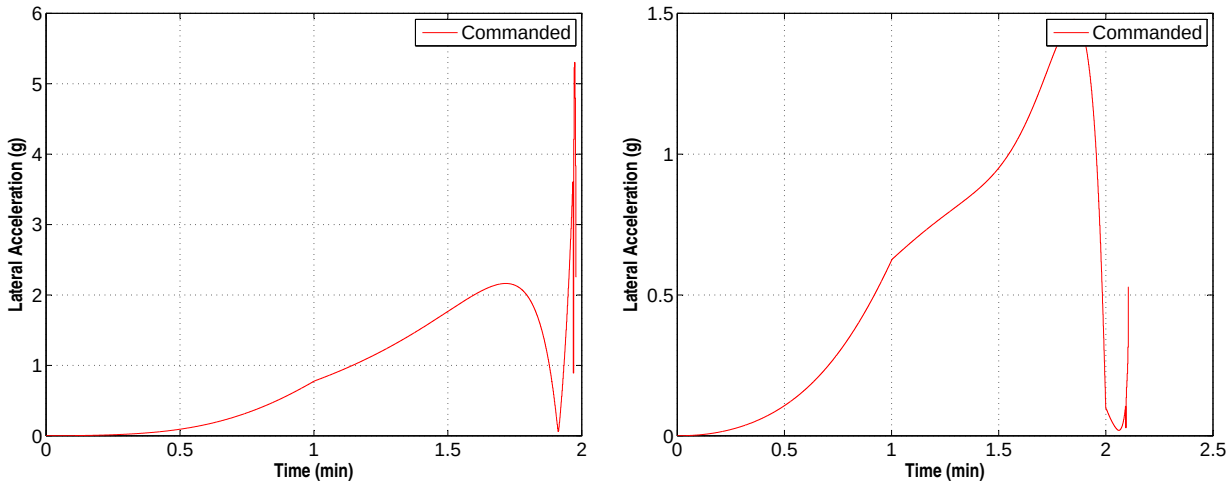

Figure 5.11: Acceleration Experienced by Interceptor Missile (San Francisco on left; Washington D.C. on right)

real-world flight control system.

If the flight control system lag is modeled as a 1^{st} order transfer function, the

relation between commanded and achieved acceleration can be given as

$$\frac{n_L}{n_c} = \frac{1}{1+sT} \tag{5.18}$$

where n_L is the achieved lateral acceleration that is integrated to obtained the interceptor missile lateral divert ($\vec{T}_p$), n_c is the commanded lateral acceleration, s is the complex frequency, and T is the system time constant[13].

The general form of an n^{th} order all-pole transfer function is written as

$$\frac{n_L}{n_c} = \frac{a}{bs^n + cs^{n-1} + \cdots + ds^2 + es + f} \tag{5.19}$$

where $a, b, c, \cdots, f$ are constants characterizing the system poles.

For the simulation executed in this chapter, the interceptor missile's flight control systems are modeled as a 3^{rd} order single time constant flight control system with the transfer function

$$\frac{n_L}{n_c} = \frac{1}{\frac{T^3}{27}s^3 + \frac{T^2}{3}s^2 + Ts + 1} \tag{5.20}$$

In the next subsection the simulation results obtained using this 3^{rd} order interceptor guidance system are shown.

13. The determination of optimal system time constant is study in itself. This was done in the background of the simulation in this chapter. It is however not detailed here. More information on designing a transfer function can be seen in Zarchan[152, 153].

5.4.6 Simulation Results With 3^{rd} Order Interceptor Guidance System

The simulation results indicate that an interceptor with a 3^{rd} order guidance system has the same intercept geometry as a zero-lag guidance system. The altitude and distance of intercept of both interceptions do not change. However, a 3^{rd} order system results in lags in the lateral divert and interceptor acceleration demands as seen in figures 5.12 and 5.13 respectively.

For the intercept between IM-1 and the San Francisco-bound target ICBM, the lateral divert increases from 975.67 m/s to 1283.25 m/s and the acceleration demands on the interceptor increases from 5.30 g to more than 10 g during the final stages of the intercept. However, to model the interceptor realistically, a maximum acceleration limit of 10 g is imposed. This can be observed from the flat lining of the commanded acceleration n_c at 10 g's in figure 5.13 on page 182. Also observed in the same figure is the lag of the system response behind the control input. This implies that even if accurate target position data is provided, the missile will experience some miss distance. Finally, the miss distance increases from 2.30 m to 203.10 m. This is a significant increase in miss distance[14].

For the intercept between IM-2 and the Washington D.C.-bound target ICBM, the lateral divert increases from 670.16 m/s to 936.44 m/s and the maximum acceleration demands on the interceptor increases from 1.48 g to 10 g's in the endgame of

14. This was accomplished without modeling a Kill Vehicle in the endgame. This will be done in later stages of the chapter.

the intercept. Also seen in figure 5.13 on page 182 for this intercept case is the lag of the system response behind the control input. Finally, for the intercept between IM-2 and the Washington D.C.-bound target ICBM, the miss distance increases from 2.87 m to 69.60 m. While, not as drastic an increase compared to the previous case, this level of miss distance still constitutes mission failure.

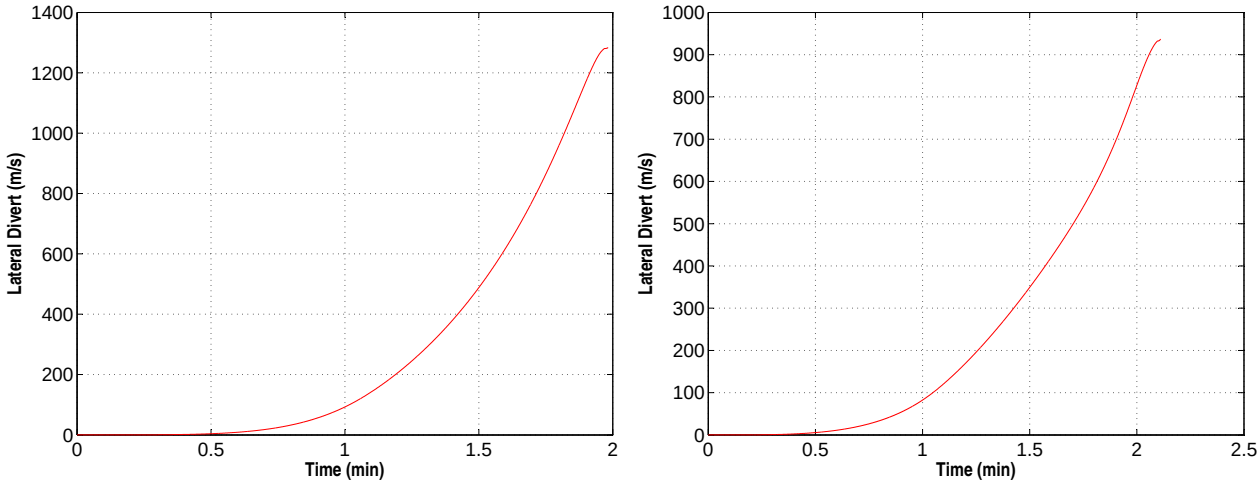

Figure 5.12: Lateral Divert demands on the Interceptor (San Francisco on left; Washington D.C. on right)

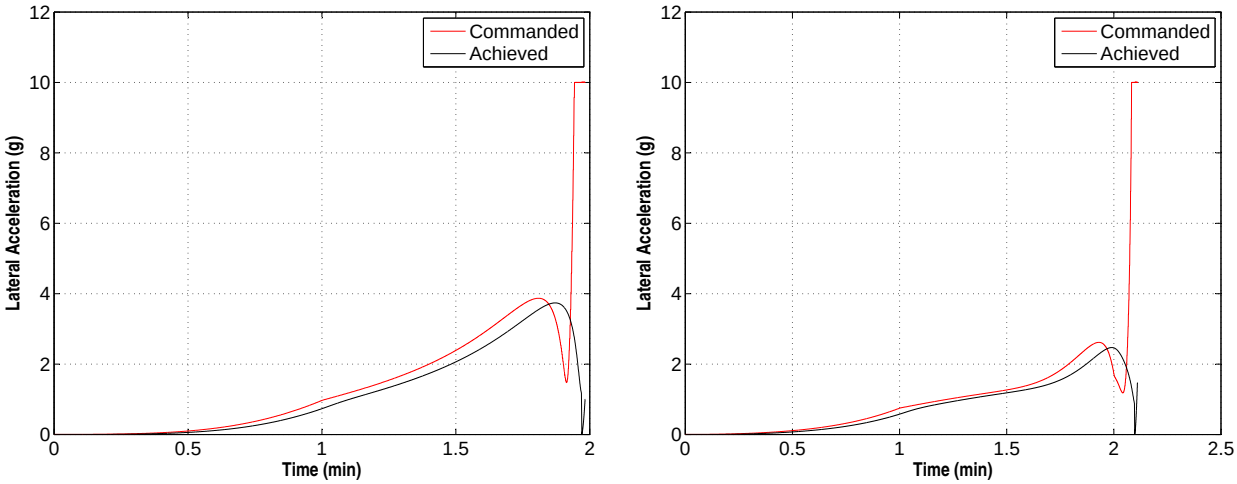

Figure 5.13: Acceleration Experienced by Interceptor Missile (San Francisco on left; Washington D.C. on right)

5.5 Sensors: Radar

Having modeled and simulated the interception between the target North Korean ICBM and the interceptor missiles, the next step is to include sensors to make the interception more realistic. This section will model Radar sensors. The next section will model the STSS space-based sensors. There are five challenges to modeling radar systems involved in the boost-phase missile defense system. They are:

1. modeling the target ICBM with sufficient electrical precision and detail
2. predicting the monostatic radar cross section (RCS) of the modeled target ICBM for all possible aspect angles that may emerge during the course of the interception
3. determining the optimum location to place the radars for the mission given operational, technical, and/or geo-political constraints
4. determining the operating parameters of the radar

5. simulating the actual intercept where the radar(s) acquires and tracks the target ICBMs

All of the five issues outlined above have been undertaken during the course of research done for this chapter. The modeling of the target ICBM (the Peacekeeper missile) was done as illustrated in table 5.2 on page 159. The model was then imported into a custom Matlab code[15] to predict the monostatic RCS of the target ICBM for all possible aspect ratios. RCS of the target ICBM is the only parameter independent of the radar system. The RCS is defined as[48]

$$\sigma = \frac{\text{Power Reflected to Receiver Per Unit Solid Angle}}{\text{Incident Power Density}/4\pi}(m^2) \tag{5.21}$$

In terms of of the incident and scattered electric field intensities, $\vec{E}_i$ and $\vec{E}_s$,

$$\sigma = \lim_{R\to\infty} 4\pi R^2 \frac{|\vec{E}_s|^2}{|\vec{E}_i|^2}(m^2) \tag{5.22}$$

15. A common approach to predict the RCS of a three-dimensional complex target is the physical optics (PO) approximation. Many software packages provide accurate RCS results with small structures and/or low frequencies. However, while working with large structures, such as ICBMs and high frequencies like X-Band, most methods result in unreasonable computational requirements due to the small wavelengths, and in turn, the requirement for a extra fine mesh structure. Obtaining accurate results for electrically large structures may take months of computation. The PO method overcomes the excessive computational requirements while working with electrically large structures. There are however trade-offs while working the PO method. This method is only accurate in the specular direction, and surface waves, multiple reflections, and edge diffraction are not included.

where R is the range to the target. The RCS values were predicted assuming that an X-Band (10 GHz) Radar was tracking the target ICBM[16].

Given the symmetry of the peacekeeper missile, a two dimensional RCS prediction for aspect angles ranging from 0 to 360 degrees is sufficient. Symmetry[17] would render the values in the third dimension similar to those obtained in the two dimensional prediction for a given aspect angle. Figure 5.14 on page 185 shows the results of the RCS prediction for all possible aspect angles of the target ICBM at various stages of its boost-phase flight.

The RCS values for the complete ICBM and ICBM after stage 1 jettison are very similar. So is the RCS values for the ICBM after stage 2 jettison and the ICBM after stage 3 jettison. For this particular ICBM model, it appears very difficult to discriminate the various stages from each other using RCS values. It is observed that fluctuations in aspect angles within the same stage are much more significant then those between different stages. The top aspect angle ($\theta = 0^o$) has a very low RCS of approximately -20 dBsm for all stages of the ICBM due to the scattering by the nose cone in all directions other than the aspect direction. As the aspect angle changes from 0^o, the first peak occurs at approximately 75^o where the slant nose cone causes a specular backscatter. The next peak occurs at $\theta = 90^o$. The peak at 90^o is caused by the exposure of the entire ICBMs body to the radar. The maximum peak RCS occurs at 180^o at the bottom aspect. Since the ICBM structure

16. X-Band radar are used since they are the most powerful in operation currently including the sea-based X-Band radar used with the Aegis ship-based missile defense systems.

17. The Peacekeeper ICBM has a nearly smooth surface and does not have any fins or protruding surfaces.

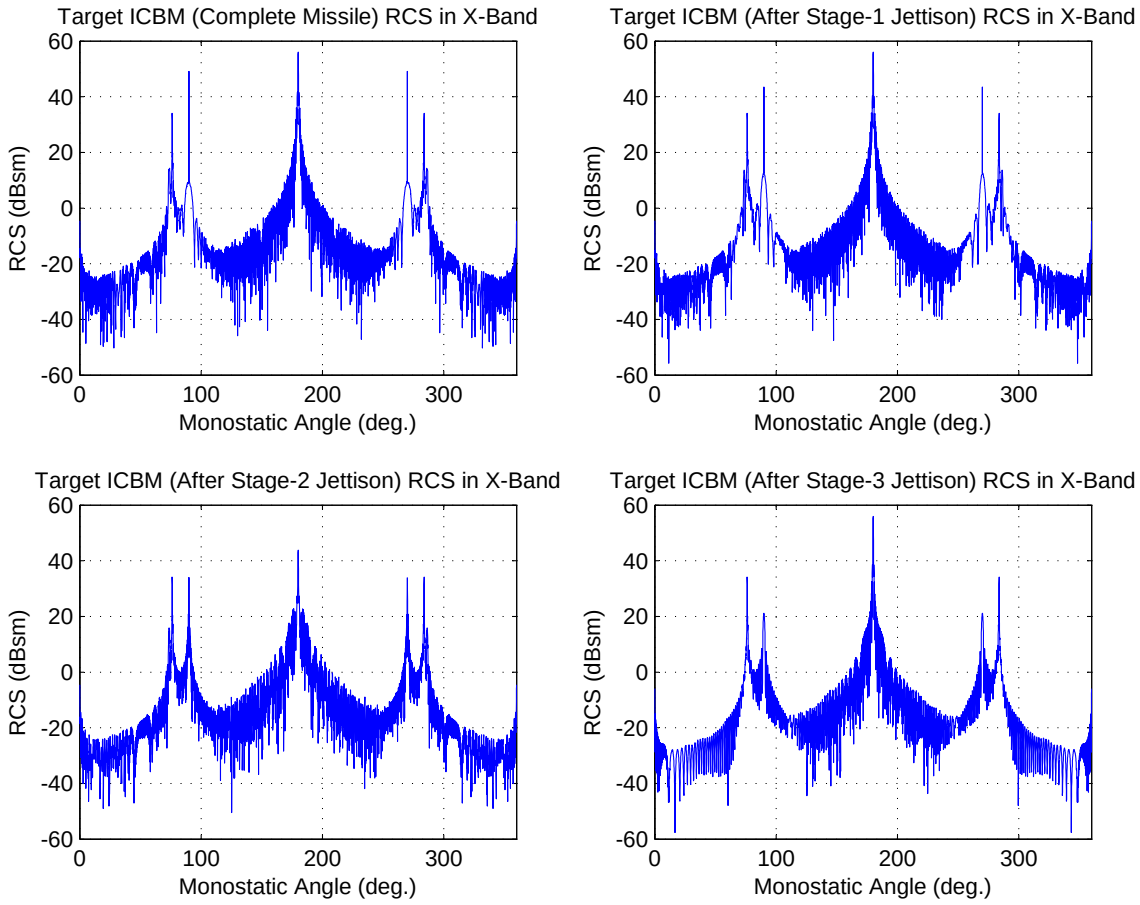

Figure 5.14: RCS Calculation of Target ICBM at Various Stages

is symmetric, the RCS changes between 180^o and 360^o are similar to the changes observed between 0^o and 90^o. RCS can be improved by viewing the target ICBM from specular directions, such as the side or bottom. However, radar sensor locations have constraints and there is rarely complete freedom to locate the radars to view the target ICBM from desired aspects. The next subsection will delve into these issues.

5.5.1 Determination of Radar(s) Location

In order to determine the optimum location to place the X-Band radars a series of simulations was performed in which the radars were sequentially located at various locations in the Sea of Japan around the North Korean ICBM launch site at various angles (ranging from 0^o to 180^o in azimuth) and distances (ranging from 350 km to 1000 km). The distribution of the possible radar locations for a given ICBM trajectory is shown below in figure 5.15.

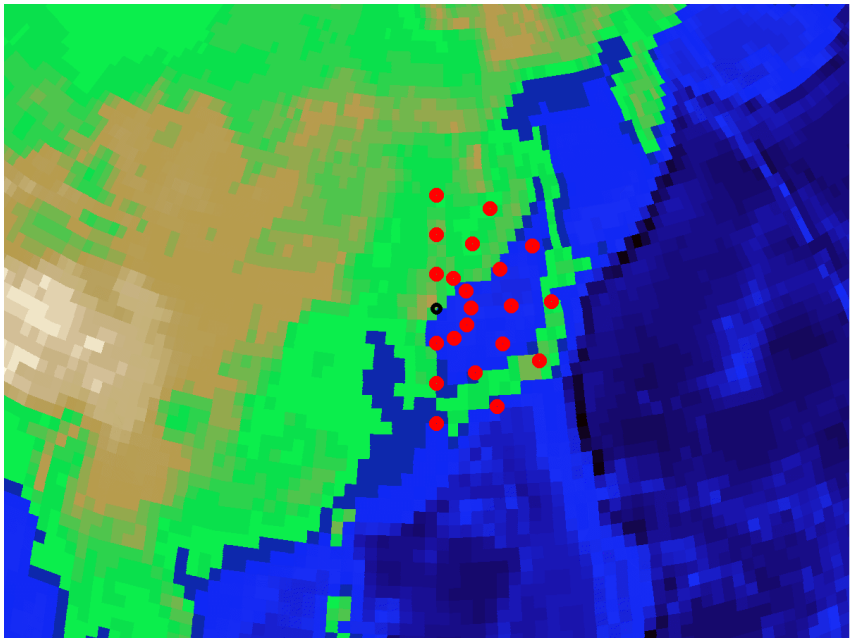

Figure 5.15: Possible X-Band Radar Locations

At each location for a given ICBM trajectory the average RCS was calculated during the boost-phase. The values of average RCS was then interpolated at other angles and distances. A plot of the average RCS of a radar tracking an ICBM

targeting San Francisco from various azimuth angles and distances from the launch location is shown below in figure 5.16.

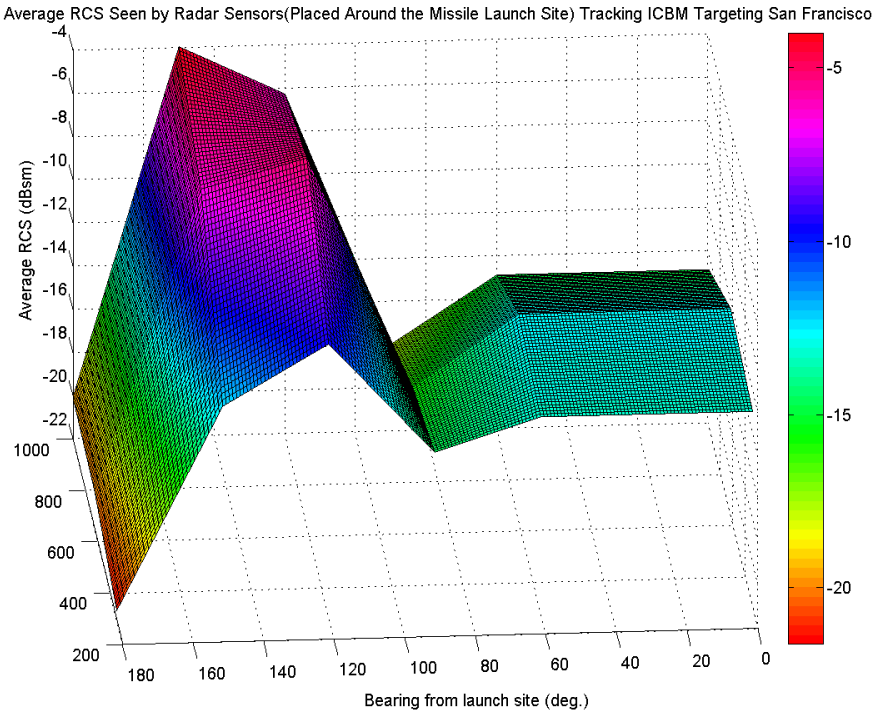

Figure 5.16: Average RCS for Various Azimuth Angles and Distances - San Francisco Trajectory

Similarly, a plot of the average RCS of an radar tracking an ICBM targeting Washington D.C. from various azimuth angles and distances from the launch location is shown below in figure 5.17 on page 188.

Examining figures 5.16 and 5.17 two inferences emerge clearly. The first is that, for every target ICBM trajectory, there is a unique optimum azimuth angle from the launch location at which maximum average RCS for the boost-phase flight

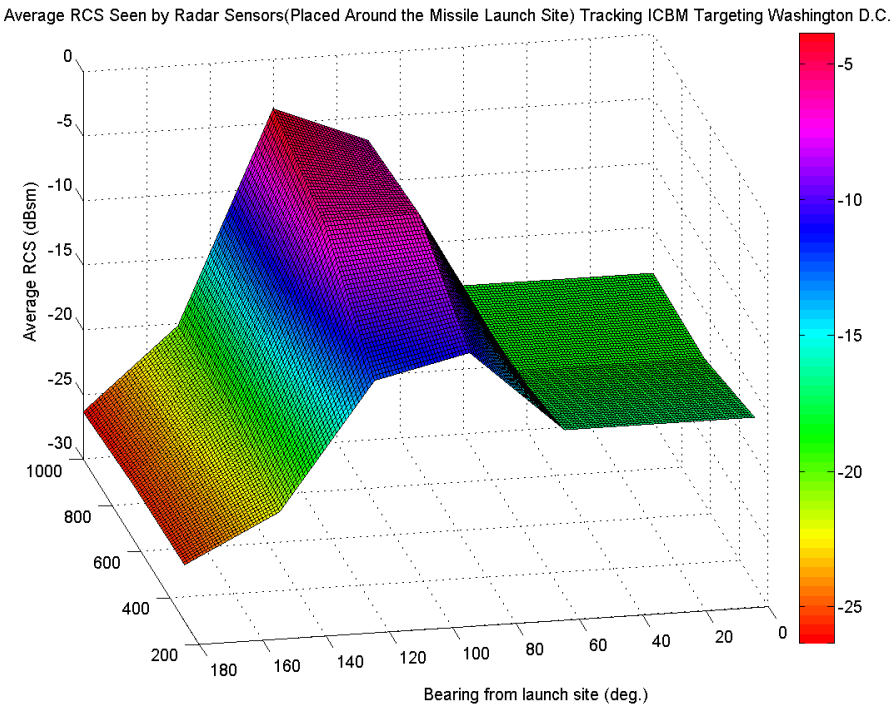

Figure 5.17: Average RCS for Various Azimuth Angles and Distances - Washington D.C. Trajectory

is obtained. For example, for a ICBM targeting San Francisco the maximum average RCS for the boost-phase is obtained at an azimuth angle of 140 degrees. Similarly, for a ICBM targeting Washington D.C. the maximum average RCS for the boost-phase is obtained at an azimuth angle of 120 degrees. The second inference that can be drawn from the plots is that the farther the radars are placed from the launch locations at a given optimum azimuth angle, the better is the average RCS for the boost-phase. At the optimum azimuth angles, the maximum average RCS is obtained at the greatest distance of 1000 km.

There is, however, a technical downside to placing the radars at the maximum possible distance. The decision to locate a radar sensor is constrained by two opposing factors. This constraint can be understood by examining the range equation for a tracking radar noted below[79, 130].

$$R_{max} = \left[\frac{N_i P_T n G_T G_R \sigma \lambda^2}{(4\pi)^3 K T B F (S/N)_{pdfa} L} \right]^{\frac{1}{4}} \tag{5.23}$$

where R_{max} is the maximum detection range, N_i is the number of pulses integrated, P_T is the peak power of the transmitter, n is the compression factor, G_T is the gain of the transmitter antenna, G_R is the gain of the receiver antenna, σ is the RCS of the target ICBM, λ is the wavelength of the radar, K is the Boltzmann constant ($1.38x10^{-23} J/deg.$), T is the antenna temperature ($290K$), B is the bandwidth, F is the system noise factor, $(S/N)_{pdfa}$ is the smallest signal-to-noise ratio capable of giving the required detection and false-alarm probability, and L is the total loss.

Equation 5.23 can be simplified by using the following assumptions:

1. N_i=1. This implies the number of integrated pulses is one,
2. if there is no pulse compression applied then n=1,
3. if a monostatic radar is used G_T=G_R=G,
4. the bandwidth B is replaced by the reciprocal of the pulsewidth i.e. $B = \frac{1}{\tau}$, and
5. neglecting other losses i.e. L=1.

Therefore, equation 5.23 simplifies to

$$R = \left[\frac{P_T G^2 \tau \sigma \lambda^2}{(4\pi)^3 KTF(S/N)_i} \right]^{\frac{1}{4}} \tag{5.24}$$

Re-arranging equation 5.24

$$(S/N)_i = \left[\frac{P_T G^2 \tau \sigma \lambda^2}{(4\pi)^3 KTF(R)^4} \right] \tag{5.25}$$

The opposing constraint in locating a radar sensor is evident from equation 5.25. The signal-to-noise ratio S/N is directly proportional to the RCS (σ). However, it is also inversely proportional to the distance between the radar and the ICBM its tracking (R). Therefore, a compromise has to be made. Further examining figures 5.16 and 5.17 on pages 187 and 188 it can be seen that RCS decreases sharply below the distance of 650 km at the optimum azimuth angle. Therefore, in the simulation attempted in this chapter the radar(s) are placed at a distance of 650 km.

Two radars are modeled in the simulation. The first radar is placed at 140 degree azimuth and a distance of 650 km optimized to track a North Korean ICBM targeting San Francisco. This translates to $36^o31'19''N$ latitude and $133^o49'18''E$ longitude. The second radar is placed at an azimuth angle of 120 degree and a distance of 650 km optimized to track an ICBM targeting Washington D.C. This translates to $38^o04'38''N$ latitude and $135^o33'58''E$ longitude. Both of the locations are to the east of the launch site in the Sea of Japan close to Japanese territory.

5.5.2 Simulation of Target ICBM RCS as Seen by the Radars

Using the optimized radar locations determined in the previous section, the target ICBMs are tracked in the simulation and their RCS is determined. In the first run of the simulation, the RCS of the ICBM targeting San Francisco is tracked by both radars, radar-1 (optimized to monitor the San Francisco-bound ICBM) and radar-2 (optimized to monitor the Washington D.C.-bound ICBM). The results are shown in figure 5.18 below. Also shown is the aspect angle of the intercept as observed by both the radars.

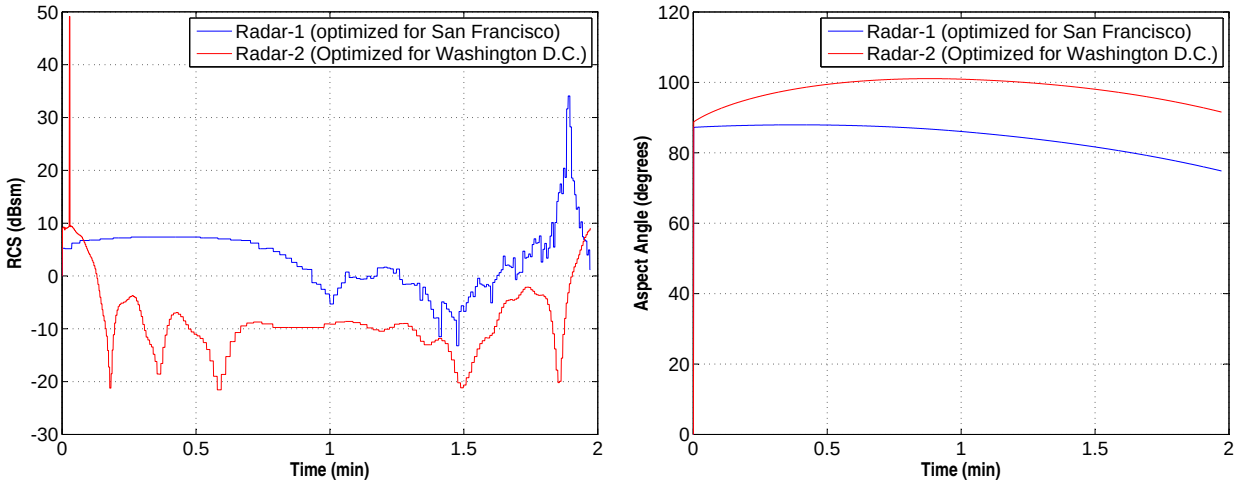

Figure 5.18: RCS of the San Francisco Bound Target ICBM

It is clear from the figure that higher RCS values are obtained for the San Francisco-bound ICBM from the radar optimized for it i.e. by radar-1. The shape of the observed RCS curve can be understood by comparing the aspect angle curve observed during the simulation shown in the right-side of figure 5.18 with the stage-wise RCS curves shown in figure 5.14 on page 185. For example, the peak RCS of

approximately 35 dBsm for the San Francisco-bound ICBM as observed by radar-1 occurs at approximately 1.85 minutes. This happens because at that time instant (approx. 1.85 minutes) the aspect angle as seen from the right half of figure 5.18 is close to 75 degrees. Going back to figure 5.14, at that particular instant after stage-1 jettison at 75 degrees, the RCS is approximately 35 dBsm.

In the second run of the simulation, the RCS of the ICBM targeting Washington D.C. as tracked by both radars, radar-1 (optimized to monitor the San Francisco bound ICBM) and radar-2 (optimized to monitor the Washington D.C.-bound ICBM) is determined. The results are shown in figure 5.19 on page 192. As expected, it is clear from the figure that higher RCS values are obtained for the Washington D.C.-bound ICBM from the radar optimized for it—by radar-2.

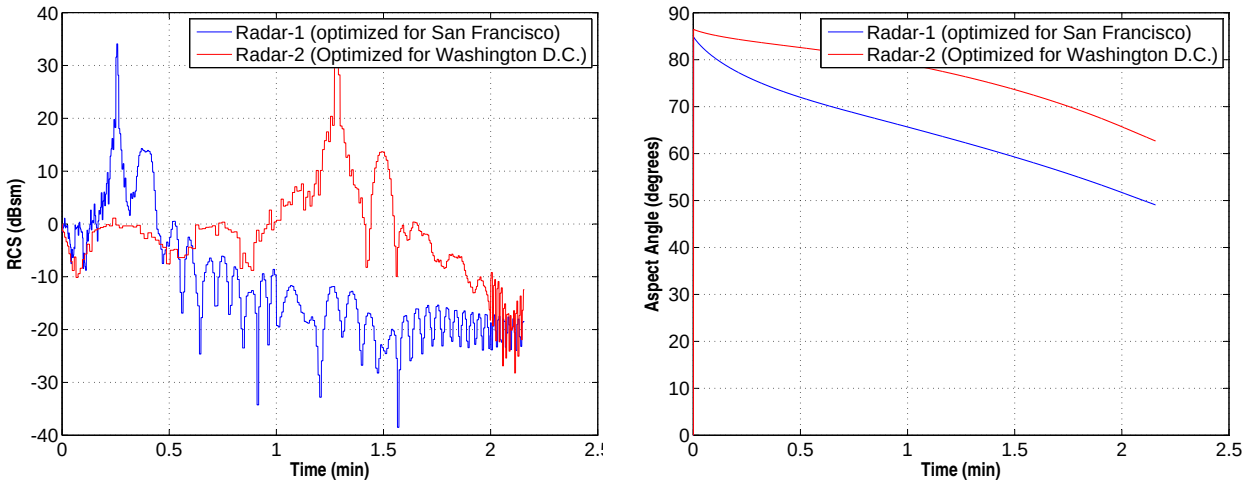

Figure 5.19: RCS of the Washington D.C. Bound Target ICBM

5.5.3 Operating Parameters of the Radar

The various parameters of the radar have to be determined in order to convert the RCS values estimated in the previous subsection into actual position estimates. The radar sensors are designed to have a minimum unambiguous range of R_{un}=1000 km. A low pulse repetition frequency (LPRF) is used. The pulse repetition frequency is calculated by using the formula

$$f_p = \frac{c}{2R_{un}} \tag{5.26}$$

where c is the speed of light (in m/s). With R_{un}=1000 km, the maximum PRF is f_p=150 Hz.

For the radar antenna, a pencil-beam is used. The gain G of the antenna is approximately given as

$$G = \frac{26000}{\theta^a_{3dB}\theta^e_{3dB}} \tag{5.27}$$

where θ^a_{3dB} is the half-power (3-dB) beamwidth in the azimuth direction, and θ^e_{3dB} is the half-power (3-dB) beamwidth in the elevation direction. Assuming the antenna is a parabolic reflector, the antenna's physical area A_p is determined by

$$A_p = \frac{G\lambda^2}{4\pi\epsilon_{ap}} \tag{5.28}$$

where ϵ_{ap} is the aperture efficiency and λ is the wavelength (in m).

From equations 5.27 and 5.28 it is evident that the antenna area is dependent on the half-power beamwidth. The area of the antenna is the limiting parameter that will influence the half-power bandwidth. Assuming an aperture efficiency of 0.5, the gain (G), antenna area and antenna diameter are calculated. It seems that a beamwidth of 0.5 x 0.5 degrees leads to a manageable antenna diameter of 4.36 m. Higher beamwidth might lead to excessive antenna diameter requirements (see Table 5.6) that may be infeasible to design and operate.

Table 5.6: Gain and Antenna Diameter for a Given Half-Power Beamwidth

Half-Power Beamwidth (Degrees)	**Gain (dB)**	**Antenna Area (m^2)**	**Antenna Diameter (m)**
0.5 x 0.5	50.17	14.90	4.36
1 x 1	44.15	3.72	2.18

The radar sensor frequency is already decided as X-Band (10 GHz). PRF is calculated as a function of the range certainty requirements as shown previously. Antenna beamwidth and gain (G) are calculated according to antenna diameter limitations as shown above. The peak power, pulsewidth and noise factor are set in the range of typical values for classical radar systems. Table 5.7 on page 195 below shows the radar parameters chosen to be used in the simulations discussed in this chapter.

Table 5.7: Radar Parameters

Parameter	**Values**
Frequency	X-Band (10 GHz)
Peak Power	1 MW
Antenna Gain	50 dB
Beamwidth	0.5 x 0.5 degrees
Pulsewidth	50 μs
PRF	150 Hz
Number of Pulses Integrated	20
Receiver Noise Factor	4

5.5.4 Simulation of Target Position Data as Determined by the Radars

Having determined the RCS as a function of the interception geometry between the interceptor(s) and target ICBM(s) in subsection 5.5.2, the RCS values can now be used along with the radar parameters determined in the previous subsection to evaluate the signal-to-noise ratio (SNR) as measured by the two radars. The SNR is then used to estimate the position errors of the target ICBM as measured by the radars. The SNR, as discussed earlier in equation 5.25 on page 190, is given by

$$(S/N)_i = \left[\frac{P_T G^2 \tau \sigma \lambda^2}{(4\pi)^3 K T F (R)^4}\right] \tag{5.29}$$

Figures 5.20 and 5.21 below show the SNR obtained by the two radars as they observe each of the interceptions.

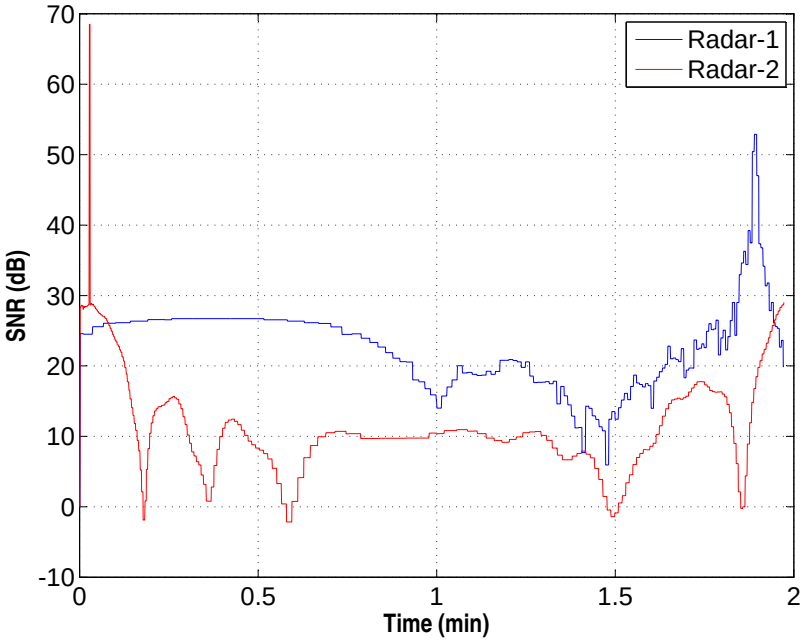

Figure 5.20: SNR for San Francisco Trajectory

However, the estimated SNR is affected by the tracking quality of the radar sensors leading to errors in the target ICBM position estimates. The most prevalent cause of error is thermal noise. The RMS error in angle (i.e. azimuth and elevation) and range due to radar thermal noise is modeled as[79]

$$\sigma_{angle} = \frac{\theta_{3dB}}{K\sqrt{2(S/N)_1 N_i}} \tag{5.30}$$

and

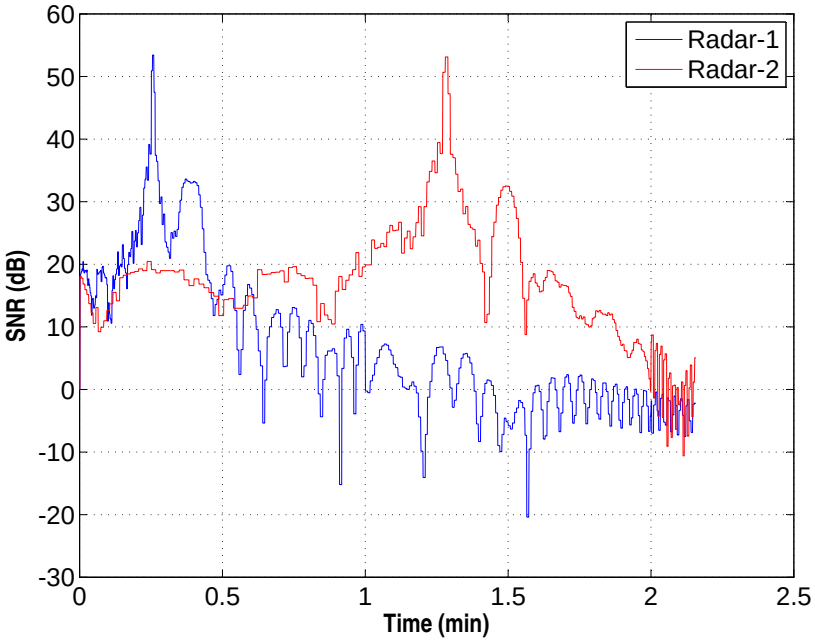

Figure 5.21: SNR for Washington D.C. Trajectory

$$\sigma_{range} = \frac{c\tau}{2} \frac{1}{K\sqrt{2(S/N)_1 N_i}} \tag{5.31}$$

where the constant K for the RMS angle error is approximately 1.7 for a monopulse tracker and the constant K for the RMS range error is between 1 and 2. Using these equations the error in radar sensor's determination of the target ICBM position is simulated. The magnitude of the RMS errors is calculated as

$$e_{RMS} = \sqrt{(x - \hat{x})^2 + (y - \hat{y})^2 + (z - \hat{z})^2} \tag{5.32}$$

where (x, y, z) is the true position of the ballistic missile and $(\hat{x}, \hat{y}, \hat{z})$ is the radar's sensor measurement of the target ICBM at any given time in the simulation. For the intercept between IM-1 and the San Francisco-bound target ICBM, the positions error given by radar-1 and radar-2 are shown in figures 5.22 and 5.23 respectively on page 199. As expected radar-1 has less error than radar-2 since it is optimized to observed the ICBM targeting San Francisco.

Similarly, for the intercept between IM-2 and the Washington D.C.-bound target ICBM, radar-2 has less error than radar-1 as shown in figures 5.24 and 5.25 on page 200. Although the optimized radar would always have less error than the other for a given target ICBM trajectory, the magnitudes of the error are random in nature. The patterns of target ICBM position error will mimic the crests and troughs indicated in the figures, however the magnitude will vary from one simulation to another.

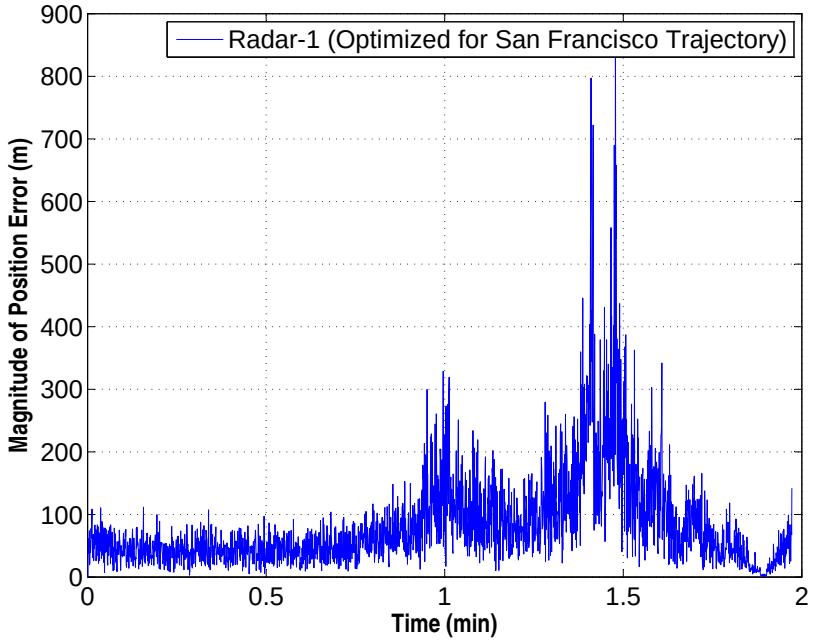

Figure 5.22: Radar-1 Position Error for San Francisco Trajectory

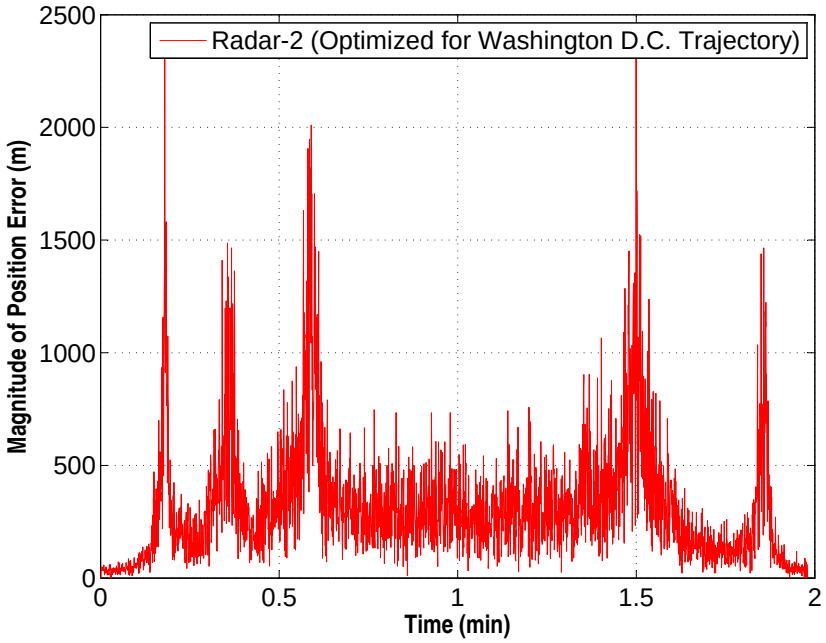

Figure 5.23: Radar-2 Position Error for San Francisco Trajectory

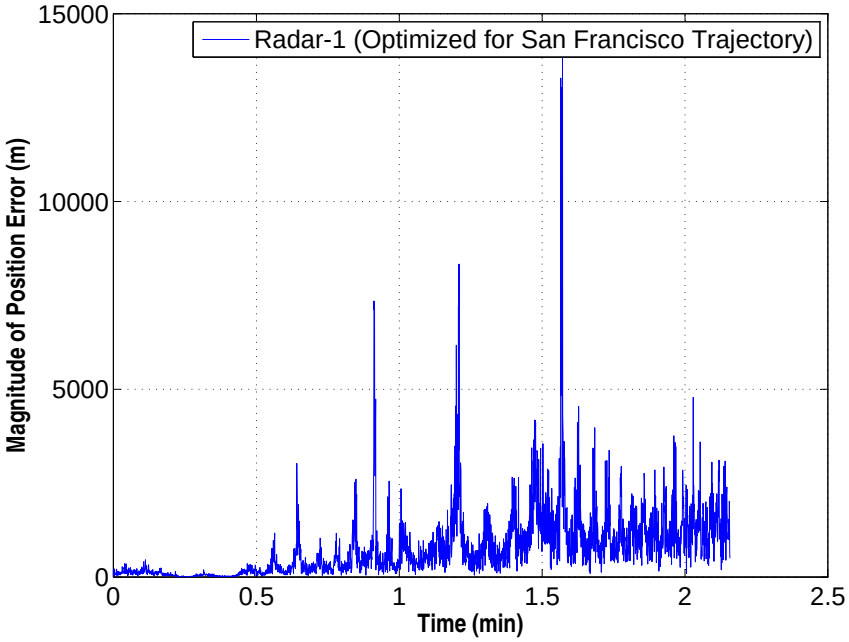

Figure 5.24: Radar-1 Position Error for Washington D.C. Trajectory

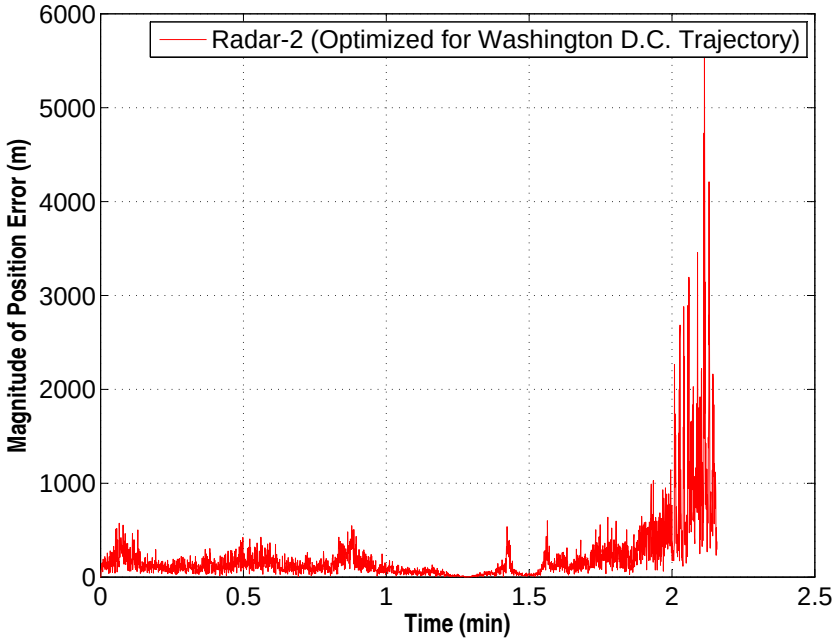

Figure 5.25: Radar-2 Position Error for Washington D.C. Trajectory

Finally the fused data from the two radars for each of the two cases of intercept (San Francisco and Washington D.C.) modeled in this chapter is shown below. The fused radar data for the IM-1 San Francisco intercept is shown in figure 5.26 below. The fused radar data for the IM-2 Washington D.C. intercept is shown in figure 5.27 on page 202. The data fusion is done using the equation below

$$\hat{p}_w(x,y,z) = \frac{\hat{p}_1(x_1,y_1,z_1) \times (S/N)_1 + \hat{p}_2(x_2,y_2,z_2) \times (S/N)_2}{(S/N)_1 + (S/N)_2} \tag{5.33}$$

where $\hat{p}_w(x,y,z)$ is the fused target position vector, $\hat{p}_1(x_1,y_1,z_1)$ and $\hat{p}_2(x_2,y_2,z_2)$ is the ICBM target position vector as determined by radar-1 and radar-2, and $(S/N)_1$ and $(S/N)_2$ is the signal to noise ratio of radar-1 and radar-2.

IM-1 - San Francisco Bound ICBM Intercept

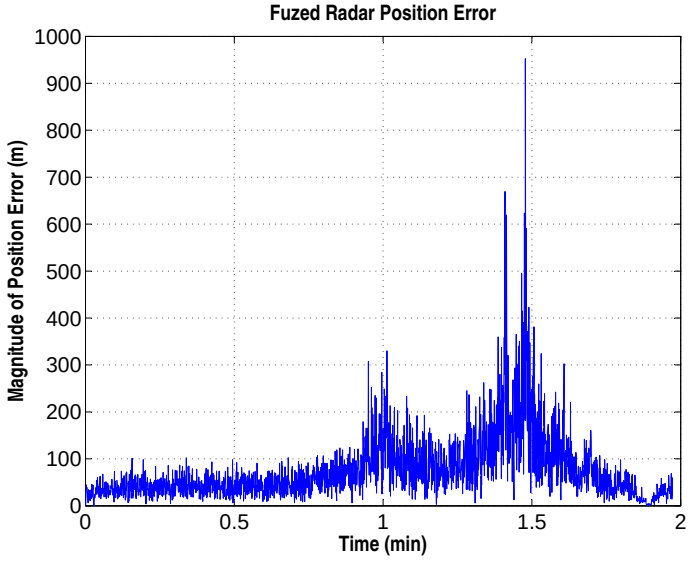

Figure 5.26: Fused Radar Position Error for San Francisco Trajectory

IM-2 - Washington D.C. Bound ICBM Intercept

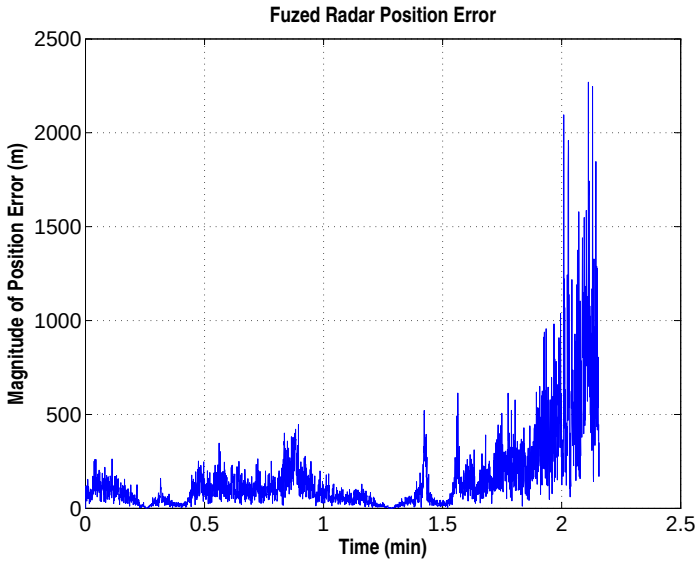

Figure 5.27: Fused Radar Position Error for Washington D.C. Trajectory

5.6 Sensors: Space Tracking and Surveillance Systems (STSS)

The previous section modeled radar sensors and estimated the magnitude of position errors (as observed by the radars) of the two tracked target ICBMs. The next section will model the STSS space-based sensors and then simulate their effect on the magnitude of position error of the tracked target ICBMs. The major concern in a space-based IR sensor "looking down" to the Earth and tracking an ICBM is the discrimination of the IR signal produced by the target of interest from the signals produced by the background. The space-based sensor must contend with sources of clutter on the surface of Earth and in the intervening atmosphere like solar reflection/radiation, earth radiation (earthshine), rain, clouds, fog, terrain

types and luminance (day-night). Inability to discriminate signal from background noise can lead to false alarms.

In ballistic missile defense, medium wavelength IR (MWIR) (3-5 μm), long wavelength IR (LWIR) (8-12 μm) and very-LWIR ($>$ 12 μm) sensors are required due to the nature of the target-background combination, which varies throughout the flight of the ICBM. To address these concerns and requirements, the STSS is equipped with a multi-color quantum well IR photodetector (QWIP) step-stare focal plane array (FPA). The term multi-color means that a single sensor has the ability to detect and track IR targets of interest in different areas of the IR spectrum. Multicolor IR sensing is important for early missile typing and booster classification, plume-to-hardbody handover, and to eliminate the effects of earthshine in exoatmospheric discrimination[143]. A multi-color IR sensor is required to maintain target tracking during the transition from boost-phase to burnout-coasting. A sample image of a Delta-II launch vehicle captured in multi-color QWIP is shown in figure 5.28 on page 204. The image clearly indicates the advantage of multi-color sensors in discriminating and identifying the body of the cold launch vehicle in the presence of the hot exhaust plume. This ability helps ensure a smooth tracking from boost-phase to post-boost-phase.

Recent developments at the Jet Propulsion Laboratory (JPL) and other centers have demonstrated the fabrication of two-band and four-band QWIP FPAs tuned to detect in the IR bands of 4-5.5 μm, 8.5-10 μm, 10-12 μm and 13-15.5 μm[18, 183, 184, 196]. Major advantages of QWIPs are their excellent uniformity, which allows for rejection of elevated backgrounds (suitable for boost-phase ICBM detection),

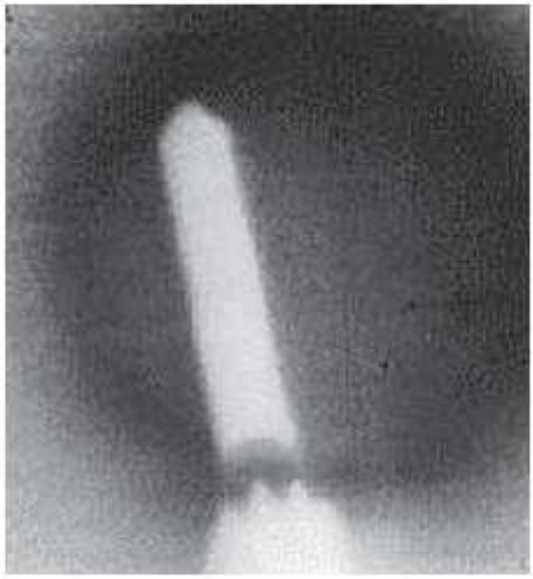

Figure 5.28: LWIR Tracking of Delta-II Launch Vehicle [183]

low cost, low power dissipation, low $1/f$ noise and their narrow-band spectrum. However, QWIPs do suffer from low quantum efficiency[143].

Apart from multi-color QWIP, the other advanced feature in STSS is the implementation of step-stare focal plane arrays (FPA). These FPA sensors have enough detectors to cover the entire sensor field of view simultaneously, without the need for scanning format implementations like the Defense Support Program (DSP) satellites. A sensor can be designed to have relatively few detectors that scan the field of view, or it can be designed to have a very large number of detectors staring at the scene to detect targets by their motion through the field of view. The technology during the development of DSP in the 1960s enabled only the former

approach[18]. In the case of STSS, due to FPA technology the individual detectors do not have to scan the field of view. They can stare at the entire sensor field of view. This approach results in longer integration times, improved sensitivity and higher SNR when compared to traditional scanning types sensors. In addition to providing improved sensitivity, staring sensors are particularly well-suited for moving target indication (MTI) applications. In MTI type applications, the sensor attempts to detect a target that is moving over a cluttered but stationary background. With the field of view of a staring sensor held fixed with respect to the stationary background, clutter can be eliminated by taking differences of successive frames of data.

For detectors staring only at the background with no target present, the differencing process results in a zero output signal. For those detectors that are traversed by the moving target, the differencing process results in a detectable, nonzero signal. In order to implement this approach from a low earth orbit a step-stare technique is used. The step-stare FPA sensor divides the total field of view into smaller steps and periodically alternates among them. In this approach, the footprint of the sensors is held in a fixed observation point for the period of time required to collect the necessary number of frames of staring data. This is the starting point of the step-stare cycle. After this data is collected, the detector footprint is moved, or *stepped* to a new observation region. This the step portion of the cycle[62].

---

18. Early strategic surveillance sensors like DSP operating in the infrared part of the spectrum achieved the necessary spatial coverage by scanning discrete infrared detectors over the search field of view. Scanning was necessary because the number of resolution cells in the search field usually exceeded the number of discrete IR detectors available to the sensor[62].

5.6.1 Target ICBM IR Spectroscopy

The first step in the process of simulating the position errors of the tracked target ICBMs as observed by the STSS satellites is to configure the IR characteristics of the target. This subsection will outline that process. Although the simulation discussed in this chapter involves only boost-phase missile defense, in order to realistically model the space-based STSS sensor it is modeled as being able to operate in boost-phase as well as in the post-boost phase of flight.

In the boost-phase of flight, the target ICBM altitude is approximately below 250 km. In this phase the missile exhaust plume is the principal contributor to the IR signature of the ICBM. The exhaust plumes of the target ICBM usually contain water vapor, carbon dioxide gas and solid particulates and are at an average temperature of 1400^{o}K and an emissivity of about 0.9[17]. The determination of the target ICBM plume's maximum radiant exitance as well as wavelength where the maximum occurs is done by applying Planck's radiation formula. The formula is given as

$$M(\lambda, T) = \epsilon(\lambda) \frac{2\pi hc^2}{\lambda^2 (e^{\frac{hc}{\lambda kT}} - 1)} \left[\frac{W}{cm^2 \mu m} \right] \tag{5.34}$$

where M is the radiant exitance, ϵ is the emissivity, λ is the radiation wavelength, T is the source temperature in K, h is the Planck's constant (6.626 x 10^{-34} J.sec), k is the Boltzmann's constant (1.38 x 10^{-23} J/K) and c is the speed of light. Using the formula the radiant exitance of the ICBM exhaust plume is plotted as shown in figure 5.29 on page 207. The maximum radiant exitance from the plume is seen

to be 5.512 W/cm^2 and corresponding peak wavelength is 2.073 μm. However, the background has to be examined before deciding the bandwidth at which the sensor should be centered for observing the boost-phase.

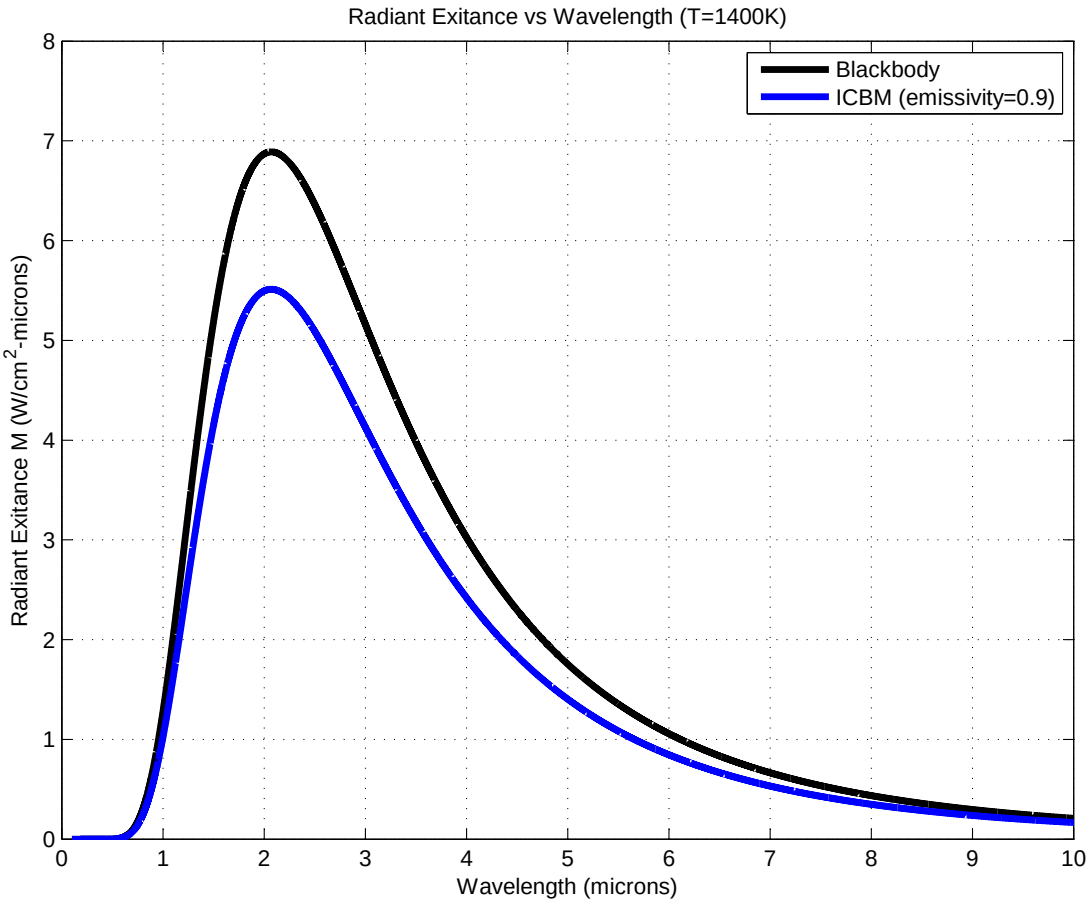

Figure 5.29: ICBM (Boost-Phase) Plume Radiant Exitance at 1400^{o}K

The background of the missile is affected by both solar radiation and earth-shine. The solar radiation is dominant for wavelengths below 3 μm as shown in figure 5.30 on page 208. This would generate significant clutter for an IR sensor during daylight observation[79]. Further, the radiation from earthshine is significant

for wavelengths greater than 5 μm[79] as seen in figure 5.31 on page 209. Considering these two limitations the IR sensor bandwidth should be from 3 to 4 μm for the narrowband QWIP.

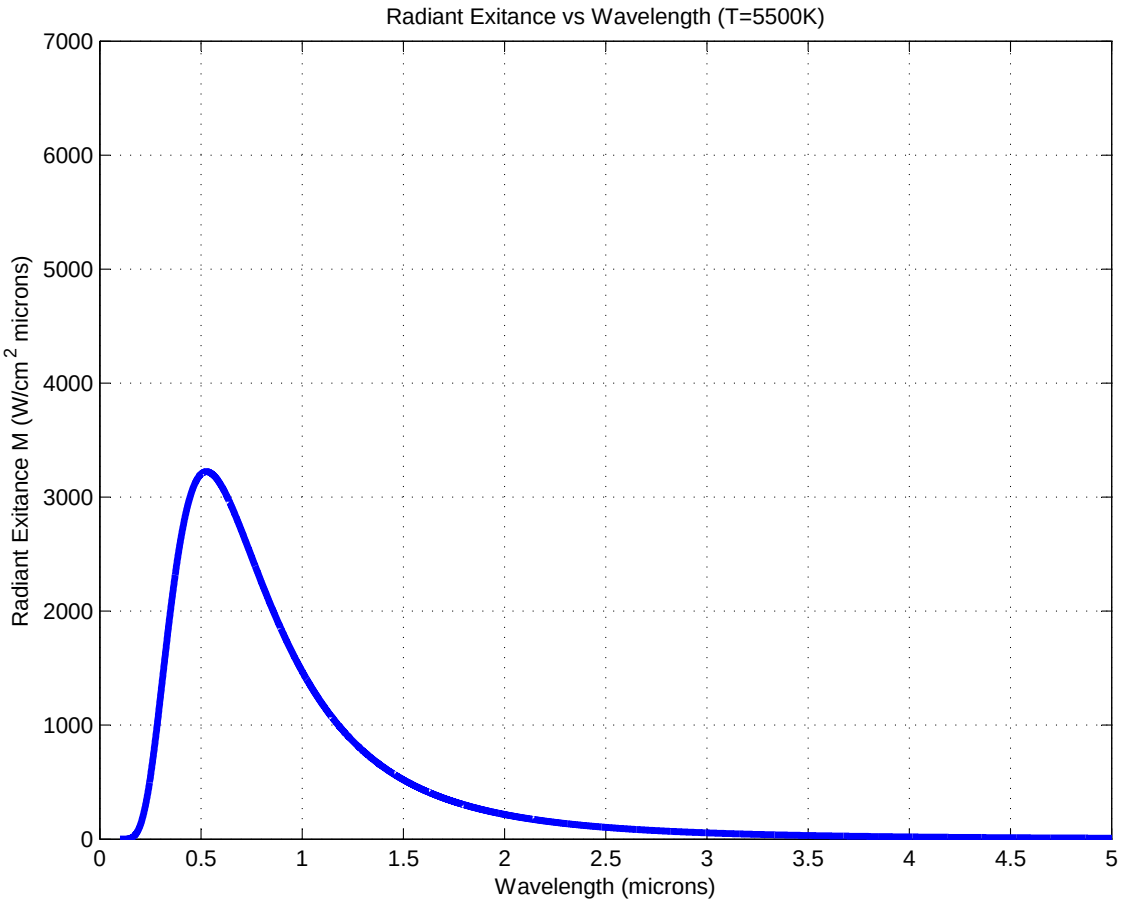

Figure 5.30: Radiant Exitance of Sun at 5500^{o}K

In the post-boost-phase, when the ICBM booster "burns-out," the IR signature of the ICBM changes significantly. At the altitude at which burn-out occurs, the temperature of the missile's surface is governed only by its surface configuration, solar radiation intensity, and whether the ICBM is rotating[17]. A typical temper-

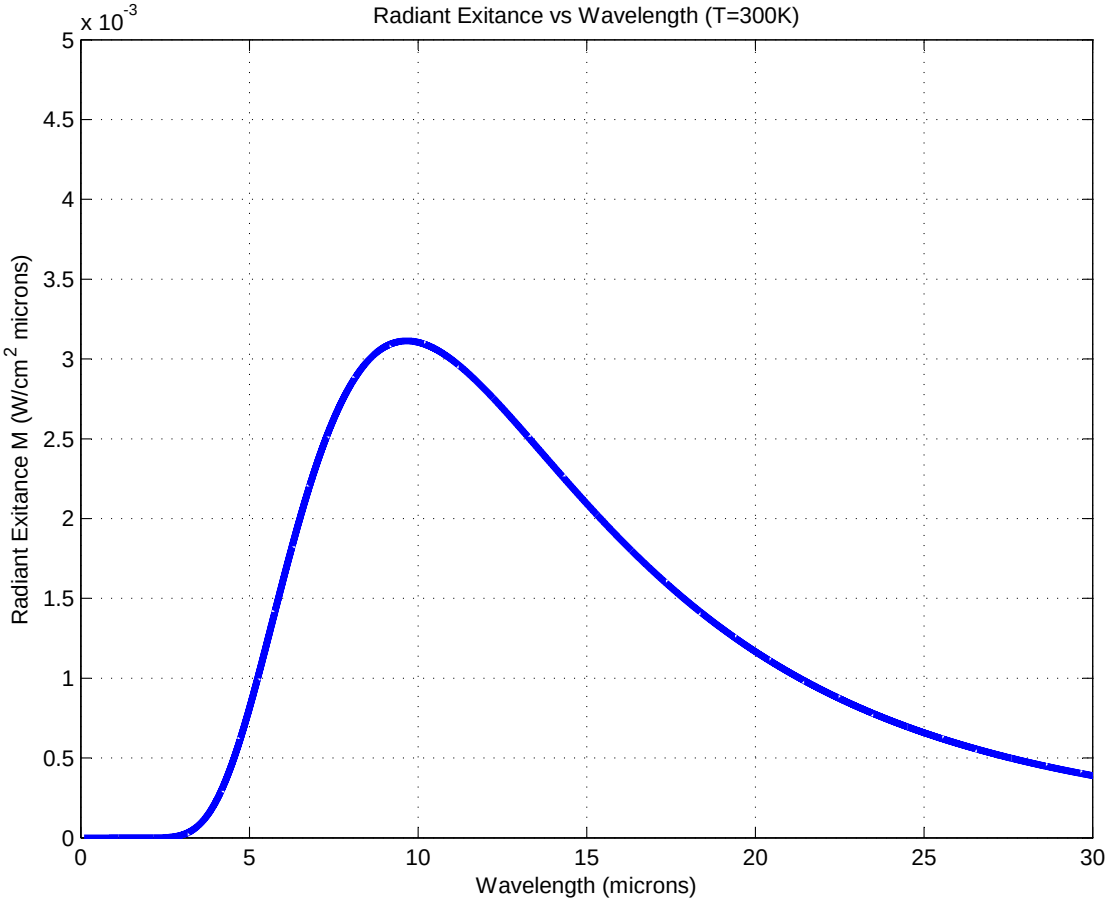

Figure 5.31: Radiant Exitance of Earth at 300^{o}K

ature for the missile surface after burn-out is 200^{o}K. The radiant exitance of the ICBM at this stage is plotted as shown in figure 5.32 on page 210 using Planck's formula.

It is seen from the plot that the maximum radiant exitance of the post-boost ICBM is approximately at 3.7 x 10^{-4} W/cm^2 and the corresponding peak wavelength is approximately at 14.51 μm. For the case of the post-boost ICBM the background characteristics actually work in favor of the ICBM. The measured exoatmospheric

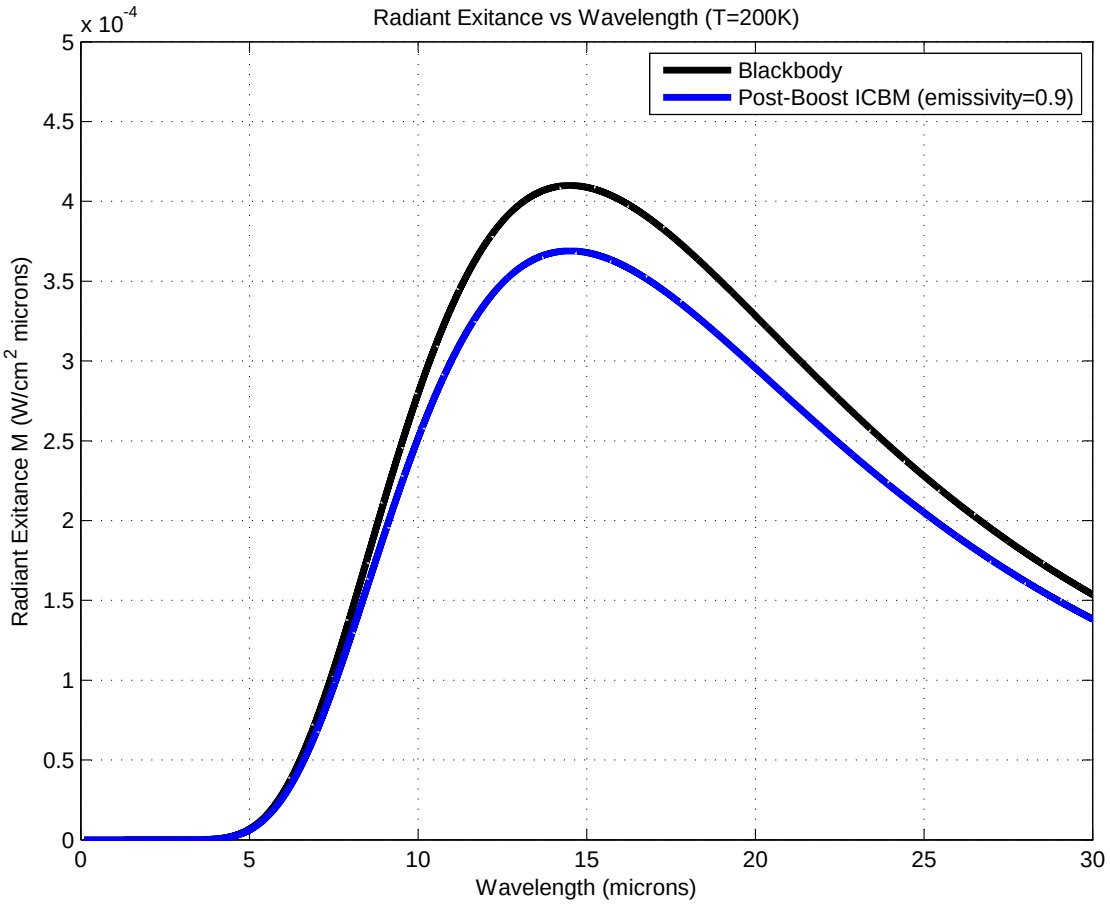

Figure 5.32: Radiant Exitance of Post-Boost ICBM at 200^{o}K

data indicates that the Earth's atmosphere totally blocks the earthshine in the carbon dioxide band between 14 and 16 μm[143]. Therefore, for this phase the bandwidth considered for the narrowband QWIP is from 14 to 15 μm.

5.6.2 Focal Plane Array (FPA) requirements

Having determined the operating bandwidths for the STSS sensors in the previous subsection this subsection will estimate the focal plane array (FPA) charac-

teristics of the STSS sensors before proceeding to calculate the sensor SNR. The main factor in outlining the requirements of a IR FPA is the azimuthal resolution. The dimensions of the target IR signature in combination with the detection range influences the FPA design. The exhaust plume of an ICBM has an approximate length of 50 m[62]. During the post-boost-phase the target ICBM IR signature is comparable to the physical dimensions of the ICBM, which has an approximate length of 20 m. Using an worst-case scenario it would be conservative to assume that the space-based IR sensor must be able to discriminate IR targets spaced 20 m apart at a distance of 1350 km. These values lead to an azimuthal resolution of approximately 15 μradians. This implies that the horizontal and vertical instantaneous field of view (HIFOV, VIFOV) of each detector element on the FPA must be 15 μradians.

The IR sensor is required to cover a total footprint equal to the area of North Korea which is approximately 120,000 square kilometers. Considering a step-stare IR sensor FPA of 20 steps, each FPA step must cover a footprint of 6000 square kilometers. Then the horizontal and vertical field of view (HFOV, VFOV) is approximately 0.06 radians. Therefore the total number of detectors on the FPA is calculated as

$$\left(\frac{HFOV}{HIFOV}\right) \times \left(\frac{VFOV}{VIFOV}\right) = \left(\frac{0.06}{15 \times 10^{-6}}\right) \times \left(\frac{0.06}{15 \times 10^{-6}}\right) = 4000 \times 4000 \quad (5.35)$$

Mid-IR and long-IR QWIP FPAs incorporating 1024 x 1024 elements have been developed and demonstrated[184]. The development of a FPA with a number

of elements more than this value requires the union of more than one array. Such a design involves complexity due to spatial alignment and temporal registration problems. However, such designs have been accomplished successfully as illustrated in figure 5.33 on page 212. The figure on the left side shows a union of nine 1024 x 1024 pixel QWIP FPAs on a GaAs wafer and the figure on the right is a 1024 x 1024 QWIP FPA.The Landsat 7 satellite is an example of an advanced satellite that has implemented FPA technology[101] of 1000 x 1000 detectors per spectral band with a ground resolution of 185 m.

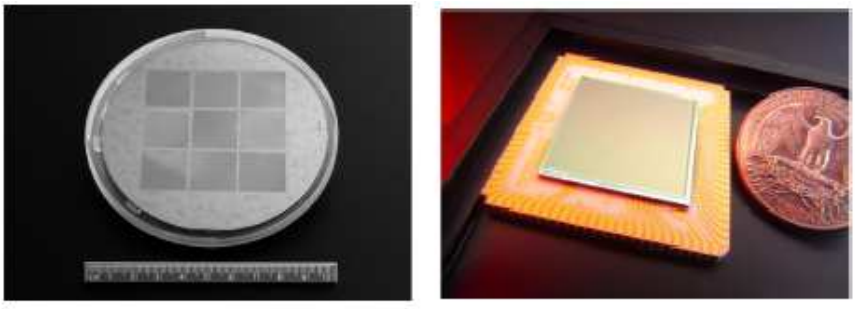

Figure 5.33: QWIP FPA wafers

[184]

5.6.3 SNR for a QWIP FPA

The SNR for an IR sensor[69] is given by

$$SNR = \left(\frac{D^*}{\sqrt{A_d \Delta f}}\right)\left(\frac{I A_{enp}}{r^2}\right) \tag{5.36}$$

where D^* is the normalized detectivity[19], A_d is the detector area, Δf is the noise equivalent bandwidth, I (W/sr) is the radiant intensity of the target source, A_{enp} is the area of the collection aperture (entrance pupil) of the detector optics and r is the detector to target range.

The performance analysis for SNR is conducted under the assumption that the IR sensor is operating under Background Limited Infrared Photodetection (BLIP) conditions. This implies that the dominant noise source is the background photon flux. All other internal noise associated with the detector itself, such as Johnson noise, Generation-Recombination noise, and 1/f noise are considered negligible. BLIP operation is common for IR scanning and staring systems[69]. Therefore, for a cooled photodetector operating under BLIP, D^* is given by

$$D^*_{BLIP}(\lambda, f) = \frac{\lambda}{2hc}\sqrt{\frac{\eta}{E_{background}}} \tag{5.37}$$

where λ is the background radiation wavelength, η is the detector quantum efficiency, h is Planck's constant, and $E_{background}$ is the total background photon irradiance.

$E_{background}$ is determined by integrating the background photon irradiance $M_{background}$ over the two IR sensor bands of consideration, MWIR and SWIR. $M_{background}$

19. This variable is the sensor sensitivity normalized to a 1 cm^2 area and 1 Hz noise equivalent bandwidth. It may be interpreted as a SNR out of detector when the radiant power of 1 W is incident on the detector, given an area of 1 cm^2 and noise equivalent bandwidth of 1 Hz.

is calculated as

$$M_{background}(\lambda, T) = \frac{2\pi c}{\lambda^4 \left(e^{\frac{hc}{\lambda kT}} - 1\right)} \left[\frac{photon}{scm^2\mu m}\right] \tag{5.38}$$

The figure of merit, D* has to be calculated for each band (MWIR and SWIR) of the multi-color IR sensor separately since the integration of the background photo irradiance in the 3-4 μm and the 14-15 μm are different. Using equations 5.37 and 5.38, D* for the two spectral areas of operation is determined for day-time luminance and night-time luminance conditions.

1. Day-time Luminance Conditions

$$D^*_{BLIP-Day}(3.5\mu m) = 6.09 \times 10^7 \left[\frac{cm\sqrt{Hz}}{W}\right] \tag{5.39}$$

$$D^*_{BLIP-Day}(14.5\mu m) = 1.75 \times 10^{10} \left[\frac{cm\sqrt{Hz}}{W}\right] \tag{5.40}$$

2. Night-time Luminance Conditions

$$D^*_{BLIP-Night}(3.5\mu m) = 5.01 \times 10^{10} \left[\frac{cm\sqrt{Hz}}{W}\right] \tag{5.41}$$

$$D^*_{BLIP-Night}(14.5\mu m) = 2.03 \times 10^{11} \left[\frac{cm\sqrt{Hz}}{W}\right] \tag{5.42}$$

The other parameters required to calculate SNR are estimated as explained

below. Detector Area A_d is given as

$$A_d = 15\mu m \times 15\mu m = 2.25 \times 10^{-10} m^2 \tag{5.43}$$

Assuming a frame rate of 100 Hz, the detector signal bandwidth Δf is calculated to be equal to 50 Hz. Given that the maximum spectral radiant exitance at day-time conditions is 5.512 W/cm^2 and at night-time conditions is 3.7 x 10^{-4} W/cm^2, the radiant intensity of the target is calculated to be 2.63 x 10^6 W/sr and 25.70 W/sr respectively for day-time and night-time conditions. Finally, the area of the collection aperture (entrance pupil) A_{enp} is determined by estimating the diameter of the detector lens using the formula

$$D_{lens} = \frac{2.44\lambda}{\Delta\theta} \tag{5.44}$$

where $\Delta\theta$ is the required angular resolution calculated earlier to be 20 μradians. For the two wavelengths under consideration, λ=3.5 μm and λ=14.5 μm the corresponding values for D_{lens} are 0.427 m and 1.8 m respectively. The larger value of 1.8 m is chosen for all further calculations in order to preserve the performance of the detector at the more demanding SWIR region. Given D_{lens}=1.8 m, the value of A_{enp}=$\pi D^2/4$=2.55 m^2.

Given all the parameters, SNR is now estimated to be

1. Day-time

$$SNR(3-4\mu m) = 43.25dB \tag{5.45}$$

$$SNR(14-15\mu m) = 17.73dB \tag{5.46}$$

2. Night-time

$$SNR(3-4\mu m) = 72.40dB \tag{5.47}$$

$$SNR(14-15\mu m) = 28.38dB \tag{5.48}$$

These achieved SNR are good enough. In a typical missile surveillance receiver, an SNR value of at least 14 dB ensures a high detection probability with low false alarm rate[17]. However, it should be remembered that this analysis was undertaken under the assumption of BLIP, neglecting other sources of noise, which could degrade the performance of the detectors to lower values than outlined here.

5.6.4 Simulation of Target Position Data as Seen by STSS

Compiling all the analysis done in the preceding subsections the specifications of the STSS system are detailed in table 5.8 on page 217. Using the data from table 5.8, simulation of the position error of the target ICBM as observed by the STSS

satellites is undertaken. In the simulations attempted, the satellites are assumed to be perfectly positioning to aid in the interception (one of the satellite IRSAT-1 is located on top of the target ICBM launch site and the other IRSAT-2 is located on top of the interceptor missile launch site). Otherwise, the simulation has to take into account the relative motion between the satellite and the ballistic missile and the fact that the different points on the surface of earth within the field of view move with different velocities with respect to the satellite, which makes the problem very complicated.

Table 5.8: STSS Parameters

Parameter	**Values**
Type	FPA step-stare
Format	4000 x 4000
Detector	Two-color QWIP
Wavelengths	3-4 μm and 14-15 μm
IHFOV-IVFOV	15 μradians
HFOV-VFOV	0.06 radians
Detector Area (A_d)	15 μm x 15 μm
Lens Diameter	1.8 m
Aperture Area	2.55 m^2
Focal Length	1 m

The STSS IR sensors are passive. They give azimuth and elevation information on the target ICBM. To derive the range to the target ICBM, two satellites have to

observe the ICBM in stereo as is attempted in the case of STSS. The intersection of the IFOV of the two satellite can be used to calculate the range to the target ICBM. This geometry between the STSS satellites and the target ICBM is illustrated in figure 5.34 below.

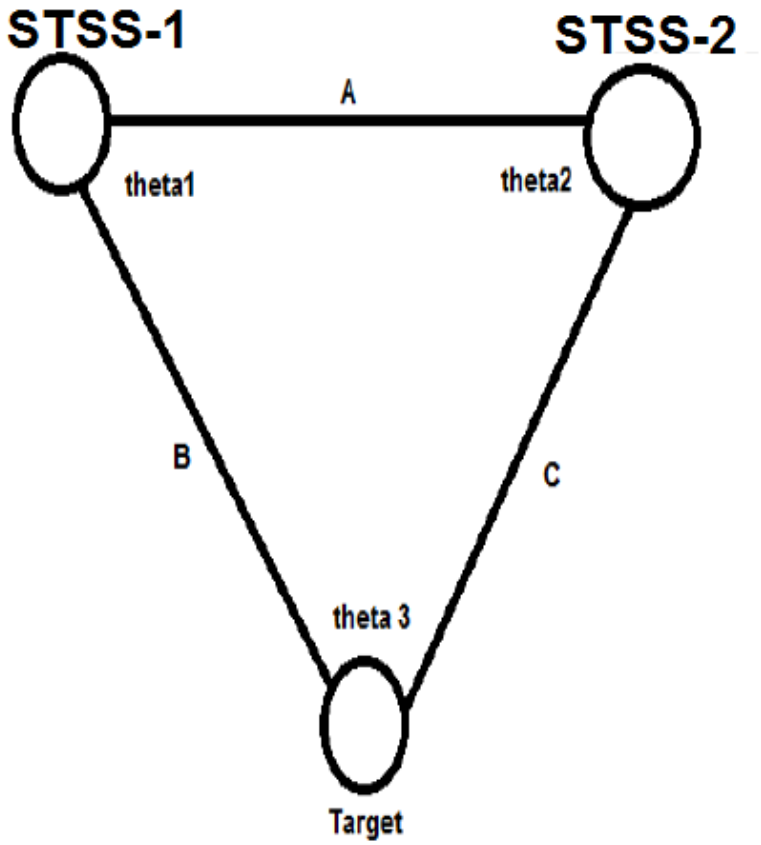

Figure 5.34: Geometry between STSS satellites and target ICBM

It is assumed that the exact position of the STSS satellites are known through on board sensors. Once the satellites have LOS to the target they can measure the angle to the target ICBM in azimuth and elevation. Given these parameters, the target ICBM position can be deduced by triangulation applying the law of sines as

indicated below.

$$\frac{A}{sin\ (\text{theta3})} = \frac{B}{sin\ (\text{theta2})} = \frac{C}{sin\ (\text{theta1})} \tag{5.49}$$

Since distance A between the satellites and all angles are known, the other distance (i.e. range) can be calculated.

In the simulation to model real-world conditions, a random uniformly distributed error is added to the measured angles. As the target must be within the IFOV lines, the error is chosen such that the midline of the IFOV can move up to ±IFOV/2 radians. The results of the simulation are shown below. Figure 5.35 on page 220 shows the error in the San Francisco-bound target ICBM position as measured by the STSS satellites during the simulation. Figure 5.36 on page 220 shows the error in the Washington D.C.-bound target ICBM position as measured by the STSS satellites during the simulation.

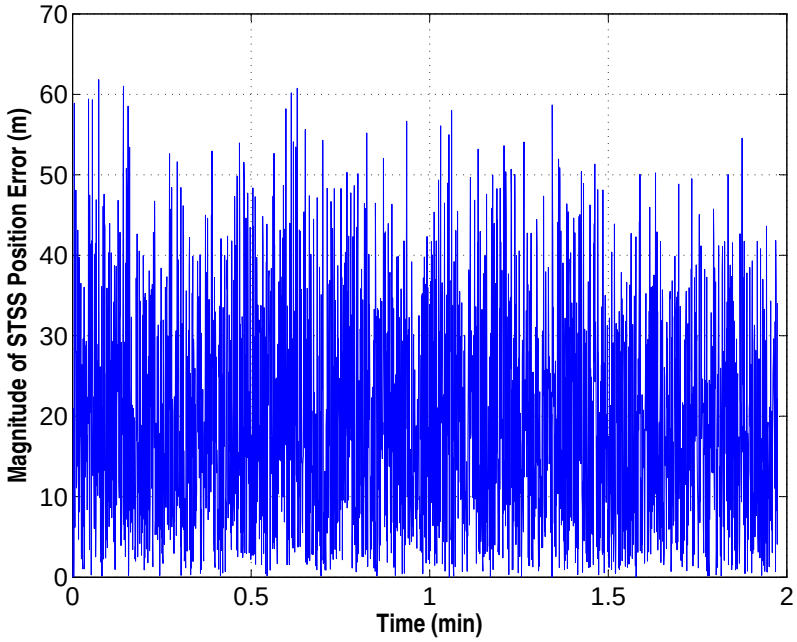

Figure 5.35: STSS Position Error for San Francisco Trajectory

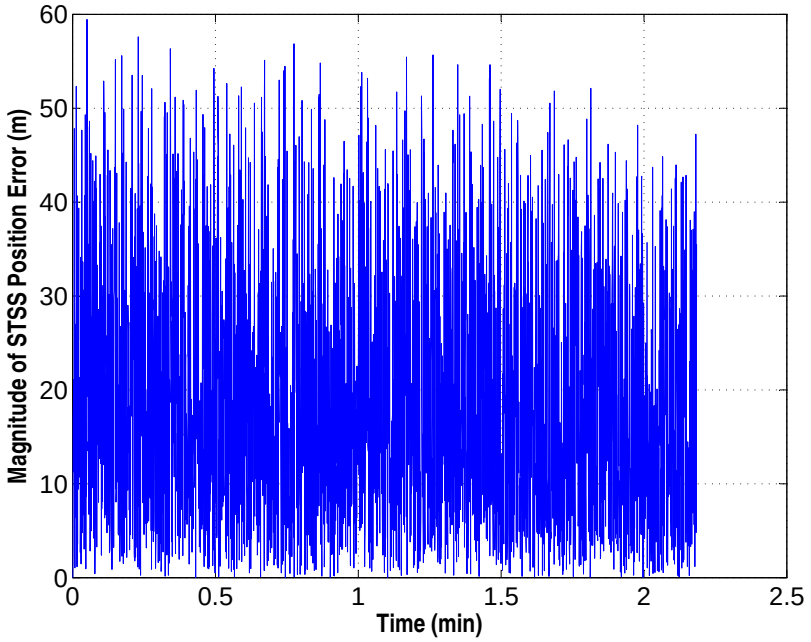

Figure 5.36: STSS Position Error for Washington D.C. Trajectory

5.7 Sensors: Kill Vehicle (KV) Sensors

Both the X-Band radar and space-based STSS sensors yield to sensors on the KV as the interceptor closes in on the target ICBM. This mechanism is adopted to ensure a hit-to-kill intercept. In order to achieve a miss distance of less than 1 m that is required for a hit-to-kill intercept it is imperative that highly accurate position data on the target is available during the endgame. The only possible way to generate such accurate data is to use sensors on the KV to track the target ICBM.

The Kill Vehicle (KV) typically consist of more than one sensor that acquires the target and helps guide the KV to the predicted interception point. In this chapter the parameters for the KV sensors is taken from the APS study on boost-phase intercept[16] which used an short-wave IR (SWIR) sensor and Light Ranging and Detection (LIDAR) sensor[20]. For the first part of the endgame the target ICBM is tracked by a short-wave IR (SWIR) sensor on the KV. The APS study decided to adopt an SWIR sensor for imaging the plume because it is simpler than an MWIR sensor and appeared adequate to allow a Light Ranging and Detection (LIDAR) sensor on the KV to locate the rocket body in the final stages of the endgame.

This chapter assumes that the decision still holds and applies an SWIR sensor in the fist part of the endgame. The SWIR sensor on the KV needs to be at an altitude of 100 km or more where atmospheric friction is sufficiently low for the

20. No attempt is made to design the sensors or to estimate its performance parameters like SNR. Details of such kind for the SWIR can be found in the APS study[16]. Details on the design and performance of a LIDAR system are well understood and documented[48, 119]. The Near Earth Asteroid Rendezvous (NEAR) spacecraft mission involved an advanced Laser rangefinder system[2].

sensor to begin operating. Therefore, for the purpose of simulation a passive SWIR sensor is functional on the KV that can detect and track the missile plume at a range of 700 km and could estimate the location of the rocket hardbody to within 100 m at a range of 100 km.

As it closes on the target, the KV shifts from homing on the plume to homing on the rocket body by handing over to its LIDAR sensor. This shift is called the plume-to-hardbody handover problem[21]. Compared to a conventional radar, the beamwidth of a LIDAR is very small due to its operation at very high frequencies. This property gives it the ability for high resolution[22].The LIDAR sensor is designed to detect and track the hardbody as soon as it is within 100 km of the target with a 10-Hz update rate and could locate the position of the aim point on the target within 0.5 m.

5.8 Simulation Results: STSS vs. Ground-based radars

Using all the insights developed in the previous sections, a comparison is made in this section between the performance of the boost-phase missile defense system using ground-based radar data versus the performance of the boost-phase missile defense system using space-based STSS data. It has already been demonstrated that

21. One mechanism is to use long-wavelength infrared (LWIR) sensors on board the kill vehicle to detect and image the rocket body's thermal emission. The radiation would have to be detected in the presence of the background LWIR emission from the plume. The other option is to use active light detection and ranging sensor (LIDAR) to determine the range to the target ICBM.

22. On the other hand, due to the narrow bandwidth they have limited search capability. Since, the endgame stage the target ICBM is already within the sights of the LIDAR there is no need for a search.

the magnitude of target ICBM position error obtained from STSS is significantly lower than the magnitude of target position error obtained from ground-based radar (compare subsections 5.6.4 and 5.5.4).

For the case of the intercept using ground-based radar, the data from the two radars are fused. This process reduced the target ICBM position error to some extent. However, in an actual setting a tuned Kalman filter needs to be applied to the radar data. For the purposes of comparing the accuracy of STSS vs. ground-based radars this is not needed and is not attempted in this chapter. Similarly, for a a multi-target, multi-interceptor scenario a joint probability data association (JPDA) algorithm[117] (i.e., a sub-optimal Bayesian algorithm) and an ellipsoidal gating[186] logic would have to be implemented to fuse the sensor tracking data. No attempts were made to create such a data processing architecture. Also, no attempt was made to fuse the DSP data with the radar data as is probably currently done. For these reasons, the results of this chapter should not be used as an absolute estimate of the miss distances obtained from a boost-phase missile defense system. To understand how a boost-phase would perform in real-world operating conditions a more detailed analysis needs to be performed. However, it can be inferred from the analysis and results shown in figures 5.37 and 5.38 below that boost-phase missile defense systems using ground-based radar data for interception will suffer from significantly larger miss distances than those using STSS data by more than an order of magnitude.

As observed from figures 5.37 and 5.38 above using position data from STSS reduces the miss distance of an intercept to between 160 and 190 m compared to

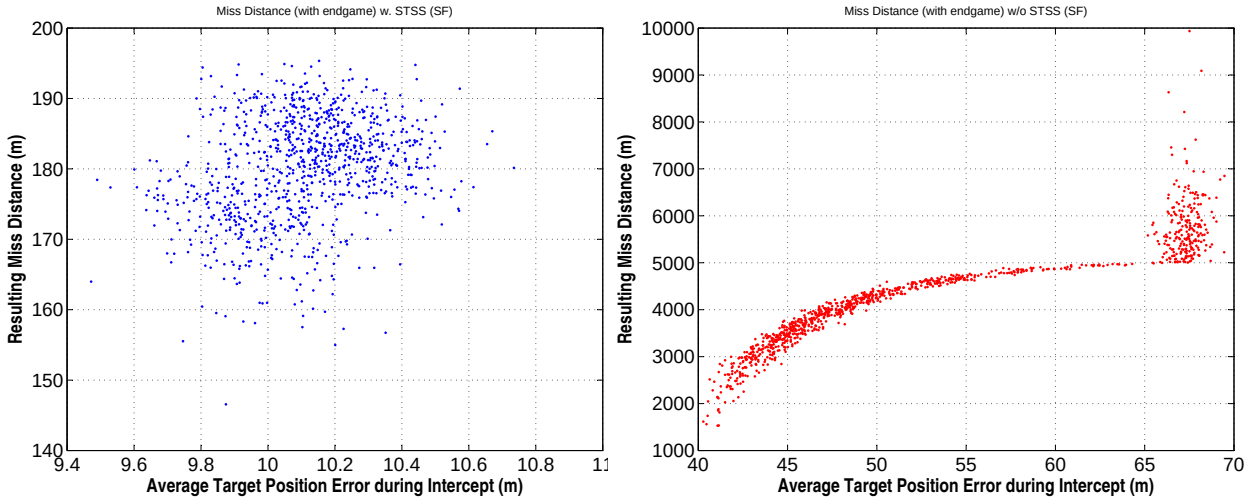

Figure 5.37: STSS vs. Ground-based Radar Performance (San Francisco Trajectory)

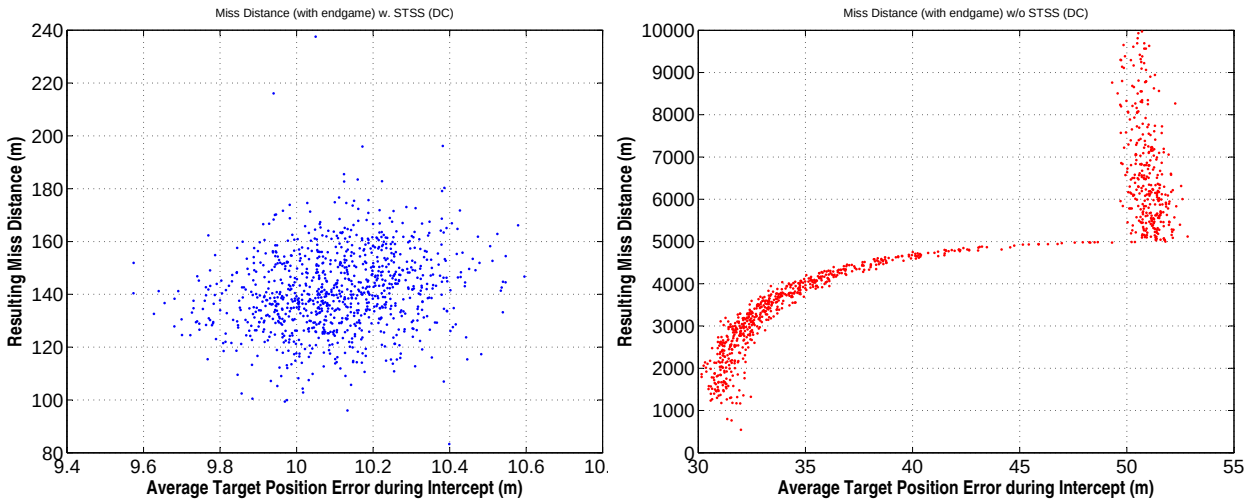

Figure 5.38: STSS vs. Ground-based Radar Performance (Washington D.C. Trajectory)

the thousands of meters of miss obtained from using X-Band radar data. This phenomenon is observed for both the San Francisco-bound and Washington D.C.-bound ICBM intercepts. The miss distance distribution for the radar data case has

a Gaussian distribution pattern and the miss distance distribution for the STSS case has an uniform distribution as expected.

5.9 Conclusion: Satellites, Missile Defense and Space Security

This chapter sequentially developed the mechanics involved in a boost-phase missile defense in order to estimate the reduction in intercept miss distances obtained by using STSS satellites. By simulating the interception between a target ICBM and a boost-phase missile defense interceptor, this chapter demonstrates that the improvements obtained from STSS satellite sensors in comparison to radar sensors are still insufficient to successfully execute a hit-to-kill boost-phase missile defense. However, the miss distances obtained with STSS are significantly lower than those obtained using radar sensors. It is conceivable that a fully populated and technologically mature STSS constellation could be a credible mechanism for missile defense against threats like North Korea.

However, this potential capability of STSS has other implications for the debate on space security. Even a limited STSS-based missile defense system might in principle reduce the effect of Chinese and possible Russian nuclear missile forces. For both Russia and China, any U.S. attempt to use space systems to augment its missile defense capabilities is of significant concern[23]. Determining whether Russia

23. From their perspective, the U.S. decision to expand missile defense capabilities into outer space represents the collapse of the Cold War bargains of strategic stability based on mutual vulnerability. During the Cold War period, the Anti-Ballistic Missile (ABM) treaty codified a situation in which the Soviet Union and the U.S. were equally vulnerable to a nuclear retaliatory strike, no matter who made the first strike. Missile defense systems were substantially limited in scope by ABM Treaty. The U.S. however withdrew from the ABM Treaty in 1991[146].

and China will be able to maintain confidence in their retaliatory missiles depends on how quickly and efficiently the U.S. could transfer STSS capabilities from a limited boost-phase system to other missile defense systems that could threaten them. If missile defense requires infrastructure—large radars or IR satellite systems—that could support a much larger system, and if the time required to build, test, and integrate the system is much greater than the time required to add more interceptors, then even a limited STSS-based missile defense system would give the U.S. a running start.

Unless the Russians and Chinese who could be threatened by the capabilities of an STSS-enabled missile defense system accept its legitimacy it would be very difficult for the U.S. to assure operational sanctuary for these satellites. If perceived as a threat to their nuclear retaliatory capabilities, China and Russia could disrupt STSS satellites, either passively or actively. They could also influence the North Korean missile program in a way that degrades the utility of a STSS-based missile defense systems. These considerations imply that if the U.S. needs to establish missile defenses against rogue threats like North Korea, then it needs to reassure other states that STSS or for that matter other satellite systems will not be used against them. It would also have to restrict the scope of its various missile defense architectures to rogue threats.

Appendix A

Failure Causes and Test Requirements for Spacecraft

Table A.1: Factors in Establishing Space Vehicle Test Requirements[55]

Factors in Space Vehicle Test Requirements
⇒ Criticality to mission ⇒ Sensitivity to Environment ⇒ Criticality to mission ⇒ Sensitivity to Environment ⇒ Severity of Environment ⇒ Knowledge or uncetainty of environment ⇒ Environmental time profile ⇒ Similarity to previously qualified articles ⇒ Ability to analyze vs. design margins ⇒ Maturity of technology ⇒ Maturity of production line ⇒ Level of assembly vs. simulation e.g. tubing and wiring vibration tested at higher levels of assembly ⇒ Product complexity ⇒ Cost of repair and retest for problems found at higher levels of assembly ⇒ Use of qualification articles for flight-alternative strategies ⇒ Benefits of dedicated qualification articles ⇒ ⇒ Fatigue life verification for repeated acceptance test of flight articles ⇒ ⇒ Available test article to evaluate upgrades/modifications ⇒ ⇒ Available testbed to evaluate mission anomalies ⇒ ⇒ Greater ability to prove design robustness ⇒ Simulation of mission environments ⇒ Prior experience with statistically significant sample of similiar products and their performance variability ⇒ Training and experience of manufacturing, assembly, integration and test personnel ⇒ Use of automated vs. operator performed manufacturing operations ⇒ Manufacturing processs controls proven to produce defect free products of similiar designs and complexity

Table A.2: Spacecraft Components and Subsystems Failure Causes[55]

	Type of Subsystem Affected													
FAILURE CAUSES	**Electrical/Electronic**	**Antenna**	**MMA**	**Solar Array**	**Battery**	**Propulsion**	**Pressure Vessel**	**Thermal Control**	**Optical**	**Structural**	**Tubing**	**Wiring/Connectors**	**Ordnance**	**Fluid**
INADEQUATE DESIGN														
Precision Surfaces/Alignment			X			X		X	X					X
Insufficient Structural Margin	X	X	X	X	X	X	X		X	X	X			X
Poor Thermal Design	X	X	X	X	X	X	X	X	X	X	X	X	X	X
Wrong Material	X	X	X	X	X	X	X	X	X	X	X	X	X	X
Insufficient Fatigue Life	X	X	X	X	X	X	X	X	X	X	X	X	X	X
Tiedown of Tubing/Wiring	X	X		X		X		X	X		X	X		X
Inadequate Envivonmental Criteria	X	X		X	X	X		X	X	X			X	X
Insufficient Life	X		X	X	X	X		X		X			X	X
Wrong Lubricants			X											
Incompatible Materials	X		X	X		X			X	X				X
Insufficient Insulation	X	X							X			X		
Insufficient Spacing/Clearance	X	X	X						X	X				
Tolerance Buildup	X	X	X						X	X				X
Cold Welding			X											
ELECTROMAGNETIC INTERFERENCE														
Inaqequate Grounding	X	X		X	X	X	X	X		X		X	X	
Insufficient Shielding	X	X										X	X	
Defective RF Seals	X	X										X	X	
High Resistance	X	X										X	X	
No RF Ground	X	X										X	X	

Table A.3: Spacecraft Components and Subsystems Failure Causes[55]

	Type of Subsystem Affected													
FAILURE CAUSES	**Electrical/Electronic**	**Antenna**	**MMA**	**Solar Array**	**Battery**	**Propulsion**	**Pressure Vessel**	**Thermal Control**	**Optical**	**Structural**	**Tubing**	**Wiring/Connectors**	**Ordnance**	**Fluid**
TESTING AND TEST PROCEDURES														
Failure to Follow Procedures	X	X	X	X	X	X	X	X	X	X	X	X	X	X
Wrong or No Procedure	X	X	X	X	X	X	X	X	X	X	X	X	X	X
Defective Test Equipment	X	X	X	X	X	X	X	X	X	X	X	X	X	X
Test Equipment Failure	X	X	X	X	X	X	X	X	X	X	X	X	X	X
Wrong Fixtures	X	X	X	X	X	X	X	X	X	X	X	X	X	X
Over/Under Torqued Bolts	X	X	X	X	X	X	X	X	X	X	X	X	X	X
Inadequate Instrumentation	X	X	X	X	X	X	X	X	X	X	X	X	X	X
Operator Error	X	X	X	X	X	X	X	X	X	X	X	X	X	X
Excessive Testing	X	X	X	X	X	X	X	X	X	X	X	X	X	X
REPAIR, REWORK AND RETEST														
Ad Hoc Procedures	X	X	X	X	X	X	X	X	X	X	X	X	X	X
Excessive Rework	X			X			X					X		
Excessive Retest	X	X	X	X	X	X			X	X				
Excessive Heat/Soldering/Welding	X			X		X						X		X
Collateral Damage	X		X	X		X								
INEXPERIENCED PERSONNEL														
Manufacturing	X	X	X	X	X	X	X	X	X	X	X	X	X	X
Handling	X	X	X	X	X	X	X	X	X	X	X	X	X	X
Assembly	X	X	X	X	X	X	X	X	X	X	X	X	X	X
Integration	X	X	X	X	X	X	X	X	X	X	X	X	X	X

Table A.4: Spacecraft Qualification Test[55]

	Primary Qualification Tests to Precipitate Failure Mechanism									
POTENTIAL FAILURE MECHANISM	**Functional**	**Vibration/Acoustic**	**Shock**	**Thermal Cycle**	**Thermal Vaccum**	**Acceleration**	**Leakage**	**Proof-Burst Pressure**	**EME**	**Life**
Mounting broken/loose	X	X	X			X			X	
Broken Part		X	X	X	X					
Shorted Part	X	X			X				X	
Defective Part	X	X		X	X				X	
Defective Board	X	X		X	X				X	
Broken/Shorted/Pinched Wires	X	X		X	X				X	
Defective/Broken Solder	X	X		X	X				X	
Contamination		X	X	X	X					
Leaky Gaskets/Seals/RF					X		X		X	
Incorrect Wiring/Routing Design	X	X							X	
Relay/Switch Chatter		X	X						X	
Adjacent Circuit Board Contact		X	X						X	
Premature Wearout		X								X
Electromagnetic Interference									X	
Insufficient Design Margin	X					X		X	X	
Corona Discharge/Arcing					X					
Inadequate Tiedown of Tubing/Wiring		X				X			X	
Inadequate Thermal Design				X	X					
Brittle Material Failure			X							
Inadequate Fatigue Life		X		X						X

Table A.5: Spacecraft Acceptance Test[55]

	Primary Acceptance Tests to Precipitate Failure Mechanism									
POTENTIAL FAILURE MECHANISM	**Functional**	**Wear-in**	**Vibration/Acoustic**	**Shock**	**Thermal Cycle**	**Thermal Vaccum**	**Leakage**	**Proof Pressure**	**Proof Load**	**EME**
Parameter Drift	X		X		X	X				
Electrical Intermittants			X	X	X	X				X
Latent Defective Parts	X		X	X	X	X				
Parts Shorting			X							
Chafed/Pinched Wires			X							
Adjacent Circuit Board Contact			X	X						
Parameters Changing Due to Deflections			X		X	X				X
Loose Hardware			X	X						X
Moving Parts Binding		X				X				
Leaky Gaskets/Seals					X	X	X			X
Lubricants Changing Characteristics		X			X	X				
Material Embrittlement				X	X	X				
Outgassing/Contamination			X	X		X				
Degradation of Electrical or Thermal Insulation						X				X
Corona Discharge/Arcing						X				X
Defective Pressure Vessels								X		
Structural Defects									X	
Defective Wiring	X									X
Defective Tubing							X			

Appendix B

Defining Field of Regard (FOR), Field of View (FOV) and Resolution

B.1 FOR and FOV

The Field of Regard (FOR) of a satellite is the total extent of *"the area of Earth that can be covered by its sensor by altering the satellite orientation (in space)."* On the other hand, the Field of View (FOV) of a satellite is *"the area of Earth that a sensor has coverage over at any moment without moving its sensor."* FOR encompasses everything that a sensor could theoretically see if it were moved on its gimballing system while FOV (which is a subset of FOR) describes what a sensor could actually see without being moved.

FOR's are mission driven. A signals intelligence mission detecting radio transmissions only needs to have line of sight to the emitter that it is trying to detect, hence its FOR extends to the horizon as seen from the satellite.Communication/BFT missions generally requires the satellite to be at a specified angle above the horizon, generally five to ten degrees, to ensure connectivity. The FOR for such a mission would be the area on the ground from where the satellite is at least 5-10 degrees above the horizon. Imagery missions have much more restrictive FORs. In order to properly analyze overhead images, the images cannot be taken from too shallow an

angle since the shallower the angle the greater is the distance to the object being imaged.

The resolution of an image[1], i.e., the ability to distinguish small, closely-spaced objects from each other, is directly related to how far the object is. The smallest feature x that can be resolved by a circular aperture of diameter D at a range R from the target using an electromagnetic wavelength λ is approximately given by the formula $x = \frac{1.22R\lambda}{D}$, showing that the resolution power is linearly related to range. Therefore, imagery satellites seldom look more than about 30 degrees off-nadir[2]. A quick survey of currently operational private for-profit satellite systems prove this (see table B.1 on page 234).

It must be noted that whether the requirement is ground-based (i.e., five degrees above the horizon for communication missions) or satellite-based (i.e., 30 degrees off-nadir for imagery), the FOR describes a specific circle on the ground. This is illustrated by figures B.1 and B.2. Both the figures show the relative sizes of these mission-driven FORs for a satellite orbiting at 185 km and 500 km, respectively. Other satellites in LEO would have FORs with similar radius ratios depending on whether their orbits are higher or lower than those depicted[67].

Finally, it is important to realize that just because a target is in the FOR of the satellite, it is not necessarily being imaged by the payload. Satellites typically do not image their entire FOR during a single pass. Especially for the high resolution

1. details on resolution requirements for military purpose and a standard definition for resolution are discussed in section B.2.
2. nadir is the direction of an imaginary line extending from the satellite straight down toward the center of the Earth.

Table B.1: Off-Nadir Capabilities of Private for-profit Satellite Systems

Satellite (Operator)	**Orbital Parameters**	**Revisit Time**	**Off-Nadir Capability**
Quickbird[177] (DigitalGlobe)	Altitude: 600 km; 97.2 deg, sun-synchronous	1-3.5 days, depending on latitude (30 deg off-nadir)	Pan: 61 cm (nadir) to 72 cm (25 deg off-nadir); MS: 2.44m (nadir) to 2.88 m (25 deg off-nadir)
Ikonos[176] (GeoEye)	Altitude: 681 km; 98.1 deg, sun-synchronous	Approximately 3 days at 40 deg latitude	Pan: 0.82 m (nadir) to 1 m (26 deg off-nadir); MS: 3.2 m (nadir) to 4 m (26 deg off-nadir)
WorldView-2[178] (DigitalGlobe)	Altitude: 770 km; sun-synchronous	1.1 days at 1 meter GSD or less 3.7 days at 20 off-nadir	Pan: 0.46 m GSD (nadir) to 0.52 m (20 deg off-nadir); MS: 1.8 m GSD (nadir) to 2.4 m GSD (20 deg off-nadir)
GeoEye-1[175] (GeoEye)	Altitude: 684 km; 98 deg, sun-synchronous	Approximately 8.3 days at 40 deg latitude and 10 deg off-nadir	Pan: 0.41 m (nadir) to 0.50 m (28 deg off-nadir)
CBERS-2[174][34] (Brazil)	Altitude: 778 km; 98.48 deg, sun-synchronous	26 days	GSD of 20 m at nadir; steerable up to +/- 32 deg across track to obtain stereoscopic imagery

imagery necessary for the tactical war fighter, only a tiny fraction of the whole FOR can be seen by the camera's FOV at any instant. Similarly, the power from the main lobe of a communication satellite would be concentrated in a smaller region of its FOR.

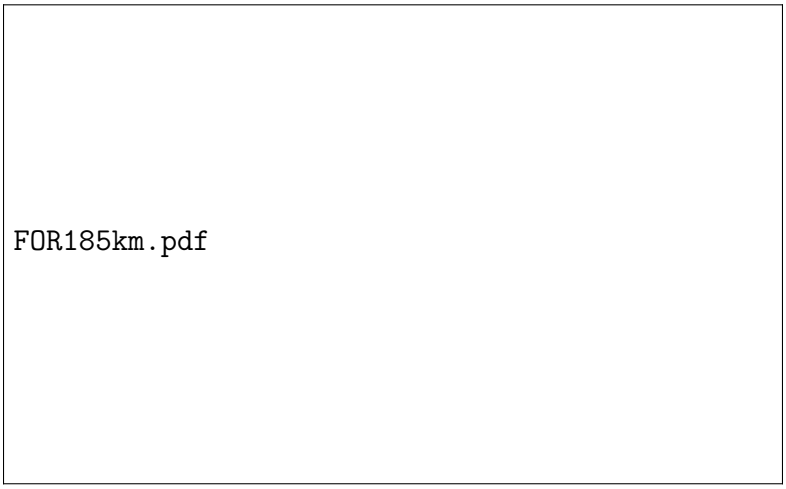

Figure B.1: Field of Regard (FOR) from 100 NM (185 km). The solid line (Horizon) represent the SIGINT FOR, the dashed lines (5/10 degree above horizon) represent communication/BFT FOR and the dotted lines (45/30 degree off-nadir) represent ISR related FOR[67].

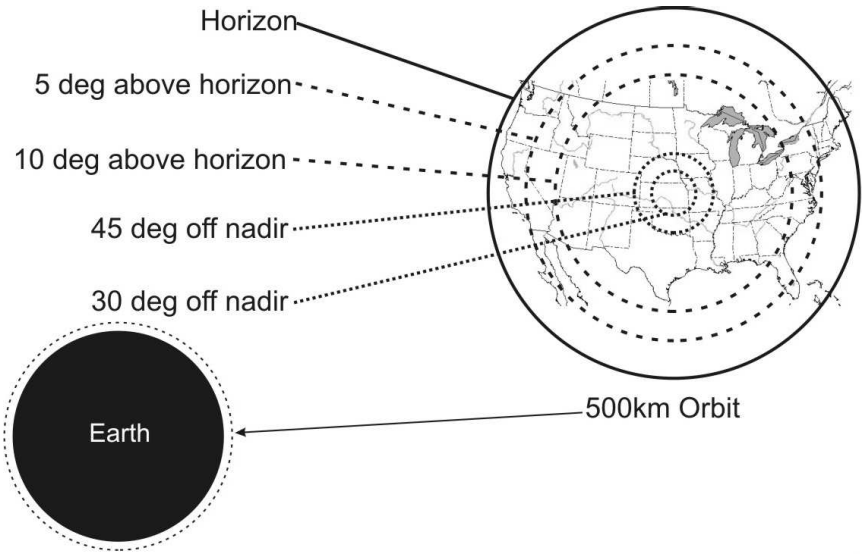

Figure B.2: Field of Regard (FOR) from 500 km. The solid line (Horizon) represent the SIGINT FOR, the dashed lines (5/10 degree above horizon) represent communication/BFT FOR and the dotted lines (45/30 degree off-nadir) represent ISR related FOR[67].

B.2 Resolution

Spatial resolution or ground resolution refers to the size of the objects on the ground that a sensor can distinguish. The easiest way to define resolution is as the minimum distance between two white spots on a black background at which the sensor can distinguish the two white spots [12].

But for electro-optical sensors used in satellites, resolution is often defined as the area on the ground that a single (square) pixel sees at any given instant i.e., its "Instantaneous Field of View", or IFOV[3]. Each pixel only gives a reading of predominant electromagnetic radiation in its IFOV. For a homogeneous feature to be detected its size generally has to be greater than one pixel. If the feature is smaller than this, it may not be detectable since the average brightness of all features in that pixel will be recorded. As a rough rule of thumb, it generally requires at least two-and-a-half pixels to distinguish an object. Thus, while a sensor with ten meter resolution by the white-dot definition can actually distinguish objects as small as about ten meters, a sensor with ten-meter resolution by the IFOV definition can only detect objects above about twenty-five meters in size. Table B.2 below uses the pixel-size IFOV definition to illustrate resolution required for various military ISR applications. For most of the analysis in this paper, this IFOV definition is used.

3. IFOV is the solid angle through which a single pixel detector is sensitive to radiation. In a scanning system this refers to the solid angle subtended by the detector when the scanning mode is stopped. IFOV is commonly expressed in milliradians.

Table B.2: Examples of Spatial Resolution[12]

REQUIRED GROUND RESOLUTION FROM COMMERICAL OBSERVATION SATELLITES (in meters)					
Target	Detection	General ID	Precise ID	Description	Technical Analysis
Bridges	6	4.5	1.5	1	0.3
Radar	3	1	0.3	0.15	0.015
Supply Dumps	1.5-3	0.6	0.3	0.03	0.03
Troop Units	6	2	1.2	0.3	0.15
Airfield Facility	6	4.5	3	0.3	0.15
Rockets/Artillery	1	0.6	0.15	0.05	0.045
Aircraft Command and Control Hq	4.5	1.5	1	0.15	0.045
Missile Sites (SSM/SAM)	3	1.5	0.6	0.3	0.045
Surface Ships	7.5-15	4.5	0.6	0.3	0.045
Nuclear Weapons Components	2.5	1.5	0.3	0.03	0.015
Vehicles	1.5	0.6	0.3	0.06	0.045
Land Minefields	3-9	6	1	0.03	0.09
Ports and Harbors	30	15	6	3	0.3
Coasts, Landing Beaches	15-30	4.5	3	1.5	0.15
Railroad Yards and Shops	15-30	15	6	1.5	0.4
Roads	6-9	6	1.8	0.6	0.4
Urban Areas	60	30	3	3	0.75
Terrain	-	90	4.5	1.5	0.75
Surfaced Submarines	7.5-30	4.5-6	1.5	1	0.03

Detection: *Location of a class of units, objects, or activity of interest*
General Identification: *Determination of a general target type*
Precise Identification: *Discrimination within target type of known types*
Description: *Size, dimension, configuration, equipment count, etc*
Technical analysis: *Detailed analysis of specific equipment*

Appendix C

Validation of Ergodic Theory

In order to validate the accuracy of the Ergodic thory based numerical estimation method used to optimize orbits for TacSats, a comparison was done between the numerical method and a orbital propagator. A satellite orbit with parameters similar to one optimized for TacSat coverage over Baghdad i.e. orbiting at an altitude of 600km and inclined at 35 degrees[1] was propogated for a period of 24 hours in STK[2] over the city of Baghdad. An illustration of the size of Baghdad chosen in STK is shown in figure C.1 below.

The results from the orbital propogation is documented below in table C.1. The coverage over Baghdad (of a optimized satellite) determined using STK's orbital propagator is compared with the coverage obtained from the numerical method based on ergodic theory. It can be seen that the variance is not enough to challenge the application of ergodic theory to the discussion of the chapter.

1. RAAN and mean anomaly was chosen to obtain maximum coverage over the region of interest.
2. STK or Satellite Tool Kit is a commerical software for orbital analysis. An evaluation copy of the software was used to undertake the analysis in this chapter.

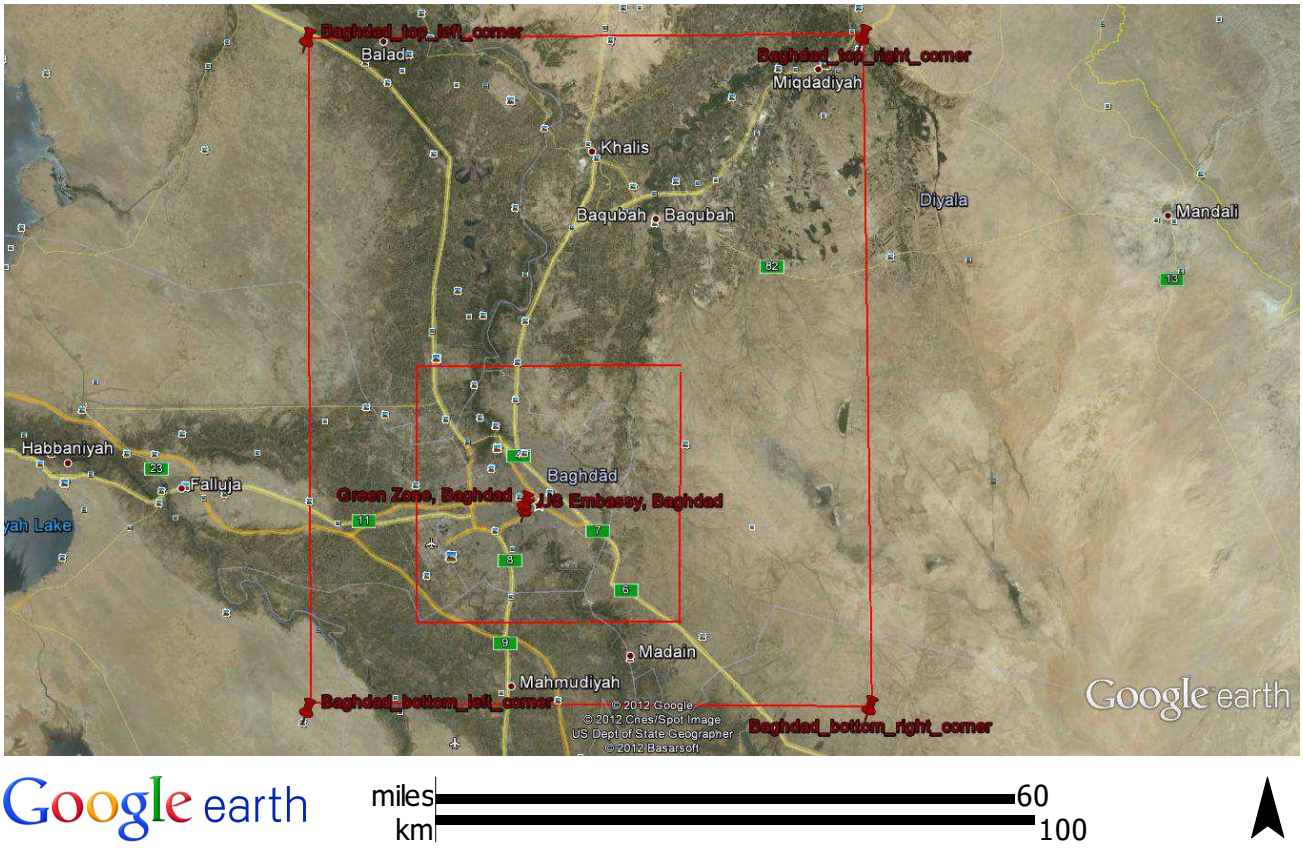

Figure C.1: Size and Extent of Baghdad as Used in the Orbital Propagator (11 Apr 2012 12:00:00.000 UTCG to 12 Apr 2012 12:00:00.000 UTCG)

Table C.1: Total Access Duration for 24 Hours

	Region of Interest/AOR	**Sensor FOR**	**Total Access Duration (min)**
Ergodic theory	Baghdad Baghdad Baghdad	Horizon 45-degree off-nadir 30-degree off-nadir	84.808 10.395 5.892
Orbital Propagation	Baghdad Baghdad Baghdad	Horizon 45-degree off-nadir 30-degree off-nadir	85 (approx.) 10.2 (approx.) 4.4 (approx.)

Appendix D

Effect of FOR Constraints on Optimized Orbits: *Jakarta* and *St. Petersburg*

This Appendix expands the inferences drawn in subsection 2.4.2 of chapter 2 (on page 44) to the other two target locations of interest: *Jakarta* and *St. Petersburg*.

D.1 *Jakarta*: Communication Mission Constraints

For a communication satellite the sensor FOR constraints are 5/10 degree above the Horizon.

Inference D.1 *At a given satellite altitude and inclination, as the FOR becomes more constrained due to operational reasons the maximum average daily coverage over the target latitude decreases. For example, it can be seen in figure D.1 that at an altitude of 500 km and an inclination of 6 degrees (Jakarta being the target location of interest at that particular latitude) with a 5 degree above the horizon FOR constraint the maximum average daily coverage is approximately 120 minutes: a 25 percent decrease in coverage (in comparison to the horizon FOR case). Similarly, it is seen in figure D.2 that at the same altitude of 500 km and 6 degrees inclination with a 10 degree above the horizon FOR constraint the maximum average daily coverage is approximately 90 minutes: a 45 percent decrease in coverage (in comparison to the horizon FOR case).*

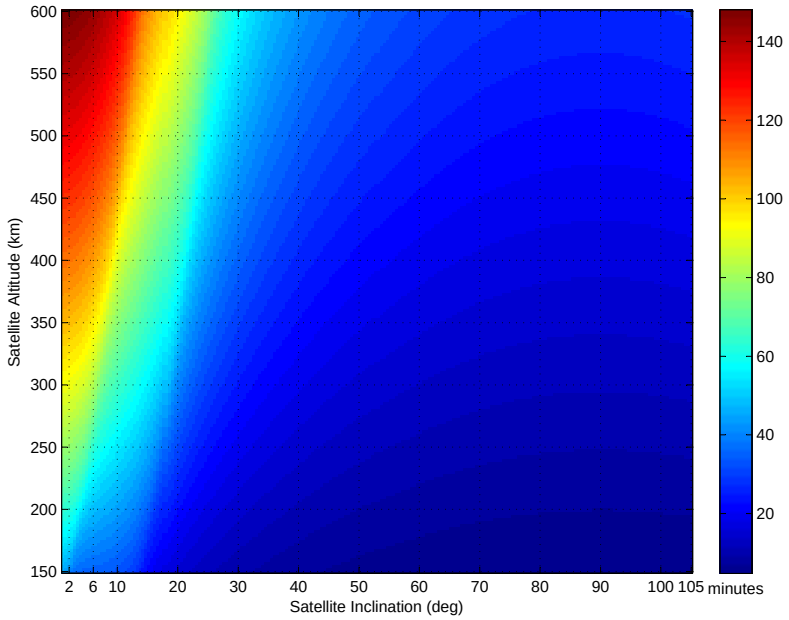

Figure D.1: Maximum Average Satellite Coverage Over *Jakarta* with a 5 Degree Above the Horizon FOR (minutes per day)

D.2 *Jakarta*: ISR Mission Constraints

For a ISR satellite the sensor FOR constraints are 30/45 degree off-nadir.

Inference D.2 *Similar to the previous inference, when the FOR is constrained by ISR requirements there are drastic losses in coverage time. For example, it can be seen in figure D.3 that at an altitude of 500 km and an inclination of 6 degrees with a 45 degree off-nadir FOR constraint the maximum daily coverage is approximately 14 minutes: a 90 percent decrease in coverage from the horizon FOR case. Similarly, it is seen in figure D.4 that at the same altitude of 500 km and 6 degrees inclination with a 30 degree off-nadir FOR constraint the maximum average daily coverage is approximately 5 minutes: a 97 percent decrease in coverage (in comparison to the*

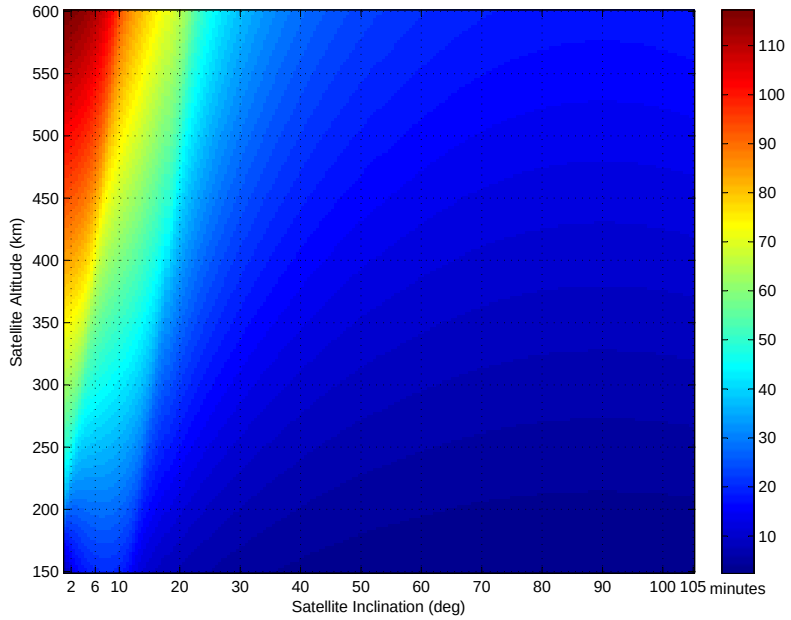

Figure D.2: Maximum Average Satellite Coverage Over *Jakarta* with a 10 Degree Above the Horizon FOR (minutes per day)

horizon FOR case).

The dramatic fall in coverage between the ideal case of horizon FOR and the 5/10 degree above the horizon requirement for communication satellites or the 30/45 degree off-nadir FOR for ISR/imaging satellites can be comprehended by examining figure B.2 in Appendix B on page 232. It is immediately clear that as the FOR becomes more constrained the area on the ground accessible for the satellite mission gets smaller hence leading to reduced mission coverage durations[1].

1. more details are in Appendix B on 232.

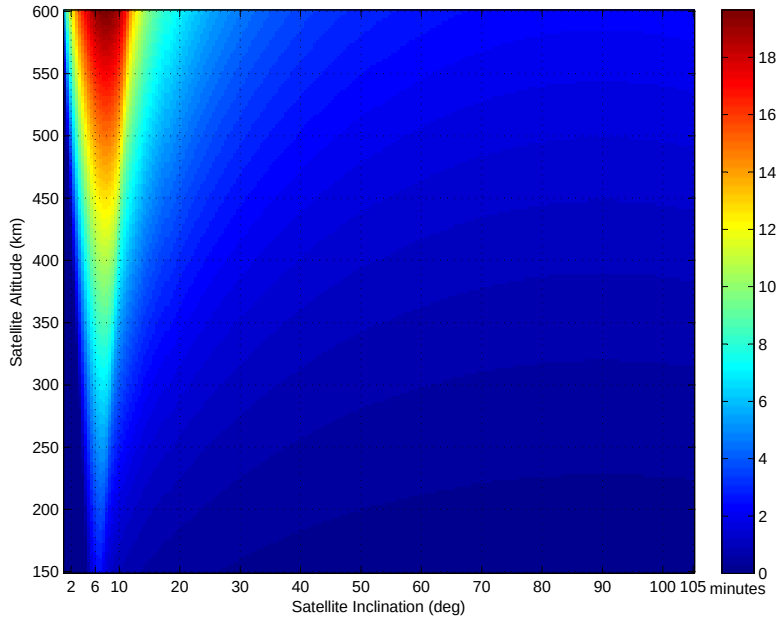

Figure D.3: Maximum Average Satellite Coverage Over *Jakarta* with a 45 Degree Off-Nadir FOR (minutes per day)

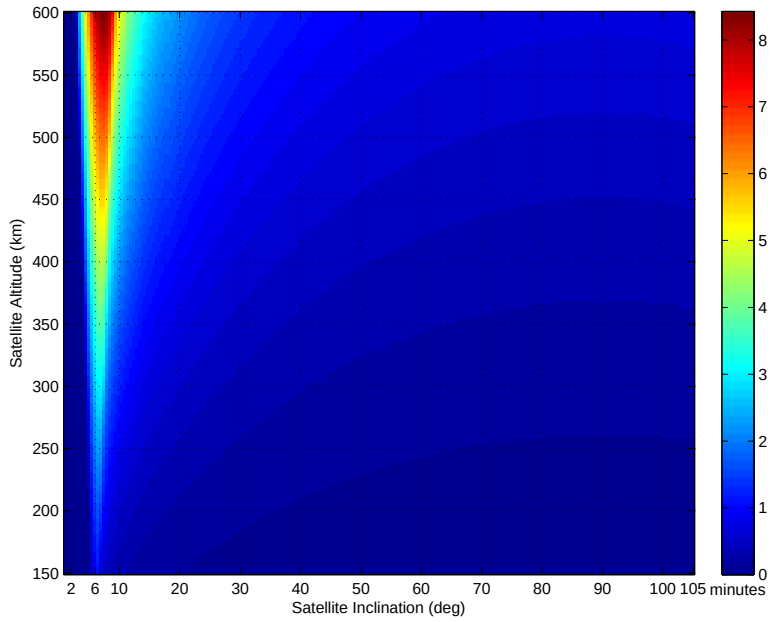

Figure D.4: Maximum Average Satellite Coverage Over *Jakarta* with a 30 Degree Off-Nadir FOR (minutes per day)

D.3 *St. Petersburg*: Communication Mission Constraints

For a communication satellite the sensor FOR constraints are 5/10 degree above the Horizon.

Inference D.3 *At a given satellite altitude and inclination, as the FOR becomes more constrained due to operational reasons the maximum average daily coverage over the target latitude decreases. For example, it can be seen in figure D.5 that at an altitude of 500 km and an inclination of 60 degrees (St. Petersburg being the target location at that particular latitude) with a 5 degree above the horizon FOR constraint the maximum average daily coverage is approximately 50 minutes: a 30 percent decrease in coverage (in comparison to the horizon FOR case). Similarly, it is seen in figure D.6 that at the same altitude of 500 km and 60 degrees inclination with a 10 degree above the horizon FOR constraint the maximum average daily coverage is approximately 40 minutes: a 40 percent decrease in coverage (in comparison to the horizon FOR case).*

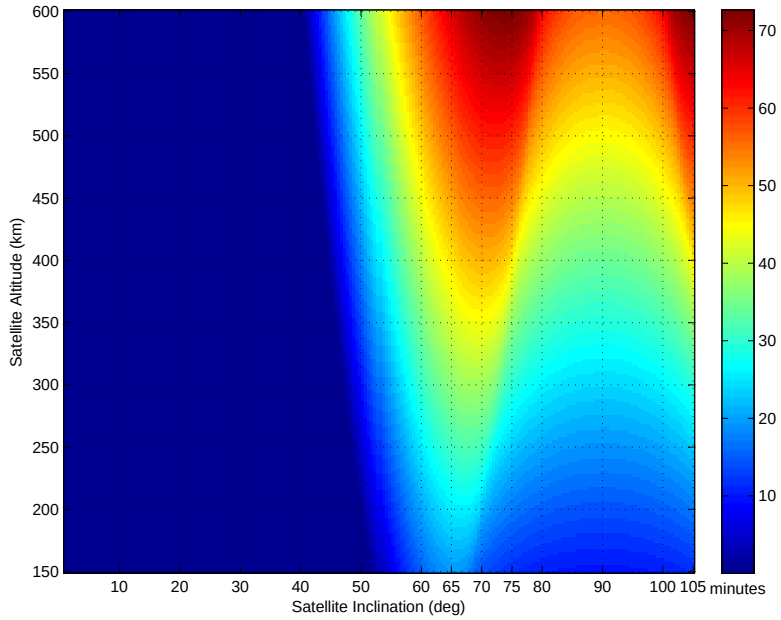

Figure D.5: Maximum Average Satellite Coverage Over *St. Petersburg* with a 5 Degree Above the Horizon FOR (minutes per day)

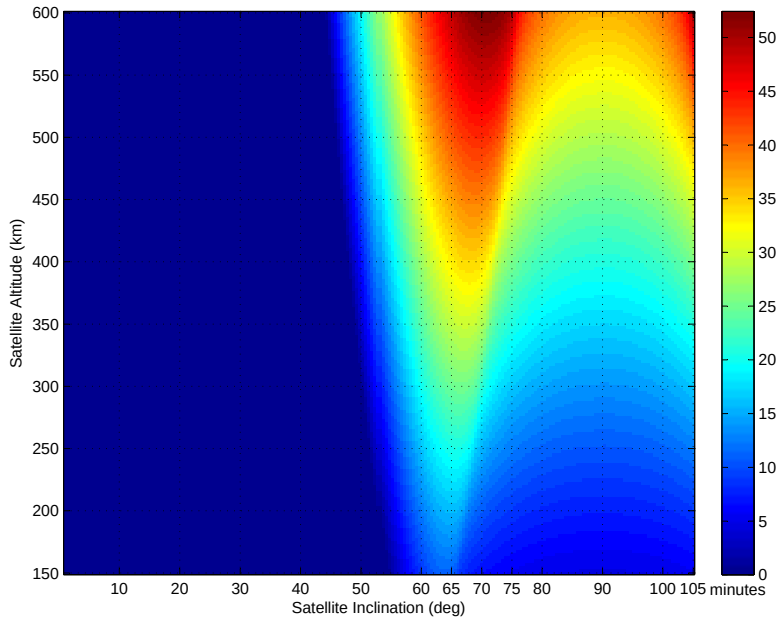

Figure D.6: Maximum Average Satellite Coverage Over *St. Petersburg* with a 10 Degree Above the Horizon FOR (minutes per day)

D.4 *St. Petersburg*: ISR Mission Constraints

For an ISR satellite the sensor FOR constraints are 30/45 degree off-nadir.

Inference D.4 *Similar to the previous inference, when the FOR is constrained by ISR and imaging requirements there are drastic losses in coverage time. For example, it can be seen in figure D.7 that at an altitude of 500 km and an inclination of 60 degrees with a 45 degree off-nadir FOR constraint the maximum daily coverage is approximately 8 minutes: a 90 percent decrease in coverage from the horizon FOR case. Similarly, it is seen in figure D.8 that at the same altitude of 500 km and 60 degrees inclination with a 30 degree off-nadir FOR constraint the maximum average daily coverage is approximately 3.5 minutes: a 95 percent decrease in coverage (in comparison to the horizon FOR case).*

As shown above, the dramatic fall in coverage between the ideal case of horizon FOR and the 5/10 degree above the horizon requirement for communication satellites or the 30/45 degree off-nadir FOR for ISR satellites can be comprehended on examining once more figure B.2 in Appendix B on page 232. It is immediately clear that as FOR becomes more constrained the area on the ground accessible for the satellite mission gets smaller hence leading to reduced mission coverages[2].

2. more details are in Appendix B on 232.

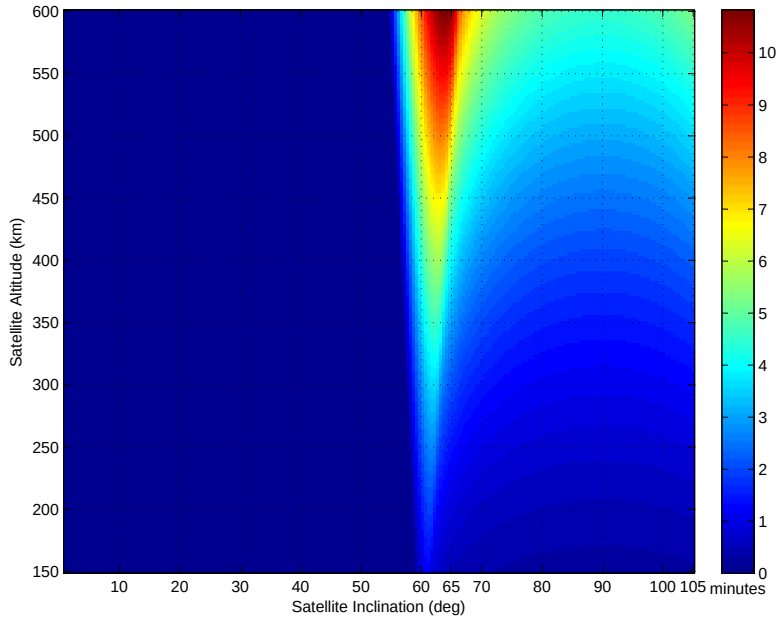

Figure D.7: Maximum Average Satellite Coverage Over *St. Petersburg* with a 45 Degree Off-Nadir FOR (minutes per day)

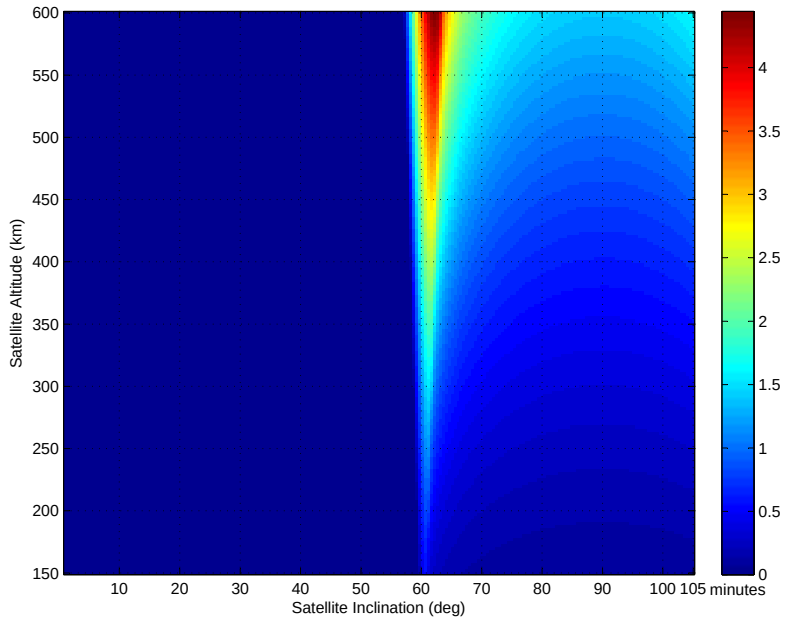

Figure D.8: Maximum Average Satellite Coverage Over *St. Petersburg* with a 30 Degree Off-Nadir FOR (minutes per day)

Appendix E

Effect of FOR constraints Across Latitudes

This appendix will illustrate and prove that

Inference E.1 *At any given altitude, the effect of various FOR constraints is to reduce the average maximum coverage across latitudes. This effect, however, is more pronounced at mid-latitude regions than in equatorial or polar regions.*

E.1 100 NM (185 km) Altitude

For the case where the satellite is orbiting at an altitude of 100 NM (185 km); when the various communication, BFT, and ISR FOR constraints are imposed there are substantial decrease in optimized maximum average coverage times across all latitudes. It will be shown in this section that even in the regions of the earth where the coverage is greatest i.e., equator and polar[1] the loss of coverage is substantial. The other regions will suffer more rapid fall in coverage.

E.1.1 Effect of FOR Constraint on Equatorial and Polar Regions

On examining figures E.1, E.2, E.3, E.4 and E.5 below the loss of coverage at equatorial and polar regions due to FOR constraints is apparent. The maximum

1. refer to inference inference 2.4 on page 41 for a discussion on the reason why equatorial and polar regions greater maximum average coverage than other regions.

coverage durations decrease progressively from 110 minutes (for the horizon FOR) to

- 80 minutes (for the 5 degree above horizon FOR) in the case of communication mission; a 27 percent decrease in coverage
- 55 minutes (for the 10 degree above horizon FOR) in the case of communication mission; a 50 percent decrease in coverage
- 14 minutes (for the 45 degree off-nadir FOR) in the case of ISR mission; a 88 percent decrease in coverage
- 8 minutes (for the 30 degree off-nadir FOR) in the case of ISR mission; a 92 percent decrease in coverage

E.1.2 Effect of FOR Constraint on Mid-Latitude Regions

On examining figures E.1, E.2, E.3, E.4 and E.5 below again the loss of coverage across mid-latitude regions (45 degree latitude) due to FOR constraints is clear. The maximum coverage durations decrease progressively from 45 minutes (for the horizon FOR) to approximately

- 25 minutes (for the 5 degree above horizon FOR) in the case of communication mission; a 45 percent decrease in coverage
- 15 minutes (for the 10 degree above horizon FOR) in the case of communication mission; a 67 percent decrease in coverage

- 3 minutes (for the 45 degree off-nadir FOR) in the case of ISR mission; a 94 percent decrease in coverage

- less than 1 minutes (for the 30 degree off-nadir FOR) in the case of ISR mission

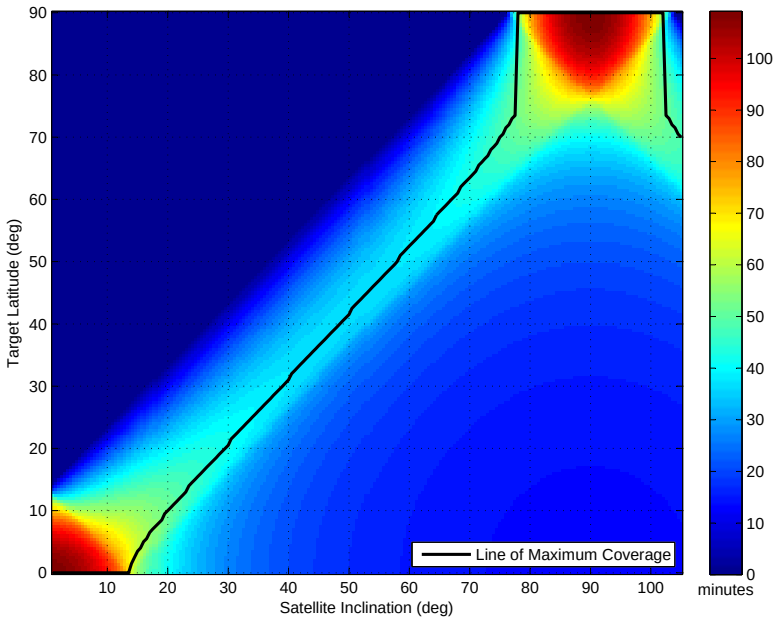

Figure E.1: HORIZON FOR Maximum Average Satellite Coverage From 100 NM (185 km) (minutes per day)

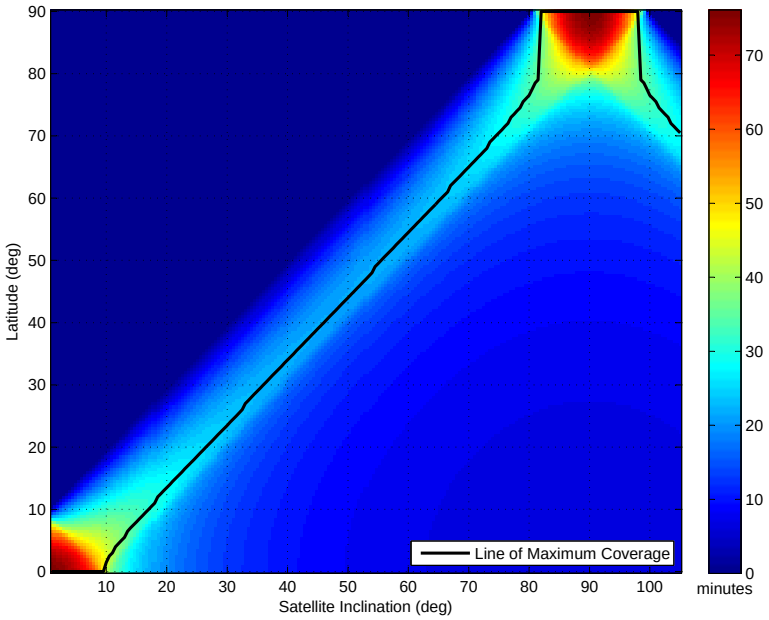

Figure E.2: 5 Degree Above the HORIZON FOR Maximum Average Satellite Coverage From 100 NM (185 km) (minutes per day)

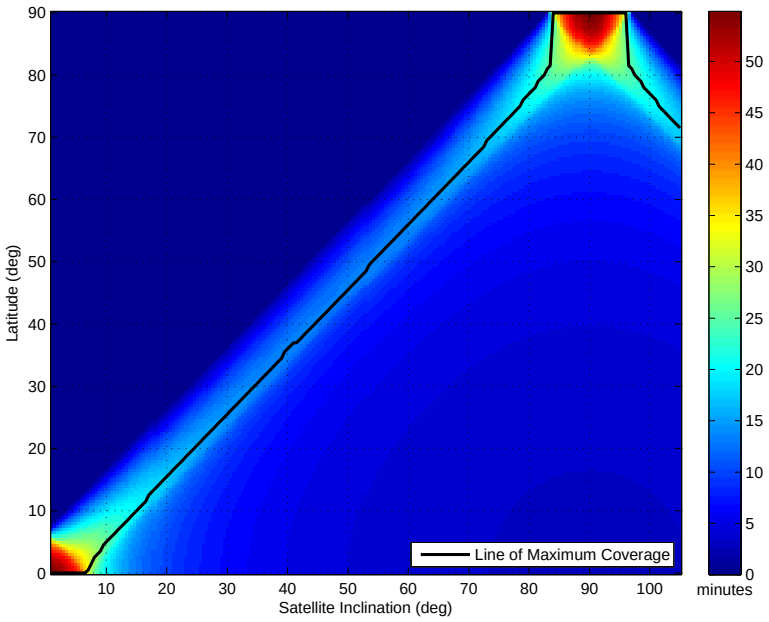

Figure E.3: 10 Degree Above the HORIZON FOR Maximum Average Satellite Coverage From 100 NM (185 km) (minutes per day)

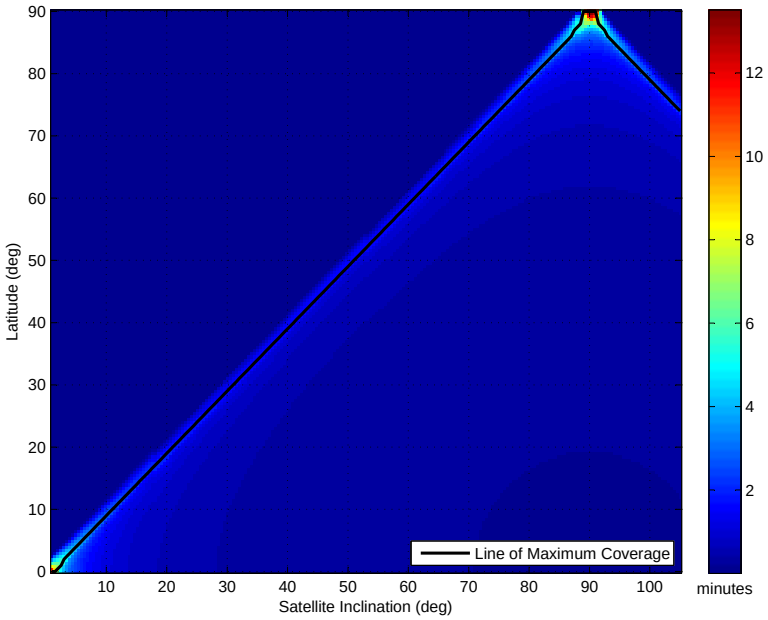

Figure E.4: 45 Degree Off-Nadir FOR Maximum Average Satellite Coverage From 100 NM (185 km) (minutes per day)

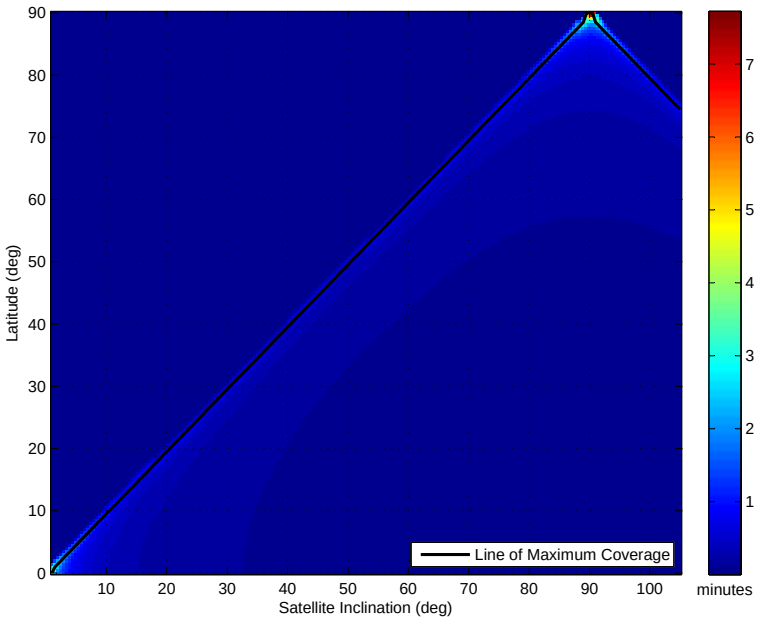

Figure E.5: 30 Degree Off-Nadir FOR Maximum Average Satellite Coverage From 100 NM (185 km) (minutes per day)

E.2 500 km Altitude

For the case where the satellite is orbiting at an altitude of 500 km; when the various communication, BFT, and ISR FOR constraints are imposed there are substantial decrease in optimized maximum average coverage times across all latitudes with mid-latitude regions suffering more drastic fall in coverages than equatorial and polar regions.

E.2.1 Effect of FOR Constraint on Equatorial and Polar Regions

On examining figures E.6, E.7, E.8, E.9 and E.10 below the loss of coverage at equatorial and polar regions due to FOR constraints is apparent. The maximum coverage durations decrease progressively from 180 minutes (for the horizon FOR) to

- 140 minutes (for the 5 degree above horizon FOR) in the case of communication mission; a 33 percent decrease in coverage
- 110 minutes (for the 10 degree above horizon FOR) in the case of communication mission; a 40 percent decrease in coverage
- 40 minutes (for the 45 degree off-nadir FOR) in the case of ISR mission; a 78 percent decrease in coverage
- 22 minutes (for the 30 degree off-nadir FOR) in the case of ISR mission; a 88 percent decrease in coverage

E.2.2 Effect of FOR Constraint on Mid-Latitude Regions

On re-examining figures E.6, E.7, E.8, E.9 and E.10 below again the loss of coverage across mid-latitude regions due to FOR constraints is clear. The maximum coverage durations decrease progressively from 80 minutes (for the horizon FOR) to approximately

- 60 minutes (for the 5 degree above horizon FOR) in the case of communication mission; a 25 percent decrease in coverage
- 45 minutes (for the 10 degree above horizon FOR) in the case of communication mission; a 44 percent decrease in coverage
- 10 minutes (for the 45 degree off-nadir FOR) in the case of ISR mission; a 92 percent decrease in coverage
- 5 minutes (for the 30 degree off-nadir FOR) in the case of ISR mission; a 94 percent decrease in coverage

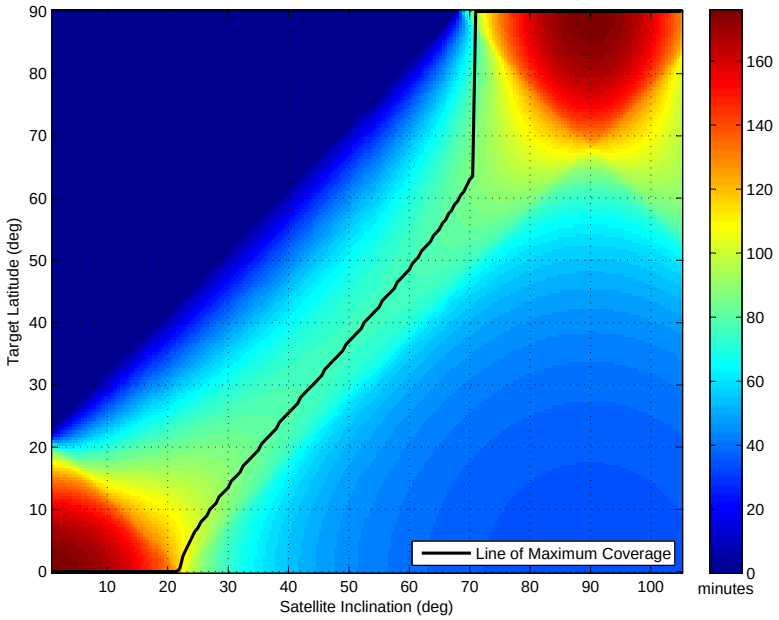

Figure E.6: HORIZON FOR Maximum Average Satellite Coverage From 500 km (minutes per day)

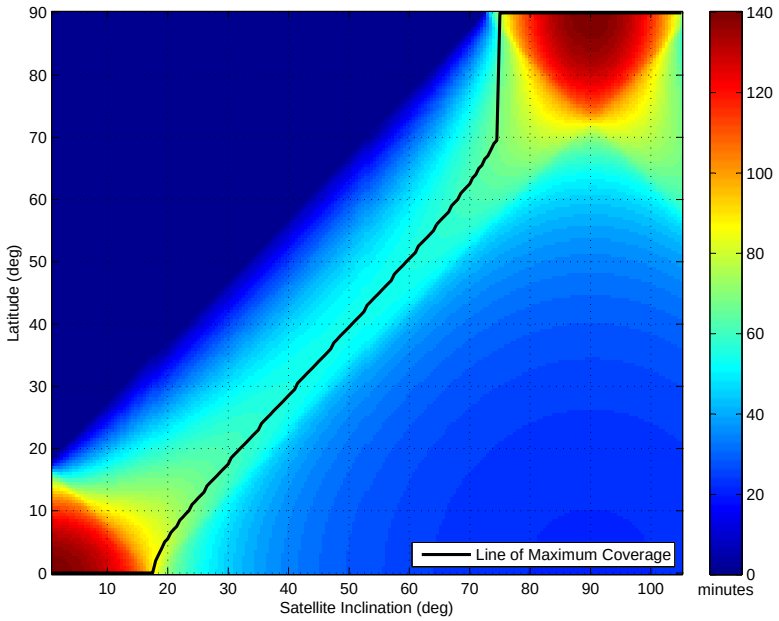

Figure E.7: 5 Degree Above the HORIZON FOR Maximum Average Satellite Coverage From 500 km (minutes per day)

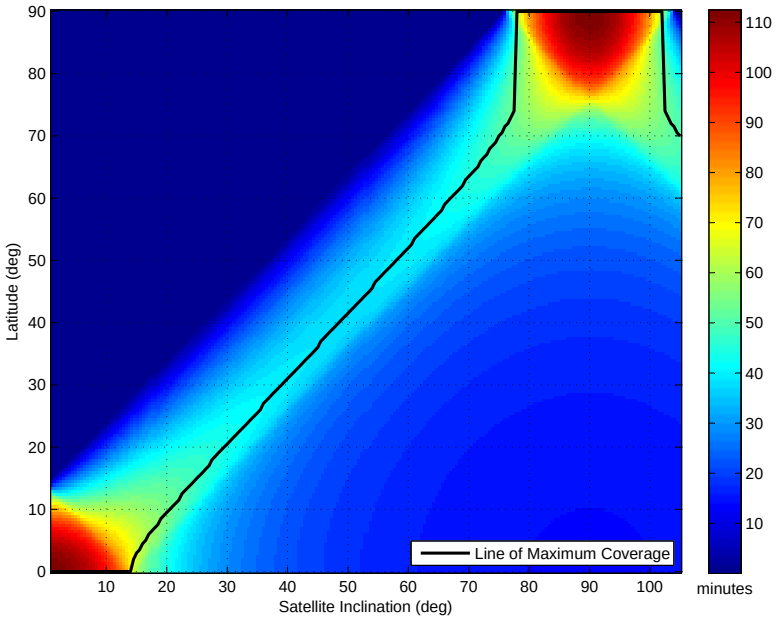

Figure E.8: 10 Degree Above the HORIZON FOR Maximum Average Satellite Coverage From 500 km (minutes per day)

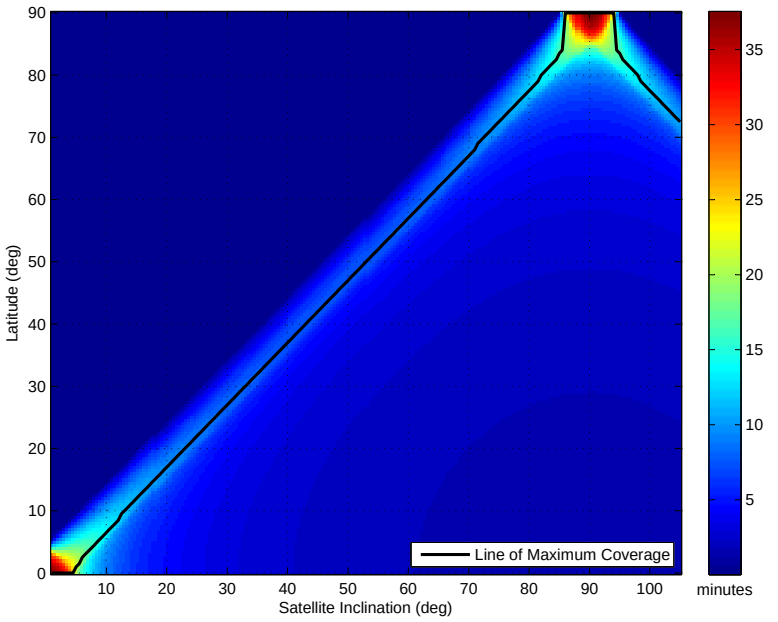

Figure E.9: 45 Degree Off-Nadir FOR Maximum Average Satellite Coverage From 500 km (minutes per day)

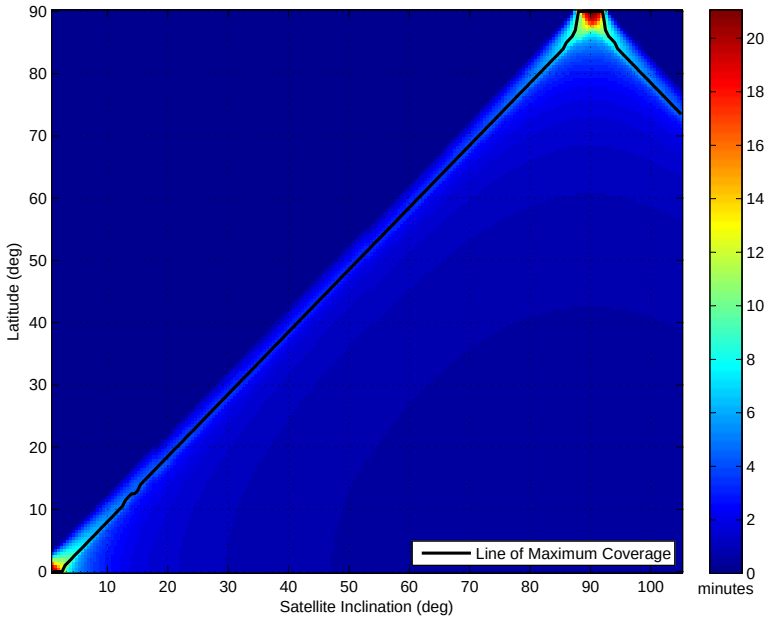

Figure E.10: 30 Degree Off-Nadir FOR Maximum Average Satellite Coverage From 500 km (minutes per day)

Appendix F

Operationally Responsive Space (ORS) Definitions and Stakeholders

The following table is adapted and improved upon from the original source[179]. The table summarizes some of the disparate definitions of Operationally Responsive Space (ORS) used by various stakeholders.

Table F.1: ORS Definitions[179]

Source	**Definition**
VADM Arthur Cebrowski,Director, USN, retired, Office of Force Transformation, OSD	A new business model that includes (1) the defining of a joint military demand function and (2) focus on providing joint military capabilities for our operational and tactical level commanders. Finally, the model incentives output rate and uses a co-evolutionary strategy of concept-technology pairing, providing for iterative advancement in operational capabilities[19].
Lt. Gen. Frank Klotz, Vice Commander, Air Force Space Command	ORS will provide affordable capability to promptly, accurately, and decisively position and operate national and military assets in and through space and near space. The ORS vision is to provide rapid, tailorable space power focused at the operational and tactical level of war[81].
Brian Green, Deputy Assistant, Secretary of Defense for Strategic Capabilities	Assured space power that is focused at the operational level of war[102].
Air University	....the ability to rapidly employ responsive space lift vehicles and satellites; service, repair or recover on-orbit satellite; and deliver space-based capabilities wherever and whenever the war fighter requests them[4].

continued on next page

continued from previous page

Source	**Definition**
GAO Report	(1) Delivers low-cost, short term joint tactical capabilities defined by field commanders (2) Complement and augment national space capabilities, not replace them (3) Serves as a testbed for the larger space program by providing a clear path for science and technology investments...providing increased access to space for testing critical research and development payloads.
2007 Defense Authorization Bill	It is the policy of the United States to demonstrate, acquire, and deploy an effective capability for operationally responsive space to support military users and operations from space, which shall consist of (1) responsive satellite payloads and buses built to common technical standards; (2) low-cost space launch vehicles and supporting range operations facilitate the timely launch and on-orbit operations of satellites; (3) responsive command and control capabilities; and (4) concepts of operations, tactics, techniques, and procedures that permit the use of responsive space assets for combat and military operations other than war[56].
USSTRATCOM	...Assured Space Power Focused on the Urgent Needs of the JFCs.
AFSPC	The ability to promptly, accurately, decisively deliver, position, and operate national and military assets in and through space....affordably

The table below summarizes the various organizations involved in the experimentation and implementation of Operationally Responsive Space (ORS) missions.

Table F.2: ORS Stakeholders[179]

Organization	**Role**
Office of Force Transformation (OFT)	Author and prime mover of current ORS initiative. Sponsor of TacSats 1-4
Naval Research Laboratory (NRL)	Program Manager for TacSats 1 and 4
Air Force Research Laboratory (AFRL)	Program Manager for TacSats 2 and 3
DARPA	Leading management of FALCON small launch vehicle program

continued on next page

continued from previous page	
Organization	**Role**
USSTRATCOM	Validates ORS Program Office requirements. Participates in ORS Program Office acquisition decisions
Executive Agent for Space (Under Secretary of the Air Force)	Acquisition authority for new ORS Program Office procurements
Air Launch LLC, Space Exploration Technologies, Corp (SpaceX)	Winners of DARPA FALCON SLV contracts
ORS Program Office	Will run DOD ORS Program. Assumes program management responsibilities previously by OFT
Air Force Space Command (AFSPC)	(1)Requirements validation (if delegated by USSTRATCOM) (2)TacSat military utility assessments (3)ORS Analysis of Alternatives (AoA) efforts
National Reconnaissance Office (NRO)	Owners/operators of spacecraft potentially requiring reconstitution
Joint Warfighting Space program office	Established in 2005 within Detachment 12 of AFSPC's Space and Missile Center

Bibliography

[1] Adam J. Hebert, "Compressing the Kill Chain," AIR FORCE Magazine, March, (2003).

[2] A. F. Cheng et al, "Near-Earth Asteroid Rendezvous: Mission Overview," Journal of Geophysical Research **Vol. 102, No. E10** (1997).

[3] AFSPC, *Final Mission Need Statement AFSPC 001-01, for Operationally Responsive Spacelift* (2001).

[4] Air University, *Space: Progess in Space Acquisition*, Air University, Maxwell Air Force Base, AL.

[5] Alan D. Campen, *Information Systems and Air Warfare* in (eds.) Alan D. Campen, *The First Information War. The Story of Communications, Computers and Intelligence Systems in the Persian Gulf War*, AFCEA International Press, Fairfax, Virginia, U.S. (1992).

[6] Alan D. Campen, *Silent Space Warriors* in (eds.) Alan D. Campen, *The First Information War. The Story of Communications, Computers and Intelligence Systems in the Persian Gulf War*, AFCEA International Press, Fairfax, Virginia, U.S. (1992).

[7] Alan D. Campen, *Electronic Templates* in (eds.) Alan D. Campen, *The First Information War. The Story of Communications, Computers and Intelligence Systems in the Persian Gulf War*, AFCEA International Press, Fairfax, Virginia, U.S. (1992).

[8] Alan D. Campen, *Communications Support to Intelligence* in (eds.) Alan D. Campen, *The First Information War. The Story of Communications, Computers and Intelligence Systems in the Persian Gulf War*, AFCEA International Press, Fairfax, Virginia, U.S. (1992).

[9] Alan Wasser, "LBJ's Space Race: What we Didn't Know Then (Part 1)," The Space Review, June, (2005)

[10] Alexander Flax, *Ballistic Missile Defense: Concepts and History* in (eds.) Franklin A. Long et al, *Weapons in Space*, American Academy of Arts and Sciences, Boston (1986).

[11] Andrew Reidy, "Russia's Anti-BMD Alliance?," The Diplomat March 22, (2012).

[12] Ann M. Florini, "The Opening Skies: Third Party Imaging Satellites and U.S. Security," International Security **Vol.13, No.2**, (1988).

[13] Annalisa L. Weigel, *Spacecraft System-Level Integration and Test Discrepancies: Characterizing Distributions and Costs*, MIT Thesis (2000).

[14] Anthony G. Knight and Aaron B. Luck, *Tactical Space - Beyond Line of Sight Alternatives for the Army and Marine Corps Ground Tactical Warfighter*, Masters Thesis, Naval Postgraduate School, CA (2007).

[15] Apoorva Bhopale and Charles J. Finley, "How ORS Will Answer the 7-Day Tier-2 Challenge," 7th Responsive Space Conference **RS7-2009-6003** (2009).

[16] American Physical Society, *Report of the American Physical Society Study Group on Boost-Phase Intercept Systems for National Missile Defense: Scientific and Technical Issues*, American Physical Society (2004).

[17] A. R. Jha, *Infrared Technology: Applications to Electro-Optics, Photonic Devices, and Sensors*, Wiley Series in Microwave and Optical Engineering, John Wiley and Sons, USA (2000).

[18] Arnold Goldberg et al, "Laboratory and Field Imaging Test Results on Single-Color and Dual-Band QWIP Focal Plane Arrays," Infrared Physics and Technology **42: 309-321** (2001).

[19] Arthur K. Cebrowski and John W. Raymond, "Operationally Responsive Space: A New Defense Business Model," Parameters (2005).

[20] Arthur K. Cebrowski, Director of Force Transformation, Office of Secretary of Defense (OSD), Senate Statement: *Before the Subcommittee on Strategic Forces, Armed Services Committtee, United States Senate*, 108^{th} Congress, 2^{nd} session, Marc25, (2004).

[21] Ashley J. Tellis, "China's Military Space Strategy," Survival, September, (2007).

[22] A. T. Aydin, P. E. Pace, and M. Tummala, "Orbit Selection for Space-based Interception of a Select ICBM Case," IEEE International Conference on Systems, Man and Cybernetics (2005).

[23] Axel Rendon, *Optimal Orbital Coverage of Theater Targets With Small Satellite Constellations*, Air Force Institute of Technology Thesis, Air Force Institute of Technology, Wright-Patterson Air Force Base, OH (2006).

[24] Baker Spring and Michaela Bendikova, "More Limits on U.S. Space Systems Unacceptable," The Heritage Foundation Webmemo, January 25, (2012).

[25] Barbara Opall-Rome Herzliya, "U.S. Seeks Space Hotline with China," Defense News, February 6, (2012).

[26] Ben Iannotta, "Drop, Then Retarget. New Datalink Would Help U.S. Navy To Redirect Missiles in Flight," DefenseNews, **February 9** (2009).

[27] Bill Gertz, "Inside the Ring," The Washington times, March 9, (2011).

[28] Bill Gertz, "New Space-Arms Control Initiative Draws Concern. Critics Say Military Activities Will be Compromised," The Washington times, January 16, (2012).

[29] Bob Brewin, "Lawmaker Bashes Proposed Space Code of Conduct," Global Secutity Newswire. March 12, (2012).

[30] Brian L. Kantsiper et al, "ORS HEO Constellations for Continuous Availability," AIAA 5th Responsive Space Conference **RS5-2007-2004** (2007).

[31] Bruce M. DeBlois, "Space Weapons: Crossing the U.S. Rubicon," International Security **Vol.29, N0.2**, 50 (2004).

[32] Bruce W. MacDonald, *China, Space Weapons, and U.S. Security*, Council on Foreign Relations Special Report (CSR N.38), (2008).

[33] Carey McCleskey, Cristina Guidi, and Kevin Brown, "Potential Strategies for Spaceport Systems Towards Airport-Like Operations," AIAA 2nd Responsive Space Conference **RS2-2004-6003** (2004).

[34] Gyanesh Chander, *An Overview of the CBERS-2 Satellite and Comparison of the CBERS-2 CCD Data with the L5 TM Data*, Accessed online at http://calval.cr.usgs.gov/JACIE_files/JACIE06/Files/37Chande.pdf, accessed on 04 March 2011.

[35] Conference on Disarmament, *Draft Treaty on Prevention of the Placement of Weapons in Outer Space and of the Threat or Use of Force against Outer Space Objects (PPWT)*, **CD/1839** (2008), Accessed online at http://www.unog.ch/ on 27th May, 2011.

[36] Charles L. Glaser and Steve Fetter, "National Missile Defense and the Future of U.S. Nuclear Weapons Policy," International Security **Vol. 26, No. 1, pp. 40-92** (2001).

[37] Christopher J. Bowie, Robert P. Haffa, Jr., and Robert E. Mullins, *Future War: What Trends in America's Post-Cold War Military Conflicts Tell Us About Early 21st Century Warfare*, Northrop Grumman, U.S. (2003).

[38] Cental Intelligence Agency, *General De Gaulle In Action: 1960 Summit Conference*, Accessed online at https://www.cia.gov/library/center-for-the-study-of-intelligence/csi-publications/csi-studies/studies/95unclass/Walters.html on 22, May 2011.

[39] Chairman of the Joint Chiefs of Staff, *Joint Vision 2010*, Washington D.C. (1997).

[40] Chairman of the Joint Chiefs of Staff, *Joint Vision 2020*, Washington D.C. (2000).

[41] Clay Dillow, "Satellite Track a Ballistic Missile Through All Phases of Flight," Navaltoday.com (2011).

[42] Major Collin A. Agee, *Peeling the Onion: The Iraqi Center of Gravity in Desert Storm*, Monograph, School of Advanced Military Studies, U.S. Army Command and General Staff College, Fort Leavenworth, Kansas (1992).

[43] Craig Covault, "Desert Storm Reinforces Military Space Directions," Aviation Week and Space Technology, April 8, (1991).

[44] Daniel L. Byman and Matthew C. Waxman, "Kosovo and the Great Air Power Debate," International Security, **Vol. 24, No.4, Spring** (2000).

[45] Daryl G. Press, "The Myth of Air Power in the Persian Gulf War and the Future of Warfare," International Security, **Vol.26, No.2, Fall** (2000).

[46] David A. Fulghum, "JDAM Errors to be Slashed," Aviation Week and Space Technology, **Vol. 142, No. 9,** February 27, (1995).

[47] David Halloway, *The Strategic Defense Initiative and the Soviet Union* in (eds.) Franklin A. Long et al, *Weapons in Space*, American Academy of Arts and Sciences, Cambridge MA (1986).

[48] David C. Jenn. *Radar and Laser Cross Section Engineering (Second Edition)*, American Institute for Aeronautics and Astronautics (AIAA) Education Series (1995).

[49] David O. Meteyer, *The Art of Peace: Dissuading China from Developing Counter-Space Weapons*, Institute for National Security Studies Occasional Paper 60, USAF Academy, Colorado (2005).

[50] David R. Mets, *The Long Search for a Surgical Strike. Precision Munitions and the Revolution in Military Affairs*, College of Aerospace Doctrine, Research and Education (CADRE), Air University, Maxwell Air Force Base, Alabama, US, CADRE Paper No. 12 (2001).

[51] David Wright and Laura Grego, "Anti-Satellite Capabilities of Planned US Missile Defense Systems," Disarmament Diplomacy **Issue No.68** (2002).

[52] David Wright and Theodore A. Postol, "A Post-Launch Examination of the Unha-2," Bulletin of Atomic Scientists (2009), Accessed online at http://www.thebulletin.org/web-edition/features/post-launch-examination-of-the-unha-2 on 11, October 2011.

[53] Dean Cheng, "China's Military Role in Space," Strategic Studies Quaterly, Spring, (2012).

[54] Desmond Ball et al, *Crisis Stability and Nuclear War*, American Academy of Arts and Sciences and Cornell University Peace Studies Program (1987).

[55] Department of Defense, *Product Verification Requirements for Launch, Upper Stage, and Space Vehicles* **MIL-STD-1540D** (1999).

[56] *John Warner National Defense Authorization Act for Fiscal Year 2007*, accessed online at http://www.govtrack.us/congress/bill.xpd?bill=h109-5122.

[57] *ABM Treaty: US Withdrawal Statement. Statement by the Press Secretary*, accessed online at http://www.dod.gov/acq/acic/treaties/abm/ABMwithdrawal.htm on 24th of May, 2011.

[58] Donald I. Blackwater, *The Long Road to Desert Storm and Beyond: The Development of Precision Guided Bombs*, School of Advanced Airpower Studies, Air University, Maxwell Air Force Base, Alabama, U.S. (1992).

[59] Donald L. Hafner, "Averting a Brobdingnagian Skeet Shoot: Arms Control Measures for Anti-Satellite Weapons," International Security **Vol.5, No.3**, Winter, (1980/81).

[60] Donald L. Hafner, *Assesing the President's Vision* in (eds.) Franklin A. Long et al, *Weapons in Space*, American Academy of Arts and Sciences, Cambridge, MA (1986).

[61] Donald M. Hodge, Maj., *The Financial Feasibility and Merits of the Small Lightweight Tactical Intelligence, Surveillance, and Reconnaissance Satellites Compared to National Systems*, Masters Thesis, U.S. Army Command and General Staff College, KA (1999).

[62] Donald W. Wilmot, William R. Owens and Robert J. Shelton, *Warning Systems* in (ed) David H. Pollock, *Volume 7: Countermeasure Systems*, The Infrared and Electro-Optical Systems Handbook, SPIE Optical Engineering Press, Washington USA (1993).

[63] Don Knight, "Concept of Operations for Operationally Responsive Space," AIAA 4th Responsive Space Conference **RS4-2006-7003** (2006).

[64] Duncan D. McKenzie, "U.S. Air Force Communications in Desert Storm," IEEE Communications Magazine **January** (1992).

[65] Dwayne A. Day, "Staring Into the Eyes of the Dragon," The Space Review **November** (2011).

[66] Dwayne Day, John Logsdon, and Brian Latell, *Eye in the Sky: The Story of the CORONA Spy Satellites*, Smithsonian Institute Press, Washington D.C. (1998).

[67] Edward B. Tomme, Lt. Col., *The Strategic Nature of Tactical Satellites*, Air Power Research Institute, Air University, AL (2006).

[68] Edward Luttwak and Stuart L. Koehl, *The Dictionary of Modern War*, Harper Collins (1991).

[69] E. L. Dereniak and G. D. Boreman, *Infrared Detectors and Systems*, Wiley, USA (1996).

[70] Eliot A. Cohen et al, *Gulf War Air Power Survey. Volume I: Planning and Command and Control*, U.S. Government Printing Office, Washington D.C. (1993).

[71] Eliot A. Cohen et al, *Gulf War Air Power Survey. Volume IV: Weapons, Tactics and Training and Space Operations*, U.S. Government Printing Office, Washington D.C. (1993).

[72] Ellen Pawlikowski, Doug Loverro, and Tom Cristler, "Space: Disruptive Challenges, New Opportunities, and New Strategies," Strategic studies Quaterly, **Spring** (2012).

[73] Everett C. Dolman and Henry F. Cooper, Jr. *Increasing the Military Uses of Space* in (eds.) Charles D. Lutes and Peter L. Hays, *Towards a Theory of SPACEPOWER: Selected Essays*, National Defense University Press, Washington D.C. (2011).

[74] Federal Aviation Administration Commercial Space Transportation, *Quaterly Launch Report - Special Report:An Overview of U.S. Commerical Space Infrastructure*, FAA Associate Administrator for Commercial Space Transportation D.C. (1998).

[75] Federal Aviation Administration Commercial Space Transportation, *2006 Commercial Space Transportation Developments and Concepts: Vehicles, Technologies and Spaceports*, FAA Office of Commercial Space Transportation D.C. (2006).

[76] Federation of American Scientists, *Executive Summary of the Report of the Commission to Assess the Ballistic Missile Threat to the United States*, Accessed online at http://www.fas.org/irp/threat/bm-threat.htm on 24th of May, 2011.

[77] Federation of American Scientists, *United States Nuclear Detonation System (USNDS)(U)*, Accessed online at http://www.fas.org/spp/military/program/nssrm/initiatives/usnds.htm on 1st of June, 2011.

[78] Federation of American Scientists, *LGM-118A Peacekeeper*, Accessed online at http://www.fas.org/nuke/guide/usa/icbm/lgm-118.htm on 11, October 2011.

[79] Filippo Neri, *Introduction to Electronic Defense Systems*, Artech House, Boston, Massachusetts (2001).

[80] Forrest E. Morgan, *Deterrence and First-Strike Stability in Space: A Preliminary Assessment*, Project Air Force, RAND Corporation, Santa Monica, CA (2010).

[81] Frank G. Klotz, Lt. Gen., *Defining Responsive Space*, Keynote address, Responsive Space Conference 2004, (2006).

[82] Frank G. Klotz, *Space, Commerce, and National Security*, A Council on Foreign Relations Paper, Council on Foreign Relations Press, New York (1998).

[83] Gene H. Edwards, III, *GPS Guided Munitions and Precision Engagement: Do National and Theater Targeting Agencies Fully Support the Joint Force Commander?*, Paper, Naval War College, Newport, RI (1998).

[84] Geoffrey Forden et al, "False Alarm, Nuclear Danger," IEEE Spectrum, **V37, Number 3** (2000).

[85] George Rathjens and Jack Ruina, *BMD and Strategic Instability* in (eds) Franklin A. Long et al, *Weapons in Space*, American Academy of Arts and Sciences, Cambridge, MA (1986).

[86] GPS World, "Desert Storm Redux," GPS World, **July/August, pp. 12** (1991).

[87] G. R. Sullivan and J. M. Dubik, "Land Warfare in the 21st Century," Military Review, **September, pp. 13-32** (1993).

[88] Human Rights Watch, *Off Target. The Conduct of the War and Civilian Casualities in Iraq*, Human Rights Watch, U.S. (2003).

[89] Jae-Hyuk Oh and In-Joong Ha, "Capturability of the 3-Dimensional Pure PNG Law," IEEE Transactions on Aerospace and Electronic Systems **Vol. 35, No. 2** (1999).

[90] James W. Canan, "Lows and High for SBIRS Early Warning," Aerospace America (2011).

[91] General James E. Cartwright, "Assured Access to Space," High Frontier **Vol.3 No. 1** (2006).

[92] James P. coyne, *Airpower in the Gulf*, Air Force Association, VA (1992).

[93] James G. Diehl and Charles E. Sloan, "Battle Damage Assessment: The Ground Truth," Joint Force Quaterly, **Issue No. 37** (2005).

[94] James F. Dunnigan and Austin Bay, *From Storm to Shield. High-Tech Weapons, Military Strategy, and Coalition Warfare in the Persian Gulf*, William Morrow and Company. Inc., New York, U.S. (1992)

[95] James R. Meisinger, *Operationally Responsive Space and the Joint Force Commander*, Naval War College, RI (2008).

[96] James W. Pardew, Jr., "The Iraqi Army's Defeat in Kuwait," Parameters, Winter, (1991-92).

[97] James R. Wertz, "Coverage, Responsiveness, and Accessibility for Various "Responsive Orbits," AIAA 3rd Responsive Space Conference **RS3-2005-2002** (2005).

[98] James R. Wertz, "Circular vs. Elliptical Orbits for Persistent Communications," AIAA 5th Responsive Space Conference **RS5-2007-2005** (2007).

[99] James R. Wertz, Richard E. Van Allen, and Christopher J. Shelner, "Aggressive Surveillance as a Key Application Area for Responsive Space," AIAA 4th Responsive Space Conference **RS4-2006-1004** (2006).

[100] Jay Raymond et al, "TacSat-1 and a Path to Tactical Space," AIAA 2nd Responsive Space Conference **RS2-2004-5003** (2004).

[101] Jennifer C. Davis and James J. Lisowski, "Developing a Remote Staring Sensor for Optimizing Successful Boost Phase Intercept," IEEE Aerospace Conference Proceedings **Vol. 4: 4-1649 - 4-1661** (2002).

[102] Jeremy Singer, "U.S. Military Working to Define Responsive Operations in Space," Armed Forces Journal (2006).

[103] Tech. Sgt. Jess D. Harvey, "Air Force 2013 Budget Invests in Critical Space Capabilities," Air Force Print News Today (2012).

[104] Jim Wolf, " Exclusive: U.S. Dangles Secret Data for Russia Missile Defense Shield Approval," Reuters, **Mar 13** (2012), Accessed online at http://www.reuters.com/article/2012/03/14/us-usa-russia-missiledefense-idUSBRE82D03A20120314 on 04.21.2012.

[105] J. J. Spiker Jr. and Bradford W. Parkinson, *Overview of GPS Operation and Design* in (eds.) J. J. Spiker and Bradford W. Parkinson, *Global Positioning System: Theory and Applications Volume I*, Progress in Astronautics and Aeronautics: Volume 164, American Institute of Aeronautics and Astronautics, Washington, DC (1996).

[106] J. J. Spiker Jr. *Satellite Constellation and Geometric Dilution of Precision* in (eds.) J. J. Spiker and Bradford W. Parkinson, *Global Positioning System: Theory and Applications Volume I*, Progress in Astronautics and Aeronautics: Volume 164, American Institute of Aeronautics and Astronautics, Washington, DC (1996).

[107] John R. Bolton and John C. Yoo, "Hands Off the Heavens," The New York Times, March 8, (2012).

[108] John Paul Hyde, Johann W. Pfeiffer and Toby C. Logan *CAFMS Goes to War* in (eds.) Alan D. Campen, *The First Information War. The Story of Communications, Computers and Intelligence Systems in the Persian Gulf War*, AFCEA International Press, Fairfax, Virginia, U.S. (1992).

[109] John A. Russ, *Precision Misses the Mark*, School of Advanced Warfighting, Marine Corps War College, Quantico, VA (2001).

[110] John D. Steinbruner, *Principles of Global Security*, Brookings Institution Press, Washington D.C. (2000).

[111] John A. Tirpak, "Precision: The Next Generation," AIR FORCE Magazine, **November** (2003).

[112] John Watson and Keith P. Zondervan, "The Missile Defense Agency's Space Tracking and Surveillance System," Crosslink (2008).

[113] Joint Publication 1-02, *Department of Defense Dictionary of Military and Associated Terms*, Office of the Joint Chiefs of Staff, Washington D.C., (1994, rev. 2000).

[114] Kaleb Dissinger, *GPS Goes to War - The Global Positioning System in Operation Desert Storm*, Army Heritage Museum, (2008), Accessed online at http://www.army.mil/article/7457/ on 03/13/2012.

[115] Karl P. Mueller, *Totem and Taboo: Depolarizing the Space Weaponization Debate* in (eds.) John M. Logsdon and Gordon Adams, *SPACE WEAPONS: Are they needed?*, Space Policy Institute, George Washington University, Washington D.C. (2003).

[116] Katelyn Noland, "DIA Head Warns Senate of China's Space Program," ExecutiveGov, February 24, (2012), accessed online at http://www.executivegov.com/2012/02/dia-head-warns-senate-of-chinas-space-program/ on March 10, (2012).

[117] K. Chang, C. Chong, Y. Bar-Shalom, "Joint Probabilistic Data Association in Distributed Sensor Networks," IEEE Transactions on Automatic Control **Vol. Ac-31, No. 10** (1986).

[118] Lt Col Kendall K. Brown, "Is Operationally Responsive Space the Future of Access to Space for the US Air Force?," Air and Space Power Journal, Summer, (2006).

[119] Khalil Seyrafi and S. A. Hovanessian, *Introduction to Electro-optical Imaging and Tracking Systems*, Artech House, Boston, USA (1993).

[120] Kimberly A. Sugrue, *Optimal Orbital Coverage of Theater Operations and Targets*, Air Force Institute of Technology Thesis, Air Force Institute of Technology, Wright-Patterson Air Force Base, OH (2007).

[121] Kurt Gottfried and Richard Ned Lebow, *Anti-Satellite Weapons: Weighing the Risks* in (eds.) Franklin A. Long et al, *Weapons in Space*, American Academy of Arts and Sciences, Cambridge, MA (1986).

[122] Laura Grego, "The Anti-Satellite Capability of the Phased Adaptive Approach Missile Defense System," Federation of American Scientists Public Interest Report, Winter (2011).

[123] Leland Joe and Issac Porche III, *Future Army Bandwidth Needs and Capabilities*, RAND Corporation, CA (2004).

[124] Lisa A. Baghal, *Assembly, Integration, and Test Methods for Operationally Responsive Space Satellites*, Air Force Institute of Technology Thesis, Wright-Patterson Air Force Base, OH (2010).

[125] Lisa Baghal, Randon Wright and Richard Galindez, "In a Tactical Minute: Lessons Learned From the First-Ever In-Theater Satellite Command and Downlink," AIAA 7th Responsive Space Conference **RS7-2009-6002** (2009).

[126] Marcia Smith, *EU Releases Revised Draft Code of Conduct for Outer Space Activities*, Spacepolicyonline.com (2010).

[127] Marco Cáceres, "Industry Insights: Cost Overruns Plague Military Satellite Programs," Aerospace America (2006).

[128] M. A. Rice and A. J. Sammes, *Command and Control: Support Systems in the Gulf War*, Volume 12: LAND WARFARE. Brassey's New Battlefield Weapons Systems and Technology Series, London (1994).

[129] Martin Streetly (ed.), *Jane's Radar and Electronic Warfare Systems 2001-2002*, 13th edition, Jane's Information Group, Alexandria, VA (2001).

[130] Merill L. Skolnik, *Introduction to Radar Systems*, McGraw Hill Publications (2001).

[131] Michael R. Frater and Michael Ryan, *Electronic Warfare for the Digitized Battlefield*, Artech House, Boston, MA (2001).

[132] Michael Krepon et al, *Preserving Freedom of Action in Space: Realizing the Potential and Limits of U.S. Spacepower* in (eds.) Charles D. Lutes and Peter L. Hays, *Towards a Theory of SPACEPOWER: Selected Essays*, National Defense University Press, Washington D.C. (2011).

[133] Michael E. O'Hanlon, *Balancing U.S. Security Interests in Space* in (eds.) Charles D. Lutes and Peter L. Hays, *Towards a Theory of SPACEPOWER: Selected Essays*, National Defense University Press, Washington D.C. (2011).

[134] Michael J. Pillsbury, *An Assessment of China's Anti-Satellite and Space Warfare Programs, Policies and Doctrines*, Report to the U.S.-China Economic and Security Review Commission, Washington D.C. (2007).

[135] Michael J. Ryan and Michael R. Frater, *Tactical Communications for the Digitized Battlefield*, Artech House, Boston, MA (2002).

[136] M.J. Ryan, *Battlefield Command Systems*, Volume 7: LAND WARFARE. Brassey's New Battlefield Weapons Systems and Technology Series into the 21st Century, Brasseys, London (2000).

[137] Martin W. Lo, "Application of Ergodic Theory to Coverage Analysis," AAS/AIAA Astrodynamics Specialist Conference (2003).

[138] Martin W. Lo, "The Long-Term Forecast of Station View Periods," NASA JPL TDA Progress Report **42-118**, (1994).

[139] Michael Hurley, Joe Hauser, Timothy Duffey, Sr., "Microsatellite Deployment On Demand," AIAA 1st Responsive Space Conference **AIAA-LA Section/SSTC 2003-3001** (2003).

[140] Michael Krepon et al, *Model Code Of Conduct For Space-Faring Nations*, Stimson Center, Washington D.C. (2007).

[141] Michael Russell Rip and James M. Hasik, *The Precision Revolution. GPS and the Future of Aerial Warfare*, Naval Institute Press, Annapolis, MD (2002).

[142] Missilethreat.com, *Reagan's SDI Speech: Announcement of Strategic Defense Initiative*, Missilethreat.com, A Project of the Claremont Institute, Accessed online at http://www.missilethreat.com/resources/pageID.263/default.asp on 22, May 2011.

[143] M. Z. Tidrow and W. R. Dyer, "Infrared Sensors for Ballistic Missile Defense," Infrared Physics and Technology **42: 333-336** (2001).

[144] Nancy Gallagher and John D. Steinbruner, *Reconsidering the Rules for Space Security*, American Academy of Arts and Sciences, Cambridge, MA (2008).

[145] National Research Council, *The Global Positioning System: A Shared National Asset*, National Academy Press, Washington, D.C. (1995).

[146] Nina Tannenwald, *Law Versus Power on the High Frontier: The Case For a Rule-Based Regime for Outer Space*, Project on Advanced Methods of Cooperative Security, CISSM, University of Maryland, College Park (2003).

[147] Office of the Secretary of Defense, "Report to the Defense and Intelligence Committees of the Congress of the United States on the Status of the Space Based Infrared System Program," Office of the Secretary of Defense, Washington D.C., USA (2005).

[148] Patrick Frakes and Paul Popejoy, "Responsive Space Operations Architecture Development for the National Security Space Community," AIAA 2nd Responsive Space Conference **RS2-2004-4001** (2004).

[149] Maj. Paul G. Gillespie, *Precision Guided Munitions: Constructing a Bomb More Potent than the A-Bomb*, Ph.D. Dissertation, Lehigh University (2002).

[150] Paul W. Gydesen, *What is the Impact to National Security Without Commercial Space Applications?*, Air War College, Air University, Maxwell Air Force Base, Alabama (2006).

[151] Paul J. Kolodziejski, "Operationally Responsive Spacelift for the U.S. Air Force," AIAA 1st Responsive Space Conference **AIAA-LA Section/SSTC 2003-1002**(2003).

[152] Paul Zarchan, *Tactical and Strategic Missile Guidance (Fifth Edition)*, Progress in Astronautics and Aeronautics, AIAA Tactical Missile Series, Virginia, USA (2007).

[153] Paul Zarchan, "Ballistic Missile Defense Guidance and Control Issues," Science and Global Security **Vol. 8, pp. 99-124** (1998).

[154] Pavel Podvig and Hui Zhang, *Russian and Chinese Responses to U.S. Military Plans in Space*, American Academy of Arts and Sciences, Cambridge MA (2008).

[155] Peter Grier, "Joint STARS Does its Stuff," Air Force Magazine, **June** (1991).

[156] Philip J. Baines and Adam C*ôté*, "Promising Confidence- and Security-Building Measure for Space Security," Disarmament Forum **Issue No.4** (2009).

[157] Philip E. Coyle and John B. Rhinelander, "Drawing the Line: The Path to Controlling Weapons in Space," Disarmament Diplomacy **Issue No.66** (2002).

[158] P. J. Sharrett et al, "GPS Performance: An Initial Assessment," 4th International Technical Meeting of the Satellite Division of the Institute of Navigation, Albuquerque, N.M., September, (1991).

[159] Rebeccah L. Heinrichs, "Hillary's Misguided Space Arms Control. Pact Could Undermine American Security in the Name of Cooperation," Washington Times, January 23, (2012).

[160] Regina Hagen and J*ü*rgen Scheffran, "Is a Space Weapons Ban Feasible? Thoughts on Technology and Verfication of Arms Control in Space," Disarmament Diplomacy **Issue No.1** (2003).

[161] Richard DalBello, *Commerical Communication Satellites: Assessing Vulnerability in a Changing World* in (eds.) John M. Logsdon and Gordon Adams, *SPACE WEAPONS: Are they needed?*, Space Policy Institute, George Washington University, Washington D.C. (2003).

[162] Richard L. Garwin, "Boost-Phase Intercept: A Better Alternative," Arms Control Today (2000).

[163] Robert Carneal, Lt. Col., "Sea-Launched TacSats for Responsive Space (STaRS)," AIAA 7th Responsive Space Conference **RS7-2009-1007** (2009).

[164] Brigadier General Robert H. Scales, Jr., *Certain Victory: The US Army in the Gulf War*, Office of the Chief of Staff, United States Army, Washington, D.C., (1993)

[165] Robert Sutter, *China and U.S. Missile Defense Proposals: Reactions and Implications*, CRS Report for Congress (1999).

[166] Ronald M. Sega and James E. Cartwright, *Plan for Operationally Responsive Space: A Report to Congressional Defense Committees*, Department of Defense, DC (2007).

[167] Ross Liemer and Christopher F. Chyba, "A Verifiable Limited Test Ban for Anti-Satellite Weapons," The Washington Quaterly **33:3** 149-163 (2010).

[168] R. P. Hallion, *Storm Over Iraq: Airpower and the Gulf War,* Smithsonian Institution Press, Washington, D.C. (1992).

[169] Ryan Pendelton Lt Col, "TacSat-3 Demonstration and Follow-On Use," AIAA 8th Responsive Space Conference **RS8-2010-7002** (2010).

[170] T. Ryan Space, Vicent Demo, and Edward Jones, "Transforming National Security Space Payloads," AIAA 2nd Responsive Space Conference **RS2-2004-2001** (2004).

[171] Sam Loeb, *Zeroing In: A Capabilities-based Alternative to Precision Guided Munitions Planning*, Pardee Rand Graduate School Dissertation, RAND Corporation, CA (2005).

[172] Satnews Daily, "Northrop Grumman' STSS Demo Sats Shoot Straight–It's A Kill (Launch)," Satnews Daily **November** (2011).

[173] Scott Schoneman et al, "Minotaur I Demonstration of Responsive Launch for the TACSAT-2 Mission," AIAA 5th Responsive Space Conference **RS5-2007-5002** (2007).

[174] Satellite Imaging Corporation, *CBERS-2 Satellite Sensor*, Accessed online at http://www.satimagingcorp.com/satellite-sensors/cbers-2.html on 04 March 2011.

[175] Satellite Imaging Corporation, *Ikonos Satellite Images and Sensor Specifications*, Accessed online at http://www.satimagingcorp.com/satellite-sensors/ikonos.html on 04 March 2011.

[176] Satellite Imaging Corporation, *GeoEye-1 Satellite Imagery/Sensor Specifications*, Accessed online at http://www.satimagingcorp.com/satellite-sensors/geoeye-1.html on 04 March 2011.

[177] Satellite Imaging Corporation, *Quickbird Satellite Images and Sensor Specifications*, Accessed online at http://www.satimagingcorp.com/satellite-sensors/quickbird.html on 04 March 2011.

[178] Satellite Imaging Corporation, *WorldView-2 Satellite Sensor*, Accessed online at http://www.satimagingcorp.com/satellite-sensors/worldview-2.html on 04 March 2011.

[179] Scott C. Larimore, Lt. Col., *Operationally Responsive Space: A New Paradigm or False Start?*, Air University Graduate Report, Air University, Maxwell Air Force Base, AL (2007).

[180] Scott C. Larimore, "Partially Continuous Earth Coverage from a Responsive Space Constellation," 5th Responsive Space Conference **RS5-2007-2001**, LA (2007).

[181] Scott Pace et al, *The Global Positioning System. Assessing National Policies*, RAND, Santa Monica, CA (1995).

[182] S. Deb, K. R. Pattipati, and Y. Bar-Shalom, "A Multisensor-Multitarget Data Association Algorithm for Heterogeneous Sensors," IEEE Trans. Aerospace Electronic Systems **AES-29(2):560-568**, (1993).

[183] S. D. Gunapala et al, "Quantum Well Infrared Photodetector Research and Development at Jet Propulsion Laboratory," Infrared Physics and Technology **42: 267-282** (2001).

[184] S. D. Gunapala et al, "1024 X 1024 Pixel Mid-wavelength and Long-Wavelength Infrared QWIP Focal Plane Arrays for Imaging Applications," Semiconductor Science and Technology **20: 473-480** (2005).

[185] Sir Peter Anson Bt. and Dennis Cummings, "The First Space War: The Contribution of Satellites to the Gulf War," RUSI Journal, Winter, (1991).

[186] S. K. Singh, M. Premalatha and G. Nair, "Ellipsoidal Gating for an Airborne Track While Scan Radar," IEEE International Radar Conference (1995).

[187] Space News Staff, "Delta 2 Rocket Launches Missile-Tracking Satellites," Space News (2009).

[188] spacetoday.net, *Report: Pentagon Cancels TacSat 1 Launch*, (2007). Accessed online at http://www.spacetoday.net/Summary/3884 on 02 March 2011.

[189] S. Rosen, C. Banning, and T. Utsch, "TACSATS: Perspectives from Air Force Space Systems Division," AIAA Space Programs and Technologies Conference **AIAA-90-3572** (1990).

[190] Stephen Clark, "Missile Defense Demo Satellites Ready for Testing," Spaceflight Now (2011).

[191] Stephen Clark, "White House Budget Would Cut Military Space Research," Spaceflight Now (2012).

[192] Steven Beardsley, "Space Clutter a Growing Concern for Pentagon," Stars and Stripes, March 23, (2012).

[193] Steven J. Rauch, *From Bull Run to Baghdad. A History of the United States Army Signal Corps 1860-2010*, Army Communicator (2010).

[194] StrategyWorld.com, "How Many JDAM Is Enough," (2008), Accessed online at http://www.strategypage.com/htmw/htairw/articles/20080924.aspx on 05.04.2012.

[195] Stuart Eves, "Small-Satellite Surveillance Missions Providing Unique Military Capabilities," 3rd Responsive Space Conference **RS3-2005-2004** (2005).

[196] S. V. Bandara et al, "Four-band Quantum Well Infrared Photodetector Array," Infrared Physics and Technology **44: 369-375** (2003).

[197] Sydney J. Freedberg, "Safe Passage: Why the Pentagon Wants an International "Code of Conduct" for Space," AoIDefense, March 22, (2012), Accessed online at http://defense.aol.com/2012/03/22/safe-passage-why-the-pentagon-wants-an-international-code-of-c/ on 03.22.2012.

[198] T. A. Keaney and E. A. Cohen, *The Gulf War Airpower survey: Summary Report*, U.S. Goverment Printing Office, Washington, D.C. (1993).

[199] T. A. Keaney and E. A. Cohen, *Revolution in Warfare? Air Power in the Persian Gulf*, Naval Institute Press, Annapolis, Maryland (1995).

[200] Terrance Yee, "Key Elements of Rapid Integration and Test," AIAA 3rd Responsive Space Conference **RS5-2005-4001** (2005).

[201] Thomas M. McGrath, *What Happens if the Stars Go Out? U.S. Army Dependence on the Global Positioning System*, Masters Thesis, U.S. Army Command and General Staff College, Fort Leavenworth, KA (2009).

[202] Timothy M. Conroy, *A COMING OF AGE: The Implications of Precision Guided Munitions for Air Power*, MA Thesis, Naval Postgraduate Thesis, Monterey, CA (1993).

[203] Timothy J. Gibson, *Rapid Preparation and Distribution of Battlefield Information* in (eds.) Alan D. Campen, *The First Information War. The Story of Communications, Computers and Intelligence Systems in the Persian Gulf War*, AFCEA International Press, Fairfax, Virginia, U.S. (1992).

[204] Titus Ledbetter III, "Lawmakers Question Proposed Cancellation of Space Test Program, ORS," Space News, March, (2012).

[205] Titus Ledbetter III, "Advanced SBIRS Sensor Capability Will Not be Available Before 2016," Space News, March, (2012).

[206] Titus Ledbetter III, "U.S. Invites Russia To Monitor Aegis Missile Intercept Test," Space News, March, (2012).

[207] Major Todd C. Westhauser, *Improving NATO's Interoperability Through U.S. Precision Weapons*, Thesis, School of Advanced Airpower Studies, Air University, Maxwell Air Force Base, Alabama, U.S. (1998).

[208] Tom Doyne et al, "ORS and TacSat Activities Including the Emerging ORS Enterprise," AIAA 5th Responsive Space Conference **RS5-2007-4001** (2007).

[209] William F. Tosney, Bruce L. Arnheim, and James B. Clark, "The Influence of Development and Test on Mission Success," Proceedings of the 4th International Symposium on Environmental Testing for Space Programs, Liege, Belgium (2001).

[210] Turner Brinton, "STSS Satellites Demonstrate 'Holy Grail' of Missile Defense," Space News (2011).

[211] Turner Brinton, "STSS Tracking Hand-Off Marks a Key Milestone," Space News (2010).

[212] Turner Brinton, "STSS Satellites Track Three Missiles in Initial Testing," Space News (2010).

[213] National Museum of the U.S. Air Force, *U.S. Air Force Fact Sheet: Tactical Communications Satellite (TACSAT 1)*, Accessed online at http://www.nationalmuseum.af.mil/ on 03.22.2011.

[214] U.S. Department of Defense, *Final Report to Congress: Conduct of the Persian Gulf War*, (1992).

[215] United States General Accounting Office Report to Congressional Committees, *Weapons Acquisition: Precision Guided Munitions in Inventory, Production, and Development*, GAO/NSIAD-95-95 (1995).

[216] United States General Accounting Office Report to Congressional Requesters, *Operation Desert Storm: Evaluation of the Air War*, GAO/PEMD-96-10 (1996).

[217] United States General Accounting Office Report to Congressional Committees, *Precision-Guided Munitions: Acquisition Plan for the Joint Air-to-Surface Standoff Missile*, GAO-NSIAD-94-144 (1996).

[218] United States Government Accountability Office, *Defense Acquisitions: Space-Based Infrared System-Low at Risk of Missing Initial Deployment Date*, GAO-01-6 (2001).

[219] United States Government Accountability Office, *Missile Defense: Alternate Approaches to Space Tracking and Surveillance System Need to Be Considered*, GAO-03-597 (2003).

[220] United States Government Accountability Office, *Military Operations: Recent Campaigns Benefited from Improved Communications and Technology, but Barriers to Continued Progress Remain*, GAO-04-547 (2004).

[221] United States Government Accountability Office, *Space Acquisitions: DOD Needs a Departmentwide Strategy for Pursuing Low-Cost, Responsive Tactical Space Capabilities*, GAO-06-449 (2006).

[222] United States Government Accountability Office, *Defense Space Activities: DOD Needs to Further Clarify the Operationally Responsive Space Concept and Plan to Integrate and Support Future Satellites*, GAO-08-831 (2008).

[223] United States Government Accountability Office, *Statement of Cristina T. Chaplain, Director Acquisition and Sourcing Management. Space Acquisitions: DOD Faces Substantial Challenges in Developing New Space Systems*, GAO-09-705T (2009).

[224] United States Government Accountability Office, *Statement of Cristina T. Chaplain, Director Acquisition and Sourcing Management. Space Acquisitions: DOD Poised to Enhance Space Capabilities, but Persistent Challenges Remain in Developing Space Systems*, GAO-10-447T (2010).

[225] United States Government Accountability Office, *Statement of Cristina T. Chaplain, Director Acquisition and Sourcing Management. Space Acquisitions: DOD Delivering New Generations of Satellites, but Space Systems Acquisition Challenges Remain*, GAO-11-590T (2011).

[226] United States Government Accountability Office, *Statement of Cristina T. Chaplain, Director Acquisition and Sourcing Management. Space Acquisitions: DOD Faces Challenges in Fully Realizing Benefits of Satellite Acquisition Improvements*, GAO-12-563T (2012).

[227] U.S. News and World Report, *Triumph Without Victory. The Unreported History of the Persian Gulf War*, Times Books, U.S. (1992).

[228] U.S. Space Command, *United States Space Command: Operation Desert Shield and Desert Storm Assessment*, (1992).

[229] Victor Mizin, *Russian Perspectives on Space Security* in (eds.) John M. Logsdon et al, *Collective Security in Space: European Perspectives*, Space Policy Institute, The George Washington University, Washington D.C. (2007).

[230] Walter J. Boyne, Colonel, USAF (Ret.), *Operation Iraqi Freedom. What Went Right, What Went Wrong, And Why*, Tom Doherty Associates Book, New York, U.S. (2003).

[231] Wendler, B., "Establishing Minimum Environmental Test Standards for Space Vehicles," 21st Aerospace Testing Seminar, CA (2003).

[232] Wikipedia, *Global Positioning System*, Accessed online at *http* : *//en.wikipedia.org/wiki/Global*$_P$*ositioning*$_S$*ystem* on 03/13/2012.

[233] William Matthews, "Tracking Missile in Stereo," Space News (2009).

[234] Y. Bar-Shalom, *Multitarget-multisensor tracking: Advanced Application*, Artech House, Boston, MA (1990).

[235] Y. Kashiwagi, *Prediction of Ballistic Missile Trajectories*, Memorandum 37, Defense Technical Information Center (1968).

[236] Yool A. Kim and Gary McLeod, "Toward a New Strategy for Operationally Responsive Space," AIAA 8th Responsive Space Conference **RS8-2010-1004** (2010).